STERILITY AND IMMUNOGENICITY OF GAMMA-IRRADIATED RESPIRATORY VIRUSES

Eve Singleton, B. Sc. (Hons).

A thesis submitted for the fulfilment of the

Degree of Doctor of Philosophy

School of Biological Sciences

The University of Adelaide

Adelaide, South Australia, Australia

July 2020

TABLE OF CONTENTS

LIST OF FIGURES AND TABLES

ABBREVIATIONS

γ	Gamma
γ-Flu	γ-irradiated influenza vaccine
γ-NDV	γ-irradiated Newcastle disease virus vaccine
γ-PN	γ-irradiated *Streptococcus pneumoniae* vaccine
γ-SFV	γ-irradiated Semliki forest virus vaccine
4-MU	4-Methylumbelliferyl
4-MUNANA	2'-(4-Methylumbelliferyl)-α-D-N-acetylneuraminic acid
^{60}Co	Cobalt-60
^{60}Ni	Nickel-60
^{137}Cs	Cesium-137
A/California	A/California/07/2009 [H1N1]
A/PR8	A/Puerto Rico/8/1934 [H1N1]
ACKR4	Atypical chemokine receptor 4
Alum	Aluminium hydroxide
ANSTO	Australian Nuclear Science and Technology Organisation
APC	Antigen presenting cell
APMC	Avian paramyxovirus
BPL	Beta-propiolactone
CEF	Chicken embryo fibroblasts
cRBC	Chicken red blood cell
CFSE	Carboxyfluorescein diacetate viiuccinimidyl ester
CPE	Cytopathic effect
CTL	Cytotoxic $CD8^+$ T lymphocytes
CTLA-4	Cytotoxic T lymphocyte-associated protein 4
CTR	Cell-Tracker Red
D_{10}	The radiation dose required to reduce bio burden by 90%
DC	Dendritic cell
DI	Dry ice
DMEM	Dulbecco's Modified Eagle's Medium
DoD	US Department of Defense
d.p.i.	Days post-immunisation
ds	Double-stranded

DS	Sterilising dose
ECE	Embryonated chicken egg
eIF-2A	Eukaryotic initiation factor 2A
ELISA	Enzyme-Linked Immunosorbent Assay
ER	Endoplasmic reticulum
F	NDV fusion protein
FBS	Foetal bovine serum
FFA	Focus-forming assay
FFIA	Focus-forming inhibition assay
FFU	Focus forming units
GI – GXXI	NDV genotype I to genotype XXI
GM-CSF	Granulocyte-macrophage colony-stimulating factor
HA	Haemagglutinin
HAU	Haemagglutination units
HBV	Hepatitis B virus
HCV	Hepatitis C virus
HIV	Human immunodeficiency virus
HN	Haemagglutinin-neuraminidase
HPAI	Highly pathogenic avian influenza
hRBC	Human red blood cell
HRP	Horse radish peroxidase
HSV	Herpes simplex virus
ICP34.5	Infected cell protein 34.5
ICP47	Infected cell protein 47
i.m	Intramuscular
i.n	Intranasal
i.p	Intraperitoneal
i.t	Intratumoral
i.v	Intravenous
IAEA	International Atomic Energy Agency
IAV	Influenza A Virus
ICP34.5	Infected cell protein 34.5
ICP47	Infected cell protein 47
IFA	Incomplete Freund’s adjuvant

IFN-I	Type I interferon
Ig	Immunoglobulin
ISO	International Organisation for Standardization
ISG	Interferon stimulated gene
kDa	KiloDaltons
kGy	KiloGray
KLH	Keyhole limpet hemocyanin
L	NDV large polymerase protein
M1	Matrix protein
M2	Membrane ion channel
MAVS	Mitochondrial antiviral signalling protein
MDCK	Madin-Darby Canine Kidney
MHC-I	Major histocompatibility complex class I
MHC-II	Major histocompatibility complex class II
MOI	Multiplicity of infection
mRNA	Messenger RNA
NA	Neuraminidase
NK	Natural killer cell
NP	Nucleoprotein
NPP	Nucleoprotein peptide
NS1	Non-structural protein 1
NS2	Non-structural protein 2
NSG	NOD *scid* gamma
OTC	Ornithine transcarbamylase
OV	Oncolytic virus
P/S	Penicillin and streptomycin
PA	Polymerase acidic protein
PAMP	Pathogen-associated molecular pattern
PB1	Polymerase basic protein 1
PB2	Polymerase basic protein 2
PBS	Phosphate buffered saline
PD-1	Programmed cell death protein 1
pDC	Plasmacytoid dendritic cell
pdmH1N1	2009 Swine flu pandemic IAV strain

PFA	Plaque-forming assay
PFU	Plaque-forming units
PKR	Protein kinase R
Poly(I:C)	Polyinosinic:polycytidylic acid
PRR	Pattern recognition receptor
R	Radioresistance value
RBS	Receptor binding site
RIG-I	Retinoic acid-inducible gene 1
ROS	Reactive oxygen species
RT	Room temperature
RV	Rotavirus
SA	Sialic acid
SAL	Sterility assurance level
SAα2,3Gal	Sialic acid-α2,3-galactose
SAα2,6Gal	Sialic acid-α2,6-galactose
SCID	Severe combined immunodeficiency disease
SDR	Standard distribution of resistance
SFV	Semliki forest virus
SH	Small hydrophobic protein
ss	Single-stranded
$TCID_{50}$	50% Tissue culture infectious dose
TCR	T cell receptor
T_H	T helper cell
TIL	Tumour-infiltrating lymphocyte
TIV	Trivalent influenza vaccine (split or subunit)
TLR	Toll-like receptor
T_{RM}	Tissue-resident memory T cell
UF	Ultrafiltration
UV	Ultraviolet
vRNP	Viral ribonucleoprotein
WHO	World Health Organisation
ZIKV	Zika virus

DECLARATION

I certify that this work contains no material which has been accepted for the award of any other degree or diploma in my name, in any university or other tertiary institution and, to the best of my knowledge and belief, contains no material previously published or written by another person, except where due reference has been made in the text. In addition, I certify that no part of this work will, in the future, be used in a submission in my name, for any other degree or diploma in any university or other tertiary institution without the prior approval of the University of Adelaide and where applicable, any partner institution responsible for the joint-award of this degree.

I acknowledge that copyright of published works contained within this thesis resides with the copyright holder(s) of those works.

I also give permission for the digital version of my thesis to be made available on the web, via the University's digital research repository, the Library Search and also through web search engines, unless permission has been granted by the University to restrict access for a period of time.

I acknowledge the support I have received for my research through the provision of an Australian Government Research Training Program Scholarship.

_____

Eve Singleton

31/07/2020

ACKNOWLEDGEMENTS

First and foremost, I would like to thank my principal supervisor Dr. Mohammed Alsharifi. Thank you for giving me the opportunity to undertake my PhD in your lab and for all of your support since I first came to your lab as an undergraduate student. I am grateful for all of time that you have spent discussing and debating science and ideas with me. Thank you for introducing me to the wide world of gamma radiation.

Secondly, I would like to thank my co-supervisors Dr. Justin Davies, Dr. Farhid Hemmatzadeh and A/Prof. Michael Beard. Thank you for your advice and assistance. In particular I would like to thank Justin for your invaluable assistance in methods of modelling sterility and Farhid for all of your help and advice regarding Newcastle disease virus.

Importantly, I would like to thank all the past and present members of the Alsharifi lab. In particular, I would like to thank Shannon David, Zoe Laan and Chloe Gates. Thank you all for your friendship and support, and for making my time in the lab so enjoyable. I would especially like to thank Shannon for all of times that you have provided training and encouragement throughout my entire time in the Alsharifi lab. I would have been lost without you.

I would also like to extend my thanks to Prof. Shaun McColl and Dr. Iain Comerford for your advice and assistance in experimental designs, and for providing reagents. I would also like to thank Jade Foeng and Todd Norton for your invaluable help and advice in setting up and monitoring tumour models in mice. A special thank you to Jade and Chloe for helping with tumour harvesting and flow cytometry.

I would also like to thank my friends and family for all your encouragement and support during my PhD. Thank you for both helping me to stay positive and providing welcome distractions. Thank you to Piper, for always making me smile.

Finally, I would like to especially thank Ryan. Thank you for your unwavering love, support and belief in me. I am truly grateful, and I honestly could not have done this without you.

PATENTS, PRESENTATIONS AND PUBLICATIONS ARISING FROM THIS THESIS

PATENTS		
Title	**Inventors**	**Status**
Gamma-irradiated NDV as an oncolytic virotherapy	**Eve Singleton**, Mohammed Alsharifi, Shaun McColl, Farhid Hemmatzedah.	Provisional application being prepared for submission.

CONFERENCE PRESENTATIONS		
Type	**Title**	**Meeting**
Poster Presentation	The development of a combined gamma-irradiated vaccine against Newcastle disease virus and influenza A virus	11th Annual Postgraduate Symposium, University of Adelaide, South Australia, July 2018
Oral Presentation	Developing a Newcastle disease virus vaccine *Winner: Best Student Talk*	12th Annual Postgraduate Symposium, University of Adelaide, South Australia, July 2019
Poster Presentation	Optimising irradiation conditions to ensure sterility and immunogenicity of whole inactivated virus vaccines.	Australasian Virology Society (AVS-10), Queenstown, New Zealand, December 2019
Oral Presentation	Gamma irradiated vaccines: concepts and applications. *Presented by Dr. Mohammed Alsharifi*	ANSTO User Meeting 2019, Sydney, New South Wales, December 2019
Poster Presentation	Optimising irradiation conditions to ensure sterility and immunogenicity of whole inactivated virus vaccines.	Australian and New Zealand Society for Immunology (ASI-48), Adelaide, South Australia, December 2019

PUBLICATIONS	
Thesis Chapter	**Title & Publication Status**
Chapter 2	**Singleton, EV**., David, SC., Davies, JB., Hirst, TR., Paton, JC., Beard, MR., Hemmatzadeh, F., Alsharifi, M. (2020). 'Sterility of gamma-irradiated pathogens: a new formula to calculate sterilising doses', *Journal of Radiation Research*, **Accepted with minor revisions**

CONTRIBUTION TO PUBLICATIONS
David, SC., Norton, T., Tyllis, T., Wilson, JJ., **Singleton, EV**., Laan, Z., Davies, J., Hirst, TR., Comerford, I., McColl, SR., Paton, JC., & Alsharifi, M. (2019). 'Direct interaction of whole-inactivated influenza A and pneumococcal vaccines enhances influenza-specific immunity'. *Nature microbiology*, *4*(8), 1316–1327.
Shahrudin, S., Chen, C., David, SC., **Singleton, EV**., Davies, J., Kirkwood, CD., Hirst, TR., Beard, M., & Alsharifi, M. (2018). Gamma-irradiated rotavirus: A possible whole virus inactivated vaccine. *PloS one*, *13*(6), e0198182.

ABSTRACT

Gamma (γ)-radiation is a method commonly applied to sterilise pathogens in the biomedical, food and pharmaceutical industries. γ-radiation inactivates pathogens by causing irreparable damage to genomes to prevent replication. However, proteins and other antigenic structures are left mostly intact. In recent years there has been increasing advocacy for highly immunogenic γ-irradiated vaccines, several of which are currently in clinical or pre-clinical trials. Importantly, various methods of mathematical modelling and sterility testing are employed to ensure the safety of a given preparation. However, these methods are designed for materials with a low bioburden, such as food and pharmaceuticals. Consequently, current methods may not be reliable or applicable to estimate the irradiation dose required to sterilise microbiological preparations for vaccine purposes, where bioburden is deliberately high. In this study, I investigated different methods of modelling sterility and developed a new formula for calculating sterilising doses that is highly applicable to viruses and bacteria.

Our research group has developed a whole-inactivated influenza A virus (IAV) vaccine using γ-radiation (γ-Flu). IAV presents a constant pandemic threat due to the mutagenic nature of the virus and the inadequacy of current vaccines to protect against emerging strains. Previous research has demonstrated the ability of γ-Flu to protect against not only vaccine-included strains but emerging strains as well. In this study, I compared γ-Flu irradiated at different temperatures and doses to meet internationally accepted sterility assurance levels. I found that, when using sterilising doses, the structural integrity and vaccine efficacy was well maintained regardless of irradiation temperature. In fact, using a higher temperature and lower radiation dose induced higher neutralising antibody responses and more effective cytotoxic T cell responses. These data provided new insights into optimal irradiation conditions as previously using frozen irradiation was considered the superior irradiation temperature.

These concepts related to preparing γ-irradiated vaccines were applied to the development of a novel vaccine against Newcastle disease virus (NDV). NDV is an important poultry pathogen that is associated with widespread livestock losses and a large economic burden. Current vaccines are available but have limited efficacy so there exists a need for alternative NDV vaccines. In this study, NDV was inactivated by γ-irradiation and structural integrity

was tested. I found overall virion structure and protein function of γ-NDV to be well maintained, however surprisingly I did not detect neutralising antibody responses after treatment in mice. Interestingly, previous studies from our group have demonstrated the ability of γ-Flu to adjuvant other γ-irradiated vaccines. In the current study, I expanded on the broader applicability of γ-Flu as an adjuvant by showing that γ-Flu can adjuvant the poorly immunogenic keyhole limpet hemocyanin. However, γ-Flu and other commonly used adjuvants were unable to enhance neutralising antibody responses to NDV. Overall, these data suggest that γ-irradiation may not be a suitable inactivation method for NDV vaccine development.

NDV is used as an oncolytic virus and many clinical trials have demonstrated the ability of NDV to treat a range of different cancers. However, research with NDV is hindered by the biosecurity risk associated with live NDV. Given the high structural integrity and protein function of γ-NDV, I hypothesised that γ-NDV could be used as an alternative cancer treatment. Importantly, γ-NDV retained its ability to kill a range of different cancer cells in vitro. This suggests that γ-NDV can be used as a broadly applicable therapeutic agent. Furthermore, I tested γ-NDV in a murine melanoma model and found that γ-NDV was able to reduce tumour growth and enhance overall survival.

CHAPTER 1

Literature Review

CHAPTER 1: LITERATURE REVIEW

Gamma (γ)-irradiation is a widely applicable sterilisation technique used in food, medical and pharmaceutical industries. Importantly, γ-radiation has been investigated as a method to inactivate pathogens for vaccine purposes. This project addressed key scientific questions related to the current mathematical modelling to calculate the radiation dose required to achieve the internationally accepted sterility assurance level (SAL) of irradiated materials, as well as investigating the immunogenicity of whole-inactivated influenza A virus (IAV) and Newcastle disease virus (NDV) vaccines. IAV and NDV are important respiratory pathogens and current vaccines for both viruses face major shortcomings. In humans, IAV is responsible for high morbidity and mortality worldwide and, in domestic poultry, IAV and NDV account for widespread livestock losses and an excessive economic burden. Importantly, previous investigations have illustrated the ability of γ-irradiated IAV (γ-Flu) to induce cross-protective immunity as well as providing adjuvant activity to co-administered whole inactivated viruses and bacteria. On the other hand, current NDV vaccines have limited efficacy against newly emerging strains and there is a clear need for better vaccines. In addition, NDV has been reported to have oncolytic activity, but the clinical use of NDV as an effective oncolytic virotherapy has been restricted due to associated biosecurity concerns.

Overall, this project investigated the effect of irradiation conditions on the immunogenicity of γ-Flu and investigated the immunogenicity of a novel γ-irradiated NDV vaccine (γ-NDV). I also addressed the possibility of co-administering γ-Flu and γ-NDV for enhanced immunogenicity. Finally, I examined the possibility of utilising γ-NDV as an oncolytic virotherapy.

1.1 GAMMA RADIATION

γ-radiation is a form of ionising radiation, and γ-rays are high frequency photons generated by the decay of radioisotopes. The most common source is Cobalt-60 (^{60}Co), which is degraded into non-radioactive Nickel (^{60}Ni), however Caesium-137 (^{137}Cs) is also used. ^{60}Co is preferred as the resulting γ-rays have higher energy and are consequently more penetrating. The breakdown of a ^{60}Co to ^{60}Ni results in the emission of an electron of 0.31 MeV and production of two γ-rays of 1.17 MeV and 1.33 MeV, whereas the breakdown of

^{137}Cs to Barium-137 only produces a single γ-ray of 0.6617 MeV. In this thesis I have used γ-rays from a ^{60}Co source to target pathogens of interest for irrevocable inactivation.

Pathogens can be inactivated by γ-radiation in two ways. Firstly, when γ-rays are absorbed they have the ability to ionise molecules by ejecting electrons. If the γ-ray interacts with an inner shell electron then an outer shell electron will drop into the inner shell, leaving the molecule ionised. Alternatively, the γ-ray can interact with and eject an outer shell electron, also resulting in ionisation. If this occurs within the nucleic acid, then the resulting ionisation causes cross-linking and breaks in genomes [1-4]. This is known as the direct effects of γ-irradiation. Direct radiation damage also occurs in proteins, but to a lesser extent as the overall protein structure is less sensitive to a single molecule becoming ionised when compared to nucleic acids.

The second mechanism of damage is through indirect effects of γ-irradiation. The ejected electrons can interact with water and oxygen molecules to generate reactive oxygen species (ROS). ROS cause further genome and protein damage [5]. Most protein damage occurs through direct effects [5]. Radiation-induced ROS include hydroxyl radicals ($OH^{\bullet}$), superoxide ($O_2^{\bullet-}$), and organic radicals ($R^{\bullet}$). It is estimated that up to 80% of indirect genome damage is caused by $OH^{\bullet}$, as dimethyl sulphoxide significantly reduces damage [6]. ROS also cause substantial damage to secondary protein structures and can lead to fragmentation of polypeptide chains and aggregation [7]. Oxidative damage to proteins can be catalysed by metal ions Fe and Cu, and can disproportionately occur in metal ion binding sites of proteins [8]. In particular, the amino acids lysine, histidine, proline and arginine appear to be most susceptible to oxidative damage [9].

1.1.1 Radiosensitivity

Radiosensitivity of a pathogen can be influenced by multiple factors including genome structure [10, 11], irradiation temperature [12-14], water [5] and oxygen levels [15, 16], and the presence of free-radical scavengers [17]. Radiosensitivity varies greatly between pathogen type and irradiation conditions. These conditions can be grouped into internal and external factors.

Internal factors cannot be changed experimentally and are inherent to the pathogen being sterilised. Genome size and structure are the most prominent internal factors. Resistance to γ-irradiation is inversely related to genome size [10, 18, 19]. A pathogen with a larger genome has an increased chance of an ionisation event occurring. Accordingly, the sterilising doses for viruses are usually higher than the sterilising doses required for bacteria, as viruses have considerably smaller genomes [20]. Furthermore, viruses with larger genomes are more susceptible to γ-radiation than viruses with smaller genomes [11]. In addition, it is hypothesised that viruses with more complex genomes are more radioresistant than viruses with simple genome structures [11, 18, 21, 22], as a virus with a double-stranded or segmented genome may require an ionisation event at each strand or segment to prevent non-damaged segments from re-assorting within a host cell upon co-infection with multiple partially-inactivated virions.

Extrinsic factors can be altered experimentally and influence the indirect effects of γ-irradiation, specifically the production and movement of ROS. The easiest condition to manipulate is irradiation temperature. Higher temperatures increase sensitivity to radiation [12-14], as at higher temperatures there is greater water availability and more movement of free radicals. We have previously shown that increased structural damage occurs when IAV is irradiated at higher temperatures [23]. In contrast, irradiation of frozen samples maintains the highest level of structural integrity [11, 24] and therefore frozen irradiation is most commonly used for sterilisation for vaccine and research purposes.

Oxygen and water availability is directly linked to the production of ROS. The presence of oxygen increases the amount of genome damage when irradiating bacteriophage T7 [25], and increases radiosensitivity [26]. Similarly, freeze-dried materials (i.e. low water availability) are more resistant to irradiation [27]. In fact, bacterial spores are considered to be highly radioresistant due to low water availability [28]. Various free radical scavengers can also enhance radioresistance and protect against protein damage. In particular, foetal bovine serum (FBS) [17, 29], manganese [30], ascorbic acid [31], glycerol [32] and N-acetyl-L-cysteine [33] have all demonstrated enhanced radioresistance when used as an excipient. The highly radioresistant bacteria *Deinococcus radiodurans* utilises manganese as one of its many resistance mechanisms [30, 34].

1.1.2 Calculating sterilising doses

The radiosensitivity of a pathogen is measured by the decimal reduction dose (D_{10}), the dose of γ-radiation required for a 1-log reduction in virus titre (i.e. a 90% reduction in infectivity). For vaccine purposes and sterilisation, the sterility assurance level (SAL) should also be considered. The SAL is an arbitrary value used to calculate sterility to a given probability. The International Atomic Energy Agency (IAEA) recommends a SAL of 10^{-6} for products intended to come into contact with compromised tissue [35]. This means that there is a one in a million chance of a single infectious particle remaining following irradiation [36]. Therefore, the required irradiation dose to give a theoretical titre of 10^{-6} infectious units in a given volume is calculated and referred to as the sterilising dose (DS). The following formula is generally used:

$$DS_{SAL} = n \times D_{10}$$

Where n is the number of $\log_{10}$ reductions required to reach a theoretical titre of 10^{-6} infectious units in a given volume, usually 1mL. Alternatively, sterilising doses can be calculated based on a standard distribution of resistance (SDR). This is based on recommendations from the International Organization for Standardization (ISO) [37]. The SDR is calculated based on a D_{10} of between 2-3 kGy. However, this is not appropriate for viruses or radioresistant pathogens that can have D_{10} values far greater than 3 kGy.

Inactivation curves are generated as a measure of sterility and can either follow one-hit or multiple-hit kinetics. One-hit, or first order, kinetics are log linear and occur where the increase in radiation dose is directly proportionate to the loss of pathogen titre. Multiple-hit kinetics are non-linear and include a shoulder of resistance where radiation damage accumulates before a significant loss of infectious titre is observed. Importantly, the existing methods of calculating DS can only be applied to pathogens displaying single-hit inactivation kinetics. Pathogens with repair mechanisms tend to have multiple hit inactivation curves and consequently the DS could be underestimated if it is calculated based on linear inactivation alone without accounting for the shoulder of resistance.

Miscalculation of the DS can have serious consequences. Most notably, this may have occurred when the US Department of Defense (DoD) inadvertently shipped live *Bacillis anthracis*, or anthrax, spores to 86 facilities over a period of 10 years [38]. Anthrax spores were irradiated at 50 kGy while frozen on dry ice. Reported D_{10} values for *B. anthracis* are

typically between 1.53 kGy and 3.35 kGy [39] for irradiation at room temperature, however frozen samples may have a considerably higher D_{10} values. Importantly, the DoD reported *B. anthracis* titres of up to 10^{12} CFU/mL [38] and consequently 50 kGy should never have been considered an appropriate sterilising dose. Given an *n* of 18 (to reduce titre from 10^{12} CFU/mL to a theoretical 10^{-6} CFU/mL) and a possible estimated D_{10} of 3.35 kGy, the substantiated DS should be a minimum of 60.3 kGy (3.35 kGy × 18 required $\log_{10}$ reduction). The inadvertent shipment of live anthrax spores by the DoD highlights an important gap in calculating sterilising doses. In fact, current methods are based on sterilising medical equipment and other healthcare products where the expected bioburden is relatively low [35, 37, 40]. Furthermore, current methods do not account for non-linear inactivation curves. In order to safely inactivate high titre and potentially radioresistant pathogens for research or vaccine purposes, new mathematical modelling methods must be developed. Mathematical modelling of inactivation has been addressed in **Chapter 2** of this thesis.

1.1.3 The effect of irradiation on structural integrity

Gamma-irradiation is widely used to sterilise materials in a variety of settings. It is used in food [41], pharmaceutical [42] and medical industries [43, 44] due to the ability of γ-radiation to inactivate pathogens through nucleic acid damage, while leaving proteins and other structures largely intact.

Sterilisation of bone and soft tissue allografts illustrates the clinical application of structurally intact γ-irradiated products. A major concern with tissue allografts is the potential for infectious agents to be transferred from donors to recipients. A study testing muscoskeletal tissue from cadaveric donors found the presence of 20 different organisms including *Pseudomonas aeruginosa* and *Klebsiella oxytoca* [45], both of which have the potential to cause disease in humans. There have also been recorded instances of viral transmission following allograft donation including hepatitis B virus (HBV), hepatitis C virus (HCV), and human immunodeficiency virus (HIV) [46, 47]. To overcome this, tissues allografts are often sterilised by γ-irradiation prior to transplantation. The standard radiation dose as suggested by the IAEA for bone allografts is 25 kGy [48]. This dose is based on the D_{10} values and bioburdens of typical contaminating species. It has been reported that γ-radiation maintains the structure of collagen better than other inactivation

methods, without causing toxicity [49-51], particularly when irradiating allografts while frozen to reduce oxidative damage [52].

In addition, γ-radiation is used in pharmaceutical settings, particularly when protein function is required after inactivation. For example, treatment of severe haemophilia requires the transfer of blood plasma or clotting factors, however this is associated with a risk of transmission of infectious viruses [53]. A study found that γ-radiation can successfully be used to inactivate HIV while having minimal effect on important coagulation factors [54]. Notably, the function of antibodies has also been demonstrated following γ-irradiation of serum [55], including a study that involves irradiation of serum collected during a clinical trial for an Ebola virus vaccine to ensure safety [56].

In order to ensure the sterility of food products, γ-radiation can also be utilised. In this setting, γ-radiation is typically be used to target food-borne pathogens such as *Escherichia coli* and *Salmonella* species. γ-irradiation does not appear to have a significant impact on taste. In fact, individuals could not differentiate between irradiated and non-irradiated trout shortly after irradiation, and after prolonged storage the taste of irradiated trout was scored higher than non-irradiated trout [57]. Other studies have also demonstrated acceptable taste of irradiated food [58, 59]. Interestingly, irradiating food allergens appears to be associated with reduced allergic reactions, suggesting epitope changes sufficient to affect IgE binding, however high doses of irradiation at ambient temperatures were required to sufficiently reduce IgE binding [60, 61].

1.1.4 γ-irradiated vaccines

γ-radiation has been has been proposed as a safe an effective method for vaccine development as it can inactivate a wide range of pathogens while maintaining structural integrity [62-64]. Several groups have demonstrated the superiority of γ-irradiation to traditional methods of vaccine inactivation, including formalin and β-propiolactone [65, 66]. Importantly, previous publications from our research group reported the development of cross-reactive γ-irradiated vaccines against influenza A virus (IAV) [66-69] and *Streptococcus pneumoniae* [70, 71]. In addition, γ-irradiated vaccines against HIV [72], and Malaria [73, 74] are currently in clinical trials, and other pathogens including

Mycobacterium spp. [75, 76], *Salmonella typhimurium* [77, 78] and *Brucella* spp. [79]. Our γ-irradiated IAV vaccine, γ-Flu, is further discussed in **Section 1.2.8**.

1.2 INFLUENZA A VIRUS

1.2.1 Overview

Influenza A virus (IAV) is a highly infectious respiratory virus from the family *Orthomyxoviridae*. IAV can cause infection in a range of host species, with infection in humans, birds and pigs being most prominent. In humans, there are between 3 and 5 million cases every year, and between 250,000 and 500,000 deaths [80]. These deaths occur most often in at-risk individuals including infants and the elderly, immunocompromised and pregnant women [81]. In humans, IAV causes a range of respiratory symptoms including coughing, sneezing, fever, vomiting and muscle aches. In birds, IAV infection can be asymptomatic or quite mild, or can cause severe illness. Symptoms can be respiratory or systemic and are demonstrated by coughing and sneezing, diarrhoea, ruffled feathers, swelling of the head and eyes and other symptoms.

There is a high economic burden associated with IAV infection due to hospitalisations and absenteeism. In Australia, the financial burden of IAV is approximately $85 million a year [82]. Antivirals are available and can reduce the severity and length of infection but need to be administered within a few days from the first onset of symptoms to be effective. While vaccination is the most effective strategy in reducing seasonal influenza infections, current vaccines only protect against strains included in the vaccine formulation and thus offer no pandemic protection. There have been four recorded IAV pandemics; 1918 Spanish flu, 1957 Asian flu, 1968 Hong Kong flu and 2009 Swine flu. In fact, there is a constant risk that novel IAV subtypes could cross the species barrier and infect humans, causing a new pandemic. This creates a need for a universal IAV vaccine to cover new and emerging strains.

1.2.2 Structure

IAV is an enveloped virus that is usually spherical and between 80-120nm in size, however human isolates can also be filamentous and over 30μm in length [83]. In fact, filamentous IAV may have a selective advantage in human infections [84]. IAV has a negative sense

single-stranded (ss) RNA genome that is made up of 8 segments. Each segment is packaged with nucleoprotein (NP) to form viral ribonucleoprotein (vRNP). The vRNP is arranged with 7 segments surrounding a central segment [85]. This arrangement occurs due to complementary RNA sequences between the segments of vRNP [86]. An RNA-dependent RNA polymerase made up of polymerase basic proteins 1 and 2 (PB1 & PB2) and polymerase acid protein (PA) is also packaged with each vRNP. The surface proteins of IAV are the receptor binding trimeric protein haemagglutinin (HA), sialic acid cleavage tetrameric protein neuraminidase (NA), and an ion channel (M2). HA is the most abundant surface protein, followed by NA then M2 [87]. Matrix protein (M1) provides support for the envelope. The virus also encodes non-structural proteins 1 and 2 (NS1 and NS2). The virion structure of IAV is shown in **Figure 1.1**.

IAV is classified into antigenically different subtypes based on the envelope proteins HA and NA. There are currently 18 known types of HA and 11 known types of NA [88]. Novel subtypes are identified through immunodiffusion and haemagglutination inhibition assays where antibodies specific to one subtype are unable to neutralise the novel subtype [89]. There are many possible combinations of HA and NA with H1N1 and H3N2 subtypes currently circulating in humans.

1.2.3 Replication

The IAV replication cycle is shown in **Figure 1.2**. IAV infects epithelial cells of the respiratory tract. The virus HA binds to sialic acid (SA)-linked galactose receptors. Human IAV strains bind preferentially to α2,6-linked sialic acid (SAα2,6Gal) receptors, whereas avian IAV bind preferentially to α2,3-linked sialic acids (SAα2,3Gal). In humans, SAα2,6Gal receptors are predominantly found in the upper respiratory tract, whereas the SAα2,3Gal receptors are found in the lower respiratory tract [90, 91]. Thus, avian strains do not transmit readily between humans as virions must travel deep into the respiratory tract to find cells permissible to replication and must then be expelled to infect other humans. However, disease is much more severe due to proximity to the lungs and an increased risk of causing lung damage.

Host trypsin-like proteases found in the respiratory tract activate the HA by cleavage from HA_0 to HA_1 and HA_2 subunits. Once the HA has attached to a host receptor the virus enters

the cell by receptor-mediated endocytosis. The low pH within the endosome causes a conformational change to expose the fusion peptide of HA_2. The fusion stalk inserts into the endosomal membrane and fuses the membrane and the viral envelope. The M2 ion channel is opened and an influx of protons and potassium ions cause the vRNP to dissociate from M1 [92] and vRNP is released into the cytoplasm. The vRNP contains nuclear localisation signals (NLS), which traffic the vRNP into the host cell nucleus [93, 94]. The virus polymerase complex, included in the vRNP, facilitates replication of the negative sense RNA. The complex produces messenger RNA that is exported from the nucleus to the cytoplasm where the viral proteins are transcribed. Within the nucleus, template positive sense RNA is used to produce more genome copies. New virions assemble at the cell membrane and are release by budding. NA cleaves the budding virions from the cell-surface sialic acids.

1.2.4 Antigenic variation

Changes to the surface antigens HA and NA enable IAV to evade adaptive immune responses and to target new species. This variation can occur by antigenic drift or antigenic shift.

Antigenic drift occurs constantly due to the low fidelity of the RNA polymerase. This introduces point mutations at a rate of approximately 1 mutation per replicated genome [95]. Mutations tend to occur in a few key antigenic sites [96]. The accumulation of these mutations leads to changes in the surface epitopes such that antibodies induced by prior infections bind less effectively and consequently leads to the rise of new IAV strains [97, 98]. In general, this reduces the efficacy of pre-existing immunity whether obtained through vaccination or a previous infection. Mutations within the receptor binding site of the HA can also influence receptor binding. A single amino acid mutation has the potential to shift receptor binding specificity from one species to another [99, 100].

Antigenic shift is considered to be quite rare. However, several times per century novel strains will arise through antigenic shift that are capable of infecting humans [101]. Antigenic shift occurs when a single cell is infected with different subtypes of IAV, potentially from different species [102, 103]. When the genome is packaged, segments from different subtypes can be incorporated into a single virion. This can result in novel HA and NA combinations that may not have been circulating in humans previously. Lack

of pre-existing immunity and human-to-human transmission of newly arising IAV strains has been associated with pandemics.

1.2.5 IAV pandemics

There have been four IAV pandemics in recent history; 1918 Spanish Flu, 1957 Asian Flu, 1968 Hong Kong Flu and the 2009 Swine Flu pandemic. Spanish Flu was caused by an H1N1 strain that is believed to be entirely avian in origin [103, 104]. During the 1918-1920 pandemic it was estimated that a third of the world's population were infected [105], and between 50-100 million people died [106], approximately 3-5% of the global population at the time. Spanish Flu was particularly virulent with a mortality rate of 2.5% compared to approximately 0.1% in a usual flu season [107, 108]. The high mortality rates could be related to secondary bacterial infections that occurred in up to 95% of Spanish flu deaths [109]. The most common bacteria isolated from Spanish Flu samples were *Streptococcus* species and *Haemophilus influenzae* [109-111]. Bacterial pneumonia as a secondary infection to IAV is associated with more severe disease and higher mortality rates [112-114], and could explain the pathogenicity of Spanish Flu. Especially when considering that antibiotics had not yet been discovered [115]. Spanish Flu also was disproportionately lethal in 20-40 year olds [116]. This is speculated to be due to a cytokine storm [117], as this age group is usually most likely to survive infection with IAV [80]. In support of this hypothesis, researchers have reverse engineered 1918 H1N1 and found that it causes severe cytokine responses and enhanced lethality in animal models [117-120].

The 1957 IAV pandemic was caused by an H2N2 strain. Initial reports of a novel respiratory disease begun in early 1957 in China and the infection spread around the world over the next few months. The disease was confirmed to be caused by IAV; however, surface molecules were different from circulating H1N1, and the strain was designated H2N2. A vaccine was quickly developed, a feat largely accredited to Maurice Hilleman [121]. 40 million vaccine doses were prepared in the US prior to the pandemic [122]. This fast-acting response is likely to have significantly reduced fatalities. Overall, the 1957 pandemic resulted in 2 million deaths worldwide, and H2N2 continued to circulate until it was displaced by H3N2 in 1968. The 1968 H3N2 pandemic caused fewer deaths than previous pandemics, approximately 1 million in total. The novel H3N2 subtype contained the NA molecule from previously circulating H2N2 strains [123], and previous NA-specific

immunity may have lessened disease severity [124]. The H3N2 strain appeared to have acquired the HA and PB1 gene segments from an avian IAV [125].

More recently, an influenza pandemic occurred in 2009. The pandemic strain was H1N1 (pdmH1N1), but antigenically differed from the seasonal strains circulating at the time [126]. The origin species was pigs, however most gene segments originally came from avian species [127]. pdmH1N1 was highly contagious and infected between 11% to 21% of the global population [128], however mortality rates were relatively low and the resulting pandemic was no more deadly than a classic flu season [129, 130].

In general, the major concern of future pandemics is the emergence of avian IAV strains. All three IAV pandemics of the 20th century were caused by re-assortment of avian gene segments to give rise to novel IAV strains that had the ability to infect humans. Importantly, in recent years several small outbreaks of avian IAV have occurred. Avian H5N1 was first isolated in humans in 1997 [131] and has since been associated with small sporadic outbreaks with limited transmissibility between humans [132]. In total, there have been 861 cases of H5N1 infection, resulting in 445 deaths [133]. Outbreaks of avian H7N9 and H9N2 have also occurred in recent years, resulting in 1568 and 33 cases, respectively [133]. The high mortality rates associated with avian IAV are concerning, particularly when considering that mutations can occur to increase infectivity of IAV through antigenic shift or antigenic drift. Evidently, a recombinant H5N1 with neuraminidase from seasonal H1N1 has shown enhanced virulence in ferrets [134]. An important feature of next generation IAV vaccines should be the ability to protect against pandemic strains not included in the vaccine formulation.

1.2.6 Immune responses to IAV

1.2.6.1 Innate immune responses

The innate immune response offers a rapid defence against viral infections. In general, it is non-specific and virus infections will be recognised by pattern recognition receptors (PRRs), particularly Toll-like receptors (TLRs) and cytosolic receptors, that interact with pathogen-associated molecular patterns (PAMPs). TLRs are an important class of PRRs that are found on the cell surface or within endosomes. In particular, IAV is recognised by TLR-3 [135], TLR-7 [136, 137] and TLR-8 [138]. TLR-3 recognises dsRNA [139], which

is a replication by-product. This is recognised when dead cells containing the viral dsRNA are phagocytosed [140]. The role of TLR-3 in protection against IAV is contentious. TLR-3 is important for the induction of pro-inflammatory cytokines and reduction of IAV replication in the lungs, however it can also enhance pathogenicity of IAV as *tlr3*$^{-/-}$ mice survive longer than wildtype mice in the case of a lethal infection [135]. TLR-7 and TLR-8 both recognise ssRNA from whole virions that are taken up by host cells into the endosome. TLR-7 is mainly expressed in the endosome of plasmacytoid dendritic cells (pDCs) [141], whereas TLR-8 is found in humans and is mainly expressed in monocytes and macrophages [142]. Activation of TLRs leads to downstream production of pro-inflammatory responses, particularly IFN-I responses.

On the other hand, cytosolic receptors, such as retinoic acid inducible gene I (RIG-I) are expressed by all nucleated cells and are capable of recognising IAV RNA within infected cells [143]. RIG-I is also present in dendritic cells and macrophages [144]. RIG-I specifically recognises 5′-triphosphate viral ssRNA [143, 145]. This results in the activation of mitochondrial antiviral signalling protein (MAVS). MAVS signalling leads to the induction of pro-inflammatory cytokines including nuclear factor κB (NF-κB), Type I Interferon (IFN-I), and other interferon response genes (ISGs). IFN-I, in the context of IAV infection, is predominantly produced by dendritic cells (DCs) and macrophages [146]. DCs play a crucial role as professional antigen presenting cells (APCs) by presenting IAV antigens to T cells [147].

1.2.6.2 Adaptive immune responses

The activation of various factors of the innate immune system leads to the activation and recruitment of the adaptive immune system. Adaptive immunity is long-lived and provides and immunological memory. This is the basis for vaccines. The adaptive immune response is characterised by two arms – humoral and cell-mediated.

Cytotoxic $CD8^+$ T cells (CTLs) are important for IAV immunity. $CD8^+$ T cells are activated by DCs presenting antigens from IAV within the draining lymph nodes [148]. Activated CTLs then migrate to the infected lungs, where they are able to directly kill IAV-infected cells. Infected cells are identified by specific interaction of T cell receptors (TCRs) with IAV antigens presented in the context of Major Histocompatibility Complex Class I proteins (MHC-I). In particular, IAV specific CTLs have been shown to recognise internal

IAV proteins NP [149, 150], M1 and polymerase proteins [151, 152]. As these proteins are highly conserved across IAV strains, T cell responses are vitally important for cross-protective immunity.

The main function of CTLs is to specifically target and kill infected respiratory epithelial cells [153]. The recognition of a peptide presented by MHC-I by the TCR will trigger several mechanisms to induce target cell cytotoxicity including the production of cytotoxic molecules such as granzymes and perforin to induce apoptosis in infected cells [154, 155], secretion of pro-inflammatory cytokines including TNFα [156], and expression of Fas ligand [154]. CTLs play an essential role in preventing the spread of IAV from the upper respiratory tract to the lungs, reducing the severity of infection [157]. In addition, IAV-specific lung-resident $CD8^+$ memory (T_{RM}) cells have been detected after IAV infection [158] or vaccination [159] and they could provide cross-protection against subsequent IAV infections.

The other aspect of cell-mediated immunity is $CD4^+$ T helper (T_H) cells. T_H cells recognise IAV infection through the presentation of IAV peptides in the context of MHC class II (MHC-II) molecules on the surface of antigen presenting cells (APCs). T_H cells are activated similarly to CTLs via DCs in draining lymph nodes [160, 161]. T_H cells then further differentiate based on the type of infection. In responses to an IAV infection, T_H cells differentiate into T_H1 cells [162]. This is mediated by cytokines including IL-12 [163] and IFN-γ [164]. Interestingly, T_H1 cells do not appear to be essential to cell-mediated immunity to IAV as depletion of $CD4^+$ cells or MHC-II does not influence survival, inflammatory responses or CTL responses [165, 166]. Instead, T_H cells appear to play a role in mediating antibody responses [167, 168].

Humoral immunity is characterised by B cells. B cells produce IAV-specific immunoglobulins. IgM is predominantly expressed during a primary or early IAV infection, prior to antibody isotype switching by B cells to produce IgG and IgA antibodies [169]. IgA is the predominant antibody isotype in the respiratory tract [170], however IgG appears to be important for reducing IAV pathogenesis [171]. In general, antibody responses mainly target the surface antigens, HA and NA, with HA-specific antibodies being both more abundant and more effective in preventing IAV infection, provided that

the antibodies match the infecting strain [169]. Anti-NA antibodies are able to prevent dissemination of new virions by blocking the release of budding virions from the host cell [172]. Anti-HA antibodies are typically directed against the variable globular head [98]. These antibodies can be neutralising if the receptor-binding site is blocked [173]. Studies have demonstrated a small subset of antibodies that are specific to the more conserved HA stalk, and can provide some cross-protective immunity [174-176]. Importantly, antibody responses are directed against the highly mutagenic surface proteins. Therefore, IAV specific antibodies are strain specific.

1.2.7 Current IAV vaccines

The currently licenced IAV vaccines in Australia are tri- or tetravalent inactivated vaccines (TIV). The trivalent vaccine includes an H1N1 strain, an H3N2 strain and an influenza B strain, and the tetravalent vaccine includes an additional influenza B strain. In the event of a pandemic, monovalent vaccines can be produced. In general, strains included in the TIV are grown in the allantoic cavity of embryonated chicken eggs, chemically inactivated using β-propiolactone and ether, and HA and NA surface antigens are then purified to be included in the vaccine formulation. These purified antigens are given intramuscularly to induce strong antibody responses. However, due to the mutagenic nature of these surface antigens the antibodies will only protect against strains included in the vaccine formulation. Consequently, the vaccine is re-formulated biannually to align with the northern and southern hemisphere flu seasons. Vaccine formulations are recommended by the World Health Organisation (WHO) based on the strains expected to be circulating. The timeframe to produce seasonal vaccines is approximately 6 months, and if unexpected strains emerge in this time then vaccine efficacy is considerably reduced [177].

In 2014 the seasonal vaccine capacity was estimated at 1.5 billion doses/year due to limited capacity in eggs [178], and in 2009 the WHO claimed that production could be increased to 4.9 billion doses of swine flu vaccine [179]. However, there was a delay in production time for the 2009 swine flu vaccine due to the low growth of the vaccine strain in embryonated chicken eggs [180]. In addition, it has been reported that the use of embryonated eggs could induce mutations to allow egg adaptation, reducing vaccine efficacy [181]. Therefore, the use of tissue culture-based methods could be used as an alternative. Importantly, despite their efficacy, the main limitation of the TIV is the inability

to provide protection against non-vaccine strains, which include seasonal as well newly emerging pandemic strains. Therefore, the development of a universal IAV vaccine is fundamentally important to human health.

1.2.8 γ-irradiated influenza vaccine

Our group has previously developed a whole-inactivated γ-irradiated IAV vaccine (γ-Flu). This vaccine involves growing IAV in embryonated chicken eggs, purifying and concentrating virus and subjecting the virus to sterilising γ-radiation while preparations are frozen on dry ice. This method of vaccine production is applicable to any IAV subtype and previous γ-Flu preparations have included H3N2 [66] and H1N1 [68] strains. Importantly, γ-Flu is able to provide cross-protective immunity [66], overcoming a major limitation of current IAV vaccines. γ-Flu prepared with an H1N1 strain was shown to protect mice against a lethal dose of avian H5N1 [68] and pdmH1N1 [182]. Previous investigations illustrated the ability of γ-Flu to induce both antibody and T cell responses [183], with particular emphasis on the cross-protective T cell responses [184, 185]. This was demonstrated experimentally in mice by the ability of adoptively transferred T cells to provide protection against a heterotypic challenge whereas mice receiving adoptive B cells were not protected [185]

Considering that γ-Flu remains structurally intact, the virus may be able to enter cells and mimic infection in terms of innate immunity and MHC-I antigen presentation [66], thus inducing stronger immune responses. This is further supported by the efficacy of different immunisation routes of γ-Flu. When given intranasally, the natural infection route, the vaccine was significantly more effective than when administered by other routes including intravenous, intraperitoneally and subcutaneously [68]. Furthermore, when comparing γ-Flu to other methods of inactivation including formalin and UV-radiation, γ-Flu provides superior protection [66].

1.2.9 Vaccine adjuvants

Vaccine preparations are commonly administered with vaccine adjuvants to elicit a stronger immune response. Adjuvants are particularly useful when considering inactivated vaccines, as innate immunity may be weaker than in live attenuated vaccines or natural

infection. Most adjuvants augment adaptive immunity through enhanced innate immune responses [186, 187]. There are several adjuvants approved for use in humans. Aluminium hydroxide salts (Alum) has been used in humans since 1932, and was the only licenced adjuvant for human vaccines for almost 70 years [188]. Alum acts as an antigen depot [189], and recruits an influx of important immune cells including DCs [190], macrophages [191] and neutrophils [192]. More recently, oil-in-water adjuvants have been approved for use in humans. Of particular interest, MF59 is an oil-in-water adjuvant currently used with inactivated IAV vaccines. [193]. Vaccines adjuvanted with MF59 produce strong antibody responses [194], and enhance differentiation [195] and antigen uptake by DCs [196].

1.2.10 Use of γ-Flu as a vaccine adjuvant

γ-Flu is a strong inducer of type I interferon responses [69]. IFN-I can stimulate the immune system and enhance responses to a given pathogen [197] and is an important component of anti-viral innate immunity [198]. This suggests that, unlike other inactivated vaccines, γ-Flu could be self-adjuvanting. Interestingly, γ-Flu has been shown to act as an adjuvant to enhance the immunogenicity of co-administered γ-irradiated vaccines. It has been reported previously that SFV-specific IgG responses and SFV-specific neutralising antibody responses were enhanced following co-administration of γ-Flu and γ-SFV in comparison to administration of γ-SFV alone [199]. This phenomenon does not appear to be limited to viral vaccines, as γ-Flu can also adjuvant γ-PN [200]. Co-administration of γ-Flu and γ-PN has been associated with enhanced antibody responses, T_H1 cells, T_H17 cells and memory $CD4^+$ cells in contrast to administration of γ-PN alone [200]. Interestingly, co-administration of γ-Flu and γ-PN has also been reported to be associated with a synergistic enhancement of IAV-specific responses [182]. In particular, γ-PN enhances IAV-specific memory responses and uptake into macrophages for antigen presentation [182] through direct interactions between IAV and *S. pneumoniae* [182, 201]. Importantly the adjuvant activity of γ-Flu appears to be functional across several different immunisation routes as both intravenous (γ-SFV) and intranasal (γ-PN) routes were tested. Consequently, γ-Flu may be widely applicable to adjuvant other vaccines to respiratory pathogens. In this study, I tested the ability of γ-Flu to enhance the immunogenicity of recombinant proteins and investigated the possibility of combining γ-Flu with γ-irradiated Newcastle Disease Virus (γ-NDV).

1.3 NEWCASTLE DISEASE VIRUS

1.3.1 Overview

Newcastle disease virus (NDV), also known as avian paramyxovirus 1 (APMV-1), is an avian respiratory virus from the family *Paramyxoviridae* and is the causative agent of Newcastle disease. There are 9 serotypes of APMV but NDV is the most important serotype as the other 8 serotypes (APMV-2 to APMV-9) induce only mild or asymptomatic infection in birds. NDV was first isolated in Newcastle-upon-Tyne, England [202] and Indonesia [203] in 1926-27. NDV mainly infects domestic poultry. In chickens, NDV can cause a range of respiratory and neurological symptoms including coughing, gasping, twisted head or neck, muscle spasms, decrease in egg quality, and swelling around the eyes and neck. There is no treatment for NDV, and infected chickens must be culled to prevent spread to the rest of the flock. Worldwide, NDV is the third highest cause of infectious disease related death in poultry, behind avian influenza and infectious bronchitis [204]. Several outbreaks have occurred in Australia in recent years and therefore a strict vaccination regime is adhered to. Mice can also be experimentally infected with NDV [205], allowing *in vivo* vaccine testing prior to progressing to avian models.

1.3.2 Structure and classification

NDV virion structure is shown in **Figure 1.3A**. NDV has a large (15.2kb) single-stranded RNA genome, and some virions carry two or more copies [206]. It is an enveloped virus with the surface proteins haemagglutinin-neuraminidase (HN), fusion protein (F), and a small hydrophobic protein (SH). The virus also carries an RNA dependent RNA polymerase (or L protein). The F protein is a determinant of virulence [207]. F proteins with polybasic cleavage sites enhance NDV virus pathogenicity as the F protein is more widely activated [208].

Strains of NDV are grouped according to their virulence. These groups are asymptomatic, lentogenic (low virulence), mesogenic (medium virulence) and velogenic (highly virulent) [209]. Lentogenic strains cause mild respiratory diseases and does not cause any mortality. Mesogenic strains cause acute respiratory disease and mortality rates are less than 10%. Velogenic strains can be further classified into respiratory and neurotropic disease, and mortality rates can reach close to 100% in some instances. There is only one NDV serotype,

and classification of NDV strains was recently restructured in 2019 according to phylogenetic analysis of the F protein [210]. Accordingly, NDV strains are separated into Class I and Class II. Class I strains are made up of a single genotype; Genotype I (GI) and includes strains isolated from wild birds. Class I strains are typically of low virulence [211]. Class II strains are further classified into Genotypes II to XXI (GII to GXXI) [210] and includes highly virulent strains that infect both wild birds and domestic poultry [212]. Recent NDV outbreaks have been caused by GII and GVII [213, 214].

1.3.3 Replication

The replication cycle of NDV is shown in **Figure 1.3B**. NDV infects cells of the respiratory or gastrointestinal tract in chickens [215]. Neurotropic NDV is also able to infect cells of the central nervous system, including neurons [216] and glial cells [217]. NDV can also infect macrophages [218] and lymphocytes [219] in chickens. Host receptors for NDV are sialic acids [220], and entry into the host cell is facilitated by HN and F proteins. HN binds to sialic acid moieties and F enables fusion between the host cell membrane and the virus envelope to allow release of the viral genome into the cell cytoplasm. NDV can also enter host cells independently of F protein at an acidic pH [221]. During virus entry the NDV surface antigens remain on the surface of the infected cell. Cell surface HN can then bind to receptors on neighbouring cells and cell-to-cell fusion can occur. This can lead to the formation of syncytia, multinucleated cells.

NDV genome replication occurs in the cell cytoplasm. For NDV to be able to replicate, the genome must contain a number of nucleotides that is divisible by 6 (i.e. 6n + 0 nucleotides long) [222], known as the “rule-of-six”. This feature is common to *paramyxoviruses* [223] and occurs because each NP subunit is exactly 6 nucleotides long [224]. The proper enclosure of the viral RNA within the NP is required for the recruitment of viral polymerase proteins [225]. mRNA templates are produced, and protein synthesis occurs in the cytoplasm and proteins are then transported to the cell membrane. Virus genome replication to produce copies of the negative-sense single stranded genome also occurs within the cytoplasm. New virions bud from the cell membrane and are released by the neuraminidase function of HN.

1.3.4 Immune responses to NDV

Initial responses to NDV infection are fast-acting non-specific innate responses. In chickens, NDV will induce several anti-viral signalling molecules including nitric oxide (NO), IFN-γ and chicken homologues of IFN-α and IFN-β [226-229]. Similarly, in mouse models NDV is a strong inducer of Type I IFN responses (IFN-I) [230, 231]. The V protein of NDV acts as an IFN-suppressor [232] and can supress apoptosis in infected cells [233]. However, V protein is highly species-specific and has limited function in mammalian cells [234]. The innate immune response plays an important role in priming the adaptive immune response.

Infection of chickens and mice with NDV induces both antibody [205, 235] and T cell responses [235, 236]. However, chickens lacking antibody responses do not survive a challenge with virulent NDV, whereas chickens lacking T cells do [237]. This suggests that antibody responses are sufficient for survival from NDV infection, whereas T cell responses are limited in their ability to provide protection. Considering that there is a single NDV serotype, antibodies generated against a given NDV strain could theoretically provide protection against other strains. In practice, this is not always the case. Vaccine strains offer better protection when they are more closely related phylogenetically to the challenge strain [238-240]. Antibodies to NDV are of isotypes IgM, IgA, and IgY (avian IgG-equivalent), and generally peak at 21-28 days after infection [241]. Importantly, the presence of neutralising antibodies are critical for survival from NDV infection [235].

Cell-mediated responses can be detected early after NDV infection [242]. Clonal expansion following vaccination with a live-attenuated vaccine has been reported for both $CD4^+$ and $CD8^+$ T cell populations [243]. The cell-mediated response also appears to be proportionate to the virulence of the NDV strain [244]. Although T cells do not appear to play a role in NDV-protection and the development of neutralising antibody responses [245], $CD8^+$ T cells play an important role in reducing virus shedding [243].

1.3.5 Current NDV vaccines

Currently, inactivated and live-attenuated NDV vaccines are commercially available. The inactivated vaccine is treated with β-propiolactone (BPL) or formalin, and then administered intramuscularly with oil-based adjuvants. This can be problematic when

dealing with a large number of chickens as it is time consuming and requires special training, thus making vaccinating with inactivated NDV an expensive process Nonetheless, the inactivated NDV vaccine is able to induce strong antibody responses and reasonable protection against live infection. In order to enhance productivity, inactivated NDV vaccines are often administered at the same time as vaccines for other diseases. Furthermore, inactivated NDV vaccines can be used as booster vaccines in commercial layers or breeders where the small number of more valuable birds can justify the expense associated with individual vaccinations.

The live-attenuated NDV vaccine is cheaper and easier to administer but it is not as effective as the inactivated vaccine. Avirulent or lentogenic strains are commonly used to formulate live-attenuated vaccines. The most commonly used strain is La Sota, which is a GII lentogenic strain. However, La Sota can cause respiratory symptoms following vaccination [246]. The vaccine is usually administered in drinking water or aerosols to allow vaccination of large number of birds quickly and easily. Protection induced by the live-attenuated vaccine is short-lived. This could be due to limited innate immunity and limited immune activation as illustrated by low interferon type I (IFN-I) and reduced pro-inflammatory signalling after La Sota immunisation compared to a challenge with virulent NDV strains [229]. It has been reported previously that IFN-I is important for lymphocyte activation in mice [197], however the effect of IFN-I signalling on lymphocyte activation in avian species has not been elucidated. In addition, the live-attenuated vaccine is heat-sensitive, and this highlights an important issue related to vaccine viability, particularly in developing countries where large distances must be travelled to reach the whole flock.

As the inactivated vaccine is more effective, it is compulsory in New South Wales and Victoria where the risk of an NDV outbreak is most prevalent. In other states there is an option to use the inactivated vaccine or the live-attenuated vaccine every 6-8 weeks [247]. Despite using commercially available vaccines, chickens can still shed virus and become sick with NDV following vaccination with both types, as neither is fully effective [239, 248]. In addition, current NDV vaccines have limited protective efficacy against Genotype VII that has recently been associated with severe NDV outbreaks. Therefore, there is an urgent need for a safe highly effective inactivated NDV vaccine capable of stimulating strong innate immunity, inducing strong antibody response and T cell response, and most

importantly that can be formulated based on virulent strains to protect against severe NDV outbreaks.

1.3.6 γ-NDV as an experimental vaccine candidate

Our lab is interested in producing a γ-irradiated NDV vaccine for use in domestic poultry, as γ-NDV has the potential to overcome several issues related to current vaccines. Firstly, as an inactivated vaccine it can be administered to chickens of all ages, and can be freeze-dried [66] to overcome availability issues in developing countries. It has been shown previously that γ-Flu is able to induce strong IFN-I responses that aid in the activation of lymphocytes [69]. This may be true for γ-NDV also, which would ensure sufficient immune stimulation upon vaccination. Importantly, recent publications have illustrated the adjuvant activity of γ-Flu on other γ-irradiated vaccines, which is associated with the ability of γ-Flu to induce strong IFN-1 responses and lymphocyte activation. Co-administration of γ-Flu with other γ-irradiated vaccines resulted in improved antibody responses [199], and promoted the development of T_{RM} cells [200]. Thus, combining γ-Flu with γ-NDV may increase immune signalling to drive development of long-lived adaptive immunity. In addition, recent outbreaks of highly pathogenic avian influenza (HPAI) has emphasised a need to implement widespread IAV vaccination in chickens. Accordingly, a combination vaccine against NDV and IAV using γ-irradiation has the potential to minimise the spread of HPAI between chickens and humans and improve current NDV vaccines in domestic poultry. Furthermore, γ-NDV may also be used as a safe inactivated oncolytic therapy to overcome the biosecurity concerns associated with the use of live NDV in a clinical setting.

1.3.7 Use of NDV as an oncolytic agent

Oncolytic viruses (OVs) have the potential to selectively target and replicate in cancer cells whilst leaving healthy cells intact. OVs are able to directly kill cells by replicating within them, or they are able to recruit components of the immune system to target the tumour (reviewed in [249]). Non-human viruses, such as NDV, are often used as safer alternatives. Several clinical trials have tested the ability of NDV to reduce tumour size in a range of cancers including colorectal carcinoma [250], breast and ovarian cancer, and glioblastoma [251]. The oncolytic properties of NDV were first identified in 1952 by Moore *et al* [252] by showing a decrease in tumour growth. This was further characterised by Prince &

Ginsberg [253] in 1957 where they showed inoculation of NDV into mice with established tumours resulted in a reduction in tumour size.

NDV has been proposed to kill cancer cells in several ways (**Figure 1.4**). In mammalian systems, NDV is a potent activator of innate signalling, which can lead to the activation of both intrinsic and extrinsic apoptotic pathways. Pro-apoptotic signalling molecules induced in cancer cells by live NDV include IFNα [254], TRAIL [255], TNFα [256], and IFNβ [257]. In addition, NDV is a fusogenic virus and thus causes syncytia formation. Syncytia tend to be short lived, as well as having an immune stimulatory effect. cDNA transcripts of individual structural proteins HN [258, 259], F protein and M protein [260] have also been shown to be oncolytic. The specificity in terms of targeting cancer cells is due to dysfunctional antiviral and apoptotic signalling. Sialic acids (the cellular receptor for NDV), and sialytransferases are also often upregulated in cancer cells (reviewed in [261]). This has not been examined from the perspective of specificity of NDV for cancer cells but could indeed be playing a role. Interestingly, in mice intratumoral administration of live NDV is able to enhance lymphocyte infiltration into distant, uninfected tumours, suggesting that replication of NDV within the tumour is not necessary to mount a response [262].

A major shortcoming of OVs is the induction of virus-specific humoral immunity, and live NDV has been shown to induce neutralising antibody responses in humans [263]. Antibodies are able to neutralise virus to prevent uptake into cancerous cells. This limits the number of times this treatment can be repeated. Furthermore, the use of replicating lytic NDV strains poses a biosecurity risk due to possible transmission from humans to birds, which may lead to outbreaks. The importation and use of these NDV strains are heavily regulated and clinical trials have halted.

1.3.8 Melanoma and current treatments

Melanoma is an aggressive form of skin cancer that develops in the pigment-producing melanocytes. Melanoma is the third most prominent cancer overall, and the most common cancer affecting 13 to 39 year-olds in Australia [264]. As with all cancers, early detection is key and prognosis depends on several factors including melanoma thickness [265, 266], ulceration [267] and proliferation rate [266]. Furthermore, in patients with metastatic

melanoma (Stage IV) the 5-year survival rate drops to 26% [264]. Most melanomas are caused by exposure to UV radiation [268], either naturally through sunlight or through artificial sources. UV light causes DNA damage by causing thymine dimers to fuse and form pyrimidine dimers [269, 270]. UV exposure can also cause indirect DNA damage through the formation of reactive oxygen species [271]. The accumulation of this genome damage can lead to cancer.

Most melanomas are initially treated with surgery. The tumour is excised with margins of between 1-3cm to reduce the risk of recurrence [272]. Where there is a risk of metastases, surgery is typically combined with adjuvant therapy, such as IFN-α or IL-2. Intermediate to high doses of IFN-α have been shown to improve relapse free survival and overall survival [273, 274]. However, high doses of IFN-α are poorly tolerated [275]. In Stage IV melanoma, where there are distant metastases, systemic therapy will also be administered. Systemic therapy includes chemotherapy, targeted therapy and immunotherapy [276]. A promising new area in cancer immunotherapy is the use of checkpoint inhibitors. In particular, the use of antibodies to target cytotoxic T lymphocyte-associated protein 4 (CTLA-4) and programmed cell-death protein 1 (PD-1) has shown widespread success (reviewed in [277]). Both CTLA-4 and PD-1 function to reduce tumour-specific T cell responses, and administration of anti-CTLA-4 and anti-PD-1 improves overall survival in previously untreatable melanoma [278, 279]. In addition, anti-CTLA-4 and anti-PD-1 can be co-administered to further enhance efficacy [280, 281]. Both antibodies, however, are associated with serious autoimmune side effects [282], as checkpoint inhibitors promote self-tolerance [283, 284].

1.3.9 Oncolytic viruses as a treatment for melanoma

The oncolytic virotherapy Talimogene laherparepvec (TVEC) was recently approved as a treatment for inoperable melanoma. TVEC is a modified strain of herpes simplex virus (HSV-1) that expresses human granulocyte-macrophage colony-stimulating factor (GM-CSF) [285]. TVEC treatment was found to be more successful than GM-CSF alone [286]. TVEC is further modified to remove the viral infected cell protein 34.5 (ICP34.5) [285]. ICP34.5 blocks the cellular antiviral responses [287]. The removal of this protein in TVEC prevents replication in healthy cells but not in cancer cells where antiviral immunity and pro-apoptotic pathways are dysregulated. In particular, dsRNA and other viral signals can

activate protein kinase R (PKR). PKR then phosphorylates eukaryotic initiation factor 2A (eIF-2A) to prevent translation and shut down virus replication [287]. The role of PKR as an oncogene is controversial as it appears to be upregulated in some cancers and down regulated in others (reviewed in [288]). Nonetheless, ICP34.5 counteracts the role of PKR by activating protein phosphatase 1A to re-phosphorylate eIF-2A, and the deletion of ICP34.5 aids TVEC specificity to cancer cells.

Another HSV mutant, HF10, is currently in clinical trials. HF10 is lacking both ICP34.5 and infected cell protein 47 (ICP47). ICP47 blocks host T cell responses [289], and could assist the tumour infiltrating lymphocytes (TILs) observed in murine cancer models treated with HF10 [290, 291], and in a clinical trial testing breast cancer treatment [292]. HF10 was able to treat melanoma in DBA/2 mice [291]. The same study found a reduction in untreated secondary tumours suggesting a systemic anti-tumour response [291].

1.3.10 Oncolytic NDV as a treatment for melanoma

Oncolytic NDV has been used as a melanoma treatment. In pre-clinical studies NDV is able to reduce tumour growth of murine melanomas and enhance TILs in the tumour site [293]. A recombinant NDV strain expressing IL-2 has also been shown to be effective at treating malignant melanoma in mice [294]. IL-2 is a currently approved immunological therapy for melanoma, however it is poorly tolerated due to systemic administration [295]. Genetically modified NDV allows for IL-2 production directly within the tumour and could reduce the systemic side effects [296]. NDV treatment has also been combined with checkpoint blockade immunotherapy. Combined treatment enhances TILs and tumour rejection [262]. In clinical trials, treatment with melanoma oncolysates prepared with NDV increased survival times [297-299] and enhanced $CD8^+$ T cell responses [298].

Limitations of NDV treatment include the induction of neutralising antibody responses and off-target effects. Neutralising antibody responses are a well-documented shortcoming of therapeutic viruses. The induction of neutralising antibodies prevents virus uptake, and consequently can hinder the efficacy and duration of treatment. In addition, treatment with oncolytic NDV can cause flu-like symptoms in clinical trials in humans including nausea and vomiting [251, 300].

1.4 RESEARCH PROJECT

1.4.1 Project rationale

In this research project, I investigated the concepts and applications related to the use of γ-radiation to inactivate viruses for vaccine purposes. γ-radiation is routinely used as a sterilisation technique in the food, medical and pharmaceutical industries. In these settings contaminating species are typically bacteria at a low bioburden and recommended sterilising doses are set accordingly. Consequently, recommended sterilisation methods are not applicable to irradiating more radioresistant species at deliberately high titres. Several γ-irradiated vaccines are currently in clinical or pre-clinical trials and in order to ensure safety, the methods for calculating sterilising doses need to be corroborated. In particular, mathematical modelling to estimate the sterilising doses must account for irradiating pathogens that; (1) have a high bioburden, (2) have a radioresistant genome causing multiple-hit inactivation kinetics, and (3) can be irradiated at different temperatures to protect structural integrity.

Irradiating vaccine preparations at different temperatures can have a marked effect on radioresistance and vaccine efficacy. At higher temperatures there is an increased production of ROS that aid inactivation but also damage antigens. For vaccine and research purposes, it is important to use an irradiation conditions that maintain structural integrity, as sterility is not the only goal. Previous investigation in our lab compared γ-Flu samples irradiated at 25 kGy and 50 kGy at room temperature or frozen on dry ice. We found that when comparing equivalent doses, frozen-irradiated vaccines performed significantly better than γ-Flu irradiated at room temperature. However, this does not account for the fact that sterilising doses are considerably lower when irradiating at warmer temperatures. In fact, irradiating at a lower dose and higher temperature may improve vaccine production and antigenic integrity.

These concepts related to sterilisation by γ-radiation can be applied to the development of novel γ-irradiated vaccines. In particular, I aim to develop a vaccine for NDV. NDV remains a prominent poultry disease despite vaccines being available. Current vaccines have major limitations due to poor coverage of GVII NDV strains and difficulty in vaccine administration. Outbreaks repeatedly occur in developing countries, even in vaccinated

flocks. We have previously demonstrated that γ-irradiated vaccines provide superior immunogenicity compared to other inactivation methods as characterised by superior antibody and T cell responses. Typically, live-attenuated vaccines induce T cell responses whereas traditional inactivated vaccines do not. Unlike chemically inactivated Flu vaccines, we have demonstrated strong T cell responses induced by γ-Flu. Similar efficacy in γ-NDV could provide a better alternative compared to existing live or chemically inactivated NDV vaccines. Importantly, due to biosecurity limitations, this thesis will use the Australian live-attenuated vaccine strain V4 to develop γ-NDV. Based on the success of this study, further development of γ-NDV will use an emerging strain such as GVII to enhance vaccine coverage.

There are further applications of γ-irradiated viruses that have not previously been explored. Namely, using γ-irradiated viruses as virotherapy. Interestingly, NDV has been used as an oncolytic virus in numerous clinical trials with widespread success. However, due to the potential for NDV to cause widespread disease and livestock losses, the use of NDV as a virotherapy has been strictly regulated. Additionally, a shortcoming of virotherapies is the potential for live viruses to cause disease. I hypothesise that γ-NDV could be used as a safe and effective oncolytic virotherapy. γ-NDV will be unable to replicate and cannot pose any outbreak risk. Furthermore, it is not expected to cause clinical symptoms when used in a clinical setting.

γ-Flu behaves in a way that mimics natural IAV infection, and similarly I expect the behaviour of γ-NDV to mimic live virus in terms of interacting with host cells, activating immune responses, and inducing cancer cell killing. Importantly, previous studies have demonstrated multiple mechanisms for oncolysis in cancer cells treated with NDV, including direct oncolytic activity for structural NDV proteins. We have also demonstrated that γ-Flu is a strong inducer of innate immunity. This is relevant to the oncolytic potential of γ-NDV, as innate signalling in tumour cells is one of the mechanisms of oncolysis.

Overall, this research project aims to address important concepts related to the use of γ-radiation to inactivate viruses for vaccine development. This research will be highly applicable to the development γ-Flu and γ-NDV vaccines, as well as other γ-irradiated

vaccines. Furthermore, this project will provide a foundation for using γ-irradiation in virotherapies, with a particular focus on γ-irradiated oncolytic NDV.

1.4.2 Hypotheses and aims

Hypothesis 1: γ-radiation is an effective inactivation method that can be optimised to develop highly effective vaccines. This method can be utilised to develop an inactivated NDV vaccine that can be co-administered with γ-Flu in domestic poultry.

Hypothesis 2: γ-irradiated NDV can be used as a novel oncolytic virotherapy.

Aim 1: To investigate the applicability of existing mathematical concepts to estimate sterilising doses for pathogens with complicated genome structures at variable irradiation conditions.

Aim 1.1. To generate inactivation curves and calculate sterilising doses for viruses with different genome structures, including IAV and NDV.

Aim 1.2. To develop accurate methods to calculate sterilising doses for pathogens with varying resistance to γ-radiation.

Aim 2: To test the effect of irradiation conditions on the immunogenicity of γ-Flu.

Aim 2.1. To test the effect of irradiation conditions on structural integrity of γ-Flu.

Aim 2.2. To establish optimal irradiation conditions for γ-Flu immunogenicity and efficacy.

Aim 3: To develop whole-inactivated γ-irradiated NDV.

Aim 3.1. To generate γ-NDV and test structural integrity.

Aim 3.2. To test immunogenicity of γ-NDV in mice.

Aim 3.3. To test co-administration of γ-NDV and γ-Flu.

Aim 4: To test the oncolytic potential of γ-NDV.

Aim 4.1. To test oncolytic activity of γ-NDV against cancer cell lines *in vitro.*

Aim 4.2. To test oncolytic activity of γ-NDV in *in vivo* mouse models.

Aim 4.3. To determine the mechanism of oncolysis induced by γ-NDV.

1.5 FIGURES

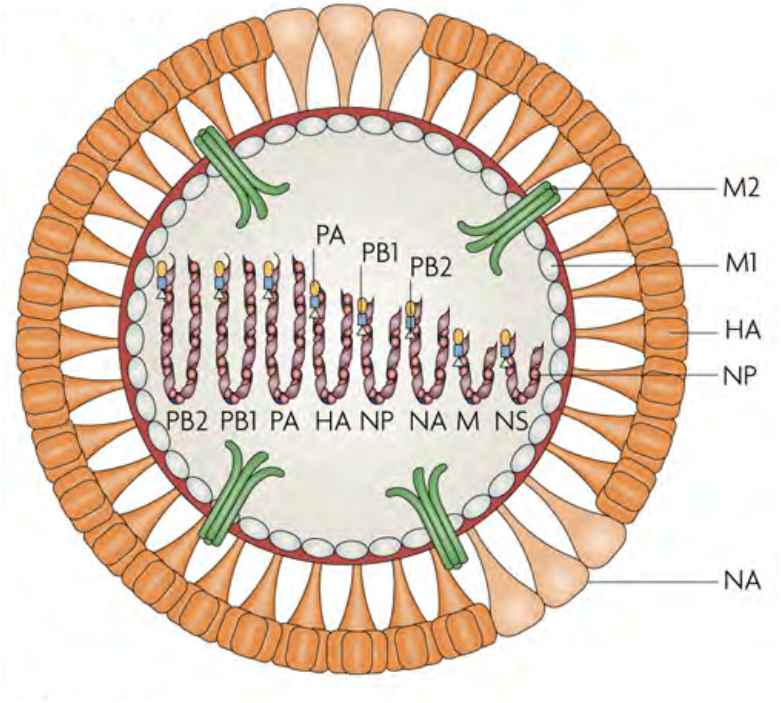

Figure 1.1. The structure of IAV. IAV is genome has 8 (-ve)ssRNA segments. The segments encode the IAV proteins. IAV is an enveloped virus and has surface antigens HA and NA and an ion channel M2. M1 provides support to the envelope. Each genome segment is protected by NP and packaged with the IAV polymerase proteins; PA, PB1 and PB2. The genes also encode non-structural proteins NS1 and NS2.
Adapted from Subbarao & Joseph, 2007 [301]**.**

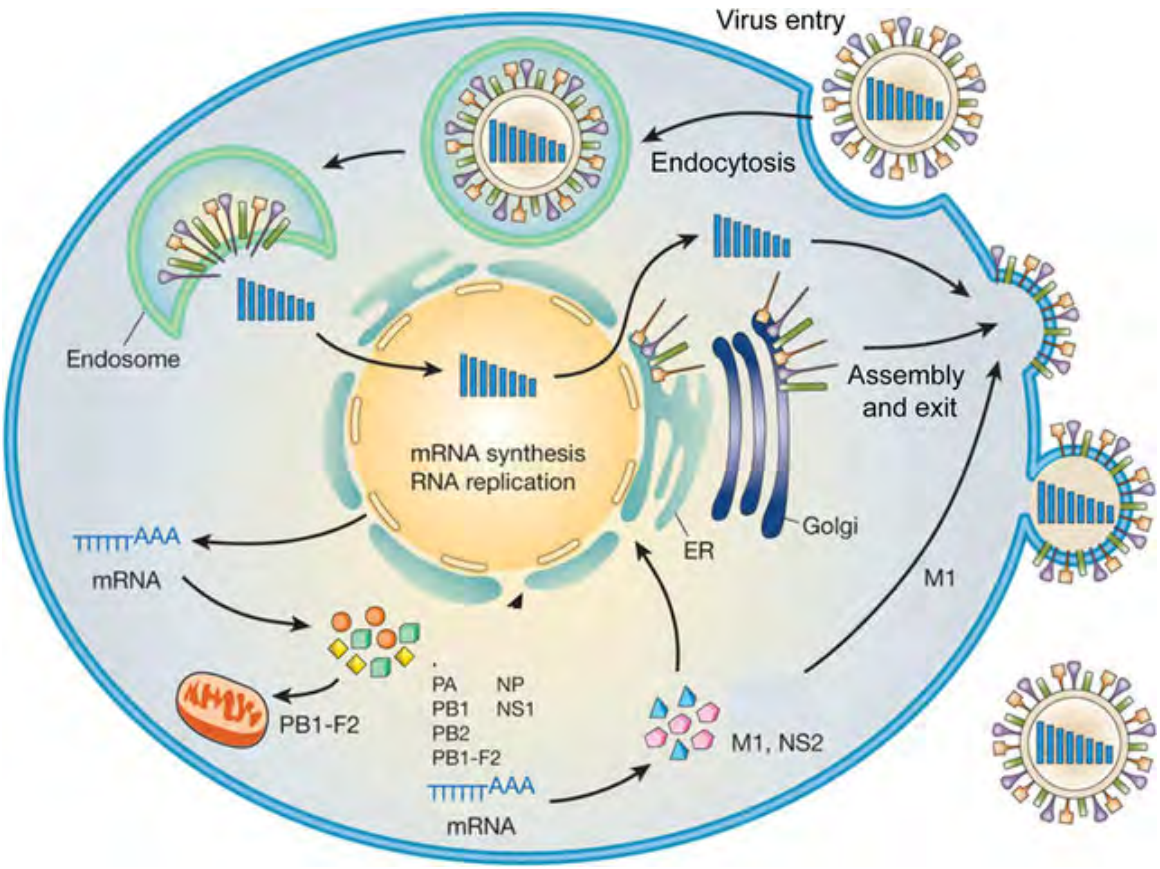

Figure 1.2. The replication cycle of IAV. IAV HA protein binds to sialic acids on the host cell to allow virus entry into host cell through receptor-mediated endocytosis. IAV escapes the endosome using the M2 ion channel and the fusion peptide of HA. The IAV vRNP is released into the cytoplasm and transported to the nucleus where replication takes place. IAV proteins are also produced in the cytoplasm with the positive sense mRNA. Proteins are transported to the cell membrane where new virions are formed by budding and released by NA.

Adapted from Arias *et al*, 2009 [302]**.**

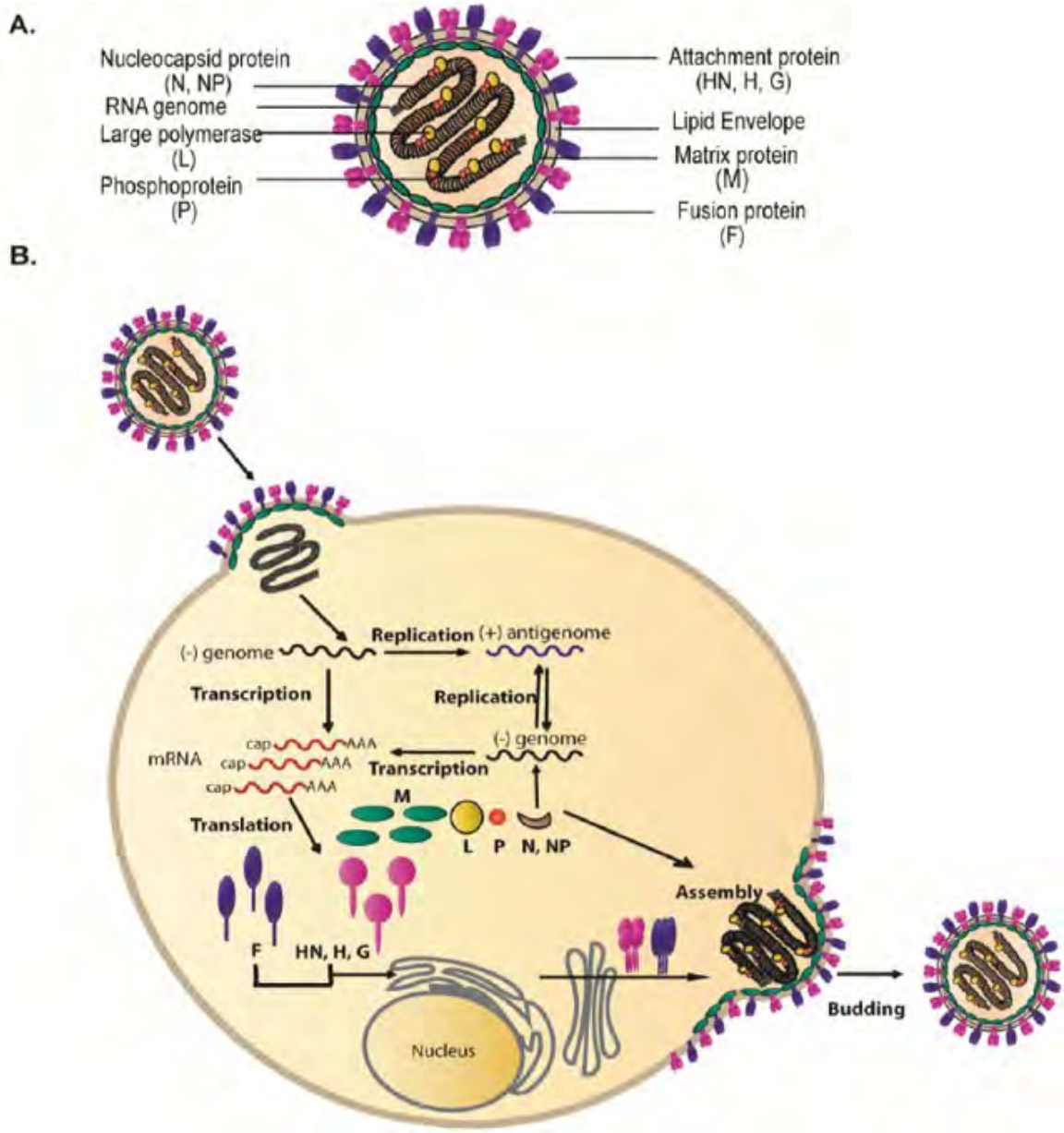

Figure 1.3. Structure and replication of paramyxoviruses. (A) NDV virions are enveloped and are made up of surface antigens HN and F, and other structural proteins NP, P, L and M. NDV also encodes non-structural proteins V and W. (B) The replication cycle of NDV within infected cells. NDV enters host cells through receptor-mediated surface fusion. Viral replication and translation occur within the cytoplasm mediated by the virus polymerase protein. New virions are then assembled at the cell membrane and are released by budding.

Adapted from El Najjar *et al*, 2014 [303]**.**

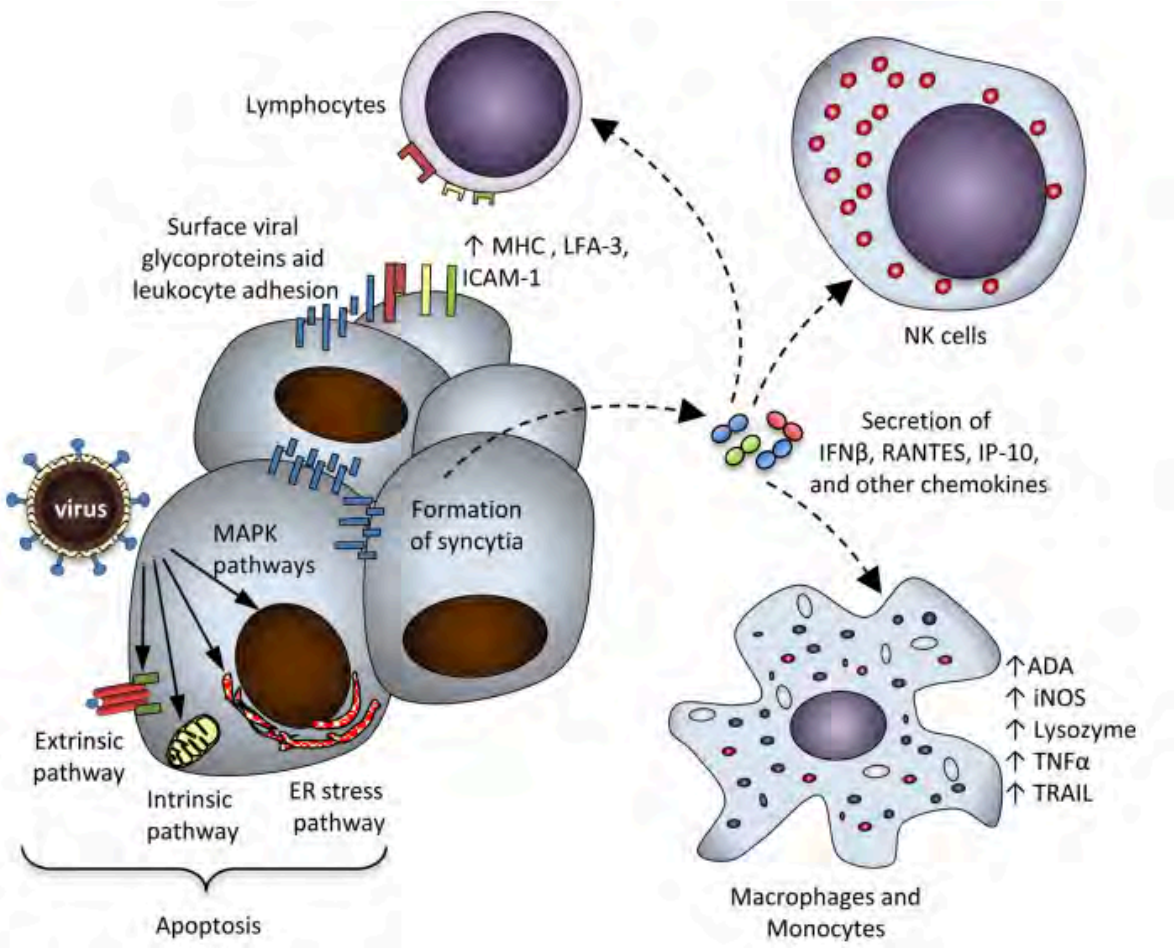

Figure 1.4. Oncolytic mechanisms of NDV. NDV is able to induce oncolysis in cancer cells using a range of different mechanisms. Replication of NDV within tumour cells can directly lyse cancer cells. The extrinsic, intrinsic and ER stress apoptotic pathways are also induced. Virus entry into cancer cells can induce syncytia formation and leave viral glycoproteins on the surface of tumour cell. Syncytia are short-lived and have an immunostimulatory effect. Similarly, viral glycoproteins help activate and recruit immune cells. Overall, NDV creates an immunostimulatory environment that recruits important anti-tumour immune cells including T cells, NK cells and macrophages.
Adapted from Zamarin *et al*, 2012 [249]**.**

CHAPTER 2

Sterility of gamma-irradiated pathogens: a new mathematical formula to calculate sterilising doses

CHAPTER 2: Sterility of gamma-irradiated pathogens: a new mathematical formula to calculate sterilising doses

2.1 INTRODUCTION

Gamma (γ) radiation is widely used to sterilise materials in a variety of settings. It is used in the food [41], pharmaceutical [42] and medical industries [43, 44] due to the ability of γ-radiation to inactivate pathogens through nucleic acid damage, whilst leaving proteins and other structures largely intact. Consequently, γ-radiation has also been proposed as an inactivation method to generate highly immunogenic vaccines [67]. Several groups have demonstrated the superiority of γ-radiation to traditional methods of vaccine inactivation, including formalin and β-propiolactone [65, 66]. In addition, previous publications illustrated the development of highly immunogenic γ-irradiated vaccines against influenza A virus (IAV) [66-69] and *Streptococcus pneumoniae* [70, 200]. Furthermore, γ-irradiated vaccines against human immunodeficiency virus (HIV) [72], and Malaria [73, 74] are currently in clinical trials.

In order to ensure vaccine safety and immunogenicity, estimating the sterilising dose under different irradiation conditions must be carefully considered. Radiosensitivity of a pathogen can be influenced by multiple factors including genome structure [10, 11], irradiation temperature [12-14], water [5] and oxygen levels [15, 16], and the presence of free-radical scavengers [17]. Importantly, resistance to γ-radiation is inversely related to genome size [10], as the chances of a single γ-ray interacting with the genome of a given pathogen is increased if the genome is larger. Accordingly, the sterilising doses required for bacterial species are usually lower than sterilising doses required for viruses [20]. In addition, it is hypothesised that viruses with more complex genomes are more radioresistant compared to viruses with simple genome structures, as a virus with a double-stranded or segmented genome may require inactivation of multiple strands or segments to prevent non-damaged segments from re-assorting in a host cell. Importantly, current standard operating procedures related to sterilisation of pathogens were developed to deal with low levels of bioburden or contamination [35, 37, 304], and a dose of 50 kGy is routinely used for sterilising pathogens that pose a biosecurity risk [36]. In this study, I investigated the effect of irradiation conditions on the irradiation dose required to sterilise highly

concentrated or radioresistant pathogens and assessed the validity of considering 50 kGy to be a widely applicable sterilising dose.

In general, the sterilising dose (DS) is calculated based on the concept of a sterility assurance level (SAL). For irradiated materials, the SAL is a given probability that any single pathogen within a sample may escape inactivation following an exposure to γ-irradiation. The International Atomic Energy Agency (IAEA) recommends a SAL of 10^{-6} for products intended to come into contact with compromised tissues [35], and so this should be applied to γ-irradiated vaccines. A SAL of 10^{-6} means that there is a one in a million chance of a single infectious particle remaining following irradiation [36]. Currently, the irradiation dose required to achieve sterility at the recommended SAL of 10^{-6} (DS_{SAL}) is calculated using the formula;

$$DS_{SAL} = n \times D_{10}, \quad (1)$$

Where n is the number of $\log_{10}$ reductions in bioburden required to reach a theoretical SAL of 10^{-6}, and D_{10} is the irradiation dose required for a single $\log_{10}$ reduction in bioburden. **Equation 1** assumes a log-linear inactivation curve, which is likely observed for viruses with simple genome structure that follow one-hit kinetics (**Figure 2.1A**). Our recent publications, however, have shown non-linear inactivation curves (**Figure 2.1B**) for rotavirus (RV) [305] and *S. pneumoniae* [71], demonstrating multiple-hit kinetics for complicated pathogens. While a D_{10} value is usually calculated based on the linear portion of the curve [16], ignoring the shoulder of resistance could lead to miscalculation of the irradiation dose required to achieve a SAL of 10^{-6} (or DS_{SAL}).

In this study I analyse the differences in D_{10} and DS_{SAL} for pathogens with different genomic structures irradiated at different temperatures. Our data show both single-hit and multiple-hit inactivation kinetics and I have formulated a simple method to calculate the DS_{SAL}. This method accounts for the shoulder of resistance in multiple-hit inactivation models and thus allows for more accurate calculation of the SAL.

2.2 MATERIALS AND METHODS

2.2.1 Cells

Madin-Darby canine kidney (MDCK), and African green monkey kidney (Vero and MA104) cells were maintained in Dulbecco's Modified Eagle's Medium (DMEM) with

10% foetal bovine serum (FBS), 1% penicillin/streptomycin (P/S) and 1% 2mM L-glutamine. For MA104 cells, 0.5% 200mM sodium pyruvate was also added. Cells were maintained at 37°C with 5% CO_2 in a humidified environment. Primary chicken embryo fibroblasts (CEF) were prepared from 10-day old chicken embryos by removing the head, limbs and viscera. Bodies were fragmented then pushed through a 70 μm single cell strainer (BD). Cells were washed 3 times with PBS by centrifugation at 1831 × *g*, then seeded into a 75cm^2 tissue culture flask in DMEM + 10% FBS and 1% P/S and kept at 37°C with 5% CO_2 in a humidified environment. After 24 hours, non-adherent cells were removed by 3 washes with PBS and fresh media was added.

2.2.2 Viruses

Viruses were used with permission from the University of Adelaide and all viruses were handled inside a Class II Biosafety Cabinet. Influenza A virus (IAV) A/Puerto Rico/8/1934 (A/PR8) H1N1 and Newcastle disease virus (NDV) V4 strain were grown in the allantoic cavity of 10 day old embryonated chicken eggs (ECE). Viruses were injected at 1 × 10^3 $TCID_{50}$/egg in PBS containing 1% P/S. Eggs were incubated at 37°C for 48 hours then chilled at 4°C overnight. Infected allantoic fluid was harvested and clarified by centrifugation at 3256 × *g* at 4°C for 10 minutes.

Semliki Forest virus (SFV) A7 strain and Zika virus (ZIKV) MRC766 (Uganda 1947) strain were grown in Vero cells, and rotavirus (RV) Rh452 was grown in MA104 cells. RV was activated by incubation at 37°C for 1 hour with 10 μg/mL TPCK-trypsin (Sigma). Viruses were added at an MOI of 0.01 and infected flasks were stored at 37°C for 24-48 hours until a cytopathic effect (CPE) of approximately 50% of the cell monolayer was observed. Supernatants were collected and clarified by centrifugation at 3256 × *g* at 4°C for 10 minutes. Infected allantoic fluids and supernatants were stored at -80°C until required.

IAV and NDV were titrated by 50% tissue culture infectious dose ($TCID_{50}$) in MDCK or CEF cells, respectively, in a 96-well round-bottomed microtitre plate. Virus was activated with 0.004% trypsin then 10-fold dilutions were added to confluent cell monolayers. Plates were incubated for 3 days at 37°C with 5% CO_2. Presence of infectious virus was determined by agglutination of 50 μL of 0.6% chicken red blood cells (cRBC) in each well.

The 50% infectious dose was determined using the method described by Reed and Muench [306] and titres were given as $TCID_{50}$/mL.

SFV and ZIKV were titrated by plaque forming assay (PFA). Confluent monolayers of Vero cells were infected with serial dilutions of virus. Adsorption of virus was allowed for 1 hour then a 0.9% agar overlay was added, and plates were incubated for 3 days (SFV) or 5 days (ZIKV). Cells were fixed with 5% formalin for 1 hour at room temperature. Overlays were removed and cells were stained with 0.2% crystal violet. Plaques were enumerated and titre was calculated as plaque-forming units (PFU)/mL.

RV was titrated by focus forming assay (FFA) as described previously [305]. Briefly, MA104 cells were seeded in 96-well flat-bottomed microtitre plates at 6.4×10^3 cells/well and plates were incubated at 37°C for 3 days until a confluent monolayer had formed. RV was activated by 10 μg/mL TPCK-trypsin for 30 minutes at 37°C. 10-fold serially diluted RV was added to wells and incubated at 37°C for 1 hour to allow virus to adhere to cells. Inoculum was removed and replaced with DMEM + 1% P/S + 1% L-Glutamine + 0.5% sodium pyruvate and plates were incubated for a further 18 hours at 37°C. Cells were then washed, and fixed and permeabilised using acetone:methanol (1:1 ratio). RV was visualised by primary staining with polyclonal mouse anti-RV sera for 1 hour at 4°C followed by Alexa Fluor® 555 goat anti-mouse IgG (Life Technologies, USA) secondary antibody for 1 hour at 4°C in the dark. Cells were also stained with 1μg/mL DAPI (Sigma) for 10 minutes at room temperature. RV-positive cells visualised using a Nikon Eclipse Ti fluorescent microscope and NIS-Elements AR software. Titre was calculated as focus-forming units (FFU)/mL.

2.2.3 *Streptococcus pneumoniae*

S. pneumoniae strain Rx1, a capsule-deficient derivative of D39 containing two additional mutations (ΔLytA, PdT) that has been described previously [70], was used. *S. pneumoniae* was inoculated into THY media at a starting OD_{600} of 0.02 then grown at 37°C + 5% CO_2 until OD reached 0.65. Bacteria were centrifuged at 4,000 × *g* for 10 minutes at 4°C then resuspended and washed 3× in PBS. Bacteria were then resuspended in PBS + 13% glycerol at approximately 10^{10} CFU/mL then frozen at -80°C until required. Viable titres were measured by CFU counts on blood agar plates.

2.2.4 Gamma irradiation

Virus and bacteria stocks were shipped to the Australian Nuclear Science and Technology Organisation (ANSTO) whilst frozen on dry ice. Samples were thawed on ice or at room temperature, or kept frozen on dry ice as specified and were exposed to increasing doses (0 – 50 kGy) of γ-radiation at different conditions (room temperature (24-27 °C), cold on ice water (4-8 °C), or frozen on dry-ice). γ-irradiation was performed using a ^{60}Co source at the Australian Nuclear Science and Technology Organisation (ANSTO, NSW). Radiation doses were measured using calibrated Fricke or ceric cerous dosimeters. Pathogens were then titrated to measure loss of infectivity at different radiation doses. Non-irradiated controls were treated to the same conditions (room-temperature, ice, or dry-ice) without exposure to γ-radiation. After irradiation all samples were stored at -80°C until required.

2.3 RESULTS

2.3.1. Inactivation curves

Different pathogens were exposed to incremental doses of γ-radiation and titres at each radiation dose were determined. IAV and NDV were both grown in 10-day old embryonated chicken eggs and they are expected to have the same media composition. This enabled a comparison between radiation-sensitivity of a non-segmented ssRNA genome (NDV) and a segmented ssRNA genome (IAV). Our data demonstrate log-linear inactivation for both viruses (**Figure 2.2**), indicating single hit inactivation kinetics.
Next, I compared the inactivation curves of SFV and ZIKV under different irradiation temperatures. Both viruses have ssRNA genomes of a comparable size and were both grown in Vero cells using DMEM with similar media composition. Both viruses demonstrated single-hit inactivation kinetics, with increased radiosensitivity at higher temperatures, as expected (**Figure 2.3**).

I then analysed the inactivation curve of RV, a more complex virus with a segmented and dsRNA genome structure. We have previously reported that the inactivation curve for dry ice-irradiated RV is non-linear and confirmed that here using a different strain of RV (**Figure 2.4**). The curve shows two distinct regions. A large shoulder of resistance is observed initially, with approximately a 2 log loss of titre occurring between 0 to 40 kGy. After this point, a rapid decline in viable titre was observed with increased radiation dose.

Importantly, calculating the sterilising dose using this inactivation curve would not be possible using current mathematical models (**Equation 1**). Interestingly, I did not detect the multiple-hit inactivation curve for RV materials irradiated on ice or at room temperature (**Figure 2.4**). This could indicate that indirect damage caused by free radicals following irradiation at higher temperatures may counteract the radioresistance of pathogens with more complex genomes.

2.3.2 Calculating sterilising doses

For viruses demonstrating single-hit kinetics, exponential lines of best fit could be determined using the equation;

$$y = ae^{-bx} \qquad (2)$$

Where y is the titre at a given radiation dose x, a is the starting titre, and b is a constant that is determined experimentally for each individual virus under a given set of irradiation conditions. **Equation 2** can then be rearranged to determine the D_{10} value (x), when $y = 0.1a$ (i.e. a 90% loss of starting titre);

$$D_{10} = \frac{ln\ (0.1)}{-b} \qquad (3)$$

Therefore, the D_{10} is higher where b is lower as would be expected for more radioresistant pathogens. The line of best fit, D_{10} values and DS_{SAL} was determined for IAV and NDV (**Table 2.1**), and ZIKV and SFV (**Table 2.2**). The D_{10} values of IAV and NDV were comparable (2.1 kGy and 2.8 kGy, respectively), whereas SFV had a higher D_{10} than ZIKV for dry-ice irradiation (5.5 kGy compared to 4.2 kGy). The D_{10} values were also calculated for ice and RT and were comparable, however an exact D_{10} value for RT-irradiated SFV could not be determined since virus was undetectable at the lowest irradiation dose used (5 kGy) in our experimental settings. Importantly, calculating a D_{10} value for pathogens with single-hit kinetics allowed us to calculate the DS_{SAL} using **Equation 1**, as shown in **Tables 1 and 2**. However, calculating the sterilising dose using **Equation 1** would not be possible for pathogens with multiple-hit kinetics as ignoring the shoulder of resistance would result in a miscalculation of the sterilising dose. Therefore, I propose a new formula to calculate the DS_{SAL} that could accommodate both single-hit and multiple-hit inactivation kinetics;

$$DS_{SAL} = R + (n \times D_{10}), \qquad (4)$$

Where R refers to the irradiation dose required to overcome the shoulder of resistance with a value of "R = 0" for pathogens that show linear inactivation curves (single-hit kinetics).

This formula takes into account the distinct regions of multiple-hit curves and should allow for more accurate calculation of sterilising doses.

When considering the inactivation curve of dry-ice irradiated RV **(Figure 2.4),** I would consider 40 kGy to be required to overcome the radioresistance (R value). The D_{10} can then be calculated for the radiation sensitive portion of the curve (above 40 kGy) using **Equation 3**. The D_{10} for the linear portion of the curve was calculated to be 3.2 kGy (based on the formula $y = 7 \times 10^{15} \times e^{-0.718x}$). To calculate DS_{SAL} using **Equation 4**, the number of $\log_{10}$ reduction in virus titre (n) required to achieve the internationally acceptable SAL of 10^{-6} was calculated. For this calculation, the viable titre at x = 40 kGy was determined to be 2.4×10^3 FFU/mL. Thus, a further reduction of 9.4 $\log_{10}$ will be required to meet a SAL of 10^{-6}. Hence the DS_{SAL} for dry-ice irradiated RV could be calculated based on **Equation 4** as follows:

$$DS_{SAL} = 40 + (9.4 \times 3.2) = 70.08 \text{ kGy}.$$

To confirm the applicability of this method, I considered the inactivation curve of the bacterial pathogen *S. pneumoniae*. This pathogen has a double stranded genome, and the inactivation curve is non-linear (**Figure 2.5**). The shoulder of resistance, or R-value, was determined to be 4 kGy. At x = 4 kGy the titre was 1.7×10^9 CFU/mL, thus 15.2 $\log_{10}$ reductions (n = 15.2) were required to reach the accepted SAL level of 10^{-6}. I calculated the D_{10} value for the log-linear curve (after 4 kGy) using the formula $y = 6 \times 10^{13} \times e^{-2.611x}$, which shows a value of 0.88 kGy. Therefore, the DS_{SAL} for *S. pneumoniae* irradiated on dry ice could be calculated using **Equation 4** as follows:

$$DS_{SAL} = 4 + (15.2 \times 0.88) = 17.38 \text{ kGy}.$$

2.4 DISCUSSION

Current recommendations for calculating sterilising doses are based on concepts and formula generated to meet requirements to sterilise food, medical equipment, and other health care products [35, 37, 40]. A dose of 25 kGy is considered the "gold standard" [35] and is often substantiated for a low bioburden. In general, the contaminating species are typically bacteria, which are more sensitive to γ-radiation than viruses [20] and spores [307]. In addition, the ISO suggests that a bioburden of 10^6 infectious units is unusually high [37]. However, materials prepared for biomedical analysis as well as for vaccine purposes are expected to have bioburden levels much higher than 10^6 infectious units.

Consequently, a DS_{SAL} below 25 kGy was not observed for any of the viruses irradiated on dry ice (**Tables 2.1 and 2.2**). Accordingly, 25 kGy should not be considered a sterilising dose for virally contaminated materials, nor for vaccine inactivation purposes without properly addressing the inactivation curve and D_{10} value, particularly when frozen materials are irradiated. For pathogens that pose a biosecurity concern a dose of 50 kGy is usually considered sufficient [36]. However, a SAL of 10^{-6} could not be reached following irradiation with 50 kGy on dry ice for ZIKV or SFV, or at 50 kGy using all irradiation conditions (dry ice, ice and RT) for RV (**Table 2.2**). Therefore, existing concepts that govern the use of γ-radiation to sterilise highly infectious pathogens should be carefully considered to ensure sterility at internationally accepted levels. This will be essential for the development of highly safe and immunogenic γ-irradiated vaccines.

Inactivation curves typically follow single-hit or multiple-hit kinetics. It was expected that inactivation of single-stranded, non-segmented RNA viruses would follow single-hit kinetics. This was confirmed with NDV (**Figure 2.2B**), SFV and ZIKV (**Figure 2.3**), as well as previous publications [11, 29]. Interestingly, IAV also appeared to follow single-hit inactivation kinetics despite having a segmented single-stranded RNA genomes (**Figure 2.2A**). We have also previously demonstrated log-linear inactivation of IAV [183]. Previous reports of inactivation curves of viruses with single-stranded segmented genomes have also demonstrated first-order kinetics [12, 21], suggesting that the ability of a segmented nature of single-stranded RNA genome of some viruses to increase radioresistance is negligible. Conversely, the inactivation curves of RV (**Figure 2.4**) and *S. pneumoniae* (**Figure 2.5**) demonstrate multiple-hit inactivation kinetics where an accumulation of damage is required to sterilise each pathogen. Reassortment of RV is relatively frequent, and has been shown to enhance resistance in response to UV treatment [308], and it could explain the large shoulder of 40 kGy observed here. *S. pneumoniae* cannot reassort, and SOS repair used by other bacterial species such as *Escherichia coli* [309] in response to γ-radiation do not appear to occur in *S. pneumoniae* [310]. However *S. pneumoniae* does utilise some repair mechanisms, such as excision repair [311]. It is also important to consider that both RV and *S. pneumoniae* have double-stranded genomes which could enhance resistance as both strands may need inactivation to render the pathogen replication-incompetent. Conversely, mammalian cells are highly susceptible to γ-radiation despite having double-stranded genomes and repair mechanisms [312, 313].

This is particularly relevant to the development of γ-irradiated cancer vaccines such as GVAX, which is currently in clinical trials [314]. Sterilising doses reported are typically between 35 Gy [315] and 100 Gy [316]. The radiosensitivity of mammalian cells is explained by a considerably larger genome than viruses and bacteria.

The ISO recommendations for calculating the sterilising dose involves setting a dose based on the calculated bioburden and a standard distribution of resistances (SDR) based on a D_{10} of between 2 – 3 kGy [37]. Where radioresistance is higher than the SDR (as would be the case for most viruses), the preparation is subjected to incremental increases in radiation dose and the proportion of positive samples is used to calculate the DS (i.e. at a SAL of 10^{-2}, there should be 0, 1 or 2 positive samples out of 100 for statistically significant substantiation of the dose used). However, extrapolating this data for a SAL of 10^{-6} does not take into account the potential for non-linear inactivation. I have proposed an alternative method where the shoulder of resistance is calculated and accounted for as well as log-linear inactivation. To ensure sterility and safety of irradiated materials, it is important to take into account the shape of the inactivation curve when considering the SAL and **Equation 4** allows for this. Importantly, mathematical modelling must also be coupled with rigid sterility testing.

It is important to note that γ-rays cause damage to pathogens by directly interacting with genomes to cause cross-linking, and single- and double-stranded breaks [1-4], and can interact with water or oxygen molecules to form free radicals. Oxidative damage causes most of the protein damage [5], but the formation and movement of free radicals can be reduced in frozen samples [317, 318]. In fact, irradiating frozen prions at incredibly high doses of up to 200 kGy showed minimal loss of transmission [319], demonstrating the resistance of proteins to γ-radiation at low temperatures. Thus, while irradiating at higher temperatures is more effective for sterilisation (**Figures 2.3 and 2.4**, [11, 12, 14]), irradiating frozen samples is expected to better maintain structural integrity [54, 183]. Therefore, γ-irradiation has routinely been performed at low temperatures to obtain more effective results for both biomedical analysis and vaccine immunogenicity. However, our data clearly illustrate that sterility at an internationally accepted level of sterility based on a SAL of 10^{-6} could not be achieved when irradiating high titres of some pathogens with 50 kGy using dry ice conditions, and even when using room-temperature irradiation for

radioresistant pathogens such as RV. Therefore, to ensure safety of irradiated materials the irradiation temperature, the appropriate method to calculate $DS_{SAL,}$ and rigid sterility testing must be considered. Overall, this study highlighted a serious gap in current practices, and I propose a new mathematical formula to calculate both the D_{10} value and DS_{SAL} to ensure safety of irradiated materials for vaccine and research purposes.

2.5 FIGURES

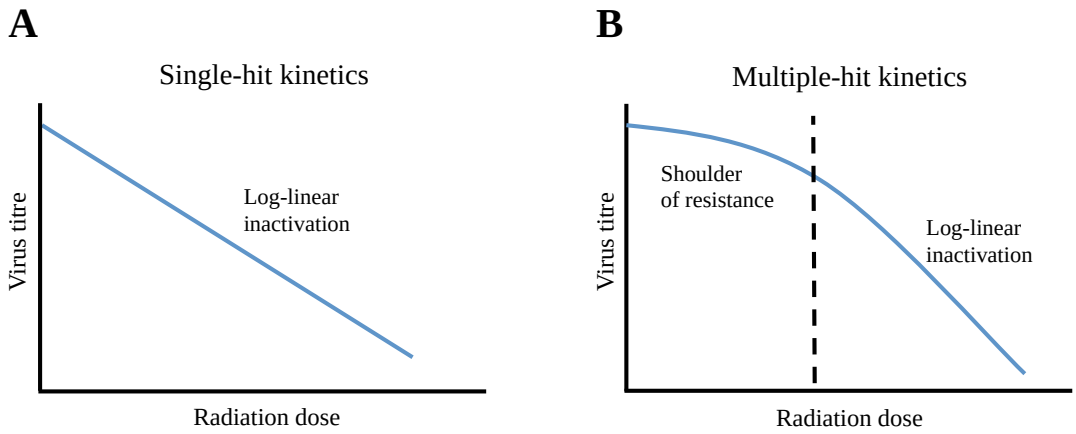

Figure 2.1. Single-hit and multiple-hit inactivation kinetics. Inactivation kinetics of viruses demonstrating a model of (A) single-hit kinetics or (B) multiple-hit kinetics. Single-hit kinetics follows log-linear inactivation, whereas multiple-hit kinetics has a shoulder of resistance before damage is accumulated and log-linear inactivation occurs.

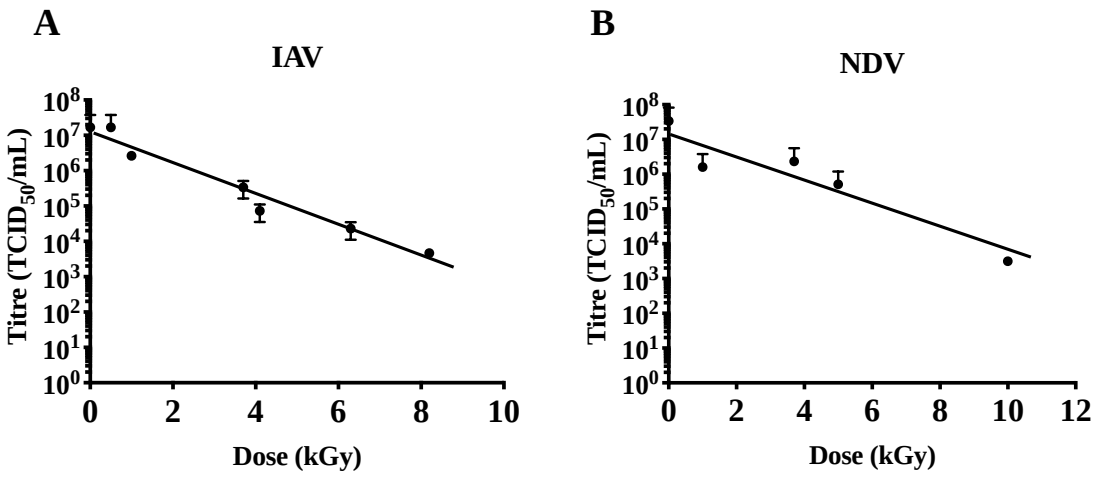

Figure 2.2. Log-linear inactivation curves of ssRNA viruses in allantoic fluid. (A) Influenza A virus and (B) Newcastle disease virus were exposed to increasing doses of γ-radiation on dry ice. Reduced virus titre (as measured by $TCID_{50}$/ml) for increasing radiation doses was used to generate inactivation curves and log-linear inactivation was observed for both viruses. Data expressed as mean ± SD (n = 2). Horizontal dashed line represents background binding of virus to RBCs in the absence of a cell monolayer.

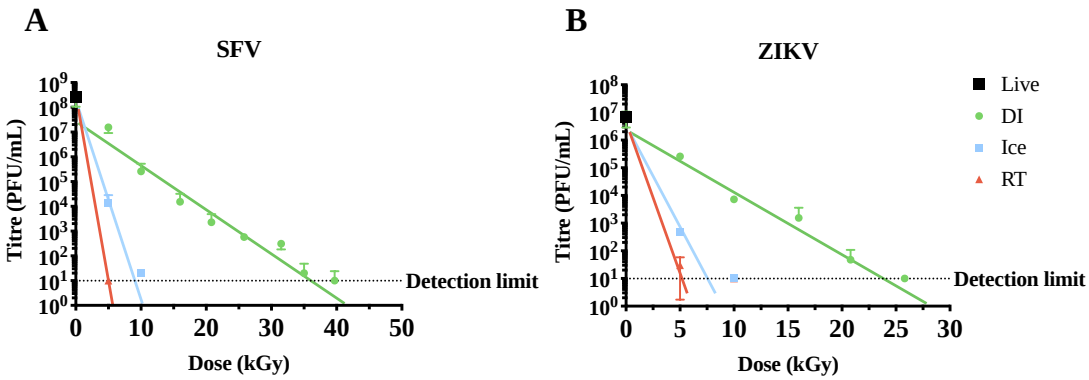

Figure 2.3. Log-linear inactivation of ssRNA viruses at different irradiation temperatures. (A) Semliki Forest virus and (B) Zika virus were exposed to increased doses of γ-irradiation on dry ice (green circles), ice (blue squares) or at room temperature (red triangles). The reduction in virus titre was estimated using plaque assay and inactivation curves were generated. Log-linear inactivation was observed for all three temperature conditions. Non-irradiated live virus was used as the starting point. Data presented as mean ± SD (n = 3). Horizontal dashed line represented detection limit.

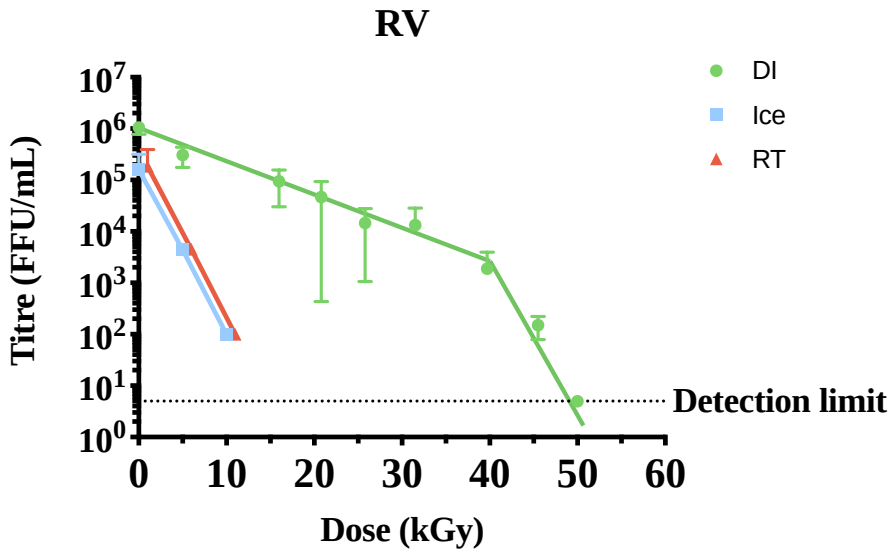

Figure 2.4. Inactivation curve of RV irradiated at different temperatures. RV was exposed to increasing doses of γ-radiation on dry ice (green circles), ice (blue squares) or at room temperature (red circles). Titre was measured by focus forming units. In contrast to both ice and RT, irradiation on DI show an inactivation curve with multiple-hit kinetics. A shoulder of resistance appears to require an irradiation dose of 40 kGy. Data presented as mean ± SD (n = 2).

Table 2.1. Inactivation formulas and sterility assurance levels of NDV and IAV.

Virus	Formula	Starting Titre ($TCID_{50}$/mL)	D_{10} (kGy)	DS (kGy)
IAV	$y = 2 \times 10^7 \times e^{-1.097x}$	1.69×10^7	2.1 ± 0.16	27.77
NDV	$y = 2 \times 10^7 \times e^{-0.823x}$	3.41×10^7	2.8 ± 0.53	37.86

Units for *x* are kGy

Table 2.2. Inactivation formulas and sterility assurance levels of ZIKV, SFV and RV.

Virus	Irradiation condition	Formula	Starting titre	D_{10} (kGy)	DS (kGy)
SFV	DI	$y = 5 \times 10^7 \times e^{-0.418x}$	2.55×10^8	5.5 ± 0.43	79.36
	Ice	$y = 3 \times 10^8 \times e^{-1.968x}$		1.2 ± 0.23	16.86
	RT	$y = 3 \times 10^8 \times e^{-3.871x}$		<1	14.41
ZIKV	DI	$y = 7 \times 10^6 \times e^{-0.625x}$	6.75×10^6	4.2 ± 0.35	54.10
	Ice	$y = 9 \times 10^6 \times e^{-1.986x}$		1.2 ± 0.06	14.87
	RT	$y = 9 \times 10^6 \times e^{-2.533x}$		0.9 ± 0.31	11.66
RV	Ice	$y = 1 \times 10^5 \times e^{-0.506x}$	1.05×10^6	4.6 ± 1.1	54.71
	RT	$y = 1 \times 10^5 \times e^{-0.521x}$		4.4 ± 0.02	53.13

Note: virus titre was measured as PFU/mL for SFV and ZIKV, and FFU/mL for RV. Units for *x* are kGy.

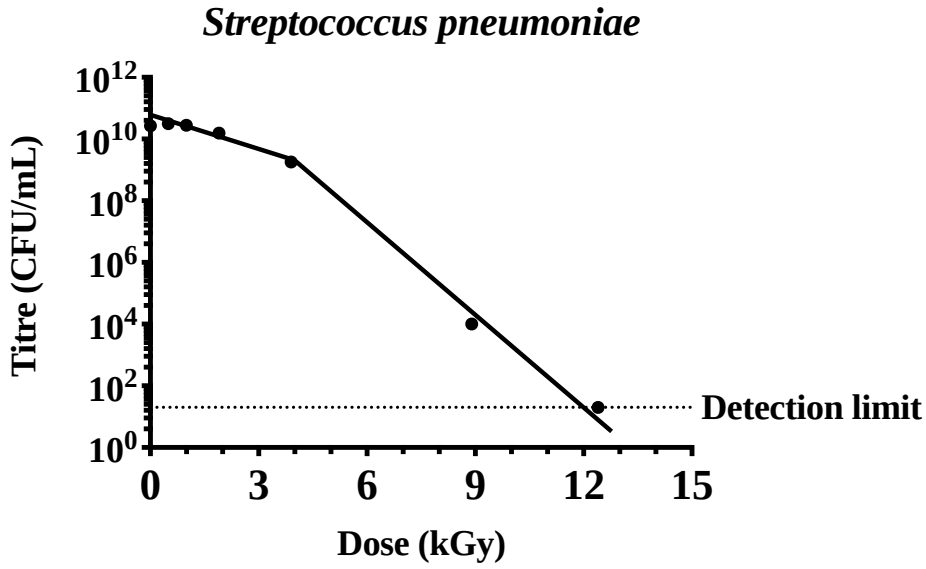

Figure 2.5. Inactivation curve of *S. pneumoniae* demonstrates multiple hit kinetics. *S. pneumoniae* was irradiated on dry ice at the indicated doses. Titre was measured by colony forming units and data presented as mean ± SEM (n = 4). Inactivation curve demonstrates multiple hit kinetics and a shoulder of resistance that require an irradiation dose of 4 kGy. **This data was collected by Shannon David.**

CHAPTER 3

Enhanced immunogenicity of whole-inactivated IAV vaccines sterilised using low dose gamma irradiation at a high irradiation temperature.

CHAPTER 3: Enhanced immunogenicity of whole-inactivated IAV vaccines sterilised using low dose gamma irradiation at a high irradiation temperature.

3.1 INTRODUCTION

Influenza A virus (IAV) is a major health concern and causes significant morbidity and mortality on a global scale. IAV causes between 250,000 and 500,000 deaths annually worldwide [80], and is associated with approximately $11 billion USD in yearly costs in the US alone [320]. The most at-risk groups for development of serious IAV symptoms or secondary compilations are infants, the elderly, the immunocompromised, and pregnant women [81]. Vaccination remains the most effective method to combat IAV infection, though current inactivated vaccines have major valency issues. Existing formulations consist of purified IAV surface proteins haemagglutinin (HA) and neuraminidase (NA) that are selected from 3 or 4 IAV strains predicted to circulate in a given year. IAV antigens are typically purified by zonal centrifugation, disrupted by detergents, and inactivated by chemical methods such as β-propiolactone or formaldehyde. While effective at protecting against these vaccine-included strains, the immune responses induced are antibody-based only and provide minimal cross-protection against strains not included in a given formulation (i.e. non-vaccine strains). These formulations must also be updated and redistributed every year due the highly mutagenic nature of IAV surface proteins. In addition, current IAV vaccines are ineffective against newly emerging seasonal strains and novel pandemic strains.

In order to increase vaccine coverage and minimise IAV-related morbidity and economic costs, new cross-protective IAV vaccines must be developed. Our group has previously demonstrated that a gamma (γ)-irradiated whole-inactivated IAV vaccine (γ-Flu) has the ability to induce cross-protective responses against vaccine-included and non-included strains [66]. Of particular importance, previous publications illustrated that mice vaccinated with a single dose of γ-Flu (consisting of the H1N1 strain) were able to survive a lethal dose of a non-vaccine H1N1 strain (drifted), a heterosubtypic H3N2 strain [182], and the highly pathogenic avian H5N1 [68]. The ability of γ-Flu-induced immune responses to protect against a wide range of non-vaccine IAV strains is specifically due to induction

of cytotoxic T-cell responses against conserved internal IAV proteins [185], unlike current inactivated IAV vaccines.

The use of γ-irradiation as an inactivation method for IAV vaccines has previously been advocated for [62, 321]. Furthermore, several vaccines using γ-radiation are currently in clinical trials including vaccines against human immunodeficiency virus [72] and malaria [73, 74]. Given these promising results, it is crucial to determine the optimal conditions to ensure both sterility and high immunogenicity of γ-irradiated vaccines. Importantly, all γ-irradiated products intended for human use must meet the internationally accepted sterility assurance level (SAL). A SAL of 10^{-6}, or a one in a million chance that an infectious unit in a sample escapes sterilisation, is recommended for vaccines [304]. The radiation dose required to reach the SAL is calculated by multiplying the decimal reduction dose, or D_{10} (the dose resulting in 1 $\log_{10}$ reduction in infectious titre), by the total number of $\log_{10}$ reductions required to reduce bioburden to a theoretical titre of 10^{-6}. The sterilising dose needed to achieve a specific SAL is therefore dependent upon starting titre and is also heavily influenced by environmental conditions. For example, viruses irradiated at lower temperatures (e.g. while frozen) are more resistant to radiation damage. It is well established that γ-radiation causes damage to pathogens via two mechanisms, termed the direct and indirect effects. The slower inactivation of frozen virus samples is due to reduction of indirect effects, as the production and movement of damaging free radicals is physically restricted [317, 318]. This preserves antigenic epitopes within vaccine preparations [54, 183], but dramatically increases the D_{10} and total sterilising doses required. High doses are inherently more damaging to the virus, and large-scale irradiation of samples whilst maintaining a frozen state is likely to pose feasibility issues. Conversely, adopting a higher irradiation temperature (e.g. room temperature) increases viral sensitivity to irradiation damage, resulting in much lower D_{10} and sterilising doses (**Chapter 2**). This reduces the total irradiation dose that a product would be exposed to, and increases feasibility of the inactivation methods when scaled-up for manufacture.

Whilst faster inactivation is desirable for most irradiated products (e.g. medical items, foods, etc.), the immunogenicity of vaccines treated in this manner is reduced due to amplification of indirect effects [12-14] and oxidative damage to surface proteins and internal components. Thus, an appropriate balance between sterilisation requirements and

vaccine antigenicity must be determined. In fact, no previous studies have compared vaccine efficacy after irradiating to different SAL values at different irradiation temperatures. In this study, we calculated the SAL for γ-Flu irradiated on dry-ice (DI), ice, or at room temperature (RT). We subsequently assessed structural integrity and vaccine efficacy of these three preparations in animal models. Interestingly, we found that vaccine efficacy was well maintained whilst irradiating at higher temperatures with lower total sterilising doses. This was unexpected and could potentially open an avenue to use lower radiation doses to reduce manufacturing time and costs associated with γ-irradiated vaccines, whilst suitably maintaining both sterility and vaccine immunogenicity.

3.2 MATERIALS AND METHODS

3.2.1 Ethics statement

This study was conducted in compliance with the *Australian Code of Practice for the Care and Use of Animals for Scientific Purposes* [322]. These studies were approved by the University of Adelaide Animal Ethics Committee under ethics approval number S-2018-013.

3.2.2 Virus Stocks

Influenza A/Puerto Rico/8/1934 [H1N1] (A/PR8) and A/California/07/2009 [H1N1] (A/California) were grown in the allantoic cavity of 10-day-old embryonated chicken eggs at 37°C for 48 hours. Eggs were then chilled at 4°C overnight, and infected allantoic fluid was harvested and clarified by centrifugation at 3272 × g for 10 minutes.

Vaccine concentration and purification was performed by haemadsorption as described previously [199]. Briefly, infected allantoic fluid was incubated with chicken erythrocytes at 4°C for 1.5 hours to allow virus adsorption to red blood cells (RBCs). Sample was then centrifuged to pellet virus-RBC complexes, and allantoic fluid supernatant was removed. Pellet was resuspended in 0.85% saline and incubated at 37°C for 1.5 hours to allow virus release from RBCs. Sample was then centrifuged to pellet RBCs, and the virus-containing supernatant was collected, aliquoted and stored at -80°C until required. Titres of concentrated IAV stocks were calculated as 3×10^9 $TCID_{50}$/mL and 1×10^6 $TCID_{50}$/mL for A/PR8 and A/California, respectively, by $TCID_{50}$ assay.

3.2.3 Gamma irradiation of IAV vaccines

Concentrated IAV stocks were inactivated by γ-irradiation at the following temperature conditions: frozen on dry-ice (DI), cold on ice water (ice, 4-8 ºC) or at room temperature (RT, 24-27 ºC), generating DI-γ-Flu, Ice-γ-Flu, and RT-γ-Flu respectively. Sterilising doses were calculated as described previously (**Chapter 2**) and were determined to be 35 kGy for DI-γ-Flu and 16 kGy for Ice- and RT-γ-Flu. Thermometers were used to measure temperature for ice and RT samples for the duration of irradiation, and non-irradiated control samples were subject to the same temperature conditions. After irradiation, all samples were stored at -80°C until required. γ-irradiation was performed using a ^{60}Co source at the Australian Nuclear Science and Technology Organisation (ANSTO, NSW). Radiation doses were measured using calibrated Fricke or ceric cerous dosimeters.

3.2.4 Virus titrations

IAV was titrated by 50% tissue culture infectious dose ($TCID_{50}$) assay using Madin-Darby canine kidney (MDCK) cells. MDCK cells were maintained in Dulbecco's Modified Eagle's Medium (DMEM) with 10% foetal bovine serum (FBS) and 1% penicillin/streptomycin (P/S). MDCK cells were kept at 37°C with 5% CO_2 and were passaged with trypsin when reached approximately 90% confluence. For $TCID_{50}$ assay, MDCK cells were seeded in 96-well round-bottomed plates at 5×10^4 cells/well. After 24h incubation, confluent cell monolayers were infected with 10-fold serial dilutions of IAV in DMEM supplemented with 8% trypsin for virus activation. Plates were incubated at 37°C for 3 days, then amplified virus in culture supernatants was detected by the addition of 0.6% packed RBCs based on pellet or mesh formation, with a mesh being considered positive for IAV. 50% infectious doses ($TCID_{50}$/mL) were calculated using the Reed and Muench method [306].

For haemagglutination assays, serial dilutions of IAV were performed in 0.85% saline in a 96-well round-bottomed microtitre plate. 0.6% packed RBCs in 50μL were added to each well and plates were scored for mesh or pellet formation. The reciprocal of the highest virus dilution showing a mesh was used to determine the total haemagglutination units (HAU/mL).

Sterility testing was also performed after γ-irradiation to ensure that the doses selected were sterile. MDCK cells were plated in 96-well flat-bottomed microtitre plates at 2×10^4 cells/well. γ-Flu was activated with 10μg/mL TPCK-trypsin at 37°C for 30 minutes then diluted 1:10 in DMEM + 1% P/S + 0.5μg/mL TPCK-trypsin. Inoculum was added to MDCK cells at an MOI-equivalent of 600 and cells were then incubated at 37°C for 24 hours to allow virus replication (passage 1). Supernatant was then collected and used to infect fresh MDCK monolayers (passage 2). This was then repeated for passage 3. At the time of collecting supernatant, cells were washed with PBS then fixed and permeabilised with 1:1 acetone:methanol (v/v) at 4°C for 15 minutes. Cells were then stained with polyclonal mouse anti-A/PR8 serum (1:200 dilution in PBS) for 1 hour at 4°C followed by Alexa-fluor® 488 goat anti-mouse IgG secondary antibody (Life Technologies, 1:500 dilution). DAPI was used to stain cell nuclei (1μg/mL in DAPI). Images were taken using the Nikon TiE inverted fluorescence microscope and analysed using NIS elements software (Tokyo, Japan).

3.2.5 Neuraminidase assay

1 in 2 serial dilutions of live and irradiated IAV samples were performed in PBS in triplicate. Samples were then incubated with 0.125mM of 2'-(4-Methylumbelliferyl)-α-D-N-acetylneuraminic acid (4-MUNANA, Sigma M8639) at 37°C for 1 hour, facilitating cleavage of 4-MUNANA by active IAV neuraminidase (NA) into the fluorescent substrate 4-Methylumbelliferyl (4-MU). 4-MU (Sigma M1381) was also included at increasing concentrations to generate standard curves. After 1 hour the assay was stopped with ice-cold 0.5M Na_2CO_3 at pH 10.5 and read using a SpectraMax fluorescent plate reader with an excitation wavelength of 365nm and emission wavelength of 450nm.

3.2.6 Transmission Electron microscopy

γ-Flu irradiated at different temperatures was loaded onto 3mm formvar/carbon coated grids (approx. 3 μL/grid) and left to settle for 3 to 5 minutes. Grids were blotted to dry, washed, then stained with 2% uranyl acetate for 3 minutes. Grids were then washed with PBS and blotted to dry prior to visualisation using the FEI Tecnai G2 Spirit TEM (Adelaide Microscopy, University of Adelaide).

3.2.7 Mice

6-8 week old female BALB/c mice were vaccinated intranasally under ketamine anaesthetic (10% ketamine, 1% xylazil in sterile water, inject IP at 10μL/gram of body weight) with 32μL of either PBS (mock-vaccine control) or γ-Flu irradiated at different temperatures (9.6×10^7 $TCID_{50}$-equivalent/mouse). All animals received a single dose only. Immune serum was collected 20 days post-immunisation by submandibular bleeding. Mice were then challenged intranasally with lethal IAV on day 21 (3 weeks post-immunisation), under ketamine anaesthetic as above. Challenge doses used were 1.6×10^2 $TCID_{50}$/mouse for A/PR8 and 1.3×10^5 $TCID_{50}$/mouse for A/California. Weight loss was measured daily for a period of 21 days post-challenge, with a 20% loss of starting body weight was used as a humane end point.

3.2.8 Antibody responses

Enzyme-linked immunosorbent assay (ELISA) was used to measure IgG responses in serum samples from vaccinated and control mice. Plates were coated with A/PR8 in bicarbonate/carbonate coating buffer and incubated overnight at room temperature. Plates were then blocked with 2% skim milk for 2 hours. Serum samples were serially diluted then added to the plate for 2 hours at room temperature. Plates were washed and horseradish peroxidase-conjugated goat anti-mouse IgG antibody (1:10,000 dilution in blocking buffer, Thermo Scientific) was added to each well. After 2 hours at room temperature, plates were washed, and colour was developed using TMB peroxidase substrate in the dark for 30 minutes then the reaction was stopped with 2M H_2SO_4. Absorbance was measured at 450nm using a Bio-Tek Instruments plate reader. The reciprocal of the highest dilution to give absorbance readings higher than naïve mice + 3 standard deviations was considered the IgG titre.

To measure neutralising antibody responses, a focus-forming inhibition assay was used. Monolayers of MDCK cells were treated with 0.1 MOI of A/PR8 that has been pre-incubated with serial dilutions of immune serum. Virus was allowed 2 hours to adhere to cells then inoculum was removed, and cells were washed with PBS. Fresh media was added, and cells were incubated at 37°C for a further 22 hours. Staining procedure and visualisation were performed as described for sterility testing. For measuring A/California neutralisation, the primary antibody used was polyclonal murine anti-A/California serum

(1:200 dilution). Secondary antibody was Alexa-fluor® 488 goat anti-mouse IgG secondary antibody (Life Technologies, 1:500 dilution).

3.2.9 Cytotoxic T lymphocyte assay

Cytotoxic T lymphocyte (CTL) assays were performed as described previously [183]. Mice were vaccinated intravenously with 3×10^8 $TCID_{50}$-equivalent of γ-Flu. 7 days later, spleens were harvested from naïve donor mice, minced, and pushed through a 70μm filter to generate a single-cell suspension. Cells were then split into equal populations, and one was pulsed with influenza nucleoprotein (NP) peptide (NPP) and stained with CFSE (NPP-Pulsed). The second population was stained with cell tracker red (CTR) only (Unpulsed). The cells were mixed at a 1:1 ratio and injected intravenously into vaccinated and non-vaccinated control mice at 10^7 cells/mouse. 24 hours later, all mice were sacrificed, and spleens were harvested and processed into a single-cell suspension prior to fixing using 1% PFA. Labelled pulsed and non-pulsed cells were acquired using the LSRII flow cytometer (BD Biosciences), and data was analysed using FlowJo software (Treestar Incorporated).

3.2.10 Statistical analysis

Statistical analysis was performed using GraphPad Prism version 8 (GraphPad Software, La Jolla, CA, USA). Quantitative results were expressed as mean ± SEM. One-way ANOVA (with Tukey's multiple comparisons test) was used for comparison of data from 3 or more groups. Survival data were analysed using Fisher's exact test (two-tailed). P-values < 0.05 (95% confidence) were considered statistically significant.

3.3 RESULTS

3.3.1 Structural integrity of γ-Flu

Sterilising doses required to exceed a SAL of 10^{-6} were calculated as described previously (**Chapter 2**). For DI-irradiation, the sterilising dose was determined to be 35 kGy (DI-γ-Flu) and for ice- and RT-irradiation the sterilising dose was calculated to be 16 kGy (Ice-γ-Flu, RT-γ-Flu). Sterility testing based on multiple *in vitro* passages was performed to ensure complete inactivation of irradiated materials. Live and irradiated IAV samples were passaged three times in MDCK cells, with supernatants from each treated monolayer (or passage) used to treat the next MDCK monolayer. After 3 passages, monolayers were fixed

and stained for IAV infection. No virus infectivity was detected in any of the MDCK monolayers treated with irradiated preparations for all 3 passages, whereas replication of live virus was amplified at each passage (**Figure 3.1**). The irradiation doses selected were thus confirmed to be sterile and appropriate for subsequent *in vitro* and *in vivo* experiments.

The structural integrity of the IAV within each vaccine preparation was then assessed by HA and NA functionality assays. While hemagglutination assay show reduced HA activity for all γ-Flu preparations compared to live IAV (**Figure 3.2A**), no significant difference was detected between the three irradiated samples despite the highly varied temperature conditions used for irradiation. Furthermore, **Figure 3.2B** demonstrates that the functionality of NA proteins in each γ-Flu preparation was not affected by irradiation, with all three vaccine formulations showing comparable NA enzymatic activity to live IAV. Transmission electron microscopy was then used to examine whole virion structure. Representative images in **Figure 3.3C** show that virions within all three irradiated preparations were intact and retained spherical IAV structure. This shows that in addition to having minimal impact on surface proteins, γ-radiation at alternate temperature conditions does not cause substantial damage to viral envelopes. It is important to note that our microscope facilities are PC1 and so do not have the capacity to image live IAV as a comparison.

3.3.2 Efficacy of γ-Flu in mice

Given that all three γ-Flu preparations appeared suitably intact in terms of virion structure and protein functionality, we next assessed their efficacy as vaccine candidates in animal models. Initially, mice were vaccinated intranasally with a single dose of each vaccine preparation (DI-γ-Flu, Ice-γ-Flu, or RT-γ-Flu), or with PBS as a mock-vaccine control. 20 days post-immunisation, serum was harvested and an ELISA was performed to determine IAV-specific IgG titres. As shown in **Figure 3.3A**, all three γ-Flu preparations induced strong IgG responses, and no significant difference was detected in IgG titres induced by the three γ-Flu preparations. Interestingly, while not significant, there was a trend towards lower IgG responses detected in serum samples from mice vaccinated with DI-γ-Flu.

Following this, a focus-forming inhibition assay was performed to determine the ability of these γ-Flu-induced antibodies to inhibit receptor binding and IAV infection. Neutralising

antibody responses are crucial for homotypic IAV protection, thus it is important to assess antibody functionality in addition to overall titre. Serum samples from γ-Flu-vaccinated and control mice were used to pre-treat live A/PR8, and virus + serum mixtures were then used to infect monolayers of MDCK cells. After a 22h incubation period, cells were stained with DAPI to visualise cell nuclei, and with murine anti-APR8 and FITC-conjugated anti-murine antibodies to visualise IAV-infected cells. Fluorescence levels of each fluorophore were quantified, and FITC-fluorescence relative to DAPI-fluorescence was calculated to determine the average IAV infectivity per cell. Quantified fluorescence of serum-treated virus samples was then compared to virus only controls. As shown in **Figure 3.3B,** no reduction in infectivity was detected for virus treated with PBS-mock control sera, indicating the murine sera from naïve animals had no effect on IAV infectivity. Conversely, infectivity was significantly reduced when A/PR8 was treated with serum from DI-, Ice- and RT-γ-Flu vaccinated mice. Interestingly, immune sera from mice vaccinated with Ice- and RT-γ-Flu was significantly more effective at neutralising A/PR8 when compared to immune sera from mice vaccinated with DI-γ-Flu. Representative images of virus neutralisation were also taken at a 1:10 serum dilution, and similarly demonstrate a clear reduction in foci for all γ-Flu groups, with antibodies induced by Ice- and RT-γ-Flu vaccination being the most effective (**Figure 3.3C**). This trend is likely due to the higher titre of total IgG present in immune sera from Ice- and RT-γ-Flu vaccinated animals, compared to those immunised with DI-γ-Flu.

Given the slight differences observed in functionality of γ-Flu-induced antibodies, we used live IAV challenges in mice to assess if these small variations would translate to detectable differences in protective efficacy. Initially, the ability of DI-, Ice-, and RT-γ-Flu to mediate homotypic protection was investigated. After receiving a single dose of each γ-Flu preparation, mice were challenged with a lethal dose of homotypic A/PR8. Vaccinated mice experienced no weight loss after this challenge (**Figure 3.4A**), nor did they experience any other clinical symptoms of infection (data not shown). Conversely, PBS-mock control mice all succumbed to this challenge by day 7 post-infection. Importantly, all vaccinated mice, irrespective of vaccine irradiation temperature, show 100% survival based on using 20% bodyweight loss as the humane end point (**Figure 3.4B**). This indicates that the antibody responses detected in **Figure 3.3**, though variable, were more than sufficient to induce robust homotypic protection.

Importantly, a key feature of γ-Flu is its ability to induce cross-protective $CD8^+$ T-cell responses against vaccine and non-vaccine IAV strains. To assess the effect of the different irradiation temperatures on the induction of $CD8^+$ T-cell responses, an *in vivo* CTL assay was performed. Here, the killing of IAV NPP-pulsed splenocytes (target cells) was assessed in vaccinated and non-vaccinated animals. **Figure 3.5** shows that in naïve control mice the 1:1 ratio of pulsed target cells to unpulsed cells was maintained, indicating no non-specific killing of targets cells *in vivo*. Conversely, I detected a substantial loss of NPP-pulsed cells relative to unpulsed cells in all three γ-Flu vaccinated groups. This demonstrates the ability of CTLs from γ-Flu-immunised mice to rapidly mount cytotoxic responses against cells presenting IAV proteins. Indeed, these pulsed target cells were all lysed within 24h of injection into immunised animals. Interestingly, animals vaccinated with Ice-γ-Flu and RT-γ-Flu showed significantly more effective CTL responses (97% and 93% killing of IAV-pulsed targets, respectively) compared to animals vaccinated with DI-γ-Flu (73% killing of IAV-pulsed targets).

Enhanced IAV-specific CTL responses should theoretically translate to enhanced cross-protection against newly emerging IAV strains. To assess this, mice were vaccinated intranasally with one of the three γ-Flu preparations (based on A/PR8 [H1N1]), or PBS as a mock-vaccine control. Three weeks later, mice were intranasally challenged with a lethal dose of A/California, the pdmH1N1 strain. As shown in **Figure 3.6**, all vaccinated and non-vaccinated mice experienced some weight loss following A/California infection, however mice vaccinated with Ice-γ-Flu showed less weight loss and faster recovery than the other vaccine groups. Furthermore, 100% survival was recorded for mice vaccinated with Ice-γ-Flu and RT-γ-Flu, whereas 86% survival occurred in mice vaccinated with DI-γ-Flu (1 out of 7 mice reached the 20% weight loss cut-off). Overall, while γ-Flu vaccination was associated with significantly less weight loss and faster recovery time in all vaccinated groups, only Ice-γ-Flu and RT-γ-Flu was associated with significantly higher survival rates compared to the unvaccinated group. This outcome is consistent with the enhanced CTL responses (**Figure 3.5**).

To rule out the possibility that the protection demonstrated in **Figure 3.6** was mediated by neutralising antibody responses, I tested the ability of serum generated by the three γ-Flu preparations to neutralise A/California. Live A/California was treated with serial dilutions

of serum generated by DI-, Ice- or RT-γ-Flu, or naïve serum as a control. Virus + serum was then added to confluent monolayers of MDCK cells and allowed to adhere for 2 hours before unbound virus was washed away. Cells were incubated for a further 2 hours at 37°C to allow virus growth then cells were fixed and stained as described for **Figure 3.3**, with murine anti-A/California serum used as a primary antibody. As expected, we observed no cross-neutralisation generated by γ-Flu in this study (**Figure 3.7**).

3.4 DISCUSSION

IAV remains an important public health concern due to its high mutation rates and potential to cause global pandemics. Current vaccines only offer strain-specific protection due to the reliance on humoral responses against highly mutagenic HA and NA surface antigens rather than cross-protective responses against the conserved internal IAV components. We have developed a new and effective whole-IAV vaccine capable of protecting against multiple IAV strains and subtypes. For this vaccine candidate, IAV is inactivated using γ-radiation (generating γ-Flu), and the heterosubtypic protection provided is specifically mediated by induction of cross-reactive cytotoxic T cell responses [185]. While previous publications illustrated the underlying mechanisms for the cross-protective immunity, this study aims to improve immunogenicity of γ-Flu by manipulating irradiation conditions. The irradiation temperature for this novel vaccine product was optimised in the present study, to facilitate use of an inactivation process that maintains vaccine efficacy while also being suitable for scale-up during future manufacture.

Sterilisation using γ-radiation for vaccine production is typically performed whilst the sample is frozen on dry ice. Our previous publications describing γ-Flu all use dry-ice irradiation [66, 68, 69, 182, 183, 185], as does a γ-irradiated *Streptococcus pneumoniae* vaccine (γ-PN) that is currently in late-phase pre-clinical testing [71]. We have specifically advocated for dry-ice irradiation over RT-irradiation when comparing like-for-like doses, as frozen γ-Flu samples have shown enhanced structural integrity and immunogenicity, particularly at the high irradiation doses required for highly pathogenic materials [183]. A Venezuelan Equine Encephalitis Virus vaccine documented in the literature is also γ-irradiated whilst frozen on dry ice [323]. Similarly, materials intended for biological analyses are usually irradiated whilst frozen. For example, serum samples from an Ebola vaccine clinical trial were irradiated frozen at 50 kGy, and antibody binding detected by

ELISA was well-maintained after this treatment [56]. Bone allografts are also often sterilised whilst frozen, as bones are less brittle when irradiated on dry ice compared to irradiation with the same dose at room temperature [52].

However, all comparative studies to our knowledge have been conducted using the same irradiation dose across different irradiation conditions instead of comparing preparations at the sterilising dose. It is well established that pathogens are more sensitive to inactivation by γ-radiation at higher temperatures [12-14], which dramatically lowers the total sterilising dose (and thus total irradiation damage) that is required. In fact, this is the first study to consider the impact of irradiation temperature on the SAL in order to directly compare the immunogenicity of IAV inactivated with sterilising doses of γ-rays at RT or cold conditions (low radiation dose) to the same IAV preparation inactivated with sterilising doses of γ-rays at frozen dry ice conditions (substantially higher radiation dose). Interestingly, our data clearly show comparable or improved vaccine-induced responses when irradiating IAV vaccine samples at higher temperatures with lower radiation doses. While previous studies have shown that more free radicals form and therefore more protein damage would occur when irradiating at higher temperatures [13], the lower dose of radiation required to reach the SAL (16 kGy for ice and RT compared to 35 kGy for DI) could explain the comparable efficacy we see. Indeed, utilising these conditions would have the advantages of faster irradiation and a negate need to keep samples frozen.

To ensure that the heightened efficacy of ice and RT-irradiated samples was not due to residual live virus, sterility was confirmed for each preparation by three passages in MDCK cells. We have previously shown this method of sterility testing to be effective in detecting as little as 2 focus-forming units in a treated sample [305]. **Figure 3.1** clearly shows all three preparations were free from viable virus over multiple passages. Furthermore, we used a very high MOI-equivalent of 600 to demonstrate sterility. Importantly, this data confirms that γ-Flu irradiated at sterilising doses does not have the ability to undergo recombination to produce viable virions. It is expected that the sterilising γ-radiation inactivated each RNA segment to prevent recombination.

We subsequently analysed the structural integrity of these sterilised γ-Flu samples by measuring HA and NA function. We found equivalent functionality for all preparations

tested (**Figure 3.2**), which suggested that the γ-Flu preparations would be highly immunogenic. In fact, we have previously published the ability of γ-Flu to induce superior IFN-I responses to commercial IAV vaccines [69] which specifically relies on the ability of IAV HA to bind to sialic acid receptors on IFN-I producing cells for virus internalisation [324]. To test vaccine efficacy *in vivo,* we measured both antibody and CTL responses, and protection against homotypic and drifted IAV infections.

We initially tested the effect of irradiation temperature on the ability of γ-Flu to induce neutralising antibody responses and homotypic protection. Interestingly, while all γ-Flu preparations induced strong A/PR8-specific IgG and neutralising responses, Ice-γ-Flu and RT-γ-Flu performed better than DI-γ-Flu (**Figure 3.3**). Nonetheless, all γ-Flu preparations induced complete protection against homotypic A/PR8 challenge (**Figure 3.4**). Interestingly, we found that Ice-γ-Flu and RT-γ-Flu also outperformed DI-γ-Flu for induction of CTL responses (**Figure 3.5**), and protection against lethal drifted challenge (**Figure 3.6**). Live IAV-induced CTL responses can target the conserved internal NP, matrix and polymerase proteins [151, 152]. Similar to live IAV infection, γ-Flu has been previously reported to induce CTL responses that target the conserved internal IAV proteins [185].

Current inactivated IAV vaccines induce antibodies of a narrow breadth, whereas responses to natural IAV infection include a small population of broadly neutralising antibodies against the HA stalk [325], an area that is highly conserved [326]. However, antibodies to the HA stalk may still be overcome by mutations [327]. Our previous work has illustrated that antibodies induced by γ-Flu are strain-specific [182], and that cross-protection arises through cell-mediated responses [185]. In the present study I confirm that antibodies generated against all three γ-Flu preparations were unable to neutralise the drifted pdmH1N1 (**Figure 3.7**), and so protection demonstrated in **Figure 3.6** is mediated by the enhanced CTL responses (**Figure 3.5**).

The reduced efficacy of DI-γ-Flu compared to RT- and ice-irradiated preparations suggest that irradiating frozen materials at a high dose is not the optimal condition to minimise the damage to viral proteins. Instead, a balanced irradiation process that includes the use of low doses of γ-rays to inactivate unfrozen materials at cold or RT conditions could be

utilised to provide highly immunogenic vaccine preparations. Indeed, Cote et al [328] showed that the irradiation conditions of anthrax spores could be adjusted to 50 kGy ice-irradiation to meet the required sterility assurance levels whilst maintaining the biological structure required for biomedical testing. This change in irradiation conditions could overcome biosecurity issues associated with the inadvertent release of live anthrax spores by the US Department of Defense [38]. A radiation-attenuated malaria vaccine PfSPZ is also reported to receive a low dose of γ-radiation at room temperature prior to harvesting the sporozoites from the mosquito [329].

RT irradiation is classically associated with higher protein damage and loss of functionality. However, precise calculation of the sterilising dose under RT conditions allowed the RT-treated γ-Flu to be hit with a substantially lower dose of irradiation. This limited both direct and indirect irradiation damage, resulting in a high level of protein activity comparable to DI-irradiated γ-Flu. This observation alone highlights the importance of comparison of *sterilising doses* when optimising irradiation conditions for vaccine purposes, rather than selecting a single high dose that is universally applied. These data also indicate that ice or RT-irradiation is far less damaging than previously thought if the concept of the SAL is properly applied. These observations offer new and improved insights into vaccine irradiation, and these concepts could be applied to other irradiated products to vastly improve the feasibility of scale-up, and reduce costs associated with low temperature irradiation.

3.5 FIGURES

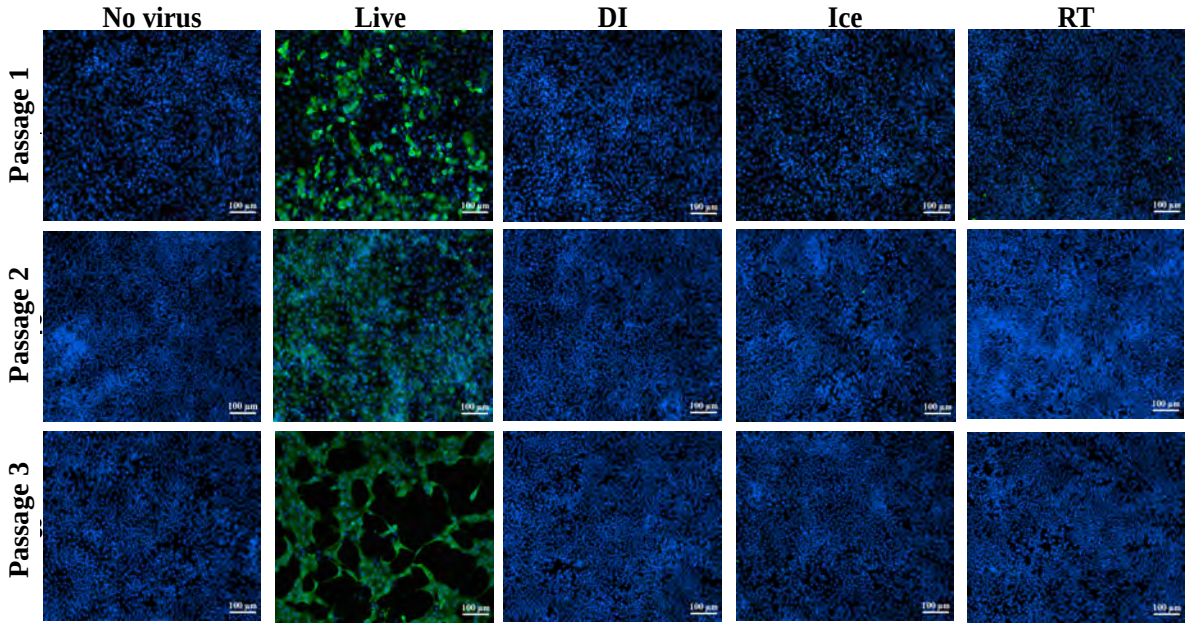

Figure 3.1. Sterility testing of γ-Flu. Sterility of γ-Flu irradiated at different temperatures and radiation doses was assessed by multiple passages in MDCK cells. Live A/PR8 or no virus were used as controls. γ-Flu was added to cells at an MOI equivalent of 600. Supernatant from passage 1 was collected 24 hours later and used to infect passage 2, this was then repeated for passage 3. Cell monolayers were stained with DAPI (blue), and IAV-positive cells were visualised with FITC-fluorescence (green). Samples were tested in triplicate, representative images are presented for each group at each passage.

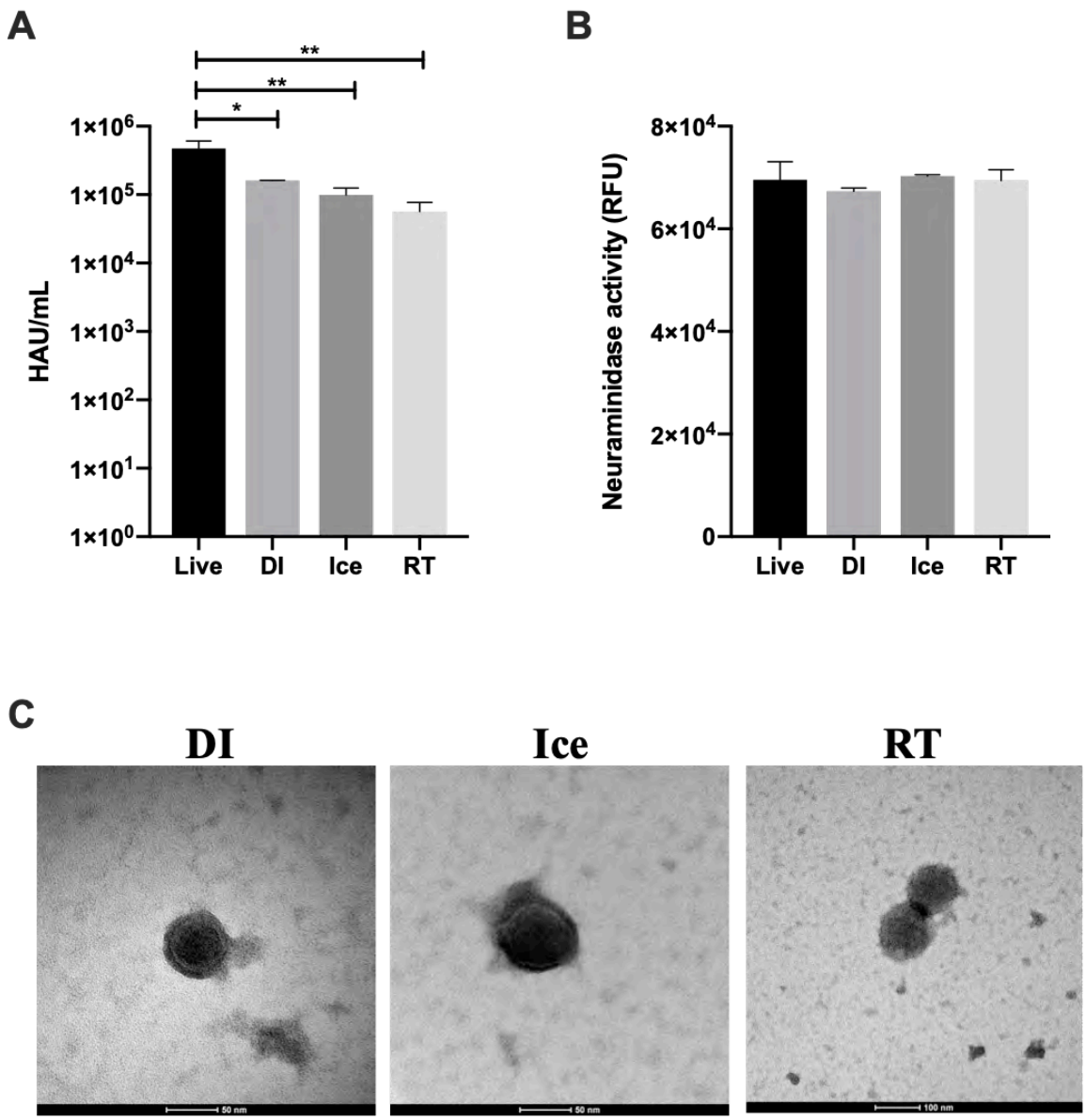

Figure 3.2. Structural integrity of IAV is maintained after γ-irradiation at different temperatures. γ-Flu preparations were inactivated with either: 16 kGy at RT, 16 kGy on ice, or 35 kGy on DI. Structural integrity of these preparations was then assessed by (A) haemagglutination assay, (B) neuraminidase assay and (C) transmission electron microscopy. Quantitative data is expressed as mean ± SEM (n=3). Data is analysed by one-way ANOVA (* $p < 0.05$, ** $p < 0.01$).

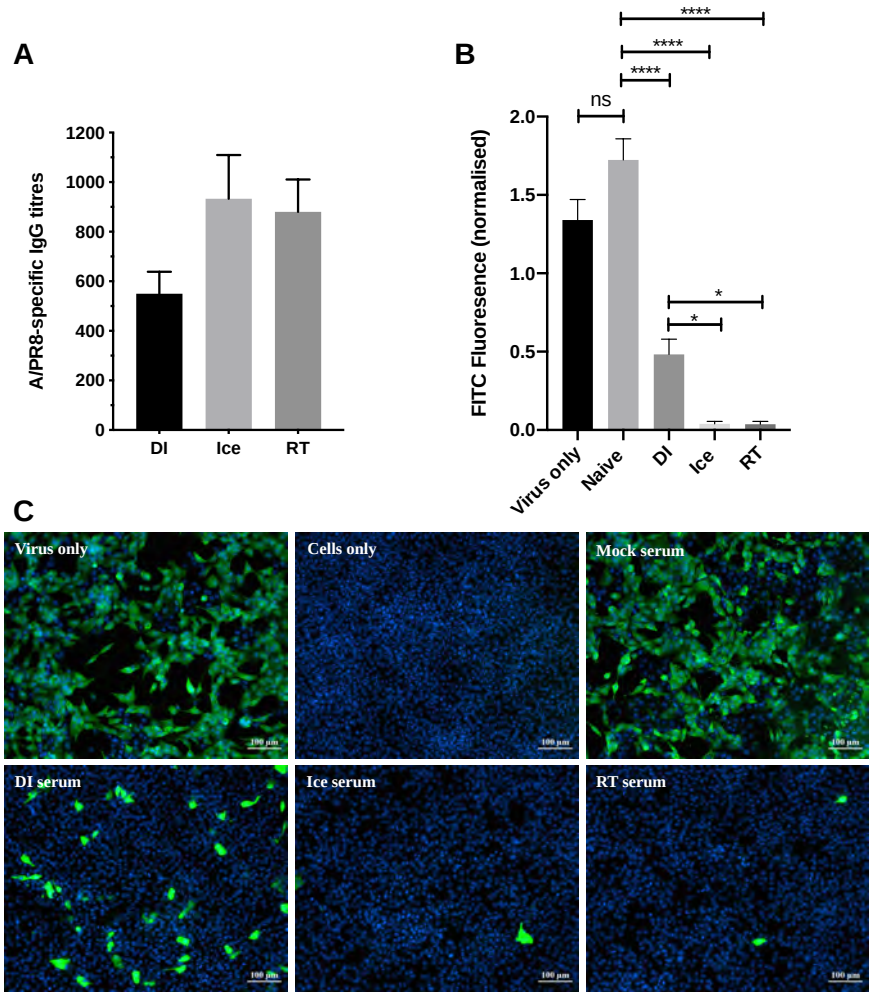

Figure 3.3. DI-γ-Flu induces reduced neutralising antibody responses when compared to Ice- and RT-γ-Flu. Mice were vaccinated intranasally with DI-γ-Flu, Ice-γ-Flu, RT-γ-Flu or PBS. Serum was collected from mice 20 days post-vaccination. (A) IgG responses were measured by direct ELISA. Data is collated from two independent experiments (n = 5 mice per repeat). Not significant by One-Way ANOVA. (B) Neutralising antibody responses were measured by focus-forming inhibition assay (FFI). Live virus was pre-treated with pooled naïve serum or pooled serum from vaccinated mice (n = 10 sera samples pooled within each vaccine group), then virus + serum mixtures were used to infect MDCK cell monolayers at MOI = 0.1. Each virus + serum mixture was tested in triplicate. FITC-fluorescence was quantified as an indicator of IAV infection and was normalised using the corresponding DAPI-fluorescence in each well (indicates the number of cell-nuclei). Data presented as mean FITC fluorescence ± SEM and analysed by one-way ANOVA (* $p < 0.05$, **** $p < 0.0001$, ns = no significance). (C) Representative images from focus-forming inhibition assay showing IAV infection levels after pre-treatment with pooled naïve and immune serum at a 1:10 dilution.

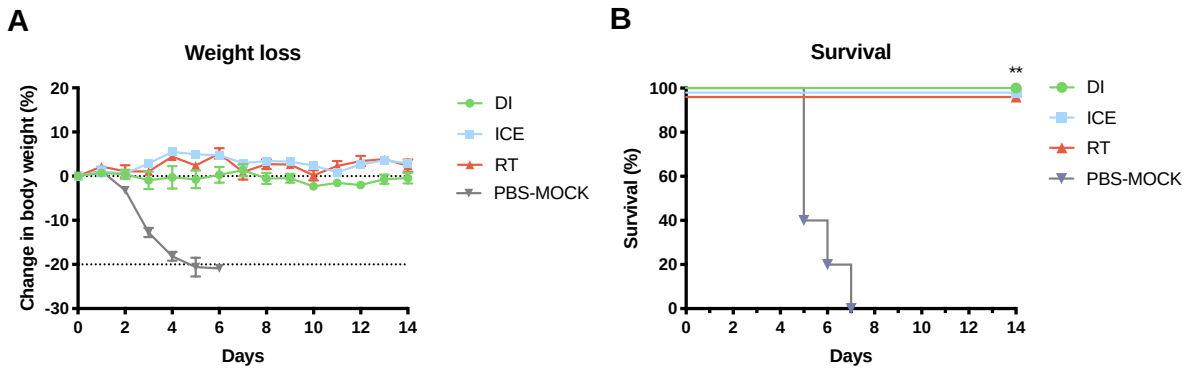

Figure 3.4. Vaccination with γ-Flu protects against lethal homotypic challenge. Mice were vaccinated intranasally with γ-Flu irradiated at different temperatures (DI, Ice and RT), or mock-vaccinated with PBS. 21 days later mice were intranasally challenged with a lethal dose of A/PR8. (A) Weight was monitored daily and a 20% loss of starting weight was considered as the humane endpoint (dotted line), at which point mice were euthanised. (B) Overall survival was plotted, and a two-tailed Fisher Exact test was used to determine statistical significance compared to the Mock control group (** $P < 0.01$, $n = 5$ mice per group).

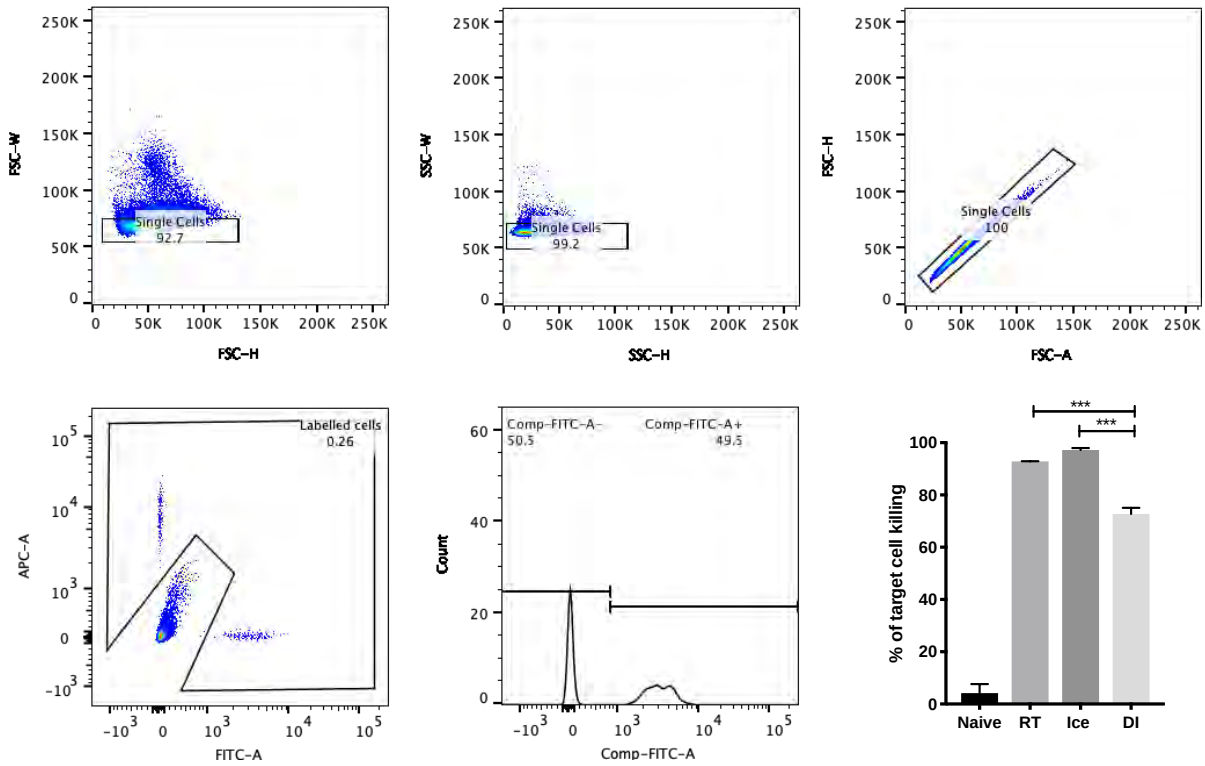

Figure 3.5. CTL responses are induced by vaccination with γ-Flu. Mice were vaccinated intravenously with γ-Flu preparations (RT-, Ice-, and DI-γ-Flu) or treated with PBS as mock control. 7 days later equal ratios of NPP-pulsed (CFSE labelled) and unpulsed (CTR labelled) splenocytes from naïve donor mice were injected into γ-Flu vaccinated mice or mock-vaccinated controls. 24 hours later splenocytes were harvested, processed and analysed using flow cytometry. Single-cell gating was performed, and the CTR+ and FITC+ cell populations of interest were isolated. Gating strategy shown above for a naïve control mouse injected with targets at a 1:1 ratio. The change in ratio of pulsed to unpulsed splenocytes after injection into vaccinated animals was then used to calculate the percentage killing of pulsed cells. Data presented here as mean percentage +/- SEM and analysed using one-way ANOVA (*** $p < 0.001$, $n = 3$).

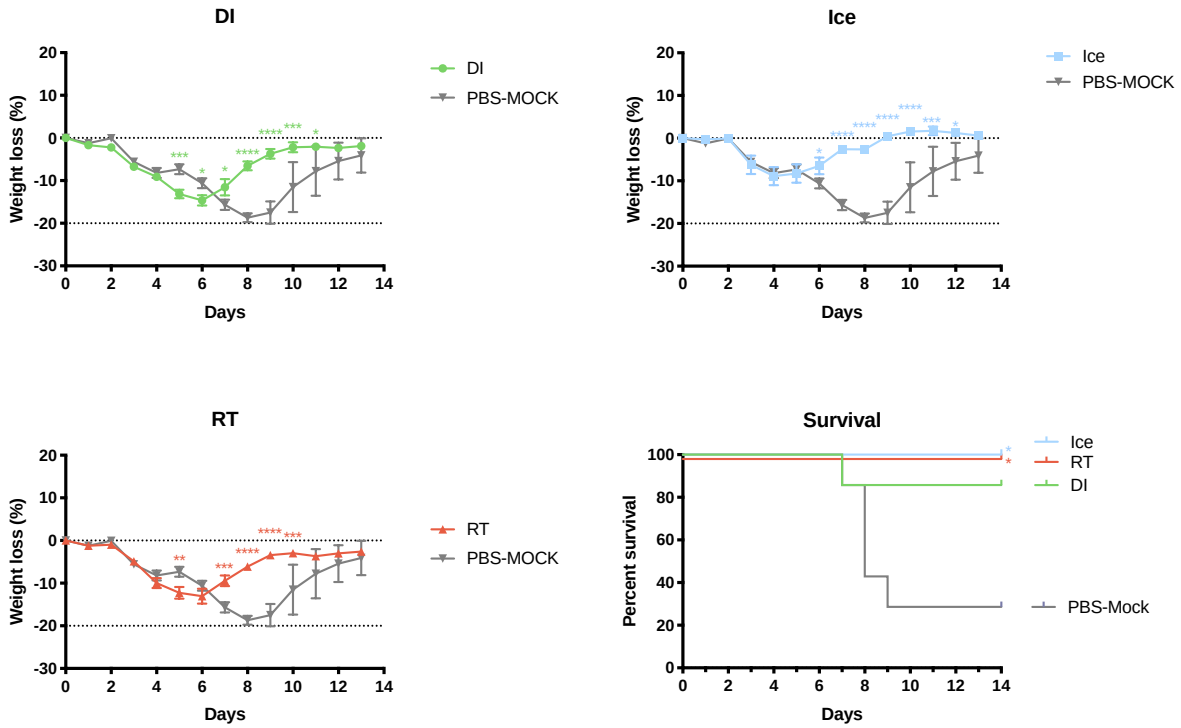

Figure 3.6. Vaccination with γ-Flu protects against lethal challenge with a drifted IAV strain. Mice were vaccinated intranasally with γ-Flu (γ-A/PR8 H1N1) irradiated at different temperatures, or PBS as mock control. 21 days later mice were challenged intranasally with a lethal dose of A/California H1N1. (A) Weight loss was measured daily, with a 20% loss of starting weight (dotted line) considered as humane end point. Weight loss was analysed by Two-Way ANOVA. Survival rates were also plotted, and a Two-Tailed Fisher-Exact test was used for analysis by comparing vaccinated groups to the PBS-MOCK vaccinated group (* $p < 0.05$), n = 7 mice/group).

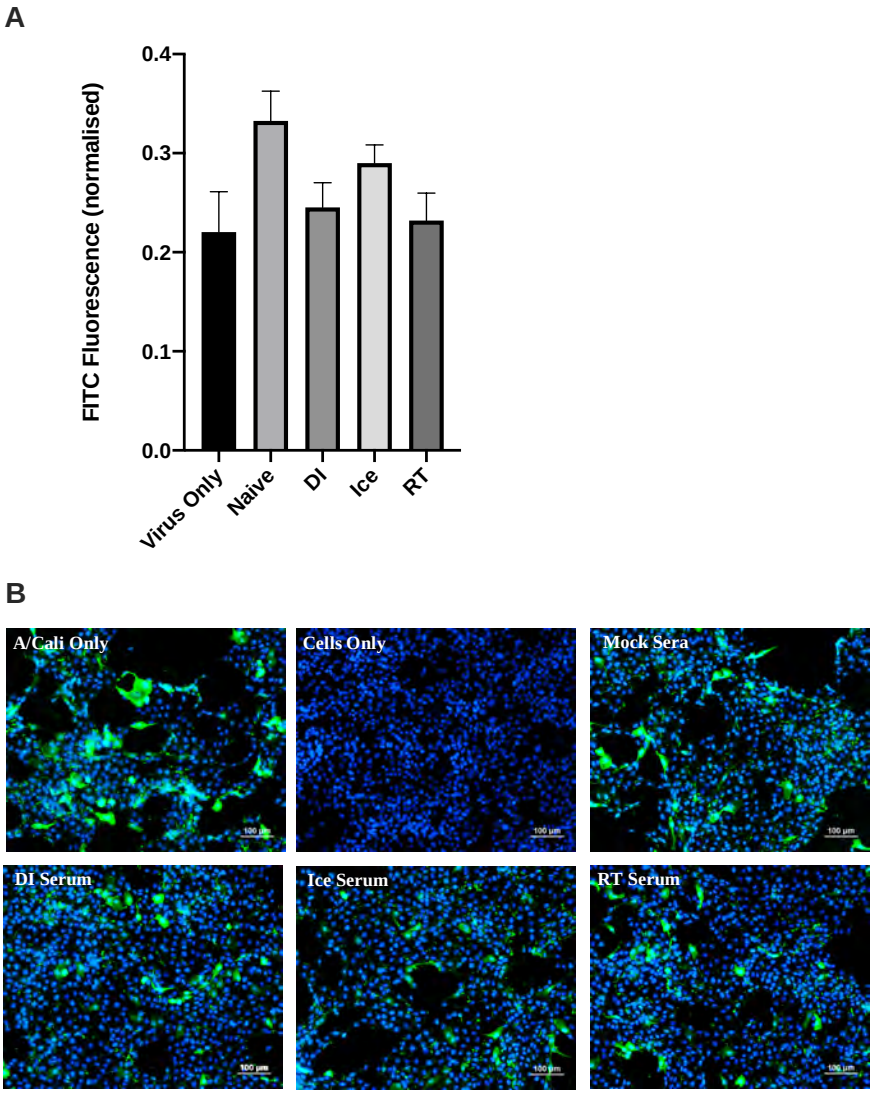

Figure 3.7. γ-Flu does not induce cross-neutralising antibody responses. Mice were vaccinated intranasally with γ-Flu (γ-A/PR8 H1N1) irradiated at room temperature (RT), on ice water (Ice) or on dry ice (DI). 20 days post-vaccination immune serum was harvested and the ability to neutralise A/California was measured by focus-forming inhibition assay. Live A/California was treated with pooled serum samples from the three vaccine groups or with serum from mock-vaccinated mice. Virus + serum mixtures were used to infect MDCK cell monolayers at an MOI of 0.1. (A) FITC-fluorescence (green) indicative of A/California replication was measured relative to DAPI-fluorescence (blue), indicative of cell nuclei. (B) Representative images of cell monolayers showing A/California infection levels after pre-treatment with a 1:10 dilution of serum samples. Experiments were performed in triplicate and quantitative data was analysed by One-Way ANOVA. Data was not significant. **This data was collected by Chloe Gates.**

CHAPTER 4

Development of gamma-irradiated NDV for use as a poultry vaccine and an oncolytic treatment.

CHAPTER 4: Development of gamma-irradiated NDV for use as a poultry vaccine and an oncolytic treatment

4.1 INTRODUCTION

Newcastle disease virus (NDV) is an avian paramyxovirus that predominantly infects chickens and other domestic poultry. Symptoms can be respiratory, gastrointestinal or neurological depending on the strain. NDV strains are highly genetically diverse [210] and are classified according to their virulence into three distinct groups – velogenic (highly virulent), mesogenic (medium virulence) and lentogenic (low virulence or avirulent) [209]. Velogenic viruses have mortality rates that can approach 100% [330, 331] and are endemic in parts of the world [332, 333], where outbreaks are associated with widespread livestock losses and a large economic burden. NDV outbreaks occurred in Australia in 2000 and 2002 and as a result Australia has adopted a strict vaccination regime [247].

Current NDV vaccines are either live-attenuated or inactivated. The Australian live-attenuated vaccine, V4, is a lentogenic strain that causes no clinical symptoms in chickens [334]. V4 is highly effective when administered by aerosol spray, however lower efficacy is observed when administered via drinking water and intranasal routes [334]. Furthermore, vaccination with V4 is susceptible to maternal antibodies that can interfere with vaccination in young chicks [335]. Inactivated vaccines consist of Group I or Group II strains that are inactivated by formalin or β-propiolactone. The inactivated vaccine is administered intramuscularly with oil adjuvant. Importantly, neither vaccine type is fully effective and vaccinated chickens can still be infected, shed virus, and become sick [248, 336]. Thus, there remains a need for alternative NDV vaccination approaches.

We have previously demonstrated that pathogens inactivated by γ-irradiation are highly immunogenic due to the limited impact of irradiation on the structural integrity of irradiated materials, particularly when using optimised irradiation conditions (**Chapter 3**, [183]). Previous research in our lab tested the immunogenicity of γ-irradiated vaccine candidates for influenza A virus (IAV) [66, 68, 69, 182, 183, 185], rotavirus (RV) [305], Semliki forest virus (SFV) [199] and *Streptococcus pneumoniae* [70, 71, 200]. Importantly, these studies have demonstrated that γ-Flu enhances neutralising antibody responses the co-administered pathogens. Considering the obvious need for a better NDV vaccine, and the importance of

humoral immunity in providing NDV-specific protection, I investigated the possibility of using γ-irradiation to inactivate NDV for vaccine purposes. The large single-stranded genome (15.2kb) makes NDV susceptible to γ-radiation [11], and irradiation conditions could be optimised to ensure structural integrity and consequently strong antibody responses, which is known to be important for protection against NDV infection [237]. In addition, considering previous publications related to the ability of γ-Flu to provide adjuvant activity to co-administered vaccines [182, 199], I investigated the possibility of combining both γ-Flu and γ-NDV in a single vaccination approach. This could enhance protection against both NDV and IAV outbreaks in birds and interfere with zoonotic transmission at the bird to human interface for avian influenza A viruses.

In addition, live NDV has garnered widespread attention due to its ability to selectively kill cancer cells. Several clinical trials have confirmed the ability of NDV to reduce tumour size in a range of cancers including colorectal carcinoma [250], breast and ovarian cancer, and glioblastoma [251]. A major shortcoming of oncolytic viruses however is the induction of humoral immunity, and live NDV has been shown to induce neutralising antibody responses in humans [263]. Antibodies are able to neutralise virus to prevent uptake into cancerous cells. This limits number of times this treatment can be repeated. Furthermore, live NDV poses a biosecurity risk and consequently the use of live NDV is heavily regulated [337]. Considering that γ-NDV is replication-incompetent so does not pose a biosecurity risk, I tested the possibility of using γ-NDV as an alternative cancer treatment.

Overall, in this study, I developed a whole-inactivated vaccine to NDV using γ-radiation (γ-NDV), illustrated the structural integrity of γ-NDV, and tested the immunogenicity of γ-NDV in mice. Surprisingly, while γ-NDV appeared to be highly immunogenic in mice and induced high-titre IgG responses, my data show these γ-NDV-specific antibody responses to be non-neutralising. In addition, I co-administered γ-NDV with γ-Flu and other adjuvants. Yet, despite the strong NDV-specific antibody responses detected in immunised mice, these antibody responses were still poorly neutralising. Importantly, γ-NDV retains oncolytic abilities, both in tissue culture and in animal models. Thus, the reduced ability of γ-NDV to induce neutralising antibody responses could help clinical application of γ-NDV as cancer therapy.

4.2 MATERIALS AND METHODS

4.2.1 Ethics statement

This study was conducted in compliance with the *Australian Code of Practice for the Care and Use of Animals for Scientific Purposes* [322]. These studies were approved by the University of Adelaide Animal Ethics Committee (ethics approval numbers S-2018-013 and S-2019-108).

4.2.2 Viruses

10-day-old embryonated chicken eggs were obtained from HiChick Breeding Company (Bethel, South Australia). Newcastle disease virus live-attenuated strain V4 and IAV strain A/Puerto Rico/8/1937 [H1N1] (A/PR8) were grown in the allantoic cavity of 10-day-old embryonated chicken eggs at 37 °C for 48 hours. Eggs were chilled overnight then infectious allantoic fluid was harvested and clarified by centrifugation at 3272 × g. Virus-containing allantoic fluid was then aliquoted and stored at -80°C until required.

For vaccine stocks, IAV was concentrated by haemadsorption to chicken red blood cells (cRBCs), and NDV was concentrated by ultrafiltration (UF). Haemadsorption was performed as described in **Chapter 3**. For UF, Amicon® Ultra-15 centrifugal filter units were used with a 100 kDa cut off (Merck). Clarified NDV was concentrated by centrifuging at 3272 × g. The preparation was resuspended in PBS and washed 3×, then resuspended in PBS for the final preparation after 10-fold concentration. NDV vaccine stocks were then aliquoted and stored at -80°C until required.

4.2.3 Cells

Chicken embryo fibroblasts (CEFs) were prepared from 10-day-old chicken embryos collected from eggs. Limbs and viscera were removed, and chicken embryos were minced. Embryos were then pushed through a 70μm filter and cells were collected in PBS in a 10mL centrifuge tube. Cells were washed 3× by centrifugation at 814 × g, and then added to tissue culture flasks. 24 hours later, non-attached cells were removed with 3 × washes with PBS then CEFs were given fresh media.

CEFs, Madin-Darby canine kidney (MDCK), African Green monkey (Vero), mouse melanoma (B16.F10), human rhabdomyosarcoma skeletal muscle cancer (RD) and human lung cancer (A549) cells were maintained in DMEM with 10% FBS and 1% P/S. Human melanoma (C32), human leukaemia (HL-60), human breast cancer (MDA), mouse breast cancer (4T1.2), mouse T cell lymphoma (EL-4), mouse B cell leukaemia (L1210) and mouse mastocytoma (P815) cells were maintained in RPMI with 10% FBS and 1% P/S, and human prostate cancer (PC3) cells were maintained in F12 media + 10% FBS and 1% P/S. All cells were kept at 37°C in a humidified environment with 5% CO_2 and cells were passaged when they reached approximately 80% confluence.

4.2.4 Virus titrations

Concentrated vaccine stocks were titrated by $TCID_{50}$ assay. Here, CEF (for NDV) or MDCK cells (for IAV) were plated at 5×10^4 cells/well in round-bottom 96-well microtitre plates and allowed to adhere overnight. 10-fold serial dilutions of virus were performed across the plate in DMEM + 8% trypsin for virus activation. Plates were incubated at 37°C for 72 hours, then 0.6% RBCs in saline were added to visualise amplified virus. Plates were scored based on a pellet or a mesh formation, where a mesh was considered positive for IAV or NDV. 50% infectious doses were then calculated using the Reed-Muench method [306]. NDV vaccine titre was determined to be 2×10^8 $TCID_{50}$/mL and IAV vaccine titre was determined to be 3×10^9 $TCID_{50}$/mL. For haemagglutination assays, IAV or NDV was serially diluted in normal saline (0.85%) in 96-well round-bottomed microtitre plates. 0.6% RBCs were added to each well and plates were scored for mesh or pellet formation. The reciprocal of the highest dilution to give a positive reading was considered the haemagglutination units (HAU).

4.2.5 Gamma irradiation

NDV and IAV were irradiated at the Australian Nuclear Science and Technology Organisation (ANSTO), NSW by exposure to 50 kGy (NDV) or 35 kGy (IAV) of gamma radiation from a ^{60}Co source. Radiation dose was measured using calibrated Fricke or ceric cerous dosimeters. Viruses were frozen on dry ice for the duration of irradiation and transportation.

4.2.6 Sterility testing

Sterility of irradiated preparations was measured by three passages in eggs and Vero cells. For egg infections, γ-NDV was diluted 1:100 in PBS + 1% penicillin/streptomycin and injected into the allantoic cavity of embryonated chicken eggs. Eggs were incubated at 37°C for 48 hours, then eggs were chilled overnight and allantoic fluid was harvested and 100μL of neat allantoic fluid was used to infect fresh eggs. This was repeated for a third passage then all three passages were tested for the presence of infectious virus by haemagglutination assay. Lack of detectable virus for all three passages was considered as a confirmation of sterility. Our previous publications have demonstrated that the method can detect as few as 2 infectious units in a preparation [305]. For sterility testing in Vero cells, cells were seeded at 5×10^4 cells/well in 96-well flat-bottomed microtitre plates then incubated overnight at 37°C. Live NDV and γ-NDV was activated with 10μg/mL TPCK-trypsin at 37°C for 1 hour. Virus was then diluted 1:10 in DMEM + 1% P/S to give a final trypsin concentration of 1μg/mL and added to Vero cells. Plates were incubated for 24 hours at 37°C then supernatant was collected and used to infect a fresh monolayer of Vero cells. This was repeated for a 3rd passage. Immunofluorescence was utilised to visualise NDV replication. Cells were fixed and permeabilised with ice-cold acetone:methanol for 10 minutes at 4°C. Plates were then washed 3 × with PBS and polyclonal chicken anti-NDV (1:200 dilution) was used as primary antibody. Plates were incubated for 1 hour at 4°C then washed 3 × with PBS. FITC-conjugated anti-chicken IgY (1:500 dilution) was added to each well and plates were further incubated for 1 hour at 4°C in the dark. Plates were washed again then DAPI staining (20 minutes at room temperature in the dark) was used to visualise cell nuclei. Plates were then visualised on Nikon TiE inverted fluorescence microscope and analysed using NIS elements software (Tokyo, Japan). Sterility testing for γ-Flu was performed as described in **Chapter 3**.

4.2.7 Neuraminidase assay

Live and irradiated virus preparations were serially diluted in PBS and 25μL of each dilution was added to microtitre plates. 25μL of 0.125mM 2'-(4-Methylumbelliferyl)-α-D-N-acetylneuraminic acid (4-MUNANA, Sigma M8639) was added to virus samples. Active neuraminidase cleaves 4-MUNANA into the fluorescent substrate 4-Methylumbelliferyl (4-MU). 4-MU was also added to plates at increasing concentrations to generate standard curves. Plates were incubated in the dark at 37°C for 1 hour with gentle shaking every 15

minutes to facilitate cleavage of 4-MUNANA. Reaction was stopped with ice-cold 0.5M Na_2CO_3 (pH 10.5) and relative fluorescence was measured using a SpectraMax fluorescent plate reader with an excitation wavelength of 365nm and an emission wavelength of 450nm.

4.2.8 Electron microscopy

Transmission electron microscopy was used to visualise structure of γ-NDV. Approximately 3μL of irradiated virus was loaded onto formvar/carbon-coated grids and incubated at room temperature for 3-5 minutes to allow attachment. Grids were blotted dry then washed with PBS and stained with 2% uranyl acetate for 3 minutes. Grids were washed with PBS then blotted to dry. Grids were visualised with an FEI Tecnai Spirit TEM (Adelaide Microscopy, University of Adelaide).

4.2.9 Giemsa stain

Vero cells, B16 cells and 4T1.2 cells were plated in 96-well flat-bottomed plates at 5×10^4 cells/well and allowed to adhere overnight at 37°C in 5% CO_2. Live or γ-NDV was activated with 0.5μg/mL of TPCK-trypsin at 37°C for 30 minutes then added to cells at an MOI of 10. Cells were incubated for 24 hours then washed 3 × with PBS and fixed with methanol for 10 minutes at room temperature. Methanol was removed and plates were allowed to air dry. Cells were then stained with Giemsa (Sigma 32884, 1:20 dilution in MilliQ water). Cells were washed again with 3 × PBS then visualised with an Olympus phase-contrast ULWCD 0.30 microscope.

4.2.10 Mice

6-8-week old female BALB/c mice were obtained from the Laboratory Animal Services, University of Adelaide, and 8-10-week old female C57BL/6J mice were obtained from the Animal Resource Centre, Western Australia. Mice were housed at the Laboratory Animal Facility, University of Adelaide, under specific pathogen free conditions and on a 12h:12h light-dark cycle. Mice were allowed a week to acclimate to housing prior to experiments commencing.

For vaccination studies, BALB/c mice were vaccinated with 6.4×10^6 $TCID_{50}$-equivalent/mouse for γ-NDV, 1×10^6 $TCID_{50}$-equivalent/mouse for γ-Flu, or 50μg/mouse

for keyhole limpet hemocyanin (Sigma, H8283). For intramuscular or subcutaneous vaccination, a total volume of 50μL per animal was used. For intranasal vaccination, mice were first anaesthetised by IP injection (10% ketamine and 1% xylazine in miliQ) prior to administering the required dose in a final volume of 32μL. For a prime-boost vaccination strategy, multiple doses of different vaccine preparations were administered at 3 weeks intervals. In addition, some experiments involved co-administration of γ-NDV with aluminium hydroxide (alum, 10%), Poly(I:C) (50μg/mouse) or incomplete Freund's adjuvant (IFA, 10%). To test vaccine immunogenicity, blood samples were collected from vaccinated animals at specific time points post-vaccination by either submandibular bleeding or from the heart cavity after mice were humanely euthanised. Serum samples were then tested *in vitro*.

For tumour induction, C57BL/6J mice were anaesthetised with isofluorane (2% isofluorane with 2L/min O_2) and 150μL of B16.F10 cells (1×10^5 cells/mouse) in PBS were injected subcutaneously. Mice were monitored daily for the development of tumours, and tumour size was measured with callipers every 2nd day from the time when tumours became palpable (day 8 in these experiments). Mice were humanely killed when tumours reached 100mm^2, or at day 28 post-tumour induction if mice had not reached the cut-off. Intratumoral treatment was administered on days 10, 13, 16 and 19 post-tumour induction. 1×10^7 $TCID_{50}$/mouse of live NDV or equivalent for γ-NDV was injected into tumours using a total volume of 50μL. An equivalent volume of PBS was used to inject control animals. For tumour endpoint analyses, tumours were induced as described above and mice were treated on days 10, 13 and 16. On day 20 mice were euthanised and tumours, spleens and draining lymph nodes were harvested and processed for flow cytometry.

4.2.11 Flow cytometry

Tumours were manually minced into small pieces then digested using a digestion buffer (1mg/mL collagenase 1A and 30 U/mL DNase in DMEM) for approximately 1 hour at 37°C with mixing every 20 minutes. Tumours, inguinal lymph nodes and spleens were then pushed through 70μm filters. RBCs in spleen and tumour samples were lysed. Cells were plated at 8×10^5 cells/well (tumours) or 1×10^6 cells/well (spleens and lymph nodes) in FACS buffer (PBS + 10mg/mL BSA + 0.04% NaN_3) and Fc receptors were blocked using mouse γ-globulin. Then, cells were stained for 1 hour at 4°C for different cell surface

molecules using fluorescent-labelled or biotinylated antibodies (see **Table 4.1)**. Where biotinylated antibodies were used, a secondary incubation with Streptavin-BV805 was performed for 20 minutes at 4°C. Live/dead staining was performed using near-infrared fixable dye (1:1000 dilution). Flow cytometry data was acquired on a Fortessa (BD Biosciences) and was analysed using FlowJo software (BD Biosciences). Cell frequencies are presented as % of viable cells or as total cells/mg of tumour.

4.2.12 ELISA

Sandwich ELISAs were performed to detect IFNα in mouse serum. 96-well ELISA plates (COSTAR) were coated with rat anti-mouse IFNα coating antibody (1:400 in Na_2HPO_4 buffer, Hycult Biotechnology). Plates were incubated overnight then washed with PBS + 0.05% tween then blocked for 2 hours with 2% skim milk (w/v) in PBS. IFNα standards (Hycult Biotechnology) were diluted to given known IFNα titres between 3.9-500 IFNα units/mL. 1:5 serial dilutions of mouse serum samples were carried out in blocking buffer. IFNα samples and standards were added to microtitre plates and incubated for 2 hours. Then, plates were washed and Rabbit anti-mouse IFNα primary antibody (1:250 dilution in blocking buffer, Sapphire Biosciences) was added and incubated for 2 hours. Plates were then washed, and horseradish peroxidase-conjugated secondary antibody was added to each well (goat anti-rabbit IgG-Peroxidase, Sigma). After a further 2-hour incubation, plates were washed then TMB colour developer (BD Biosciences) was added and plates incubated in the dark at RT for 30 minutes. Colour developer was stopped with 2M H_2SO_4.

To measure total IgG responses, maxisorp ELISA plates were coated with live whole-NDV (2×10^6 $TCID_{50}$/well) or KLH (500ng/well) in bicarbonate coating buffer (0.6% $NaHCO_3$, 0.303% Na_2CO_3 in MilliQ water, pH 9.6) and incubated overnight at room temperature. Plates were washed 3 × with 0.05% tween in PBS then blocked with 2% skim milk for 2 hours. Plates were washed again, then serial dilutions of serum collected from mice were added to the ELISA plate. 2 hours later plates were washed again and horseradish peroxidase conjugated goat-anti mouse IgG secondary antibody (1:10,000 dilution in blocking buffer, Thermo Scientific) was added. After 2 hours at room temperature unbound secondary antibody was washed away, and TMB peroxidase substrate was used to develop colour in the dark for 30 minutes. The reaction was stopped with 2M H_2SO_4. Absorbance of all ELISA plates were measured at 450nm using a Bio-Tek Instruments plate reader. IgG

titres were calculated as the reciprocal of the highest serum dilution that gave absorbance readings higher than those of naïve serum ± 3 standard deviations or as fold-increase relative to naïve serum.

4.2.13 Virus neutralisation

Vero cells or B16 cells were plated in 96-well flat-bottom microtitre plates at 6×10^4 cells/well and incubated at 37°C overnight. Live NDV was activated with 10μg/mL TPCK-trypsin at 37°C for 1 hour. Meanwhile, serum samples were heated-inactivated at 56°C for 30 minutes to inactivate complement. Serum samples were then serially diluted in PBS and added to activated NDV at a 1:1 ratio. Virus and serum was then added to cells at an MOI of 0.1 and incubated at 37°C for 2 hours to allow virus adherence. Plates were then washed 3 × with PBS and fresh DMEM + 1% P/S was added to each well. Plates were incubated at 37°C for 22 hours, then cells were fixed, stained and visualised as described in **Section 4.2.6**. To calculate neutralisation, the FITC-specific fluorescence and DAPI-specific fluorescence levels were both quantified using NIS elements software (Tokyo, Japan). The FITC-specific fluorescence readings were then normalised using the corresponding DAPI-specific readings, to account for small differences in total cell number between sample wells. A significant reduction in normalised FITC fluorescence for wells inoculated with immune-sera treated virus compared to naïve sera-treated virus was considered to indicate virus neutralisation. Where % neutralisation was analysed, the reduction in FITC-fluorescence in immune sera-treated samples was calculated relative to FITC-fluorescence in naïve sera-treated samples.

Table 4.1. Antibodies used in flow cytometry

Antigen	Fluorophore
CD45	BUV395
CD3	Biotin, then StrepBV805
CD4	BUV496
CD8	APC
NK1.1	PE

4.3 RESULTS

4.3.1 Development of γ-NDV vaccine

Egg grown NDV was clarified, concentrated, and exposed to a radiation dose of 50 kGy while frozen on dry ice. To ensure sterility, both live and γ-NDV were passaged three times in eggs and in tissue culture. No infectious virus was detected in eggs treated with γ-NDV at all three passages, in contrast to control live NDV (**Table 4.2**). Similarly, no infectivity was detected when the γ-NDV was passaged 3 times in tissue cultures in contrast to live NDV, as illustrated in **Figure 4.1** for passage 3. This confirms that 50 kGy is sufficient to inactivate NDV.

Previous studies have illustrated the ability of γ-radiation to produce vaccines with a high level of structural integrity. To assess if this is also the case for irradiated NDV, I examined the functional activity of the surface protein HN. I tested the possible effect of γ-irradiation on the ability of γ-NDV to cause haemagglutination. As shown in **Figure 4.2A**, γ-NDV retained high functional activity of HA protein as illustrated by the binding to sialic acid receptors on RBCs to cause haemagglutination, but this level of activity was slightly reduced compared to live NDV. Additionally, my data illustrate the ability of γ-NDV to utilise the neuraminidase activity of HN protein to cleave sialic acids at comparable levels to that observed for live NDV (**Figure 4.2B**). Despite the reduced level of haemagglutination, these data indicate that the structure of HN protein is well maintained. Finally, I used electron microscopy to observe the effects of γ-radiation on whole virion structure and the TEM images illustrated the structural integrity of γ-NDV (**Figure 4.2C**). The TEM images demonstrate the high variability in virion size, which is expected for NDV. Overall, my data suggest that γ-NDV is structurally intact and the surface proteins have normal functions, indicating that γ-NDV could be used as a vaccine candidate to induce strong immune responses.

4.3.2 Immune responses to γ-NDV

Mice were vaccinated intramuscularly with γ-NDV to align with current vaccination routes in chickens [247]. Two vaccinations were carried out three weeks apart, with 6.4×10^6 $TCID_{50}$-equivalent of γ-NDV per mouse. Serum samples were collected 20 days after the first immunisation, and again three weeks after the second vaccination. Presence of NDV-

specific IgG was determined by direct ELISA, with titres being calculated relative to naïve serum (**Figure 4.3A**). My data indicate that IgG titres are relatively low after one dose of γ-NDV. However, after a booster dose of γ-NDV, the IgG titres were significantly higher. Surprisingly, this increase in IgG responses did not correlate with an increase in neutralising titres, as there was no significant reduction in live NDV infection following treatment of NDV with immune sera prior to infecting monolayers of Vero cells compared to NDV treated with naïve serum (**Figures 4.3B and 4.3C**).

In order to enhance neutralising antibody responses, I investigated the possibility of co-administering γ-NDV and γ-Flu. Our previous publications have demonstrated the adjuvant activity of γ-Flu when co-administered with other γ-irradiated vaccines [199, 200]. To test the broader applicability of γ-Flu as an adjuvant, I investigated the ability of γ-Flu to enhance the immunogenicity of keyhole limpet hemocyanin (KLH), which is a well-documented poorly immunogenic protein. Several immunisation routes were tested including intramuscularly, intranasally and sub-cutaneously. Mice were immunised twice at 2 weeks intervals and immune sera was tested for KLH specific antibody responses. I found that a single dose of γ-Flu was able to vastly increase IgG responses to KLH when given intramuscularly and intranasally (**Figure 4.4A**), and subcutaneous γ-Flu enhanced responses to KLH after 2 doses (**Figure 4.4B**). This shows the strong adjuvant ability of γ-Flu.

Next, I tested the ability of γ-Flu to enhance the immunogenicity of γ-NDV, particularly in relation to the ability of γ-NDV to induce neutralising antibody responses. Mice were immunised intramuscularly with γ-NDV only or γ-NDV + γ-Flu and serum samples were collected 3 weeks later. Surprisingly, no significant increase in NDV-specific IgG titres was detected following co-administration of γ-NDV + γ-Flu in contrast to vaccination with γ-NDV only (**Figure 4.5A**). Considering that the adjuvant activity of γ-Flu was previously reported to be associated with an enhanced type I interferon signalling, I measured IFNα levels in mice immunised with γ-Flu, γ-NDV or γ-NDV + γ-Flu. My data show that γ-NDV did not induce IFNα responses in mice. Surprisingly, while I expected the ability of γ-Flu to induce IFNα responses to provide adjuvant activity to γ-NDV, my data indicated that IFNα levels following co-vaccination with γ-Flu + γ-NDV were actually lower compared

to administration of γ-Flu alone (**Figure 4.5B**). The inhibition of innate signalling by γ-NDV may explain the inability of γ-Flu to provide adjuvant activity to γ-NDV. A potential mechanism to explain the observed reduction in IFNα levels is the competition between γ-NDV and γ-Flu to bind to same host receptors.

In order to circumvent competition for receptor binding between γ-Flu and γ-NDV, other commonly used adjuvants were tested. Mice were vaccinated twice 2 weeks apart with γ-NDV alone or with IFA, alum, poly(I:C) or γ-Flu as an adjuvant. Serum samples were collected 2 weeks after the first and second vaccinations and tested for NDV-specific antibody responses. As shown in **Figure 4.6**, IgG responses were enhanced when γ-NDV was co-administered with IFA and alum. In contrast, both poly(I:C) and γ-Flu did not enhance the immunogenicity of γ-NDV (**Figure 4.6**). Given the enhanced IgG responses, I also measured neutralising antibody responses by FFIA to determine whether adjuvantation was able to improve neutralising responses. Serum from mice vaccinated twice with the different groups was used to measure neutralisation. Interestingly, despite the enhanced IgG responses following vaccination with γ-NDV + IFA or alum, I did not detect any neutralising antibody responses (**Figure 4.7**). There was no significant difference in normalised FITC-fluorescence (indicative of NDV replication) when comparing serum from mice treated with γ-NDV only to any of the adjuvanted groups.

4.3.3 γ-NDV as an oncolytic virotherapy

Based on the high structural integrity of γ-NDV paired with the lack of neutralising antibody responses, I investigated the possibility of using γ-NDV as a novel oncolytic sterile virotherapy. Usually repeated treatments are used for virotherapy administration. Thus, I administered 4 doses of live or γ-NDV, then collected serum and measured antibody responses. I detected similar IgG levels after repeat intravenous injections of live and γ-NDV, and importantly confirmed that live NDV is able to induce far stronger neutralising antibody responses than γ-NDV (**Figures 4.8A** and **4.8B**). In fact, my data illustrate that immune serum harvested from mice that received 4 doses of live NDV was able to almost completely neutralise NDV. However, in γ-NDV treated mice the neutralisation was less than 20%. This reduction in neutralising antibody responses highlighted the possibility of using γ-NDV as a novel oncolytic sterile virotherapy.

An initial screen of 11 murine and human cancer cells was performed and in vitro oncolysis was measured using an MTT assay. My data illustrate the effectiveness of γ-NDV against a range of different cancers including solid tumours and blood cancers (**Table 4.3**). Cytotoxicity of live and γ-NDV was shown at 24-48 hours for B16, 4T1.2, PC3 and RD cells (**Figure 4.9**). Syncytia formation is a possible mechanism for oncolysis and based on the high structural integrity of γ-NDV it is expected that γ-NDV would be able to fuse with host cells and induce syncytia formation among adjacent cells. This was confirmed using B16 cells and 4T1.2 cells (**Figure 4.10**), but minimal morphological changes were observed for Vero cells (**Figure 4.10**), which is a non-cancerous cell line. This demonstrates the specificity of γ-NDV to cancer cells. These assays were performed *in vitro*, and so only demonstrate the direct killing of cancer cells by γ-NDV.

The indirect mechanisms of oncolysis during virotherapy involve activation of both innate and adaptive immunity and the recruitment of immune cells to the tumour microenvironment. These responses are expected to be relevant to the potential use of γ-NDV as an oncolytic therapy. B16 cells as a relevant murine melanoma model was selected to investigate γ-NDV-mediated oncolysis *in vivo*. In this model, B16 cells were injected subcutaneously into 8-10 week-old C57BL/6J mice. Mice were then treated intratumourally with live NDV or γ-NDV on days 10, 13, 16 and 19 post-tumour induction. Injection of PBS was used as a negative control. Tumour size was measured every 2nd day and presented in **Figure 4.11A**. Importantly, while tumour growth was delayed in mice treated with live and γ-NDV, treatment with γ-NDV appeared to be more effective than treatment with live NDV based on a significant reduction in tumour sizes at an earlier time points observed for mice treated with γ-NDV compared to mice treated with live NDV. Mice were humanely euthanised when tumour size reached 100mm^2 and overall survival was plotted and presented in **Figure 4.11B**. Notably, a significantly higher percentage of mice treated with γ-NDV (43%) and live NDV (29%) survived compared to mice with untreated melanomas, where no mice survived past day 21. Furthermore, when survival time was considered, a significantly prolonged survival time was observed in both treatment groups (live and γ-NDV) when compared to untreated mice (**Figure 4.11C**). The mean survival time for untreated mice was 17.6 days compared to 22.4 and 24.5 days for mice treated with live and γ-NDV, respectively. We detected no significant differences in

survival when comparing live NDV and γ-NDV treatment, suggesting that γ-NDV may be a viable alternative to enhance safety.

Previous studies have demonstrated that an important mechanism of NDV-mediated oncolysis is through activation and recruitment of immune cells to the tumour microenvironment. Consequently, I investigated cell-mediated immune responses following treatment of melanomas with live or γ-NDV. B16 cells were injected subcutaneously into C57BL/6J mice and were subsequently treated with live NDV, γ-NDV or PBS on days 10, 13 and 16 post-tumour induction. On day 20 tumours, spleens and draining lymph nodes were harvested and processed for flow cytometry. Gating strategy is shown in **Supplementary Figure 1**. Total tumour-infiltrating lymphocytes ($CD45^+$) were measured in all three tissues (**Figure 4.12**). Interestingly, when considering the proportion of live cells, there was a significant increase in lymphocytes in live NDV-treated tumours (**Figure 4.12A**). Interestingly, while the proportion of lymphocytes as a percentage of live cells was comparable between γ-NDV- and PBS-treated tumours (**Figure 4.12A**), there was a trend towards increased tumour-infiltrating lymphocytes (TILS) in γ-NDV treated tumours when considering the total number of cells within the tumour (**Figure 4.12B**). There were no significant differences in the proportion of lymphocytes in the inguinal lymph node or spleens (**Figure 4.12C** and **Figure 4.12D**).

Further analysis attempted to deduce the types of lymphocytes within the tumour. Flow cytometry was used to measure T cells ($CD45^+$ $CD3^+$), T_H cells ($CD45^+$ $CD3^+$ $CD4^+$) and CTLs ($CD45^+$ $CD3^+$ $CD8^+$). My data show an increased proportion of T cells in tumours treated with live NDV, and proportion of $CD4^+$ T cells in both live and γ-NDV-treated tumours (**Figure 4.13**). Furthermore, when considering total cell number within the tumour there was a trend towards increased T cells in γ-NDV-treated melanomas compared to melanomas treated with live NDV or PBS, however this trend did not reach statistical significance. Interestingly, I observed a decrease in T cells within the spleen of both live NDV and γ-NDV treated mice, which was statistically significant for γ-NDV treatment (**Figure 4.13**). This may suggest that T cells are migrating from the spleen to γ-NDV-treated tumours. There were no overall changes in T cell numbers within the draining lymph node.

NK cells are an important component of anti-cancer immunity and previous studies have demonstrated that NK cells can be activated by NDV. I used flow cytometry to measure NK cells ($CD45^+$ $NK1.1^+$). The proportion of NK cells within the tumour was comparable between groups (**Figure 4.14A**). However, there did appear to be an increase in total NK cells in γ-NDV-treated tumours. Again, this was not statistically significant (**Figure 4.14B**). The proportion of NK cells in the draining lymph nodes and spleens were also comparable between groups (**Figure 4.14C** and **Figure 4.14D**). Overall, this data does not compellingly implicate any cell type as mediating the reduction of tumour size and increased survival in mice treated with γ-NDV observed in **Figure 4.11**, but may be due to infiltration of lymphocytes into the tumour.

In addition to analysing cellular responses following oncolytic therapy, serum samples from treated mice were harvested at day 20 and tested for the ability to neutralise NDV. Live NDV was treated with pooled serum samples from mice treated with live NDV, γ-NDV or PBS and a FFIA was performed in Vero and B16 cells (**Figure 4.15**). Surprisingly, we found that serum collected from tumour-bearing C57BL/6 mice treated with live and γ-NDV was able to neutralise live NDV to prevent infection in both cell types. This is contradictory to our earlier data that showed limited neutralising efficacy in mice treated with γ-NDV (**Figures 4.3**, **4.7** and **4.8**). It is important to note that C57BL/6J mice were used in **Figure 4.15**, whereas previous studies used BALB/c mice. Furthermore, in the B16 model mice received 1×10^7 $TCID_{50}$-equivalent/mouse at 3 time points, 3 days apart, and the high dose used in **Figure 4.8** was 2×10^7 $TCID_{50}$-equivalent/mouse at 4 times points, 2 weeks apart. These differences in experimental design my influence the ability of mice to induce neutralising antibody responses.

4.4 DISCUSSION

γ-NDV was initially developed as a poultry vaccine and surprisingly did not induce neutralising antibody responses. IgG antibodies are important for neutralisation, however the specific IgG subclasses that mediate this appear to differ between virus types. IgG1 appears to be important for neutralisation of West Nile virus [338], whereas IgG3 and IgG4 are important for herpes simplex virus [339] and IgG1 and IgG3 are important for human immunodeficiency virus neutralisation [340, 341]. The subclasses important for NDV neutralisation have not been elucidated.

We have previously shown that highly maintained structural integrity translates to strong immunogenicity of γ-irradiated vaccines [23]. Interestingly, I did not observe that for γ-NDV, even though structural integrity was well maintained (**Figure 4.2**). In fact, I observed strong IgG responses in response to γ-NDV immunisation, but these did not translate to functional neutralisation of live virus (**Figure 4.3**). Infection of chickens and mice with NDV induces both antibody [205, 235] and T cell responses [235, 236]. However, chickens lacking antibody responses do not survive a challenge with virulent NDV, whereas chickens lacking T cells do [237]. This suggests that antibody responses are essential for NDV survival in vaccinated birds. This indicates that γ-NDV may not be a suitable vaccine candidate.

Importantly, my data show no enhancement of neutralising antibody responses despite administering γ-NDV with different adjuvants (**Figures 4.5 – 4.7**). Poly(I:C) and γ-Flu provide adjuvantation in a similar manner through stimulation of IFN-I responses [69, 342], whereas alum and oil adjuvants act as stabilisers and can help recruit immune cells to the immunisation site [189, 343]. Furthermore, alum shifts the immune responses to a T_H2 response that is characterised by enhanced antibody responses [189, 344, 345]. The underlying cause of the lack of neutralising antibody responses in mice treated with γ-NDV has not been elucidated. Nonetheless, while γ-NDV may not be a suitable poultry vaccine, it does open an avenue for the use of γ-NDV as an oncolytic virotherapy.

Despite major advances in cancer treatment, the prognosis of some cancers has not improved in recent years. The use of virotherapy to target cancers is a promising area of research, however there are health and biosecurity risks associated with using pathogenic viruses in humans. Virotherapies are further limited by viral clearance through neutralising antibody responses. The use of virulent NDV as an oncolytic therapy has been halted due to associated outbreak risks in domestic poultry [337]. Alternative NDV therapies have involved using attenuated strains [346], although non-lytic strains are less effective against cancer cells [347]. γ-NDV represents a unique approach where inactivated virus can be used as a virotherapy. **Table 4.2** and **Figure 4.1** shows that γ-NDV is completely sterile and does not recover viability after multiple passages, meaning it could be safety administered in humans without an outbreak risk.

The killing of cancer cells *in vitro* showed direct oncolysis induced by γ-NDV. In mammalian cells, NDV is a potent activator of innate signalling, which can lead to the activation of both intrinsic and extrinsic apoptotic pathways. Pro-apoptotic signalling molecules induced in cancer cells by live NDV include IFNα [254], TRAIL [255], TNFα [256], and IFNβ [257]. HN binding to sialic acid on host cells appears to be important for oncolysis as a loss of sialic acids on the cell surface can impair oncolytic activity [348]. Furthermore, neuraminidase inhibitors can block the activation of NK cells, indicating that the cleavage of sialic acids is also important for oncolytic activity [349].

The ability of γ-NDV to bind to cellular receptors (**Figure 4.2A**) and cleave sialic acids (**Figure 4.2B**) supports the oncolytic potential of γ-NDV. Similarly, studies have shown that surface antigens HN and F when expressed on the surface of tumour cells [259, 349-351] or CEF DF1 cells [351] will lead to cell death. This is abrogated by HN-specific neutralising antibodies, but not F protein neutralising antibodies [350]. Although, interestingly, an NDV strain with a more widely activated F protein was more effective at inducing syncytia and lysing cancer cells [352] and so the F protein does indeed contribute to oncolysis. Syncytia formation (**Figure 4.11**) by γ-NDV demonstrates efficacy of both HN and F proteins and syncytia contribute to cell death and immune stimulation [353, 354]. Membrane-bound HN appears to be important for HN-induced oncolysis, however limited oncolysis is still observed with cytoplasmic and secreted HN [258]. M protein alone has also been shown to be oncolytic [260]. M protein has a BH3 domain that shares homology with Bcl2 proteins. This enables the M protein to interact with Bax and activate the intrinsic pathway of apoptosis [260]. However, Bax-knockout cells are still apoptosed by NDV [355].

The importance of HN is further accentuated by the upregulation of sialic acids in some cancers (reviewed in [261]), allowing a mechanism for NDV to specifically target cancer cells. Furthermore, enhanced sialic acids on cancer cells has been identified as a cause of chemotherapy resistance, specifically cis-platin resistance [356] and suggests that NDV could specifically target resistant cancer cells. Indeed, live NDV is an effective treatment in cis-platin resistant A549 cells [351, 357], and we have demonstrated here that γ-NDV is also effective in the same A549 cell line (**Table 4.3**). The susceptibility of chemotherapy resistant cells to NDV could be utilised to develop combination therapies wherein NDV is

co-administered with cis-platin. Overall, the ability of different individual proteins to induce oncolysis suggests a multi-faceted mechanism of oncolysis.

Indirect mechanisms of oncolysis may play a further role in oncolysis via the activation and recruitment of immune cells to tumour sites. Oncolytic NDV has an immune stimulatory effect and is able to recruit cells to the tumour microenvironment. Whilst the direct killing of B16 cells by γ-NDV is not as effective as live NDV *in vitro* (**Figure 4.9**), my data illustrated a similar behaviour of both treatments when directly compared in an animal model (**Figure 4.11**). Importantly, I observed a higher proportion of lymphocytes in NDV-treated tumours, and a trend towards infiltration of lymphocytes into γ-NDV-treated tumours (**Figure 4.12**). The presence of tumour-infiltrating lymphocytes (TILs) is associated with enhanced cancer prognosis in patients [358, 359]. I also analysed NK and T cells. Both cell types have previously shown to be important in NDV oncolytic virotherapy [360-362], and depletion of NK cells and T cells abrogates oncolysis in an HSV intracranial metastatic melanoma model [363]. There was a trend towards increased T cells (**Figure 4.13**) and NK cells (**Figure 4.14**) in the tumour after treatment with γ-NDV, however this data was not significant. Interestingly, I detected significantly higher T_H cells in tumours treated with live NDV and γ-NDV (**Figure 4.13**). $CD4^+$ T cells may be important for establishing a memory response against tumour reoccurrence [364].

Interestingly, I detected neutralising antibody responses against NDV in mice with tumours that had been treated with live and γ-NDV (**Figure 4.14**), despite consistently not detecting neutralising responses in previous assays (**Figures 4.3, 4.7 & 4.8**). The NDV tumour experiments utilised the B16 melanoma model, which requires C57BL/6 mice [365]. It is important to note that I used BALB/c mice as a pre-clinical model for developing an NDV vaccine because NDV is able to cause clinical infection in BALB/c mice [205]. Previous studies have demonstrated a difference in antibody kinetics between BALB/c and B6 mice [366-368]. Indeed, this could be the underlying factor for the observed differences in neutralising antibody responses and this will be further elucidated in future studies. The difference in neutralising antibody responses may also be caused by inflammatory responses within the tumour microenvironment. Regardless, both treatments were successful in treating B16 tumours and γ-NDV may indeed be a good vaccine candidate when tested in chickens, a more suitable animal model.

Despite using V4, a lentogenic strain, there was effective oncolysis with both live and irradiated NDV, with γ-NDV outperforming live NDV in a B16 tumour model. This proof-of-concept can also be applied to highly virulent strains that are expected to elicit stronger immune responses but cannot be used due to current biosecurity regulations. Importantly, this study demonstrates that NDV does not need to replicate to induce an oncolytic effect. In fact, Zamarin et al [262] found reduced growth in secondary tumours after treatment of the primary tumour with NDV, even though no viral RNA was detected in the secondary tumour site.

4.5 FIGURES

Table 4.2. Sterility testing of γ-NDV in embryonated chicken eggs. 10-day-old embryonated chicken eggs were inoculated with live NDV, γ-NDV or PBS then incubated for 48 hours at 37°C. Allantoic fluid was then harvested and used to infect fresh 10-day-old eggs (Passage 2). This was repeated for a 3rd Passage. Harvested allantoic fluid was then tested for NDV infection by haemagglutination assay ("+" indicates allantoic fluid could haemagglutinate RBCs and "-" indicates no haemagglutination). 5 eggs were infected per group per passage.

	Passage 1	**Passage 2**	**Passage 3**
Live NDV	+++++	+++++	+++++
γ-NDV	- - - - -	- - - - -	- - - - -
PBS	- - - - -	- - - - -	- - - - -

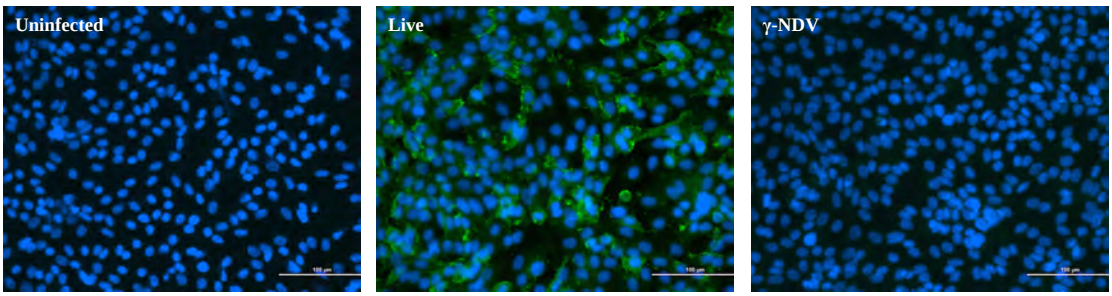

Figure 4.1. Sterility testing of γ-NDV in Vero cells. Live and γ-NDV were activated with 1μg/mL trypsin at 37°C for 1 hour. Vero cell monolayers were then treated with the preparations at MOI of 40 and incubated for 24 hours. As a control, monolayers were also treated with allantoic fluid from uninfected 12-days old embryonated eggs. Supernatant was collected and used to infect fresh Vero cell monolayers and incubated for a further 24 hours. This was then repeated for a third passage, and cells were then fixed and stained with DAPI to visualise cell nuclei and treated with chicken anti-NDV and anti-chicken IgY FITC-conjugated antibodies to visualise NDV-infected cells. Infection levels of Passage 3 are shown here. Images are representative of 3 wells per sample, and 2 independent experiments.

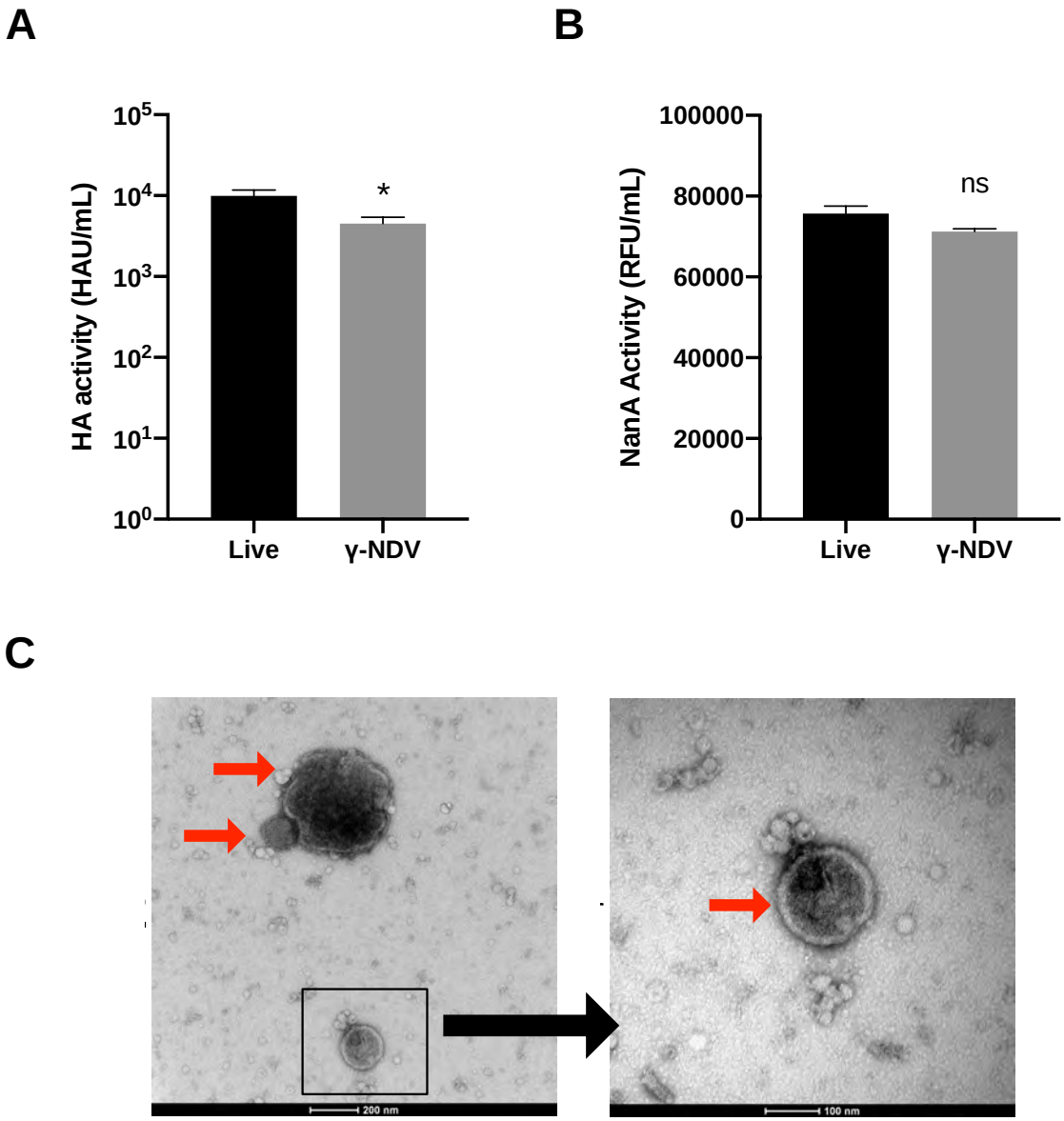

Figure 4.2. Structure of NDV is maintained after γ-irradiation. NDV was inactivated by exposure to 50 kGy of γ-radiation and the (A) neuraminidase activity, (B) haemagglutinin activity and (C) whole virion structure were analysed. Haemagglutinin activity was measured by the ability of the virus to agglutinate RBCs. Neuraminidase activity was measured by cleavage of 4-MUNANA into the fluorescent substrate 4-MU. The relative fluorescent intensity was then measured for each sample. Live NDV was used as a positive control. For whole virion structure, γ-NDV was imaged using a transmission electron microscope. Red arrows indicate NDV virions and black arrow indicates area enlarged for the second panel. Quantitative data is expressed as mean ± SEM (n = 3, collated from 2 independent experiments). Data was analysed by one-way ANOVA (* $p < 0.05$).

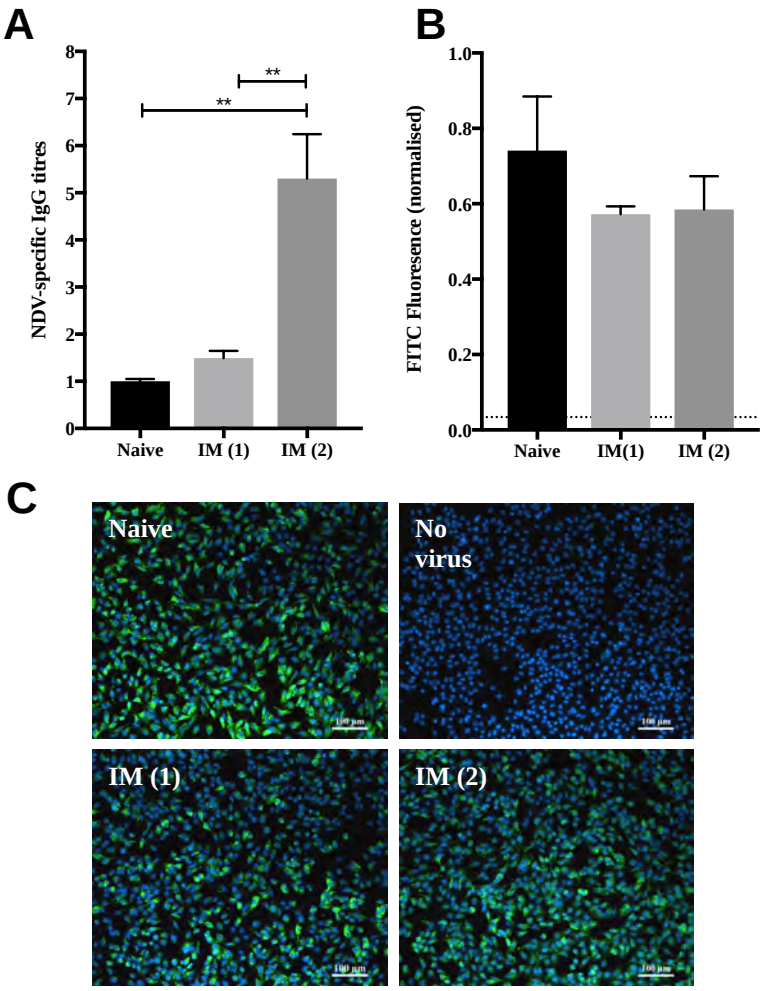

Figure 4.3. γ-NDV does not induce neutralising antibody responses. 6-8-week old BALB/c mice were immunised intramuscularly with two doses of γ-NDV three weeks apart or were unvaccinated as controls and serum samples were collected 20 days after each vaccination. (A) NDV-specific IgG responses were determined by direct ELISA. (B) Neutralising antibody responses were determined by focus forming inhibition assay. Live virus was pre-treated with pooled immune serum from 5 mice, then added to monolayers of Vero cells at an MOI of 0.1 and allowed to attach for 2 hours. Cells were then washed and incubated with a fresh media for a further 22 hours. Cells were fixed and stained with a chicken anti-NDV antibody and a FITC-conjugated anti-chicken IgY secondary antibody. A fluorescence microscope was used to quantify FITC-fluorescence (representative of NDV infection) relative to DAPI-fluorescence (cell nuclei). (C) Representative images were also taken of each sample at a 1:10 serum dilution (representative of 3 wells tested per serum group). Quantitative data was presented as mean ± SEM and analysed by one-way ANOVA (** $p < 0.01$).

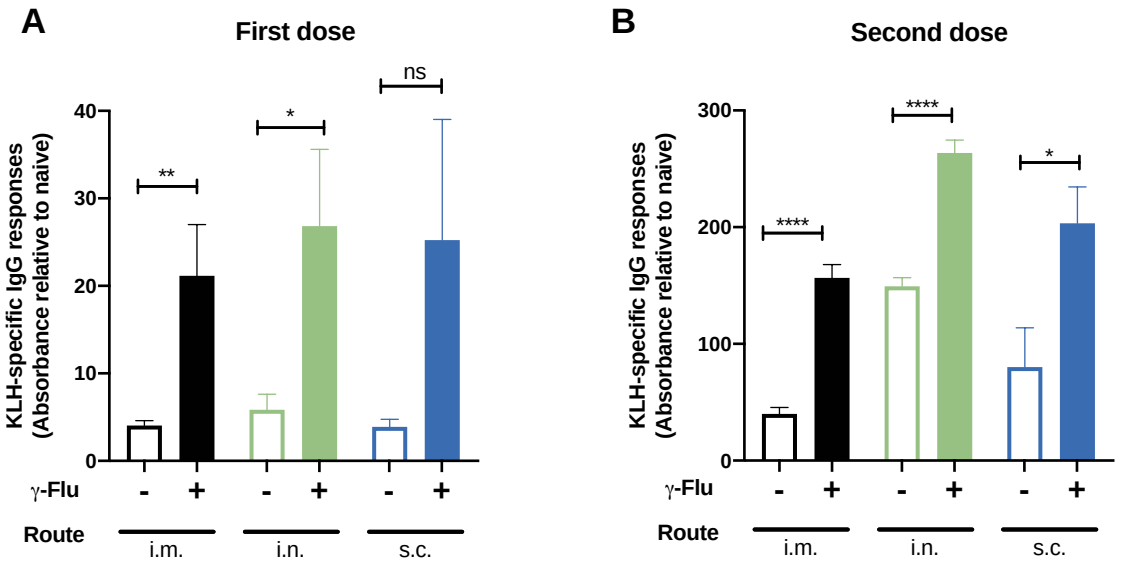

Figure 4.4. γ-Flu provides adjuvant activity to keyhole limpet hemocyanin. BALB/c mice were immunised intramuscularly (i.m), intranasally (i.n) or subcutaneously (s.c) with 50μg KLH/mouse with or without γ-Flu (1×10^6 $TCID_{50}$-equivalent/mouse). Mice received 2 doses at 3 weeks intervals and serum samples were collected (A) 20 days post 1st vaccination or (B) 2nd vaccination. KLH-specific IgG titres were measured by ELISA and fold-increase relative to naïve serum was used as IgG titres. Data is presented as mean ± SEM (n = 5) and was analysed by one-way ANOVA (* $p < 0.05$, ** $p < 0.01$, **** $p < 0.0001$, ns = not significant).

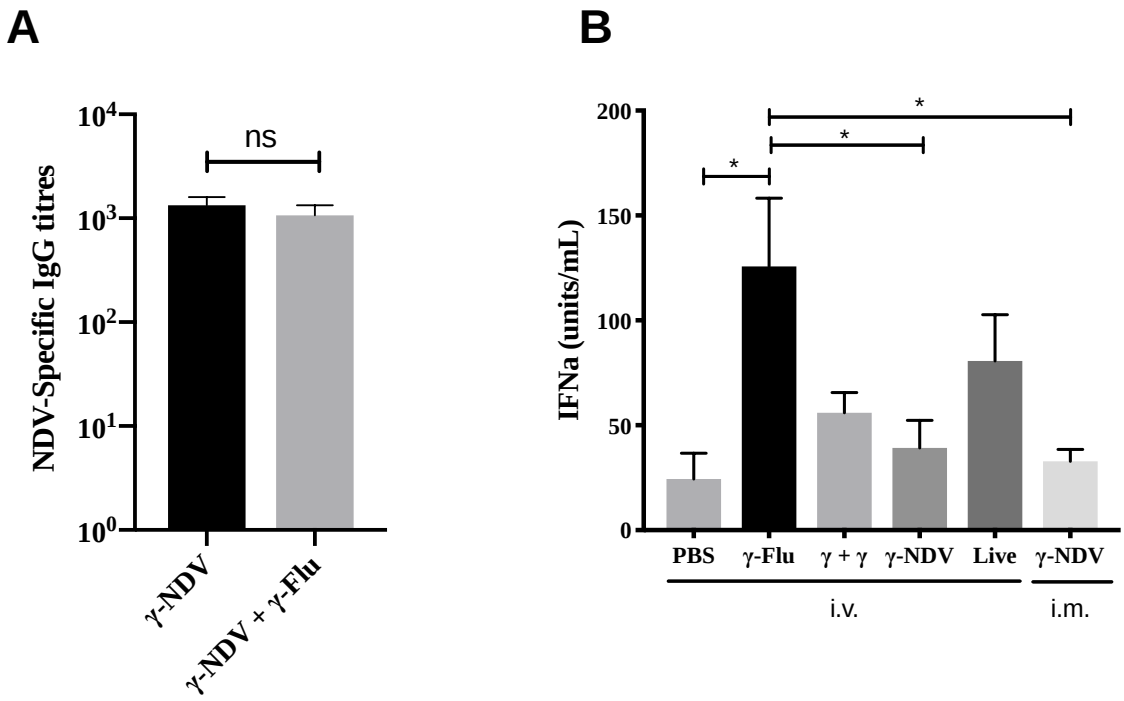

Figure 4.5. Co-administration of γ-Flu and γ-NDV does not enhance immune responses. (A) BALB/c mice were vaccinated intramuscularly with γ-NDV with or without γ-Flu. Three weeks later serum samples were collected, and NDV-specific IgG responses were measured by direct ELISA. (B) Serum samples were collected 24-hours after intravenous (i.v) or intramuscular (i.m) administration of γ-Flu, γ-Flu + γ-NDV (γ + γ), γ-NDV, or live NDV (Live). IFNα responses to vaccine preparations were determined by Sandwich ELISA. Data is presented as mean ± SEM (n = 5) and was analysed by one-way ANOVA (ns = not significant, * $p < 0.05$).

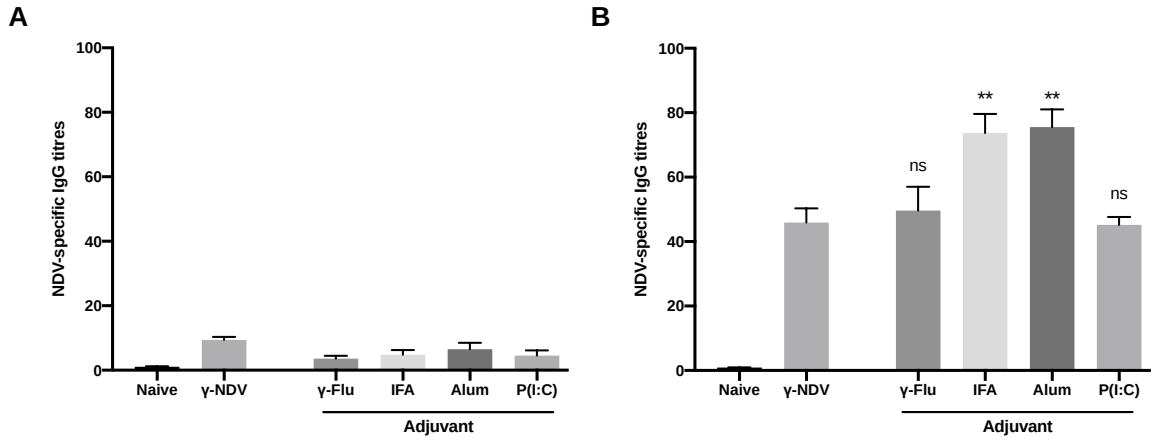

Figure 4.6. The effect of different adjuvants on IgG responses to γ-NDV. BALB/c mice were vaccinated twice 2 weeks apart with γ-NDV alone or γ-NDV mixed with different adjuvants; γ-Flu, incomplete Freund's adjuvant (IFA), aluminium hydroxide (Alum) or poly(I:C) (P(I:C)). Serum samples harvested (A) 2 weeks after the 1st vaccination and (B) the 2nd vaccination were tested for NDV-specific IgG responses using direct ELISA. Data is presented as mean ± SEM (n = 5, compiled from two independent experiments) and was analysed by one-way ANOVA and adjuvanted IgG responses were compared to IgG responses generated by γ-NDV alone (** $p < 0.01$).

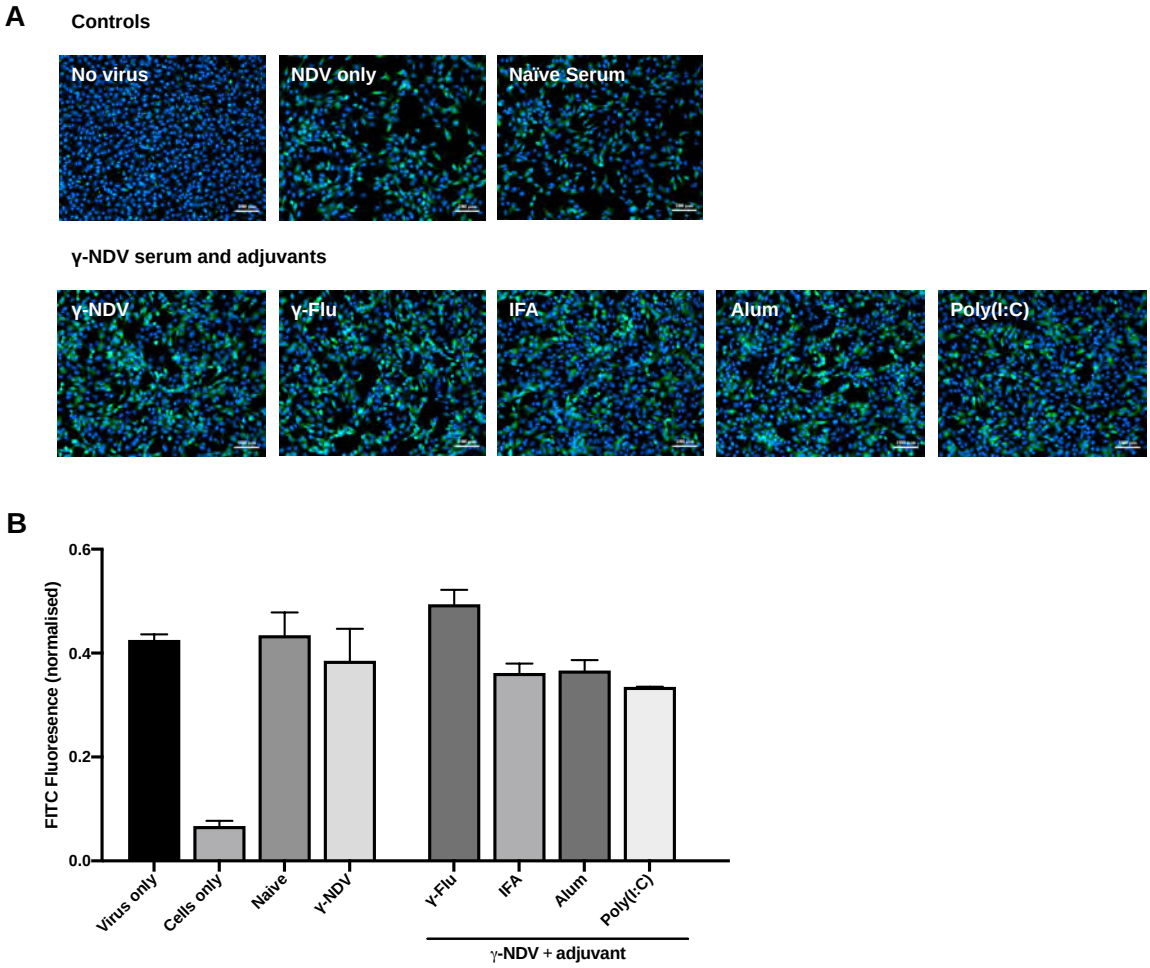

Figure 4.7. γ-NDV does not induce neutralising antibody responses despite the use of adjuvants. BALB/c mice were vaccinated twice intramuscularly with γ-NDV ± adjuvants. Two weeks after the second immunisation serum was harvested. Live NDV was pre-treated with serum samples in triplicate then added to confluent monolayers of Vero cells. Virus was allowed 2 hours to attach then plates were washed, fresh media was given, and plates were incubated for a further 22 hours. Cells were fixed then stained and visualised using DAPI-fluorescence (cell nuclei) and FITC-fluorescence (NDV infection). (A) Images of each well were taken at a 1:10 serum dilution. (B) FITC-fluorescence relative to DAPI-fluorescence was quantified. Data is presented as mean ± SEM and was analysed by one-way ANOVA. There is no significant neutralisation when comparing live virus only or naïve serum to any of the serum groups from vaccinated mice.

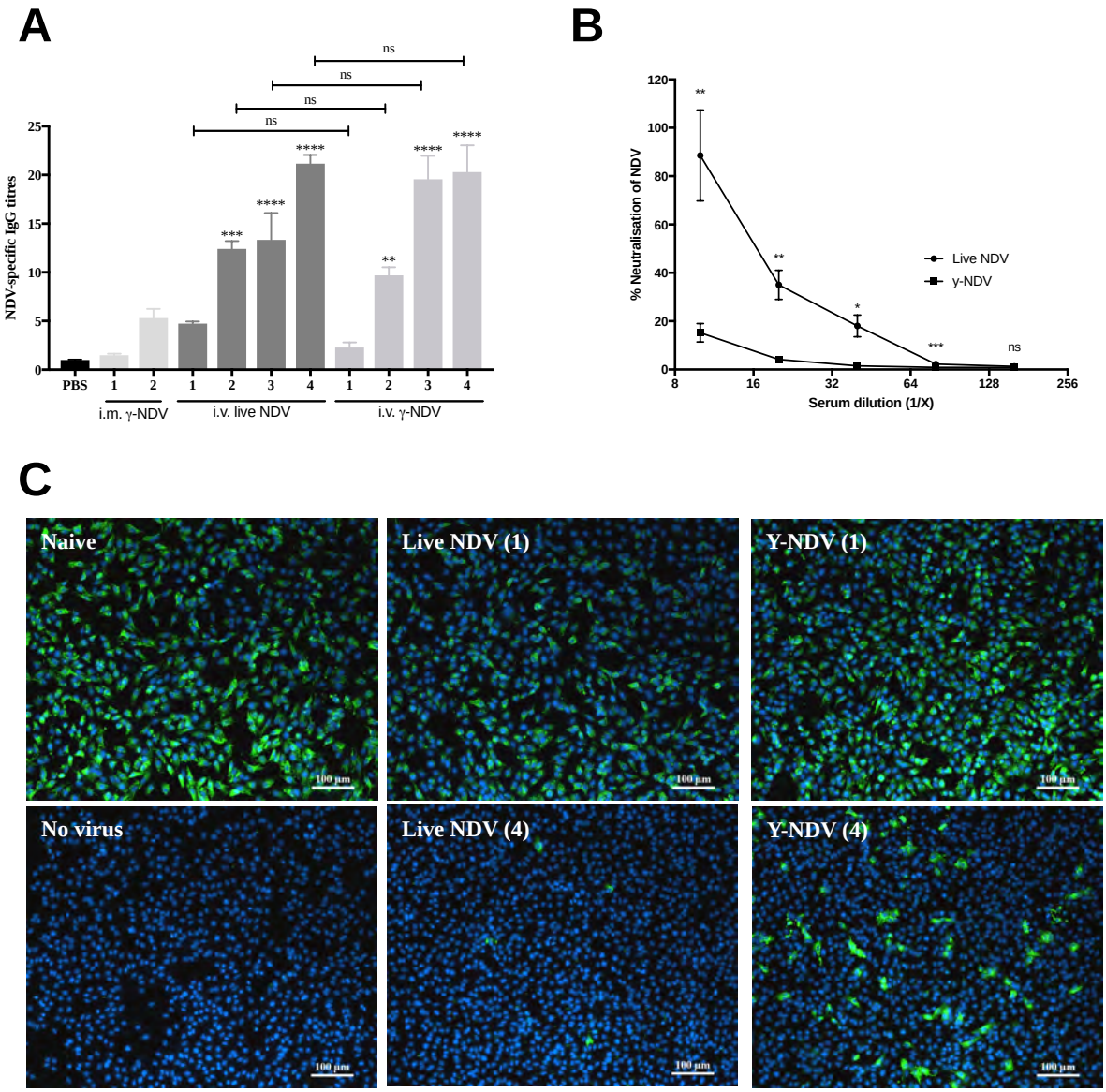

Figure 4.8. Neutralising antibody responses after repeated immunisations with γ-NDV. BALB/c mice were immunised intramuscularly 2 times with γ-NDV or intravenously up to 4 times with live or γ-NDV. (A) NDV-specific IgG responses were measured by direct ELISA. (B) % neutralisation of live NDV by serum from mice immunised 4 times i.v with live or γ-NDV was measured by comparing FITC-fluorescence in naïve sera-treated samples versus immune sera-treated samples. (C) Representative images of a reduction in foci after virus treatment with sera (at a 1:10 dilution) from i.v immunised mice (after vaccination with 1 or 4 doses of live or γ-NDV, as indicated in each panel). Data is presented as mean ± SEM (n = 4) and was analysed by one-way ANOVA (* $p < 0.05$, ** $p < 0.01$, *** $p < 0.001$, **** $p < 0.0001$).

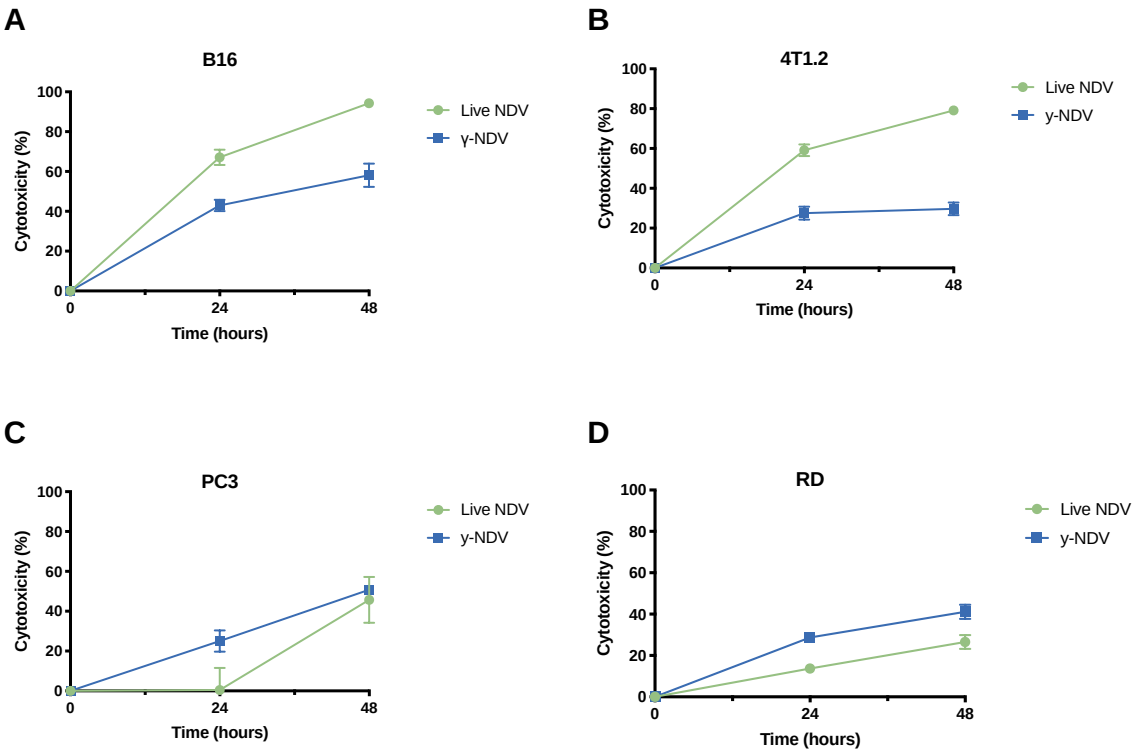

Figure 4.9. Cytotoxicity of live and γ-NDV in mouse and human cancers. Cell monolayers were established and treated with live or γ-NDV (MOI = 20). MTT staining was used to measure cell death in (A) mouse melanoma B16 cells, (B) mouse breast cancer 4T1.2 cells, (C) human prostate cancer PC3 cells, and (D) human muscle cancer RD cells. Absorbance was measured at 562nm and cytotoxicity was measured using the formula [100 – (absorbance treated cells/absorbance untreated cells)]. Cytotoxicity was presented as mean ± SEM (n = 3).

Table 4.3. Cytotoxicity of γ-NDV in different cancer cell lines. Cells were treated with γ-NDV or untreated (control). MTT assay was performed 48 hours later and used to calculate cytotoxicity.

Cell line	Description	Cytotoxicity at 48 hours (%)
C32	Human melanoma	28.9 ± 2.00
MDA	Human breast cancer	44.0 ± 2.51
PC3	Human prostate cancer	50.8 ± 1.85
RD	Human muscle cancer	41.1 ± 4.89
A549	Human lung cancer	22.1 ± 7.43
HL-60	Human leukaemia	41.8 ± 6.49
B16	Mouse melanoma	49.9 ± 8.29
4T1.2	Mouse breast cancer	29.7 ± 5.45
EL-4	Mouse T cell lymphoma	65.8 ± 0.45
L1210	Mouse B cell leukaemia	33.1 ± 3.02
P815	Mouse mastocytoma	9.43 ± 3.56

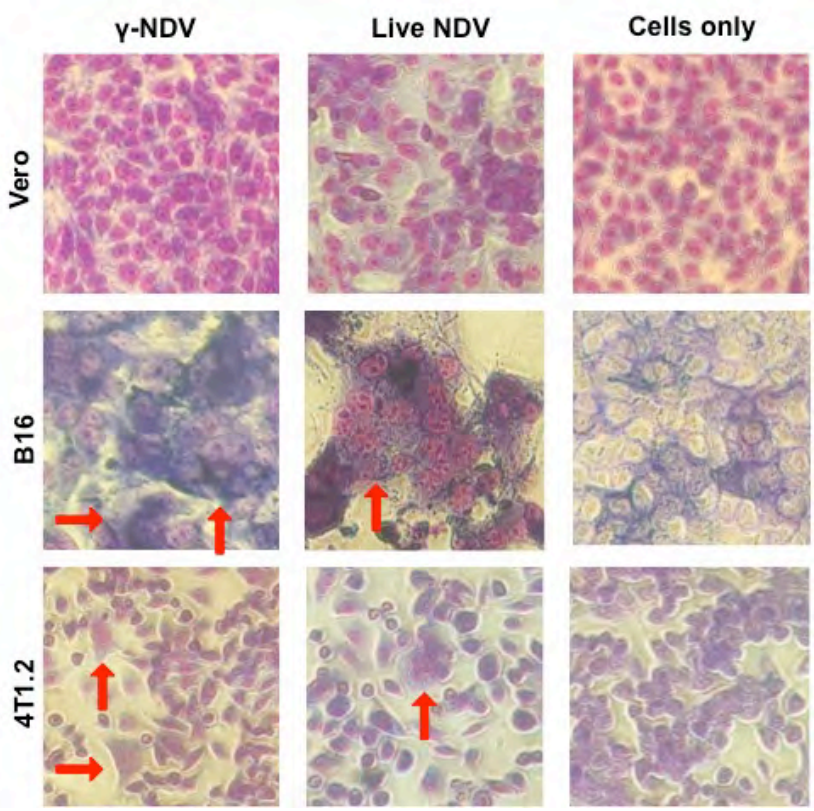

Figure 4.10. Syncytia formation is induced by γ-NDV. Vero, B16 and 4T1.2 cell monolayers were treated with live or γ-NDV, or untreated as controls. Cells were incubated for 24 hours then fixed with methanol and stained with Giemsa to visualise multi-nucleated cells. Syncytia are indicated by red arrows and evident in B16 cells and 4T1.2 cells treated with live NDV and γ-NDV, but not Vero cells.

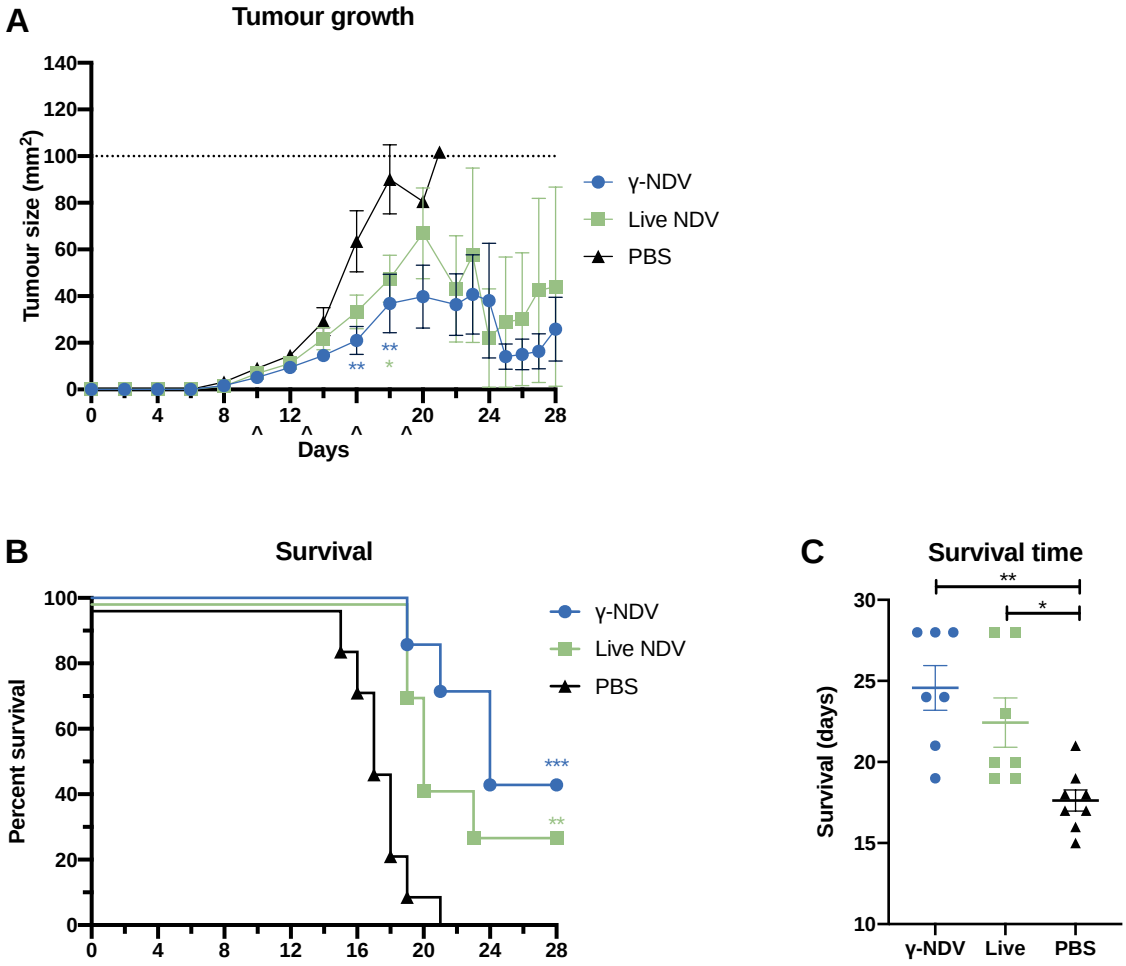

Figure 4.11. Treatment of B16 tumours with γ-NDV. B16.F10 cells were injected subcutaneously into C57BL/6Jmice. Tumours were treated with live NDV, γ-NDV or PBS on days 10, 13, 16 and 19 (indicated by ^). (A) Tumours became palpable at day 8 and were measured every 2nd day with callipers. Mice were humanely euthanised when tumour size reached 100mm^2. (B) Overall survival was plotted and (C) survival time in days was measured. Surviving mice were euthanised at day 28 post-tumour induction. Data is presented as mean ± SEM (n = 7-8). For (A) and (C) data was analysed by one-way ANOVA comparing all groups. For survival analysis a Mantel-Cox test was used (* $p < 0.05$, ** $p < 0.01$, *** $p < 0.001$).

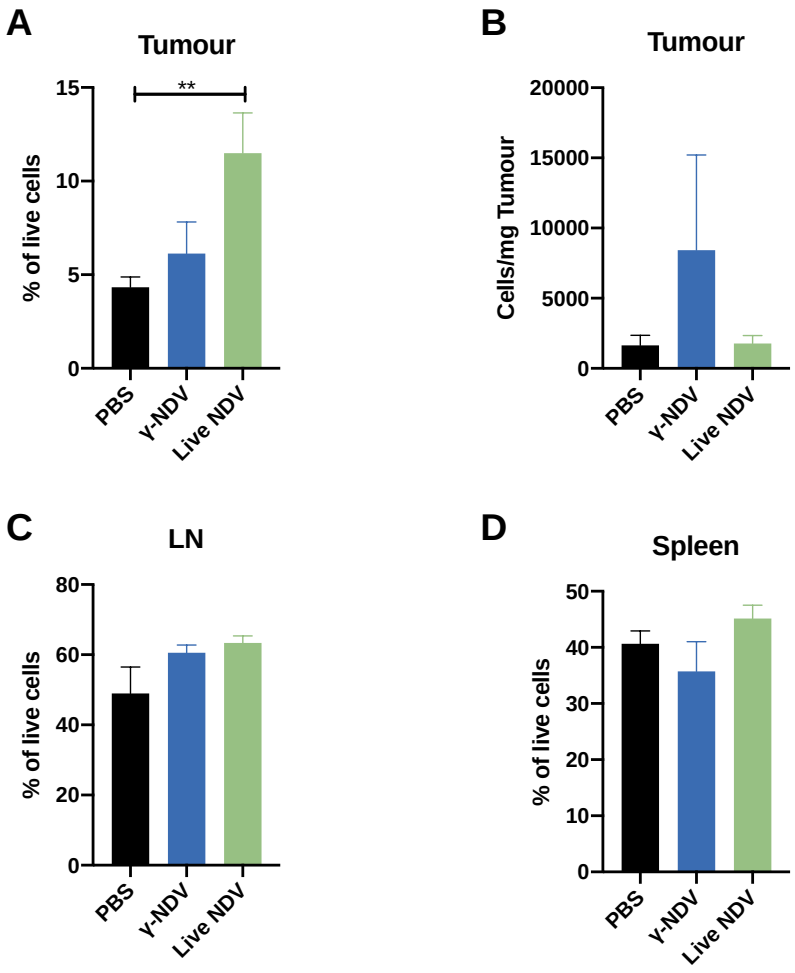

Figure 4.12. Lymphocyte responses following treatment with oncolytic NDV. B16 tumours were induced by subcutaneous injection into C57BL/6J mice. The, mice were treated intratumorally with live NDV, γ-NDV or PBS (control) at days 10, 13 and 16 post-tumour induction. (A, B) Tumours, (C) draining lymph node and (D) spleens were harvested at day 20 and lymphocytes ($CD45^+$) were quantified using flow cytometry. Data is presented as mean ± SEM (n = 7) and was analysed by one-way ANOVA (** $p < 0.01$).

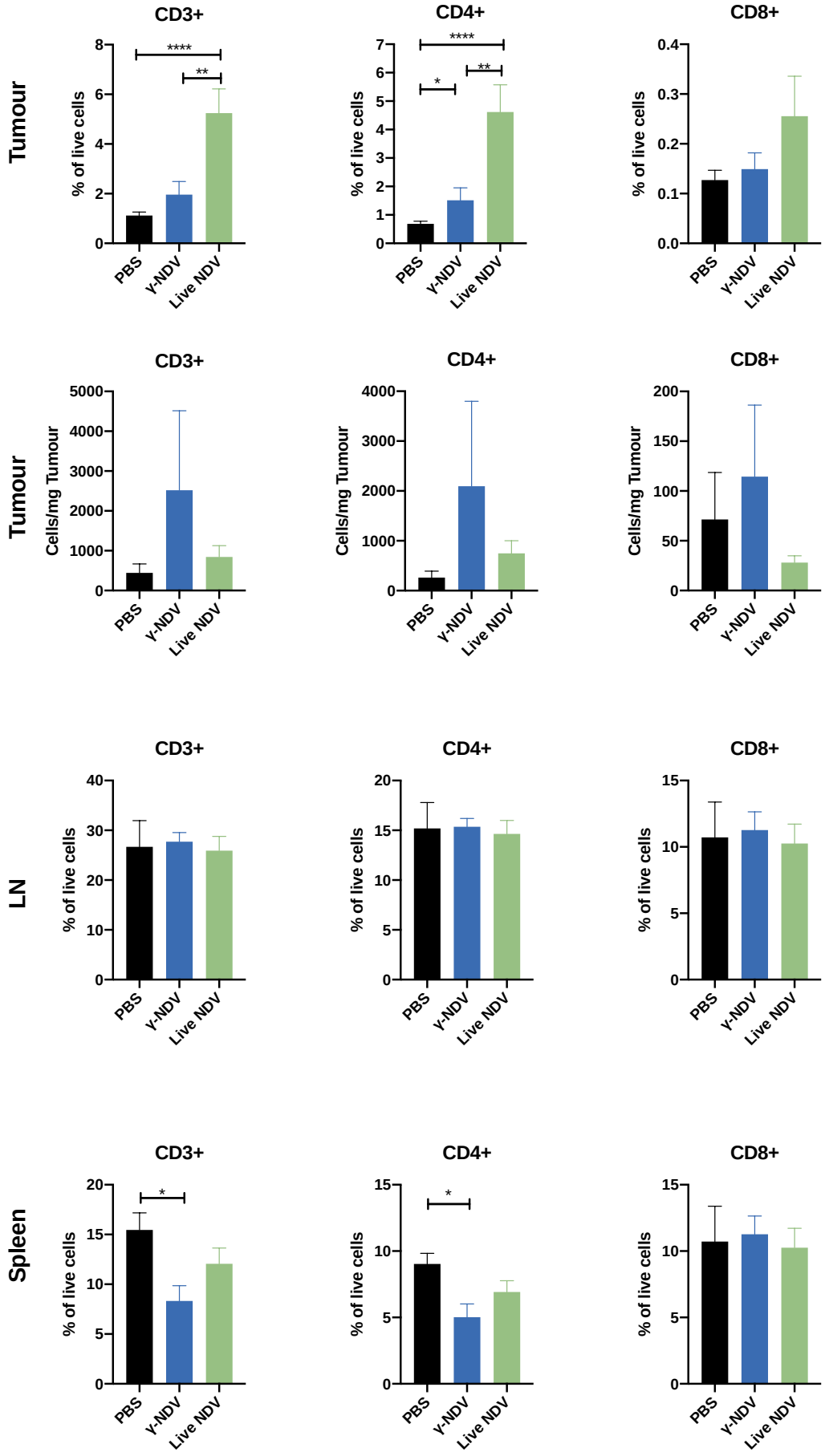
Tumour
LN
Spleen
CD3+
CD4+
CD8+
% of live cells
Cells/mg Tumour
PBS
γ-NDV
Live NDV
****
**
*

Figure 4.13. T cell responses following treatment with oncolytic NDV. B16 tumours were induced by subcutaneous injection of B16 cells into C57BL/6J mice. Then, mice were treated intratumorally with live NDV, γ-NDV or PBS (control) at days 10, 13 and 16 post-tumour induction. Tumours, draining lymph node and spleens were harvested at day 20 and T cells ($CD45^+$ $CD3^+$), T helper cells ($CD45^+$ $CD3^+$ $CD4^+$) and cytotoxic T cells ($CD45^+$ $CD3^+$ $CD8^+$) were quantified using flow cytometry. Data is presented as mean ± SEM (n = 7) and was analysed by one-way ANOVA (* $p < 0.05$, ** $p < 0.01$, **** $p < 0.0001$).

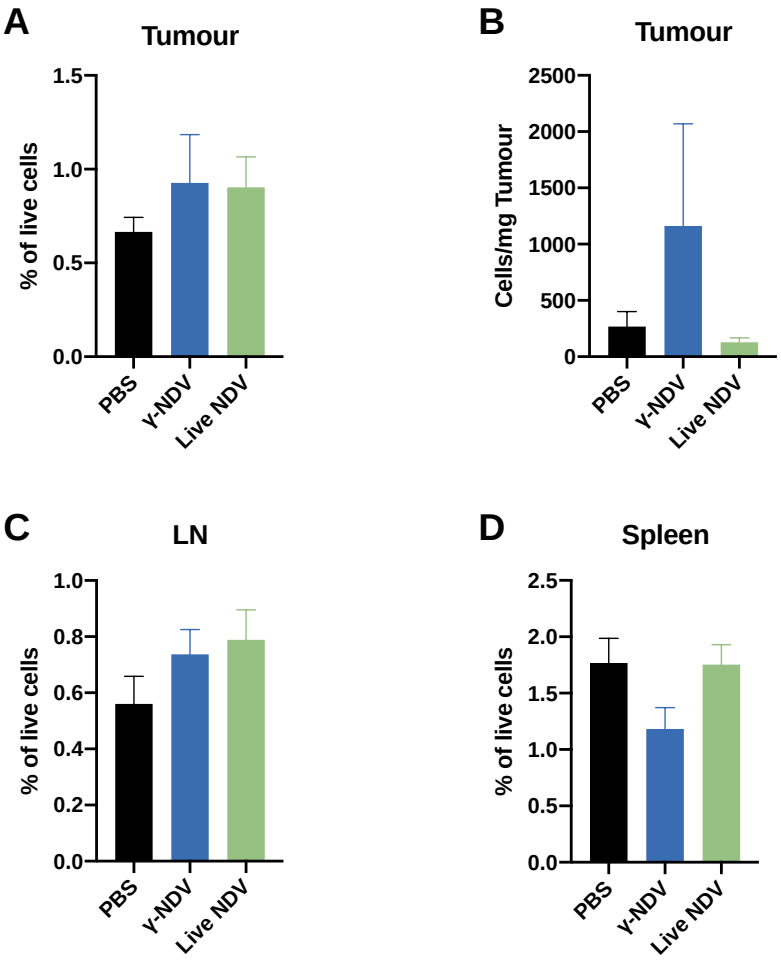

Figure 4.14. NK cell responses following treatment with oncolytic γ-NDV. B16 tumours were induced by subcutaneous injection of B16 cells into C57BL/6J mice. Then, mice were treated intratumorally with live NDV, γ-NDV or PBS (control) at days 10, 13 and 16 post-tumour induction. Tumours, draining lymph node and spleens were harvested at day 20 and NK cells ($CD45^+$ $NK1.1^+$) cells were quantified using flow cytometry. Data is presented as mean ± SEM (n = 7) and was analysed by one-way ANOVA (not significant).

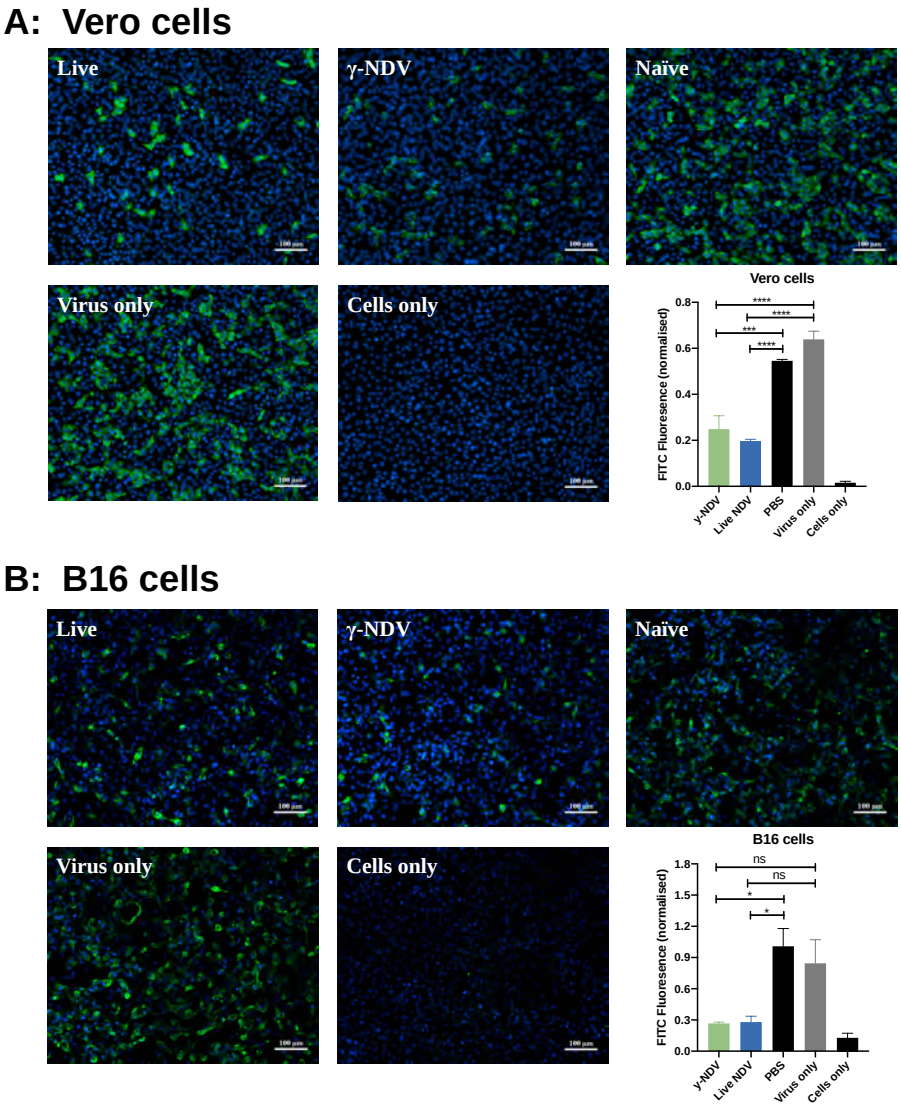

Figure 4.15. Neutralising antibody responses in C57BL/6 mice induced by intratumoral treatment with γ-NDV. B16 tumours were induced by subcutaneous injection of B16 cells into C57BL/6J mice. Then, mice were treated intratumorally with live NDV, γ-NDV or PBS (control) at days 10, 13 and 16 post-tumour induction and at day 20 serum was collected. To measure neutralisation, live NDV was treated with dilutions of pooled serum from mice treated with live NDV, γ-NDV or PBS. Virus + serum was then added to (A) Vero cells or (B) B16 cells at an MOI of 0.1. Plates were washed 2 hours later to remove unattached virus then plates were incubated for a further 22 hours, stained with DAPI (cell nucleus) and FITC (NDV infection) then visualised using a Nikon TiE inverted fluorescence microscope. FITC relative to DAPI was quantified as a measure of neutralisation. Quantitative data was analysed by one-way ANOVA (* $p < 0.05$, *** $p < 0.001$, **** $p < 0.0001$, ns = not significant).

CHAPTER 5

Final Discussion

5. FINAL DISCUSSION

5.1 Final Discussion

This project investigated concepts and applications related to using γ-radiation to sterilise pathogens for research purposes and for the development of clinically relevant vaccines. Findings in this thesis provide recommendations for calculating sterilising doses that are expected to be widely applicable to different pathogens irradiated under different conditions. Furthermore, I have investigated the influence of irradiation conditions on vaccine efficacy when irradiating to the sterilising dose. These novel findings can facilitate the production of more effective vaccines in future. This thesis also provides the foundations for a γ-irradiated oncolytic virotherapy, a novel application of γ-radiation.

As the applications for γ-radiation grows, so too must the standards for meeting sterilisation requirements. Calculating sterilising doses correctly is imperative to delivering γ-irradiated products safely. Current recommendations for calculating sterilising doses were written for sterilising medical equipment or pharmaceuticals where bioburden is typically low. This thesis highlights an important gap in current standards related to the use of γ-radiation to inactivate viruses for both vaccine and biomedical analysis and I propose a new formula and method for calculating sterilising doses. This formula can be applied to pathogens displaying multiple-hit and single-hit kinetics, whereas previous methods could only account for single-hit kinetics. Importantly, multiple-hit kinetics is observed where pathogens may be more radioresistant. For example, inactivation curves for *B. anthracis* demonstrate a shoulder of resistance [369]. Although the authors noted this shoulder, it was ignored for the purpose of calculating sterilising doses. This could lead to the miscalculation of sterilising doses, particularly when we see a large shoulder such as that observed for rotavirus (**Figure 2.4**). This new formula is easy to apply to any pathogen, regardless of genome structure, titre and irradiation conditions. Furthermore, this formula is highly applicable to the further development of γ-irradiated vaccines, and to other γ-irradiated products such as irradiation of pathogens that pose a biosecurity concern for research purposes.

In this thesis, I demonstrate that pathogens are most susceptible to γ-radiation at higher temperatures. Importantly, calculated sterilising doses are considerably lower for viruses

irradiated at room temperature and on ice water compared to irradiation on dry ice. Previous studies have demonstrated that structural damage caused by irradiation is increased when the irradiation process was conducted at higher temperatures [11, 24, 183], however these studies compared irradiated samples exposed to the same dose of radiation. Considering the widely accepted concept of Sterility Assurance Level and the impact of irradiation conditions on inactivation curves, data presented in **Chapter 3** represents the first study to compare structural integrity and immunogenicity of materials inactivated by exposure to sterilising doses that have been estimated based on variation in irradiation conditions. Using influenza A virus as an experimental model, I surprisingly found better-maintained structural integrity and an enhanced immunogenicity of γ-Flu preparations that had been irradiated at warmer temperatures compared to those irradiated on dry ice. This is contradictory to the previously accepted understanding of γ-irradiated vaccines and opens an avenue for using high temperature/low dose irradiation conditions, which would be faster and cheaper to scale up for the clinical development of irradiated vaccines. These data highlight the importance of considering the sterilising dose for the applied irradiation conditions in order to minimise oxidative damage. Importantly, any changes to external factors may influence the sterilising dose and may shift oxidative damage, and so sterilising doses must be calculated for each pathogen for specified irradiation conditions to avoid inadvertently releasing pathogens that have escaped sterility.

The concepts identified in this thesis were applied to the development of an inactivated vaccine candidate for NDV to overcome the limitation of existing live and chemically inactivated vaccines. NDV is an important avian pathogen that is associated with large livestock losses and a great economic burden globally. We expected γ-radiation to produce a highly effective vaccine, as previous studies have demonstrated γ-irradiation to be a superior inactivation method compared to other methods [65, 66]. γ-NDV had high levels of protein function and structural integrity and generated high IgG responses. However, various mouse vaccination experiments conducted using BALB/c mice indicated that γ-NDV does not induce neutralising responses. Neutralising antibody responses are critical to vaccine-induced immunity [237] and consequently γ-NDV may not be a suitable vaccine candidate. It is important to note that experiments performed in **Chapter 3** and **Chapter 4** were carried out concurrently, and dry ice irradiation was used for the development of γ-NDV as it was expected to elicit the strongest immune responses based on previous studies

that investigated the immunogenicity of other γ-irradiated vaccines. Based on results from **Chapter 3**, γ-NDV could be irradiated at a lower dose and higher temperature to improve immunogenicity.

Interestingly, when collecting serum from C57BL/6J mice with B16 tumours treated with live NDV and γ-NDV, I did detect NDV-specific neutralising antibody responses. The reason for the observed difference between C57BL/6J and BALB/c mice has not been elucidated in this thesis. However, immune responses in C57BL/6 and BALB/c mice are geared towards T_H1 or T_H2 responses, respectively [370, 371], and antibody kinetics differs between the two mouse strains [366-368]. Importantly, the difference in neutralising responses may be due to the animal model used. Furthermore, C57BL/6 mice were used in the context of a melanoma model. It is expected that B16 melanoma cells express a high concentration of sialic acid receptors that γ-NDV can utilise to be internalised to enhance immune responses. These same receptors may not be available in a non-tumour model. Additionally, in the B16 tumour model mice were given repeated high-dose γ-NDV treatments in quick succession. This overload of antigen could also explain the induction of neutralising antibody responses in C57BL/6 mice. Based on the differences in neutralising antibody responses observed between C57BL/6 mice and BALB/c mice, it is possible that γ-NDV is still a suitable vaccine candidate that requires further testing in a chicken model.

This research has developed a novel application by using γ-radiation to develop γ-irradiated virotherapies. Oncolytic virotherapies is a growing area of research and many clinical trials are on-going to assess efficacy. Furthermore, the first oncolytic virotherapy, TVEC, was approved for use in humans in 2015. Most oncolytic virotherapies are genetically modified to restrict specificity to cancer cells and to reduce infectivity. With γ-irradiation, these modifications may not be necessary. Data in this thesis demonstrate that γ-NDV retains specificity for cancer cells and may actually promote faster tumour regression than live NDV. In addition, a major limitation for the clinical use of virulent NDV as a virotherapy is the biosecurity risk that may lead to a disease outbreak in poultry but using γ-irradiated NDV negates this risk.

There have been several reported instances of severe reactions and death in clinical trials using viral gene therapies. Most gene-therapy clinical trials are targeted to cancer treatment [372]. In a clinical trial in 1998 to treat an ornithine transcarbamylase (OTC) deficiency, an adenovirus vector was designed to deliver OTC directly to the liver, the organ where OTC functions. Shortly after adenovirus administration, an 18-year-old trial participant suffered a severe adverse reaction and ultimately died from multiple organ failure attributed to the adenovirus treatment [373]. The reason for such a severe reaction to an adenovirus vector is largely unknown [374]. The first successful gene therapy clinical trial was completed in 2000, where a retroviral vector was used to treat severe combined immunodeficiency disease (SCID) [375]. However, this treatment was associated with at least 2 incidences of lymphoproliferative disease resulting in a leukaemia-like disorder due to the random integration of the gene into the patients DNA [376].

While γ-irradiation is unlikely to be useful when applied to viral gene therapies, as the virus must be able to produce the protein of interest, this could instead be applied to γ-irradiated bacteria. Bacteria have considerably larger genomes and so are sterilised at low radiation doses (e.g. *S. pneumoniae* has a DS_{SAL} of 17.4 kGy, **Chapter 2**). However, it is expected that individual genes are less damaged by γ-irradiation. Our group has previously demonstrated that γ-radiation inactivated *S. pneumoniae* can still produce RNA from inducible genes (Laan *et al*, currently unpublished). Bacteria can be used to target tumours in two ways; firstly, bacteria can induce tumour regression and secondly bacteria can deliver genes to mammalian cells within the tumours, a process known as 'bactofection'. Oncolytic bacteria include *Streptococcus* [377], *Salmonella* [378] and *Clostridium* species. Interestingly, heat-killed *Streptococcus* spp. are able to cause tumour regression [377]. In Bactofection delivery systems, the gene of interest is contained on a plasmid to be delivered to host cells. A range of genes has been successfully utilised in clinical and pre-clinical modelling (reviewed in [379]). Importantly, plasmid DNA is still transformable, albeit with reduced efficacy, using doses of up to 20 kGy [380], a dose that would inactivate most bacterial species. Given the pathogenicity of bacteria used in gene therapy and the ability for γ-irradiated bacteria to produce RNA despite genome damage, γ-irradiated bacteria gene delivery systems could be an avenue worth pursuing.

5.2 Future Directions

An area that warrants further investigation is to better characterise the antibody responses to γ-NDV. My data consistently demonstrates a lack of neutralising antibody responses in a BALB/c model, irrespective of administration route, adjuvants used or booster immunisations. However, in the context of a cancer model in C57BL/6 mice there were neutralising antibody responses. There may be species, or even strain, specificity for inducing neutralising antibody responses to NDV. Indeed, there has been observed differences in antibody kinetics between BALB/c and C57BL/6 mice in the literature [366-368]. Additionally, there are many instances of different susceptibilities to disease between mouse strains [381]. Future studies should examine whether the difference in antibody responses are caused by (1) different animal models, (2) administering multiple high antigen doses in quick succession or (3) the pro-inflammatory environment within the tumour. It is also important to identify antibody-binding sites in neutralising and non-neutralising populations using epitope mapping. These findings could improve current NDV vaccines and could be used to increase virotherapy efficacy. Importantly, future studies will include conventional methods of preparing killed vaccines such as formalin or β-propiolactone. These studies will identify whether the reduced neutralising responses were inherent to inactivation by γ-radiation.

An interesting finding in this thesis was the ability of γ-NDV to specifically target and kill cancer cells. Due to biosecurity restrictions, all work in this thesis was completed using V4, a lentogenic live-attenuated vaccine strain. However, more virulent strains are more effective at targeting cancer cells [347]. Future research should focus on testing γ-irradiated mesogenic and velogenic strains. More virulent strains are able to induce stronger cytokines responses [229] and thus could induce enhanced oncolysis. Velogenic strains have more polybasic amino acids at the cleavage site, which means that it is cleaved by a wider range of proteases and so is more active to induce entry into host cells. However, other NDV proteins are also associated with virulence. Virulent NDV is able to shift macrophage polarisation from M2 to M1, whereas lentogenic NDV does not [382]. HN is also related to virulence and HN strains from velogenic NDV have enhanced haemagglutinin and neuraminidase activity [383]. Overall, we expect developing γ-NDV using a velogenic strain to have enhanced oncolytic effects.

In this research project, I tested 11 different human and murine cancer cells *in vitro*, and selected B16, a mouse melanoma model for further *in vivo* testing. Our *in vitro* testing demonstrated that γ-NDV was effective in many different types of cancer including breast cancer, prostate cancer and leukaemia (**Table 4.3**). Further studies could demonstrate the efficacy of γ-NDV in treating these tumour models in mice. In addition, it is important to test γ-NDV efficacy in a human xenograft model as part of pre-clinical testing. Human cell lines can be transplanted into Nod *scid* gamma (NSG) mice. NSG mice are the most severely immunocompromised mouse model to date and lack lymphocytes and NK cells [384]. This makes NSG mice a good animal model for human xenografts [385]. Interestingly, as NSG mice lack important components of both innate and adaptive immunity, the indirect mechanisms of oncolysis will be excluded (i.e. recruitment of the immune system). Therefore, in addition to providing valuable pre-clinical testing of human cancers, this model will also shine further light on the mechanism of action of γ-NDV. The ability of γ-NDV to kill cancer cells *in vitro* demonstrates that direct mechanisms of oncolysis are occurring. Importantly, current pre-clinical testing of live NDV on human xenografts cannot be completed due to the ability of live virus to replicate unchecked in the immunocompromised mice.

An important area of cancer treatments is combination therapy. Treatments must differentiate between cancerous and non-cancerous cells. Traditional treatments, such as chemotherapy, target rapidly replicating cells. However, the proportion of dividing cells within the tumour is relatively low. Human tumours are also highly heterogeneous and so within any given population of tumour cells there will be proportions resistant to different treatments. To overcome tumour heterogeneity, a combination of different treatments is recommended. Of interest, the development of immune checkpoint inhibitors, particularly against CTLA-4 and PD-1, has improved mean survival times and immune responses to tumours [386-388]. CTLA-4 efficacy is enhanced when combined with oncolytic NDV treatment [262]. Another area of interest is atypical chemokine receptor 4 (ACKR4). ACKR4 down-regulates CCR7, an important chemokine receptor involved in the migration of tumour antigen-presenting DCs to draining lymph nodes and the subsequent priming of tumour-specific cytotoxic T cells [389]. Up-regulation of CCR7 is related to increased infiltration of lymphocytes into the tumour and overall survival [389, 390]. Recent research at the University of Adelaide has demonstrated that in tumour models in ACKR4-deficicent

mice, there is an increase in tumour-infiltrating cytotoxic T cells and reduced tumour growth [391]. Treatment with antibodies against CTLA-4 and PD-1 are also enhanced in ACKR4-deficient mice [391]. Further research with γ-NDV could test the possibility of a combination with other cancer therapies including those targeting CTLA-4, PD-1 and ACKR4.

5.3. Conclusions

Overall, the work in this thesis has highlighted a critical gap in the methodology used to calculate sterilising doses, and I have proposed a new widely applicable formula to be used in the future. In this research project, I hypothesised that γ-radiation conditions could be optimised to develop highly effective vaccines. Indeed, I was able to modify irradiation temperature and dose to enhance immunogenicity of γ-Flu vaccines. However, the findings in this thesis did not support my hypothesis that highly immunogenic NDV vaccines could be generated using γ-radiation and further studies need to be performed in chickens to demonstrate efficacy.

I hypothesised that γ-irradiated NDV could be used as a novel oncolytic virotherapy. Importantly, structural integrity and protein function was well maintained and sterility was achieved. Data in this thesis demonstrates the ability for γ-NDV to specifically lyse a range of cancer cells *in vitro*. Furthermore, γ-NDV was able to effectively treat melanoma in mouse models. This important finding could be applied to enhance safety and efficacy of current cancer treatments.

REFERENCES

REFERENCES

1. Schulte-Frohlinde, D.; Opitz, J.; Gorner, H.; Bothe, E., Model studies for the direct effect of high-energy irradiation on DNA. Mechanism of strand break formation induced by laser photoionization of poly U in aqueous solution. *Int J Radiat Biol Relat Stud Phys Chem Med* **1985,** 48, (3), 397-408.
2. Henner, W. D.; Grunberg, S. M.; Haseltine, W. A., Sites and structure of gamma radiation-induced DNA strand breaks. *J Biol Chem* **1982,** 257, (19), 11750-4.
3. Lomax, M. E.; Folkes, L. K.; O'Neill, P., Biological consequences of radiation-induced DNA damage: relevance to radiotherapy. *Clin Oncol (R Coll Radiol)* **2013,** 25, (10), 578-85.
4. Van Der Schans, G. P., Gamma-ray induced double-strand breaks in DNA resulting from randomly-inflicted single-strand breaks: temporal local denaturation, a new radiation phenomenon? *Int J Radiat Biol Relat Stud Phys Chem Med* **1978,** 33, (2), 105-20.
5. Feldberg, R. S.; Carew, J. A., Water radiolysis products and nucleotide damage in gamma-irradiated DNA. *Int J Radiat Biol Relat Stud Phys Chem Med* **1981,** 40, (1), 11-7.
6. Repine, J. E.; Pfenninger, O. W.; Talmage, D. W.; Berger, E. M.; Pettijohn, D. E., Dimethyl sulfoxide prevents DNA nicking mediated by ionizing radiation or iron/hydrogen peroxide-generated hydroxyl radical. *Proc Natl Acad Sci U S A* **1981,** 78, (2), 1001-3.
7. Lee, S.; Lee, S.; Bin Song, K., Effect of gamma-irradiation on the physicochemical properties of porcine and bovine blood plasma proteins. *Food Chem* **2003,** 82, (4), 521-526.
8. Stadtman, E. R.; Oliver, C. N., Metal-catalyzed oxidation of proteins. Physiological consequences. *J Biol Chem* **1991,** 266, (4), 2005-8.
9. Stadtman, E. R., Metal ion-catalyzed oxidation of proteins: biochemical mechanism and biological consequences. *Free Radic Biol Med* **1990,** 9, (4), 315-25.
10. Jordan, R. T.; Kempe, L. L., Inactivation of some animal viruses with gamma radiation from cobalt-60. *Proc Soc Exp Biol Med* **1956,** 91, (2), 212-5.
11. Sullivan, R.; Fassolitis, A. C.; Larkin, E. P.; Read, R. B., Jr.; Peeler, J. T., Inactivation of thirty viruses by gamma radiation. *Appl Microbiol* **1971,** 22, (1), 61-5.

12. Elliott, L. H.; Mccormick, J. B.; Johnson, K. M., Inactivation of Lassa, Marburg, and Ebola Viruses by Gamma-Irradiation. *J Clin Microbiol* **1982,** 16, (4), 704-708.
13. Kempner, E. S.; Haigler, H. T., The influence of low temperature on the radiation sensitivity of enzymes. *J Biol Chem* **1982,** 257, (22), 13297-9.
14. Thayer, D. W.; Boyd, G., Effect of irradiation temperature on inactivation of Escherichia coli O157:H7 and Staphylococcus aureus. *J Food Prot* **2001,** 64, (10), 1624-6.
15. Teoule, R.; Bonicel, A.; Bert, C.; Cadet, J.; Polverelli, M., Identification of radioproducts resulting from the breakage of thymine moiety by gamma irradiation of E. coli DNA in an aerated aqueous solution. *Radiat Res* **1974,** 57, (1), 46-58.
16. Gazso, L., Physical, chemical and biological dose modifying factors. In *Radiation inactivation of bioterrorism agents*, Gazso, L. P., CC, Ed. IOS Press: Amsterdam, 2005; pp 59-68.
17. Sullivan, R.; Scarpino, P. V.; Fassolitis, A. C.; Larkin, E. P.; Peeler, J. T., Gamma radiation inactivation of coxsackievirus B-2. *Appl Microbiol* **1973,** 26, (1), 14-7.
18. Rohwer, R. G., Scrapie Infectious Agent Is Virus-Like in Size and Susceptibility to Inactivation. *Nature* **1984,** 308, (5960), 658-662.
19. Kenny, M. T.; Albright, K. L.; Emery, J. B.; Bittle, J. L., Inactivation of rubella virus by gamma radiation. *J Virol* **1969,** 4, (6), 807-10.
20. Farkas, J., Physical Methods of Food Preservation In Doyle MP, B. L., Ed. 2007.
21. Thomas, F. C.; Davies, A. G.; Dulac, G. C.; Willis, N. G.; Papp-Vid, G.; Girard, A., Gamma ray inactivation of some animal viruses. *Can J Comp Med* **1981,** 45, (4), 397-9.
22. Miekka, S. I.; Forng, R. Y.; Rohwer, R. G.; MacAuley, C.; Stafford, R. E.; Flack, S. L.; MacPhee, M.; Kent, R. S.; Drohan, W. N., Inactivation of viral and prion pathogens by gamma-irradiation under conditions that maintain the integrity of human albumin. *Vox Sang* **2003,** 84, (1), 36-44.
23. David, S. C.; Lau, J.; Singleton, E. V.; Babb, R.; Davies, J.; Hirst, T. R.; McColl, S. R.; Paton, J. C.; Alsharifi, M., The effect of gamma-irradiation conditions on the immunogenicity of whole-inactivated Influenza A virus vaccine. *Vaccine* **2017**.
24. Da Silva Aquino, K. A., Sterilization by Gamma Irradiation. In *Gamma Radiation*, Adrovic, F., Ed. InTech: Vienna, Austria, 2012; pp 171-206.
25. van der Schans, G. P.; van der Drift, A. C., Comparsion of the oxygen-enhancement ratio for gamma-ray-induced double-strand breaks in the DNA of bacteriophage T7

as determined by two different methods of analysis. *Int J Radiat Biol Relat Stud Phys Chem Med* **1975,** 27, (5), 437-46.

26. Tallentire, A., An Observed 'Oxygen Effect' during Gamma-irradiation of Dried Bacterial Spores. *Nature* **1958,** 182, (4641), 1024-1025.
27. Miekka, S. I.; Busby, T. F.; Reid, B.; Pollock, R.; Ralston, A.; Drohan, W. N., New methods for inactivation of lipid-enveloped and non-enveloped viruses. *Haemophilia* **1998,** 4, (4), 402-8.
28. Moeller, R.; Raguse, M.; Reitz, G.; Okayasu, R.; Li, Z.; Klein, S.; Setlow, P.; Nicholson, W. L., Resistance of Bacillus subtilis spore DNA to lethal ionizing radiation damage relies primarily on spore core components and DNA repair, with minor effects of oxygen radical detoxification. *Appl Environ Microbiol* **2014,** 80, (1), 104-9.
29. Hume, A. J.; Ames, J.; Rennick, L. J.; Duprex, W. P.; Marzi, A.; Tonkiss, J.; Muhlberger, E., Inactivation of RNA Viruses by Gamma Irradiation: A Study on Mitigating Factors. *Viruses* **2016,** 8, (7).
30. Daly, M. J.; Gaidamakova, E. K.; Matrosova, V. Y.; Vasilenko, A.; Zhai, M.; Venkateswaran, A.; Hess, M.; Omelchenko, M. V.; Kostandarithes, H. M.; Makarova, K. S.; Wackett, L. P.; Fredrickson, J. K.; Ghosal, D., Accumulation of Mn(II) in Deinococcus radiodurans facilitates gamma-radiation resistance. *Science* **2004,** 306, (5698), 1025-8.
31. Mendonca, A. F., Inactivation by irradiation. In *Control of Foodborne Microorganisms*, Vijay K. Juneja, J. N. S., Ed. CRC Press: 2001; p 552.
32. Basha, S. G.; Krasavin, E. A.; Kozubek, S.; Amirtaev, K. G., [The effect of glycerine on gamma-induced mutagenesis in Salmonella typhimurium cells]. *Radiobiologiia* **1990,** 30, (2), 185-9.
33. Allaveisi, F.; Hashemi, B.; Mortazavi, S. M., Radioprotective effect of N-acetyl-L-cysteine free radical scavenger on compressive mechanical properties of the gamma sterilized cortical bone of bovine femur. *Cell Tissue Bank* **2015,** 16, (1), 97-108.
34. Battista, J. R., Against all odds: the survival strategies of Deinococcus radiodurans. *Annu Rev Microbiol* **1997,** 51, 203-24.
35. International Atomic Energy Agency, Good radiation practice (GRP). *IAEA Guidelines for industrial radiation and sterilization of disposable medical products (cobalt-60 gamma irradiation)* **1990**.

36. Department of Agriculture Fisheries and Forestry Biosecurity, 'Gamma Irradiation as a Treatment to Address Pathogens of Animal Biosecurity Concern - Final Policy Review'. In Canberra, CC BY 3.0, 2014.
37. International Organisation for Standardization, Sterilization of Health Care Products - Radiation - Part 2: Establishing the Sterilization Dose. **2013**, ISO 11137-2:2013.
38. United States Department of Defense (Committee for Comprehensive Review of DoD Laboratory Procedures, P., and Protocols Associated with Inactivating Bacillus anthracis Spores); *Review Committee Report: Inadvertent Shipment of Live Bacillus anthracis Spores by DoD*; Department of Defense: July 13, 2015.
39. Helfinstine, S. L.; Vargas-Aburto, C.; Uribe, R. M.; Woolverton, C. J., Inactivation of Bacillus endospores in envelopes by electron beam irradiation. *Appl Environ Microbiol* **2005,** 71, (11), 7029-32.
40. Hendry, J. H., *Radiation Sterilization of Tissue Allografts: Requirements for Validation and Routine Control : a Code of Practice*. International Atomic Energy Agency: 2007.
41. Food and Drug Administration (FDA), Irradiation in the Production, Processing and Handling of Food. In 2017; Vol. 3.
42. International Atomic Energy Agency, Manual on Radiation Sterilization of Medical and Biological Materials. **1973**.
43. Singh, R.; Singh, D.; Singh, A., Radiation sterilization of tissue allografts: A review. *World J Radiol* **2016,** 8, (4), 355-69.
44. Doue, B., Radiation doses and dose distribution during industrial sterilization by gamma rays and acclerated electron beams (Part I). *Medical Device Technol.* **2001**, 32-35.
45. Dennis, J. A.; Martinez, O. V.; Landy, D. C.; Malinin, T. I.; Morris, P. R.; Fox, W. P.; Buck, B. E.; Temple, H. T., A comparison of two microbial detection methods used in aseptic processing of musculoskeletal allograft tissues. *Cell Tissue Bank* **2011,** 12, (1), 45-50.
46. Ison, M. G.; Llata, E.; Conover, C. S.; Friedewald, J. J.; Gerber, S. I.; Grigoryan, A.; Heneine, W.; Millis, J. M.; Simon, D. M.; Teo, C. G.; Kuehnert, M. J.; Team, H.-H. T. T. I., Transmission of human immunodeficiency virus and hepatitis C virus from an organ donor to four transplant recipients. *Am J Transplant* **2011,** 11, (6), 1218-25.

47. Tugwell, B. D.; Patel, P. R.; Williams, I. T.; Hedberg, K.; Chai, F.; Nainan, O. V.; Thomas, A. R.; Woll, J. E.; Bell, B. P.; Cieslak, P. R., Transmission of hepatitis C virus to several organ and tissue recipients from an antibody-negative donor. *Ann Intern Med* **2005,** 143, (9), 648-54.

48. Singh, R.; Singh, D.; Singh, A., Radiation sterilization of tissue allografts: A review. *World journal of radiology* **2016,** 8, (4), 355.

49. Arizono, T.; Iwamoto, Y.; Okuyama, K.; Sugioka, Y., Ethylene oxide sterilization of bone grafts. Residual gas concentration and fibroblast toxicity. *Acta Orthop Scand* **1994,** 65, (6), 640-2.

50. Binnet, M. S.; Akan, B.; Kaya, A., Lyophilised medial meniscus transplantations in ACL-deficient knees: a 19-year follow-up. *Knee Surg Sports Traumatol Arthrosc* **2012,** 20, (1), 109-13.

51. Pruss, A.; Gobel, U. B.; Pauli, G.; Kao, M.; Seibold, M.; Monig, H. J.; Hansen, A.; von Versen, R., Peracetic acid-ethanol treatment of allogeneic avital bone tissue transplants--a reliable sterilization method. *Ann Transplant* **2003,** 8, (2), 34-42.

52. Hamer, A. J.; Stockley, I.; Elson, R. A., Changes in allograft bone irradiated at different temperatures. *J Bone Joint Surg Br* **1999,** 81, (2), 342-4.

53. Lederman, M. M.; Ratnoff, O. D.; Scillian, J. J.; Jones, P. K.; Schacter, B., Impaired cell-mediated immunity in patients with classic hemophilia. *N Engl J Med* **1983,** 308, (2), 79-83.

54. Kitchen, A. D.; Mann, G. F.; Harrison, J. F.; Zuckerman, A. J., Effect of gamma irradiation on the human immunodeficiency virus and human coagulation proteins. *Vox sanguinis* **1989,** 56, (4), 223-9.

55. Grieb, T.; Forng, R. Y.; Brown, R.; Owolabi, T.; Maddox, E.; McBain, A.; Drohan, W. N.; Mann, D. M.; Burgess, W. H., Effective use of gamma irradiation for pathogen inactivation of monoclonal antibody preparations. *Biologicals* **2002,** 30, (3), 207-16.

56. Grant-Klein, R. J.; Antonello, J.; Nichols, R.; Dubey, S.; Simon, J., Effect of Gamma Irradiation on the Antibody Response Measured in Human Serum from Subjects Vaccinated with Recombinant Vesicular Stomatitis Virus-Zaire Ebola Virus Envelope Glycoprotein Vaccine. *Am J Trop Med Hyg* **2019,** 101, (1), 207-213.

57. Moini, S.; Tahergorabi, R.; Hosseini, S. V.; Rabbani, M.; Tahergorabi, Z.; Feas, X.; Aflaki, F., Effect of gamma radiation on the quality and shelf life of refrigerated rainbow trout (Oncorhynchus mykiss) fillets. *J Food Prot* **2009,** 72, (7), 1419-26.

58. Assuncao, E.; Reis, T. A.; Baquiao, A. C.; Correa, B., Effects of Gamma and Electron Beam Radiation on Brazil Nuts Artificially Inoculated with Aspergillus flavus. *J Food Prot* **2015,** 78, (7), 1397-401.

59. Hajare, S. N.; Gautam, S.; Nair, A. B.; Sharma, A., Formulation of a nasogastric liquid feed and shelf-life extension using gamma radiation. *J Food Prot* **2014,** 77, (8), 1308-16.

60. Seo, J. H.; Kim, J. H.; Lee, J. W.; Yoo, Y. C.; Kim, M. R.; Park, K. S.; Byun, M. W., Ovalbumin modified by gamma irradiation alters its immunological functions and allergic responses. *Int Immunopharmacol* **2007,** 7, (4), 464-72.

61. Zhenxing, L.; Hong, L.; Limin, C.; Jamil, K., The influence of gamma irradiation on the allergenicity of shrimp (Penaeus vannamei). *Journal of food engineering* **2007,** 79, (3), 945-949.

62. Alsharifi, M.; Mullbacher, A., The gamma-irradiated influenza vaccine and the prospect of producing safe vaccines in general. *Immunol Cell Biol* **2010,** 88, (2), 103-4.

63. Seo, H. S., Application of radiation technology in vaccines development. *Clin Exp Vaccine Res* **2015,** 4, (2), 145-58.

64. Alsharifi, M.; David, S., Virus Inactivation Using a High Dose of Gamma-Irradiation: A Possible Approach for Safer Vaccines Against Highly Infectious Agents. *Journal of Vaccines & Vaccination* **2017,** 08.

65. Wiktor, T. J.; Aaslestad, H. G.; Kaplan, M. M., Immunogenicity of rabies virus inactivated by β-propiolactone, acetylethyleneimine, and ionizing irradiation. *Appl Microbiol* **1972,** 23, (5), 914-8.

66. Furuya, Y.; Regner, M.; Lobigs, M.; Koskinen, A.; Müllbacher, A.; Alsharifi, M., Effect of inactivation method on the cross-protective immunity induced by whole 'killed' influenza A viruses and commercial vaccine preparations. *J Gen Virol* **2010,** 91, (Pt 6), 1450.

67. Alsharifi, M.; Mullbacher, A., The γ-irradiated influenza vaccine and the prospect of producing safe vaccines in general. *Immunol Cell Biol* **2009,** 88, (2), 103.

68. Alsharifi, M.; Furuya, Y.; Bowden, T. R.; Lobigs, M.; Koskinen, A.; Regner, M.; Trinidad, L.; Boyle, D. B.; Mullbacher, A., Intranasal flu vaccine protective against seasonal and H5N1 avian influenza infections. *PLoS One* **2009,** 4, (4), e5336.

69. Furuya, Y.; Chan, J.; Wan, E.-C.; Koskinen, A.; Diener, K. R.; Hayball, J. D.; Regner, M.; Müllbacher, A.; Alsharifi, M., Gamma-Irradiated Influenza Virus Uniquely Induces IFN-I Mediated Lymphocyte Activation Independent of the TLR7/MyD88 Pathway (Immune Responses to Inactivated Influenza Viruses). *PLoS ONE* **2011,** 6, (10), e25765.

70. Babb, R.; Chen, A.; Hirst, T. R.; Kara, E. E.; McColl, S. R.; Ogunniyi, A. D.; Paton, J. C.; Alsharifi, M., Intranasal vaccination with gamma-irradiated *Streptococcus pneumoniae* whole-cell vaccine provides serotype-independent protection mediated by B-cells and innate IL-17 responses. *Clin Sci (Lond)* **2016,** 130, (9), 697-710.

71. David, s. c.; Laan, Z.; Minhas, V.; Chen, A.; Davies, J.; Hirst, T. R.; McColl, S. R.; Alsharifi, M.; Paton, J. C., Enhanced safety and immunogenicity of a psaA mutant whole-cell inactivated pneumococcal vaccine. *Immunology and Cell Biology* **2019**.

72. Choi, E.; Michalski, C. J.; Choo, S. H.; Kim, G. N.; Banasikowska, E.; Lee, S.; Wu, K.; An, H. Y.; Mills, A.; Schneider, S.; Bredeek, U. F.; Coulston, D. R.; Ding, S.; Finzi, A.; Tian, M.; Klein, K.; Arts, E. J.; Mann, J. F.; Gao, Y.; Kang, C. Y., First Phase I human clinical trial of a killed whole-HIV-1 vaccine: demonstration of its safety and enhancement of anti-HIV antibody responses. *Retrovirology* **2016,** 13, (1), 82.

73. Seder, R. A.; Chang, L. J.; Enama, M. E.; Zephir, K. L.; Sarwar, U. N.; Gordon, I. J.; Holman, L. A.; James, E. R.; Billingsley, P. F.; Gunasekera, A.; Richman, A.; Chakravarty, S.; Manoj, A.; Velmurugan, S.; Li, M.; Ruben, A. J.; Li, T.; Eappen, A. G.; Stafford, R. E.; Plummer, S. H.; Hendel, C. S.; Novik, L.; Costner, P. J.; Mendoza, F. H.; Saunders, J. G.; Nason, M. C.; Richardson, J. H.; Murphy, J.; Davidson, S. A.; Richie, T. L.; Sedegah, M.; Sutamihardja, A.; Fahle, G. A.; Lyke, K. E.; Laurens, M. B.; Roederer, M.; Tewari, K.; Epstein, J. E.; Sim, B. K.; Ledgerwood, J. E.; Graham, B. S.; Hoffman, S. L.; Team, V. R. C. S., Protection against malaria by intravenous immunization with a nonreplicating sporozoite vaccine. *Science* **2013,** 341, (6152), 1359-65.

74. Ishizuka, A. S.; Lyke, K. E.; DeZure, A.; Berry, A. A.; Richie, T. L.; Mendoza, F. H.; Enama, M. E.; Gordon, I. J.; Chang, L. J.; Sarwar, U. N.; Zephir, K. L.; Holman, L. A.; James, E. R.; Billingsley, P. F.; Gunasekera, A.; Chakravarty, S.; Manoj, A.;

Li, M.; Ruben, A. J.; Li, T.; Eappen, A. G.; Stafford, R. E.; K, C. N.; Murshedkar, T.; DeCederfelt, H.; Plummer, S. H.; Hendel, C. S.; Novik, L.; Costner, P. J.; Saunders, J. G.; Laurens, M. B.; Plowe, C. V.; Flynn, B.; Whalen, W. R.; Todd, J. P.; Noor, J.; Rao, S.; Sierra-Davidson, K.; Lynn, G. M.; Epstein, J. E.; Kemp, M. A.; Fahle, G. A.; Mikolajczak, S. A.; Fishbaugher, M.; Sack, B. K.; Kappe, S. H.; Davidson, S. A.; Garver, L. S.; Bjorkstrom, N. K.; Nason, M. C.; Graham, B. S.; Roederer, M.; Sim, B. K.; Hoffman, S. L.; Ledgerwood, J. E.; Seder, R. A., Protection against malaria at 1 year and immune correlates following PfSPZ vaccination. *Nat Med* **2016,** 22, (6), 614-23.

75. Nishihara, H.; Lawrence, C. A.; Taplin, G. V.; Carpenter, C. M., Immunogenicity of Gamma-Irradiated Mycobacterium Tuberculosis H37rv (Giv) in Mice. *Am Rev Respir Dis* **1963,** 88, 827-32.
76. Lighter, J.; Fisher, J. Tuberculosis vaccine and method of using same. 2013.
77. Ammar, A.; El-Bialy, A.; Yousef, S.; Nemer, M. E., Evaluation of irradiated vaccine prepared from *Salmonella typhimurium* isolated from buffalo calves. *Int J Res Pure Appl Microbiol* **2014,** 4, (1), 10-14.
78. Begum, R. H.; Rahman, H.; Ahmed, G., Development and evaluation of gamma irradiated toxoid vaccine of Salmonella enterica var Typhimurium. *Vet Microbiol* **2011,** 153, (1-2), 191-7.
79. Dabral, N.; Martha Moreno, L.; Sriranganathan, N.; Vemulapalli, R., Oral immunization of mice with gamma-irradiated Brucella neotomae induces protection against intraperitoneal and intranasal challenge with virulent B. abortus 2308. *PLoS One* **2014,** 9, (9), e107180.
80. Influenza (Seasonal) fact sheet No 211. www.who.int/mediacentre/factsheets/fs211/en/ (07/02/2016),
81. Mauskopf, J.; Klesse, M.; Lee, S.; Herrera-Taracena, G., The burden of influenza complications in different high-risk groups: a targeted literature review. *Journal of Medical Economics, 2013, Vol.16(2), p.264-277* **2013,** 16, (2), 264-277.
82. Newall, A. T.; Scuffham, P. A.; Hodgkinson, B., Economic report into the cost of influenza to the Australiam health system. *Report to the Influenza Specialist Group* **2007**.
83. Mosley, V. M.; Wyckoff, R. W., Electron micrography of the virus of influenza. *Nature* **1946,** 157, 263.

84. Seladi-Schulman, J.; Steel, J.; Lowen, A. C., Spherical influenza viruses have a fitness advantage in embryonated eggs, while filament-producing strains are selected in vivo. *Journal of virology* **2013,** 87, (24), 13343-13353.

85. Noda, T.; Sugita, Y.; Aoyama, K.; Hirase, A.; Kawakami, E.; Miyazawa, A.; Sagara, H.; Kawaoka, Y., Three-dimensional analysis of ribonucleoprotein complexes in influenza A virus. *Nat Commun* **2012,** 3, 639.

86. Dadonaite, B.; Gilbertson, B.; Knight, M. L.; Trifkovic, S.; Rockman, S.; Laederach, A.; Brown, L. E.; Fodor, E.; Bauer, D. L. V., The structure of the influenza A virus genome. *Nat Microbiol* **2019,** 4, (11), 1781-1789.

87. Hutchinson, E. C.; Charles, P. D.; Hester, S. S.; Thomas, B.; Trudgian, D.; Martinez-Alonso, M.; Fodor, E., Conserved and host-specific features of influenza virion architecture. *Nat Commun* **2014,** 5, 4816.

88. Influenza Type A Viruses. http://www.cdc.gov/flu/avianflu/influenza-a-virus-subtypes.htm (26/09/2016),

89. A revision of the system of nomenclature for influenza viruses: a WHO memorandum. *Bulletin of the World Health Organization* **1980,** 58, (4), 585.

90. Nelli, R. K.; Kuchipudi, S. V.; White, G. A.; Perez, B. B.; Dunham, S. P.; Chang, K.-C., Comparative distribution of human and avian type sialic acid influenza receptors in the pig. *BMC Veterinary Research* **2010,** 6, 4-4.

91. Trebbien, R.; Larsen, L. E.; Viuff, B. M., Distribution of sialic acid receptors and influenza A virus of avian and swine origin in experimentally infected pigs. *Virology Journal* **2011,** 8.

92. Stauffer, S.; Feng, Y.; Nebioglu, F.; Heilig, R.; Picotti, P.; Helenius, A., Stepwise priming by acidic pH and a high K+ concentration is required for efficient uncoating of influenza A virus cores after penetration. *J Virol* **2014,** 88, (22), 13029-46.

93. Martin, K.; Helenius, A., Transport of incoming influenza virus nucleocapsids into the nucleus. *J Virol* **1991,** 65, (1), 232-44.

94. Wu, W. W.; Sun, Y. H.; Pante, N., Nuclear import of influenza A viral ribonucleoprotein complexes is mediated by two nuclear localization sequences on viral nucleoprotein. *Virol J* **2007,** 4, 49.

95. Drake, J. W., Rates of Spontaneous Mutation Among RNA Viruses. *Proceedings of the National Academy of Sciences of the United States of America* **1993,** 90, (9), 4171-4175.

96. Both, G. W.; Sleigh, M. J.; Cox, N. J.; Kendal, A. P., Antigenic drift in influenza virus H3 hemagglutinin from 1968 to 1980: multiple evolutionary pathways and sequential amino acid changes at key antigenic sites. *J Virol* **1983,** 48, (1), 52-60.

97. Koelle, K.; Cobey, S.; Grenfell, B.; Pascual, M., Epochal evolution shapes the phylodynamics of interpandemic influenza A (H3N2) in humans. *Science* **2006,** 314, (5807), 1898-903.

98. Smith, D. J.; Lapedes, A. S.; de Jong, J. C.; Bestebroer, T. M.; Rimmelzwaan, G. F.; Osterhaus, A. D.; Fouchier, R. A., Mapping the antigenic and genetic evolution of influenza virus. *Science* **2004,** 305, (5682), 371-6.

99. Nobusawa, E.; Ishihara, H.; Morishita, T.; Sato, K.; Nakajima, K., Change in receptor-binding specificity of recent human influenza A viruses (H3N2): A single amino acid change in hemagluttinin altered its recognition of sialyloligosaccharides. *Journal of Virology* **2000,** 278, 587-596.

100. Rogers, G. N.; Paulson, J. C.; Daniels, R. S.; Skehel, J. J.; Wilson, I. A.; Wiley, D. C., Single amino acid substitutions in influenza haemagglutinin change receptor binding specificity. *Nature* **1983,** 304, (5921), 76.

101. Potter, C. W., A history of influenza. *Journal of applied microbiology* **2001,** 91, (4), 572-9.

102. Holmes, E. C.; Ghedin, E.; Miller, N.; Taylor, J.; Bao, Y.; St George, K.; Grenfell, B. T.; Salzberg, S. L.; Fraser, C. M.; Lipman, D. J.; Taubenberger, J. K., Whole-genome analysis of human influenza A virus reveals multiple persistent lineages and reassortment among recent H3N2 viruses. *PLoS Biol* **2005,** 3, (9), e300.

103. Nelson, M. I.; Holmes, E. C., The evolution of epidemic influenza. *Nat Rev Genet* **2007,** 8, (3), 196-205.

104. Reid, A. H.; Taubenberger, J. K.; Fanning, T. G., Evidence of an absence: the genetic origins of the 1918 pandemic influenza virus. *Nat Rev Microbiol* **2004,** 2, (11), 909-14.

105. Burnet, F.; Clark, E., Influenza: A Survey of the Last 50 Years in the Light of Modern Work on the Virus of Epidemic Influenza. *Journal of the American Medical Association* **1942,** 120, (5), 408-408.

106. Johnson, N. P.; Mueller, J., Updating the accounts: global mortality of the 1918-1920 "Spanish" influenza pandemic. *Bull Hist Med* **2002,** 76, (1), 105-15.

107. Marks, G.; Beatty, W. K., Epidemics, New York: C. *Scribner's Sons* **1976**.

108. Iuliano, A. D.; Roguski, K. M.; Chang, H. H.; Muscatello, D. J.; Palekar, R.; Tempia, S.; Cohen, C.; Gran, J. M.; Schanzer, D.; Cowling, B. J.; Wu, P.; Kyncl, J.; Ang, L. W.; Park, M.; Redlberger-Fritz, M.; Yu, H.; Espenhain, L.; Krishnan, A.; Emukule, G.; van Asten, L.; Pereira da Silva, S.; Aungkulanon, S.; Buchholz, U.; Widdowson, M. A.; Bresee, J. S.; Global Seasonal Influenza-associated Mortality Collaborator, N., Estimates of global seasonal influenza-associated respiratory mortality: a modelling study. *Lancet* **2018,** 391, (10127), 1285-1300.

109. Morens, D. M.; Taubenberger, J. K.; Fauci, A. S., Predominant role of bacterial pneumonia as a cause of death in pandemic influenza: implications for pandemic influenza preparedness. *J Infect Dis* **2008,** 198, (7), 962-70.

110. Blake, F. G.; Small, J. C.; Rivers, T. M., *Epidemic respiratory disease: the pneumonias and other infections of the respiratory tract accompanying influenza and measles*. CV Mosby: 1921.

111. Roos, C., Notes on the bacteriology, and on the selective action of B. influenzae Pfeiffer. *The Journal of Immunology* **1919,** 4, (4), 189-201.

112. McCullers, J. A., Insights into the interaction between influenza virus and pneumococcus. *Clin Microbiol Rev* **2006,** 19, (3), 571-82.

113. Smith, M. W.; Schmidt, J. E.; Rehg, J. E.; Orihuela, C. J.; McCullers, J. A., Induction of pro- and anti-inflammatory molecules in a mouse model of pneumococcal pneumonia after influenza. *Comp Med* **2007,** 57, (1), 82-9.

114. Nelson, G. E.; Gershman, K. A.; Swerdlow, D. L.; Beall, B. W.; Moore, M. R., Invasive pneumococcal disease and pandemic (H1N1) 2009, Denver, Colorado, USA. *Emerg Infect Dis* **2012,** 18, (2), 208-16.

115. Fleming, A., On the Antibacterial Action of Cultures of a Penicillium, with Special Reference to their Use in the Isolation of B. influenzæ. *British journal of experimental pathology* **1929,** 10, (3), 226-236.

116. Taubenberger, J. K.; Morens, D. M., 1918 Influenza: the mother of all pandemics. *Emerg Infect Dis* **2006,** 12, (1), 15-22.

117. Tumpey, T. M.; Basler, C. F.; Aguilar, P. V.; Zeng, H.; Solorzano, A.; Swayne, D. E.; Cox, N. J.; Katz, J. M.; Taubenberger, J. K.; Palese, P.; Garcia-Sastre, A., Characterization of the reconstructed 1918 Spanish influenza pandemic virus. *Science* **2005,** 310, (5745), 77-80.

118. de Wit, E.; Siegers, J. Y.; Cronin, J. M.; Weatherman, S.; van den Brand, J. M.; Leijten, L. M.; van Run, P.; Begeman, L.; van den Ham, H. J.; Andeweg, A. C.;

Bushmaker, T.; Scott, D. P.; Saturday, G.; Munster, V. J.; Feldmann, H.; van Riel, D., 1918 H1N1 Influenza Virus Replicates and Induces Proinflammatory Cytokine Responses in Extrarespiratory Tissues of Ferrets. *J Infect Dis* **2018,** 217, (8), 1237-1246.

119. Kobasa, D.; Jones, S. M.; Shinya, K.; Kash, J. C.; Copps, J.; Ebihara, H.; Hatta, Y.; Kim, J. H.; Halfmann, P.; Hatta, M.; Feldmann, F.; Alimonti, J. B.; Fernando, L.; Li, Y.; Katze, M. G.; Feldmann, H.; Kawaoka, Y., Aberrant innate immune response in lethal infection of macaques with the 1918 influenza virus. *Nature* **2007,** 445, (7125), 319-23.
120. Kash, J. C.; Tumpey, T. M.; Proll, S. C.; Carter, V.; Perwitasari, O.; Thomas, M. J.; Basler, C. F.; Palese, P.; Taubenberger, J. K.; Garcia-Sastre, A.; Swayne, D. E.; Katze, M. G., Genomic analysis of increased host immune and cell death responses induced by 1918 influenza virus. *Nature* **2006,** 443, (7111), 578-81.
121. Tulchinsky, T. H., Maurice Hilleman: Creator of Vaccines That Changed the World. *Case Studies in Public Health* **2018**, 443.
122. Hilleman, M. R.; Flatley, F. J.; Anderson, S. A.; Luecking, M. L.; Levinson, D. J., Antibody response in volunteers to Asian influenza vaccine. *J Am Med Assoc* **1958,** 166, (10), 1134-40.
123. Schulman, J. L.; Kilbourne, E. D., Independent variation in nature of hemagglutinin and neuraminidase antigens of influenza virus: distinctiveness of hemagglutinin antigen of Hong Kong-68 virus. *Proc Natl Acad Sci U S A* **1969,** 63, (2), 326-33.
124. Monto, A. S.; Kendal, A. P., Effect of neuraminidase antibody on Hong Kong influenza. *Lancet* **1973,** 1, (7804), 623-5.
125. Kawaoka, Y.; Krauss, S.; Webster, R. G., Avian-to-human transmission of the PB1 gene of influenza A viruses in the 1957 and 1968 pandemics. *J Virol* **1989,** 63, (11), 4603-8.
126. Schnitzler, S. U.; Schnitzler, P., An update on swine-origin influenza virus A/H1N1: a review. *Virus Genes* **2009,** 39, (3), 279-92.
127. Garten, R. J.; Davis, C. T.; Russell, C. A.; Shu, B.; Lindstrom, S.; Balish, A.; Sessions, W. M.; Xu, X.; Skepner, E.; Deyde, V.; Okomo-Adhiambo, M.; Gubareva, L.; Barnes, J.; Smith, C. B.; Emery, S. L.; Hillman, M. J.; Rivailler, P.; Smagala, J.; de Graaf, M.; Burke, D. F.; Fouchier, R. A.; Pappas, C.; Alpuche-Aranda, C. M.; Lopez-Gatell, H.; Olivera, H.; Lopez, I.; Myers, C. A.; Faix, D.; Blair, P. J.; Yu, C.; Keene, K. M.; Dotson, P. D., Jr.; Boxrud, D.; Sambol, A. R.;

Abid, S. H.; St George, K.; Bannerman, T.; Moore, A. L.; Stringer, D. J.; Blevins, P.; Demmler-Harrison, G. J.; Ginsberg, M.; Kriner, P.; Waterman, S.; Smole, S.; Guevara, H. F.; Belongia, E. A.; Clark, P. A.; Beatrice, S. T.; Donis, R.; Katz, J.; Finelli, L.; Bridges, C. B.; Shaw, M.; Jernigan, D. B.; Uyeki, T. M.; Smith, D. J.; Klimov, A. I.; Cox, N. J., Antigenic and genetic characteristics of swine-origin 2009 A(H1N1) influenza viruses circulating in humans. *Science* **2009,** 325, (5937), 197-201.

128. Kelly, H.; Peck, H. A.; Laurie, K. L.; Wu, P.; Nishiura, H.; Cowling, B. J., The age-specific cumulative incidence of infection with pandemic influenza H1N1 2009 was similar in various countries prior to vaccination. *PLoS One* **2011,** 6, (8), e21828.
129. Simonsen, L.; Spreeuwenberg, P.; Lustig, R.; Taylor, R. J.; Fleming, D. M.; Kroneman, M.; Van Kerkhove, M. D.; Mounts, A. W.; Paget, W. J.; Teams, G. L. C., Global mortality estimates for the 2009 Influenza Pandemic from the GLaMOR project: a modeling study. *PLoS Med* **2013,** 10, (11), e1001558.
130. Dawood, F. S.; Iuliano, A. D.; Reed, C.; Meltzer, M. I.; Shay, D. K.; Cheng, P. Y.; Bandaranayake, D.; Breiman, R. F.; Brooks, W. A.; Buchy, P.; Feikin, D. R.; Fowler, K. B.; Gordon, A.; Hien, N. T.; Horby, P.; Huang, Q. S.; Katz, M. A.; Krishnan, A.; Lal, R.; Montgomery, J. M.; Molbak, K.; Pebody, R.; Presanis, A. M.; Razuri, H.; Steens, A.; Tinoco, Y. O.; Wallinga, J.; Yu, H.; Vong, S.; Bresee, J.; Widdowson, M. A., Estimated global mortality associated with the first 12 months of 2009 pandemic influenza A H1N1 virus circulation: a modelling study. *Lancet Infect Dis* **2012,** 12, (9), 687-95.
131. Chan, P. K., Outbreak of avian influenza A(H5N1) virus infection in Hong Kong in 1997. *Clin Infect Dis* **2002,** 34 Suppl 2, S58-64.
132. Lai, S.; Qin, Y.; Cowling, B. J.; Ren, X.; Wardrop, N. A.; Gilbert, M.; Tsang, T. K.; Wu, P.; Feng, L.; Jiang, H.; Peng, Z.; Zheng, J.; Liao, Q.; Li, S.; Horby, P. W.; Farrar, J. J.; Gao, G. F.; Tatem, A. J.; Yu, H., Global epidemiology of avian influenza A H5N1 virus infection in humans, 1997-2015: a systematic review of individual case data. *Lancet Infect Dis* **2016,** 16, (7), e108-e118.
133. Avian Influenza Weekly Update Number 746. In World Health Organisation 2020.
134. Zhang, Y.; Zhang, Q.; Kong, H.; Jiang, Y.; Gao, Y.; Deng, G.; Shi, J.; Tian, G.; Liu, L.; Liu, J.; Guan, Y.; Bu, Z.; Chen, H., H5N1 hybrid viruses bearing 2009/H1N1 virus genes transmit in guinea pigs by respiratory droplet. *Science* **2013,** 340, (6139), 1459-63.

135. Le Goffic, R.; Balloy, V.; Lagranderie, M.; Alexopoulou, L.; Escriou, N.; Flavell, R.; Chignard, M.; Si-Tahar, M.; Levine, B., Detrimental Contribution of the Toll-Like Receptor (TLR)3 to Influenza A Virus–Induced Acute Pneumonia. *PLoS Pathogens* **2006,** 2, (6).

136. Diebold, S. S.; Kaisho, T.; Hemmi, H.; Akira, S.; Reis E Sousa, C., Innate antiviral responses by means of TLR7-mediated recognition of single-stranded RNA. *Science (New York, N.Y.)* **2004,** 303, (5663), 1529.

137. Lund, J. M.; Alexopoulou, L.; Iwasaki, A.; Flavell, R. A.; Sato, A.; Karow, M.; Adams, N. C.; Gale, N. W., Recognition of single-stranded RNA viruses by Toll-like receptor 7. *Proceedings of the National Academy of Sciences of the United States of America* **2004,** 101, (15), 5598-5603.

138. Lee, N.; Wong, C. K.; Hui, D. S. C.; Lee, S. K. W.; Wong, R. Y. K.; Ngai, K. L. K.; Chan, M. C. W.; Chu, Y. J.; Ho, A. W. Y.; Lui, G. C. Y.; Wong, B. C. K.; Wong, S. H.; Yip, S. P.; Chan, P. K. S., Role of human Toll-like receptors in naturally occurring influenza A infections. *Influenza and Other Respiratory Viruses* **2013,** 7, (5), 666-675.

139. Alexopoulou, L.; Holt, A. C.; Medzhitov, R.; Flavell, R. A., Recognition of double-stranded RNA and activation of NF-kappaB by Toll-like receptor 3. *Nature* **2001,** 413, (6857), 732-8.

140. Schulz, O.; Diebold, S. S.; Chen, M.; Naslund, T. I.; Nolte, M. A.; Alexopoulou, L.; Azuma, Y. T.; Flavell, R. A.; Liljestrom, P.; Reis e Sousa, C., Toll-like receptor 3 promotes cross-priming to virus-infected cells. *Nature* **2005,** 433, (7028), 887-92.

141. Lund, J. M.; Alexopoulou, L.; Sato, A.; Karow, M.; Adams, N. C.; Gale, N. W.; Iwasaki, A.; Flavell, R. A., Recognition of single-stranded RNA viruses by Toll-like receptor 7. *Proc Natl Acad Sci U S A* **2004,** 101, (15), 5598-603.

142. Ablasser, A.; Poeck, H.; Anz, D.; Berger, M.; Schlee, M.; Kim, S.; Bourquin, C.; Goutagny, N.; Jiang, Z.; Fitzgerald, K. A.; Rothenfusser, S.; Endres, S.; Hartmann, G.; Hornung, V., Selection of molecular structure and delivery of RNA oligonucleotides to activate TLR7 versus TLR8 and to induce high amounts of IL-12p70 in primary human monocytes. *J Immunol* **2009,** 182, (11), 6824-33.

143. Pichlmair, A.; Schulz, O.; Tan, C. P.; Naslund, T. I.; Liljestrom, P.; Weber, F.; Reis e Sousa, C., RIG-I-mediated antiviral responses to single-stranded RNA bearing 5'-phosphates. *Science* **2006,** 314, (5801), 997-1001.

144. Kato, H.; Sato, S.; Yoneyama, M.; Yamamoto, M.; Uematsu, S.; Matsui, K.; Tsujimura, T.; Takeda, K.; Fujita, T.; Takeuchi, O.; Akira, S., Cell type-specific involvement of RIG-I in antiviral response. *Immunity* **2005,** 23, (1), 19-28.

145. Hornung, V.; Ellegast, J.; Kim, S.; Brzozka, K.; Jung, A.; Kato, H.; Poeck, H.; Akira, S.; Conzelmann, K. K.; Schlee, M.; Endres, S.; Hartmann, G., 5'-Triphosphate RNA is the ligand for RIG-I. *Science* **2006,** 314, (5801), 994-7.

146. Garcia-Sastre, A.; Biron, C. A., Type 1 interferons and the virus-host relationship: a lesson in detente. *Science* **2006,** 312, (5775), 879-82.

147. GeurtsvanKessel, C. H.; Bergen, I. M.; Muskens, F.; Boon, L.; Hoogsteden, H. C.; Osterhaus, A. D.; Rimmelzwaan, G. F.; Lambrecht, B. N., Both conventional and interferon killer dendritic cells have antigen-presenting capacity during influenza virus infection. *PLoS One* **2009,** 4, (9), e7187.

148. Ho, A. W.; Prabhu, N.; Betts, R. J.; Ge, M. Q.; Dai, X.; Hutchinson, P. E.; Lew, F. C.; Wong, K. L.; Hanson, B. J.; Macary, P. A.; Kemeny, D. M., Lung CD103+ dendritic cells efficiently transport influenza virus to the lymph node and load viral antigen onto MHC class I for presentation to CD8 T cells. *J Immunol* **2011,** 187, (11), 6011-21.

149. Yewdell, J. W.; Bennink, J. R.; Smith, G. L.; Moss, B., Influenza A virus nucleoprotein is a major target antigen for cross-reactive anti-influenza A virus cytotoxic T lymphocytes. *Proc Natl Acad Sci U S A* **1985,** 82, (6), 1785-9.

150. Taylor, P. M.; Askonas, B. A., Influenza nucleoprotein-specific cytotoxic T-cell clones are protective in vivo. *Immunology* **1986,** 58, (3), 417-20.

151. Jameson, J.; Cruz, J.; Ennis, F. A., Human cytotoxic T-lymphocyte repertoire to influenza A viruses. *J Virol* **1998,** 72, (11), 8682-9.

152. Gotch, F.; McMichael, A.; Smith, G.; Moss, B., Identification of viral molecules recognized by influenza-specific human cytotoxic T lymphocytes. *J Exp Med* **1987,** 165, (2), 408-16.

153. Hufford, M. M.; Kim, T. S.; Sun, J.; Braciale, T. J., Antiviral CD8+ T cell effector activities in situ are regulated by target cell type. *J Exp Med* **2011,** 208, (1), 167-80.

154. Topham, D. J.; Tripp, R. A.; Doherty, P. C., CD8+ T cells clear influenza virus by perforin or Fas-dependent processes. *J Immunol* **1997,** 159, (11), 5197-200.

155. Johnson, B. J.; Costelloe, E. O.; Fitzpatrick, D. R.; Haanen, J. B.; Schumacher, T. N.; Brown, L. E.; Kelso, A., Single-cell perforin and granzyme expression reveals

the anatomical localization of effector CD8+ T cells in influenza virus-infected mice. *Proc Natl Acad Sci U S A* **2003,** 100, (5), 2657-62.

156. Brehm, M. A.; Daniels, K. A.; Welsh, R. M., Rapid production of TNF-alpha following TCR engagement of naive CD8 T cells. *J Immunol* **2005,** 175, (8), 5043-9.

157. Pizzolla, A.; Nguyen, T. H. O.; Smith, J. M.; Brooks, A. G.; Kedzieska, K.; Heath, W. R.; Reading, P. C.; Wakim, L. M., Resident memory CD8(+) T cells in the upper respiratory tract prevent pulmonary influenza virus infection. *Sci Immunol* **2017,** 2, (12).

158. Pizzolla, A.; Nguyen, T. H.; Sant, S.; Jaffar, J.; Loudovaris, T.; Mannering, S. I.; Thomas, P. G.; Westall, G. P.; Kedzierska, K.; Wakim, L. M., Influenza-specific lung-resident memory T cells are proliferative and polyfunctional and maintain diverse TCR profiles. *J Clin Invest* **2018,** 128, (2), 721-733.

159. Zens, K. D.; Chen, J. K.; Farber, D. L., Vaccine-generated lung tissue-resident memory T cells provide heterosubtypic protection to influenza infection. *JCI Insight* **2016,** 1, (10).

160. Ingulli, E.; Mondino, A.; Khoruts, A.; Jenkins, M. K., In vivo detection of dendritic cell antigen presentation to CD4(+) T cells. *J Exp Med* **1997,** 185, (12), 2133-41.

161. Lukens, M. V.; Kruijsen, D.; Coenjaerts, F. E.; Kimpen, J. L.; van Bleek, G. M., Respiratory syncytial virus-induced activation and migration of respiratory dendritic cells and subsequent antigen presentation in the lung-draining lymph node. *J Virol* **2009,** 83, (14), 7235-43.

162. Deng, N.; Weaver, J. M.; Mosmann, T. R., Cytokine diversity in the Th1-dominated human anti-influenza response caused by variable cytokine expression by Th1 cells, and a minor population of uncommitted IL-2+IFNgamma- Thpp cells. *PLoS One* **2014,** 9, (5), e95986.

163. Magram, J.; Connaughton, S. E.; Warrier, R. R.; Carvajal, D. M.; Wu, C. Y.; Ferrante, J.; Stewart, C.; Sarmiento, U.; Faherty, D. A.; Gately, M. K., IL-12-deficient mice are defective in IFN gamma production and type 1 cytokine responses. *Immunity* **1996,** 4, (5), 471-81.

164. Zhang, Y.; Apilado, R.; Coleman, J.; Ben-Sasson, S.; Tsang, S.; Hu-Li, J.; Paul, W. E.; Huang, H., Interferon gamma stabilizes the T helper cell type 1 phenotype. *J Exp Med* **2001,** 194, (2), 165-72.

165. Allan, W.; Tabi, Z.; Cleary, A.; Doherty, P. C., Cellular events in the lymph node and lung of mice with influenza. Consequences of depleting CD4+ T cells. *J Immunol* **1990,** 144, (10), 3980-6.

166. Bodmer, H.; Obert, G.; Chan, S.; Benoist, C.; Mathis, D., Environmental modulation of the autonomy of cytotoxic T lymphocytes. *Eur J Immunol* **1993,** 23, (7), 1649-54.

167. Mozdzanowska, K.; Furchner, M.; Maiese, K.; Gerhard, W., CD4+ T cells are ineffective in clearing a pulmonary infection with influenza type A virus in the absence of B cells. *Virology* **1997,** 239, (1), 217-25.

168. Topham, D. J.; Doherty, P. C., Clearance of an Influenza A Virus by CD4+ T Cells Is Inefficient in the Absence of B Cells. *Journal of Virology* **1998,** 72, (1), 882.

169. Murphy, B. R.; Clements, M. L., The systemic and mucosal immune response of humans to influenza A virus. *Curr Top Microbiol Immunol* **1989,** 146, 107-16.

170. Asahi, Y.; Yoshikawa, T.; Watanabe, I.; Iwasaki, T.; Hasegawa, H.; Sato, Y.; Shimada, S.; Nanno, M.; Matsuoka, Y.; Ohwaki, M.; Iwakura, Y.; Suzuki, Y.; Aizawa, C.; Sata, T.; Kurata, T.; Tamura, S., Protection against influenza virus infection in polymeric Ig receptor knockout mice immunized intranasally with adjuvant-combined vaccines. *J Immunol* **2002,** 168, (6), 2930-8.

171. Seibert, C. W.; Rahmat, S.; Krause, J. C.; Eggink, D.; Albrecht, R. A.; Goff, P. H.; Krammer, F.; Duty, J. A.; Bouvier, N. M.; Garcia-Sastre, A.; Palese, P., Recombinant IgA is sufficient to prevent influenza virus transmission in guinea pigs. *J Virol* **2013,** 87, (14), 7793-804.

172. Marcelin, G.; Sandbulte, M. R.; Webby, R. J., Contribution of antibody production against neuraminidase to the protection afforded by influenza vaccines. *Rev Med Virol* **2012,** 22, (4), 267-79.

173. Whittle, J. R.; Zhang, R.; Khurana, S.; King, L. R.; Manischewitz, J.; Golding, H.; Dormitzer, P. R.; Haynes, B. F.; Walter, E. B.; Moody, M. A.; Kepler, T. B.; Liao, H. X.; Harrison, S. C., Broadly neutralizing human antibody that recognizes the receptor-binding pocket of influenza virus hemagglutinin. *Proc Natl Acad Sci U S A* **2011,** 108, (34), 14216-21.

174. Tan, G. S.; Krammer, F.; Eggink, D.; Kongchanagul, A.; Moran, T. M.; Palese, P., A pan-H1 anti-hemagglutinin monoclonal antibody with potent broad-spectrum efficacy in vivo. *J Virol* **2012,** 86, (11), 6179-88.

175. Ekiert, D. C.; Friesen, R. H.; Bhabha, G.; Kwaks, T.; Jongeneelen, M.; Yu, W.; Ophorst, C.; Cox, F.; Korse, H. J.; Brandenburg, B.; Vogels, R.; Brakenhoff, J. P.; Kompier, R.; Koldijk, M. H.; Cornelissen, L. A.; Poon, L. L.; Peiris, M.; Koudstaal, W.; Wilson, I. A.; Goudsmit, J., A highly conserved neutralizing epitope on group 2 influenza A viruses. *Science* **2011,** 333, (6044), 843-50.

176. Ekiert, D. C.; Bhabha, G.; Elsliger, M. A.; Friesen, R. H.; Jongeneelen, M.; Throsby, M.; Goudsmit, J.; Wilson, I. A., Antibody recognition of a highly conserved influenza virus epitope. *Science* **2009,** 324, (5924), 246-51.

177. Chambers, B. S.; Parkhouse, K.; Ross, T. M.; Alby, K.; Hensley, S. E., Identification of Hemagglutinin Residues Responsible for H3N2 Antigenic Drift during the 2014-2015 Influenza Season. *Cell Rep* **2015,** 12, (1), 1-6.

178. McLean, K. A.; Goldin, S.; Nannei, C.; Sparrow, E.; Torelli, G., The 2015 global production capacity of seasonal and pandemic influenza vaccine. *Vaccine* **2016,** 34, (45), 5410-5413.

179. Recommendations of the Strategic Advisory Group of Experts (SAGE) on influenza A (H1N1) vaccines. 19 May 2009. In World Health Organization.

180. Abelin, A.; Colegate, T.; Gardner, S.; Hehme, N.; Palache, A., Lessons from pandemic influenza A(H1N1): the research-based vaccine industry's perspective. *Vaccine* **2011,** 29, (6), 1135-8.

181. Skowronski, D. M.; Janjua, N. Z.; De Serres, G.; Sabaiduc, S.; Eshaghi, A.; Dickinson, J. A.; Fonseca, K.; Winter, A. L.; Gubbay, J. B.; Krajden, M.; Petric, M.; Charest, H.; Bastien, N.; Kwindt, T. L.; Mahmud, S. M.; Van Caeseele, P.; Li, Y., Low 2012-13 influenza vaccine effectiveness associated with mutation in the egg-adapted H3N2 vaccine strain not antigenic drift in circulating viruses. *PLoS One* **2014,** 9, (3), e92153.

182. David, S. C.; Norton, T.; Tyllis, T.; Wilson, J. J.; Singleton, E. V.; Laan, Z.; Davies, J.; Hirst, T. R.; Comerford, I.; McColl, S. R.; Paton, J. C.; Alsharifi, M., Direct interaction of whole-inactivated influenza A and pneumococcal vaccines enhances influenza-specific immunity. *Nat Microbiol* **2019,** 4, (8), 1316-1327.

183. David, S. C.; Lau, J.; Singleton, E. V.; Babb, R.; Davies, J.; Hirst, T. R.; McColl, S. R.; Paton, J. C.; Alsharifi, M., The effect of gamma-irradiation conditions on the immunogenicity of whole-inactivated Influenza A virus vaccine. *Vaccine* **2017,** 35, (7), 1071-1079.

184. Müllbacher, A.; Lobigs, M.; Alsharifi, M.; Regner, M., Cytotoxic T-cell immunity as a target for influenza vaccines. *Lancet Infect Dis* **2006,** 6, 255-256.

185. Furuya, Y.; Chan, J.; Regner, M.; Lobigs, M.; Koskinen, A.; Kok, T.; Manavis, J.; Li, P.; Mullbacher, A.; Alsharifi, M., Cytotoxic T Cells Are the Predominant Players Providing Cross-Protective Immunity Induced by γ-Irradiated Influenza A Viruses. *The Journal of Virology* **2010,** 84, (9), 4212.

186. McCartney, S.; Vermi, W.; Gilfillan, S.; Cella, M.; Murphy, T. L.; Schreiber, R. D.; Murphy, K. M.; Colonna, M., Distinct and complementary functions of MDA5 and TLR3 in poly(I:C)-mediated activation of mouse NK cells. *J Exp Med* **2009,** 206, (13), 2967-76.

187. McKee, A. S.; MacLeod, M. K.; Kappler, J. W.; Marrack, P., Immune mechanisms of protection: can adjuvants rise to the challenge? *BMC Biol* **2010,** 8, 37.

188. Di Pasquale, A.; Preiss, S.; Tavares Da Silva, F.; Garcon, N., Vaccine Adjuvants: from 1920 to 2015 and Beyond. *Vaccines (Basel)* **2015,** 3, (2), 320-43.

189. Kool, M.; Fierens, K.; Lambrecht, B. N., Alum adjuvant: some of the tricks of the oldest adjuvant. *J Med Microbiol* **2012,** 61, (Pt 7), 927-934.

190. Kool, M.; Soullie, T.; van Nimwegen, M.; Willart, M. A.; Muskens, F.; Jung, S.; Hoogsteden, H. C.; Hammad, H.; Lambrecht, B. N., Alum adjuvant boosts adaptive immunity by inducing uric acid and activating inflammatory dendritic cells. *J Exp Med* **2008,** 205, (4), 869-82.

191. McKee, A. S.; Munks, M. W.; MacLeod, M. K.; Fleenor, C. J.; Van Rooijen, N.; Kappler, J. W.; Marrack, P., Alum induces innate immune responses through macrophage and mast cell sensors, but these sensors are not required for alum to act as an adjuvant for specific immunity. *J Immunol* **2009,** 183, (7), 4403-14.

192. Calabro, S.; Tortoli, M.; Baudner, B. C.; Pacitto, A.; Cortese, M.; O'Hagan, D. T.; De Gregorio, E.; Seubert, A.; Wack, A., Vaccine adjuvants alum and MF59 induce rapid recruitment of neutrophils and monocytes that participate in antigen transport to draining lymph nodes. *Vaccine* **2011,** 29, (9), 1812-23.

193. Podda, A., The adjuvanted influenza vaccines with novel adjuvants: experience with the MF59-adjuvanted vaccine. *Vaccine* **2001,** 19, (17-19), 2673-80.

194. Ott, G.; Barchfeld, G. L.; Chernoff, D.; Radhakrishnan, R.; van Hoogevest, P.; Van Nest, G., MF59. Design and evaluation of a safe and potent adjuvant for human vaccines. *Pharm Biotechnol* **1995,** 6, 277-96.

195. Seubert, A.; Monaci, E.; Pizza, M.; O'Hagan, D. T.; Wack, A., The adjuvants aluminum hydroxide and MF59 induce monocyte and granulocyte chemoattractants and enhance monocyte differentiation toward dendritic cells. *J Immunol* **2008,** 180, (8), 5402-12.

196. Dupuis, M.; Murphy, T. J.; Higgins, D.; Ugozzoli, M.; van Nest, G.; Ott, G.; McDonald, D. M., Dendritic cells internalize vaccine adjuvant after intramuscular injection. *Cell Immunol* **1998,** 186, (1), 18-27.

197. Alsharifi, M.; Lobigs, M.; Regner, M.; Lee, E.; Koskinen, A.; Mullbacher, A., Type I interferons trigger systemic, partial lymphocyte activation in response to viral infection. *J Immunol* **2005,** 175, (7), 4635-40.

198. Ivashkiv, L. B.; Donlin, L. T., Regulation of type I interferon responses. *Nat Rev Immunol* **2014,** 14, (1), 36-49.

199. Babb, R.; Chan, J.; Khairat, J. E.; Furuya, Y.; Alsharifi, M., Gamma-Irradiated Influenza A Virus Provides Adjuvant Activity to a Co-Administered Poorly Immunogenic SFV Vaccine in Mice. *Front Immunol* **2014,** 5, 267.

200. Babb, R.; Chen, A.; Ogunniyi, A. D.; Hirst, T. R.; Kara, E. E.; McColl, S. R.; Alsharifi, M.; Paton, J. C., Enhanced protective responses to a serotype-independent pneumococcal vaccine when combined with an inactivated influenza vaccine. *Clin Sci (Lond)* **2017,** 131, (2), 169-180.

201. Rowe, H. M.; Meliopoulos, V. A.; Iverson, A.; Bomme, P.; Schultz-Cherry, S.; Rosch, J. W., Direct interactions with influenza promote bacterial adherence during respiratory infections. *Nat Microbiol* **2019,** 4, (8), 1328-1336.

202. Doyle, T. M. In *A hitherto unrecorded disease of fowls due to a filter-passing virus*, 1927; 1927.

203. Kraneveld, F. C., A poultry disease in the Dutch East Indies. *Ned. Indisch. Bl. Diergeneeskd.* **1926,** 38, 448-450.

204. Bank, W., World Livestock Disease Atlas. A Quantitative Analysis of Global Animal Health Data.(2006–2009). Washington, DC. In 2011.

205. Khattar, S. K.; Kumar, S.; Xiao, S.; Collins, P. L.; Samal, S. K., Experimental infection of mice with avian paramyxovirus serotypes 1 to 9. *PLoS One* **2011,** 6, (2), e16776.

206. Goff, P. H.; Gao, Q.; Palese, P., A majority of infectious Newcastle disease virus particles contain a single genome, while a minority contain multiple genomes. *J Virol* **2012,** 86, (19), 10852-6.

207. de Leeuw, O. S.; Koch, G.; Hartog, L.; Ravenshorst, N.; Peeters, B. P., Virulence of Newcastle disease virus is determined by the cleavage site of the fusion protein and by both the stem region and globular head of the haemagglutinin-neuraminidase protein. *J Gen Virol* **2005,** 86, (Pt 6), 1759-69.

208. Romer-Oberdorfer, A.; Werner, O.; Veits, J.; Mebatsion, T.; Mettenleiter, T. C., Contribution of the length of the HN protein and the sequence of the F protein cleavage site to Newcastle disease virus pathogenicity. *J Gen Virol* **2003,** 84, (Pt 11), 3121-3129.

209. Saif, Y. M.; Fadly, A. M.; Glisson, J. R.; McDougald, L. R.; Nolan, L. K.; Swayne, D. E., *Diseases of poultry*. John Wiley & Sons: 2011.

210. Dimitrov, K. M.; Abolnik, C.; Afonso, C. L.; Albina, E.; Bahl, J.; Berg, M.; Briand, F. X.; Brown, I. H.; Choi, K. S.; Chvala, I.; Diel, D. G.; Durr, P. A.; Ferreira, H. L.; Fusaro, A.; Gil, P.; Goujgoulova, G. V.; Grund, C.; Hicks, J. T.; Joannis, T. M.; Torchetti, M. K.; Kolosov, S.; Lambrecht, B.; Lewis, N. S.; Liu, H.; Liu, H.; McCullough, S.; Miller, P. J.; Monne, I.; Muller, C. P.; Munir, M.; Reischak, D.; Sabra, M.; Samal, S. K.; Servan de Almeida, R.; Shittu, I.; Snoeck, C. J.; Suarez, D. L.; Van Borm, S.; Wang, Z.; Wong, F. Y. K., Updated unified phylogenetic classification system and revised nomenclature for Newcastle disease virus. *Infect Genet Evol* **2019,** 74, 103917.

211. Alexander, D. J.; Campbell, G.; Manvell, R. J.; Collins, M. S.; Parsons, G.; McNulty, M. S., Characterisation of an antigenically unusual virus responsible for two outbreaks of Newcastle disease in the Republic of Ireland in 1990. *Vet Rec* **1992,** 130, (4), 65-8.

212. Diel, D. G.; da Silva, L. H.; Liu, H.; Wang, Z.; Miller, P. J.; Afonso, C. L., Genetic diversity of avian paramyxovirus type 1: proposal for a unified nomenclature and classification system of Newcastle disease virus genotypes. *Infect Genet Evol* **2012,** 12, (8), 1770-9.

213. Radwan, M. M.; Darwish, S. F.; El-Sabagh, I. M.; El-Sanousi, A. A.; Shalaby, M. A., Isolation and molecular characterization of Newcastle disease virus genotypes II and VIId in Egypt between 2011 and 2012. *Virus Genes* **2013,** 47, (2), 311-6.

214. Farooq, M.; Saliha, U.; Munir, M.; Khan, Q. M., Biological and genotypic characterization of the Newcastle disease virus isolated from disease outbreaks in commercial poultry farms in northern Punjab, Pakistan. *Virology Reports* **2014,** 3, 30-39.

215. Zaffuto, K. M.; Estevez, C. N.; Afonso, C. L., Primary chicken tracheal cell culture system for the study of infection with avian respiratory viruses. *Avian Pathol* **2008,** 37, (1), 25-31.

216. Ecco, R.; Susta, L.; Afonso, C. L.; Miller, P. J.; Brown, C., Neurological lesions in chickens experimentally infected with virulent Newcastle disease virus isolates. *Avian Pathol* **2011,** 40, (2), 145-52.

217. Butt, S. L.; Moura, V.; Susta, L.; Miller, P. J.; Hutcheson, J. M.; Cardenas-Garcia, S.; Brown, C. C.; West, F. D.; Afonso, C. L.; Stanton, J. B., Tropism of Newcastle disease virus strains for chicken neurons, astrocytes, oligodendrocytes, and microglia. *BMC Vet Res* **2019,** 15, (1), 317.

218. Lam, K. M., Growth of Newcastle disease virus in chicken macrophages. *J Comp Pathol* **1996,** 115, (3), 253-63.

219. Lam, K. M.; Vasconcelos, A. C., Newcastle disease virus-induced apoptosis in chicken peripheral blood lymphocytes. *Vet Immunol Immunopathol* **1994,** 44, (1), 45-56.

220. Villar, E.; Barroso, I. M., Role of sialic acid-containing molecules in paramyxovirus entry into the host cell: a minireview. *Glycoconjugate journal* **2006,** 23, (1-2), 5-17.

221. Sanchez-Felipe, L.; Villar, E.; Munoz-Barroso, I., Entry of Newcastle Disease Virus into the host cell: role of acidic pH and endocytosis. *Biochim Biophys Acta* **2014,** 1838, (1 Pt B), 300-9.

222. Peeters, B. P.; Gruijthuijsen, Y. K.; de Leeuw, O. S.; Gielkens, A. L., Genome replication of Newcastle disease virus: involvement of the rule-of-six. *Arch Virol* **2000,** 145, (9), 1829-45.

223. *Fields virology*. 3rd ed. ed.; Raven Press: New York, 1996.

224. Egelman, E. H.; Wu, S. S.; Amrein, M.; Portner, A.; Murti, G., The Sendai virus nucleocapsid exists in at least four different helical states. *J Virol* **1989,** 63, (5), 2233-43.

225. Kolakofsky, D.; Pelet, T.; Garcin, D.; Hausmann, S.; Curran, J.; Roux, L., Paramyxovirus RNA synthesis and the requirement for hexamer genome length: the rule of six revisited. *J Virol* **1998,** 72, (2), 891-9.

226. Ahmed, K. A.; Saxena, V. K.; Ara, A.; Singh, K. B.; Sundaresan, N. R.; Saxena, M.; Rasool, T. J., Immune response to Newcastle disease virus in chicken lines

divergently selected for cutaneous hypersensitivity. *Int J Immunogenet* **2007,** 34, (6), 445-55.

227. Sick, C.; Schultz, U.; Munster, U.; Meier, J.; Kaspers, B.; Staeheli, P., Promoter structures and differential responses to viral and nonviral inducers of chicken type I interferon genes. *J Biol Chem* **1998,** 273, (16), 9749-54.
228. Munir, S.; Sharma, J. M.; Kapur, V., Transcriptional response of avian cells to infection with Newcastle disease virus. *Virus Res* **2005,** 107, (1), 103-8.
229. Rue, C. A.; Susta, L.; Cornax, I.; Brown, C. C.; Kapczynski, D. R.; Suarez, D. L.; King, D. J.; Miller, P. J.; Afonso, C. L., Virulent Newcastle disease virus elicits a strong innate immune response in chickens. *J Gen Virol* **2011,** 92, (Pt 4), 931-9.
230. Hoss, A.; Zwarthoff, E. C.; Zawatzky, R., Differential expression of interferon alpha and beta induced with Newcastle disease virus in mouse macrophage cultures. *J Gen Virol* **1989,** 70 (Pt 3), 575-89.
231. Zawatzky, R.; Wurmbaeck, H.; Falk, W.; Homfeld, A., Endogenous interferon specifically regulates Newcastle disease virus-induced cytokine gene expression in mouse macrophages. *J Virol* **1991,** 65, (9), 4839-46.
232. Huang, Z.; Krishnamurthy, S.; Panda, A.; Samal, S. K., Newcastle disease virus V protein is associated with viral pathogenesis and functions as an alpha interferon antagonist. *J Virol* **2003,** 77, (16), 8676-85.
233. Wang, C.; Chu, Z.; Liu, W.; Pang, Y.; Gao, X.; Tang, Q.; Ma, J.; Lu, K.; Adam, F. E. A.; Dang, R.; Xiao, S.; Wang, X.; Yang, Z., Newcastle disease virus V protein inhibits apoptosis in DF-1 cells by downregulating TXNL1. *Vet Res* **2018,** 49, (1), 102.
234. Park, M. S.; Garcia-Sastre, A.; Cros, J. F.; Basler, C. F.; Palese, P., Newcastle disease virus V protein is a determinant of host range restriction. *J Virol* **2003,** 77, (17), 9522-32.
235. Reynolds, D. L.; Maraqa, A. D., Protective immunity against Newcastle disease: the role of cell-mediated immunity. *Avian Dis* **2000,** 44, (1), 145-54.
236. Cannon, M. J.; Russell, P. H., Secondary in vitro stimulation of specific cytotoxic cells to Newcastle disease virus in chickens. *Avian Pathol* **1986,** 15, (4), 731-40.
237. Cheville, N. F.; Beard, C. W., Cytopathology of Newcastle disease. The influence of bursal and thymic lymphoid systems in the chicken. *Lab Invest* **1972,** 27, (1), 129-43.

238. Miller, P. J.; King, D. J.; Afonso, C. L.; Suarez, D. L., Antigenic differences among Newcastle disease virus strains of different genotypes used in vaccine formulation affect viral shedding after a virulent challenge. *Vaccine* **2007,** 25, (41), 7238-46.

239. Miller, P. J.; Estevez, C.; Yu, Q.; Suarez, D. L.; King, D. J., Comparison of viral shedding following vaccination with inactivated and live Newcastle disease vaccines formulated with wild-type and recombinant viruses. *Avian Dis* **2009,** 53, (1), 39-49.

240. Hu, S.; Ma, H.; Wu, Y.; Liu, W.; Wang, X.; Liu, Y.; Liu, X., A vaccine candidate of attenuated genotype VII Newcastle disease virus generated by reverse genetics. *Vaccine* **2009,** 27, (6), 904-10.

241. Al-Garib, S. O.; Gielkens, A. L.; Gruys, D. E.; Hartog, L.; Koch, G., Immunoglobulin class distribution of systemic and mucosal antibody responses to Newcastle disease in chickens. *Avian Dis* **2003,** 47, (1), 32-40.

242. Ghumman, J. S.; Wiggins, A. D.; Bankowski, R. A., Antibody response and resistance of turkeys to Newcastle disease vaccine strain LaSota. *Avian Dis* **1976,** 20, (1), 1-8.

243. Russell, P. H.; Dwivedi, P. N.; Davison, T. F., The effects of cyclosporin A and cyclophosphamide on the populations of B and T cells and virus in the Harderian gland of chickens vaccinated with the Hitchner B1 strain of Newcastle disease virus. *Vet Immunol Immunopathol* **1997,** 60, (1-2), 171-85.

244. Rauw, F.; Gardin, Y.; Palya, V.; van Borm, S.; Gonze, M.; Lemaire, S.; van den Berg, T.; Lambrecht, B., Humoral, cell-mediated and mucosal immunity induced by oculo-nasal vaccination of one-day-old SPF and conventional layer chicks with two different live Newcastle disease vaccines. *Vaccine* **2009,** 27, (27), 3631-42.

245. Timms, L.; Alexander, D. J., Cell-mediated immune response of chickens to Newcastle disease vaccines. *Avian Pathol* **1977,** 6, (1), 51-9.

246. Winterfield, R. W.; Dhillon, A. S., Comparative immune response from vaccinating chickens with lentogenic Newcastle disease virus strains. *Poult Sci* **1981,** 60, (6), 1195-1203.

247. National Newcastle disease management plan 2013-16. In Agriculture, D. o., Ed. Australian Animal Health Council: 2013.

248. Rehmani, S. F.; Wajid, A.; Bibi, T.; Nazir, B.; Mukhtar, N.; Hussain, A.; Lone, N. A.; Yaqub, T.; Afonso, C. L., Presence of virulent Newcastle disease virus in vaccinated chickens in farms in Pakistan. *J Clin Microbiol* **2015,** 53, (5), 1715-8.

249. Zamarin, D.; Palese, P., Oncolytic Newcastle disease virus for cancer therapy: old challenges and new directions. *Future Microbiol* **2012,** 7, (3), 347-67.

250. Bohle, W.; Schlag, P.; Liebrich, W.; Hohenberger, P.; Manasterski, M.; Moller, P.; Schirrmacher, V., Postoperative active specific immunization in colorectal cancer patients with virus-modified autologous tumor-cell vaccine. First clinical results with tumor-cell vaccines modified with live but avirulent Newcastle disease virus. *Cancer* **1990,** 66, (7), 1517-23.

251. Freeman, A. I.; Zakay-Rones, Z.; Gomori, J. M.; Linetsky, E.; Rasooly, L.; Greenbaum, E.; Rozenman-Yair, S.; Panet, A.; Libson, E.; Irving, C. S.; Galun, E.; Siegal, T., Phase I/II trial of intravenous NDV-HUJ oncolytic virus in recurrent glioblastoma multiforme. *Mol Ther* **2006,** 13, (1), 221-8.

252. Moore, A. E.; Diamond, L. C.; Mackay, H. H.; Sabachewsky, L., Influence of hemagglutinating viruses on tumor cell suspensions. II. Newcastle disease virus and Ehrlich carcinoma. *Proc Soc Exp Biol Med* **1952,** 81, (2), 498-501.

253. Prince, A. M.; Ginsberg, H. S., Studies on the cytotoxic effect of Newcastle disease virus (NDV) on Ehrlich ascites tumor cells. II. The mechanism and significance of in vitro recovery from the effect of NDV. *J Immunol* **1957,** 79, (2), 107-12.

254. Elankumaran, S.; Chavan, V.; Qiao, D.; Shobana, R.; Moorkanat, G.; Biswas, M.; Samal, S. K., Type I interferon-sensitive recombinant newcastle disease virus for oncolytic virotherapy. *J Virol* **2010,** 84, (8), 3835-44.

255. Washburn, B.; Weigand, M. A.; Grosse-Wilde, A.; Janke, M.; Stahl, H.; Rieser, E.; Sprick, M. R.; Schirrmacher, V.; Walczak, H., TNF-related apoptosis-inducing ligand mediates tumoricidal activity of human monocytes stimulated by Newcastle disease virus. *J Immunol* **2003,** 170, (4), 1814-21.

256. Lorence, R. M.; Rood, P. A.; Kelley, K. W., Newcastle disease virus as an antineoplastic agent: induction of tumor necrosis factor-alpha and augmentation of its cytotoxicity. *J Natl Cancer Inst* **1988,** 80, (16), 1305-12.

257. Washburn, B.; Schirrmacher, V., Human tumor cell infection by Newcastle Disease Virus leads to upregulation of HLA and cell adhesion molecules and to induction of interferons, chemokines and finally apoptosis. *Int J Oncol* **2002,** 21, (1), 85-93.

258. Sui, H.; Bai, Y.; Wang, K.; Li, X.; Song, C.; Fu, F.; Zhang, Y.; Li, L., The anti-tumor effect of Newcastle disease virus HN protein is influenced by differential subcellular targeting. *Cancer Immunol Immunother* **2010,** 59, (7), 989-99.

259. Ni, J.; Galani, I. E.; Cerwenka, A.; Schirrmacher, V.; Fournier, P., Antitumor vaccination by Newcastle Disease Virus Hemagglutinin-Neuraminidase plasmid DNA application: changes in tumor microenvironment and activation of innate anti-tumor immunity. *Vaccine* **2011,** 29, (6), 1185-93.

260. Molouki, A.; Hsu, Y. T.; Jahanshiri, F.; Abdullah, S.; Rosli, R.; Yusoff, K., The matrix (M) protein of Newcastle disease virus binds to human bax through its BH3 domain. *Virol J* **2011,** 8, 385.

261. Pearce, O. M.; Laubli, H., Sialic acids in cancer biology and immunity. *Glycobiology* **2016,** 26, (2), 111-28.

262. Zamarin, D.; Holmgaard, R. B.; Subudhi, S. K.; Park, J. S.; Mansour, M.; Palese, P.; Merghoub, T.; Wolchok, J. D.; Allison, J. P., Localized oncolytic virotherapy overcomes systemic tumor resistance to immune checkpoint blockade immunotherapy. *Sci Transl Med* **2014,** 6, (226), 226ra32.

263. Laurie, S. A.; Bell, J. C.; Atkins, H. L.; Roach, J.; Bamat, M. K.; O'Neil, J. D.; Roberts, M. S.; Groene, W. S.; Lorence, R. M., A phase 1 clinical study of intravenous administration of PV701, an oncolytic virus, using two-step desensitization. *Clin Cancer Res* **2006,** 12, (8), 2555-62.

264. Australian Institue of, H.; Welfare, Cancer in Australia 2019. **2019**.

265. Breslow, A., Thickness, cross-sectional areas and depth of invasion in the prognosis of cutaneous melanoma. *Ann Surg* **1970,** 172, (5), 902-8.

266. Balch, C. M.; Gershenwald, J. E.; Soong, S. J.; Thompson, J. F.; Atkins, M. B.; Byrd, D. R.; Buzaid, A. C.; Cochran, A. J.; Coit, D. G.; Ding, S.; Eggermont, A. M.; Flaherty, K. T.; Gimotty, P. A.; Kirkwood, J. M.; McMasters, K. M.; Mihm, M. C., Jr.; Morton, D. L.; Ross, M. I.; Sober, A. J.; Sondak, V. K., Final version of 2009 AJCC melanoma staging and classification. *J Clin Oncol* **2009,** 27, (36), 6199-206.

267. Soong, S. J.; Ding, S.; Coit, D.; Balch, C. M.; Gershenwald, J. E.; Thompson, J. F.; Gimotty, P.; Force, A. M. T., Predicting survival outcome of localized melanoma: an electronic prediction tool based on the AJCC Melanoma Database. *Ann Surg Oncol* **2010,** 17, (8), 2006-14.

268. Koh, H. K.; Geller, A. C.; Miller, D. R.; Grossbart, T. A.; Lew, R. A., Prevention and early detection strategies for melanoma and skin cancer. Current status. *Arch Dermatol* **1996,** 132, (4), 436-43.

269. Douki, T.; Reynaud-Angelin, A.; Cadet, J.; Sage, E., Bipyrimidine photoproducts rather than oxidative lesions are the main type of DNA damage involved in the genotoxic effect of solar UVA radiation. *Biochemistry* **2003,** 42, (30), 9221-6.

270. Rochette, P. J.; Therrien, J. P.; Drouin, R.; Perdiz, D.; Bastien, N.; Drobetsky, E. A.; Sage, E., UVA-induced cyclobutane pyrimidine dimers form predominantly at thymine-thymine dipyrimidines and correlate with the mutation spectrum in rodent cells. *Nucleic Acids Res* **2003,** 31, (11), 2786-94.

271. Pavel, S.; van Nieuwpoort, F.; van der Meulen, H.; Out, C.; Pizinger, K.; Cetkovska, P.; Smit, N. P.; Koerten, H. K., Disturbed melanin synthesis and chronic oxidative stress in dysplastic naevi. *Eur J Cancer* **2004,** 40, (9), 1423-30.

272. van Zeijl, M. C.; van den Eertwegh, A. J.; Haanen, J. B.; Wouters, M. W., (Neo)adjuvant systemic therapy for melanoma. *Eur J Surg Oncol* **2017,** 43, (3), 534-543.

273. Kirkwood, J. M.; Ibrahim, J. G.; Sondak, V. K.; Richards, J.; Flaherty, L. E.; Ernstoff, M. S.; Smith, T. J.; Rao, U.; Steele, M.; Blum, R. H., High- and low-dose interferon alfa-2b in high-risk melanoma: first analysis of intergroup trial E1690/S9111/C9190. *J Clin Oncol* **2000,** 18, (12), 2444-58.

274. Eggermont, A. M.; Suciu, S.; MacKie, R.; Ruka, W.; Testori, A.; Kruit, W.; Punt, C. J.; Delauney, M.; Sales, F.; Groenewegen, G.; Ruiter, D. J.; Jagiello, I.; Stoitchkov, K.; Keilholz, U.; Lienard, D.; Group, E. M., Post-surgery adjuvant therapy with intermediate doses of interferon alfa 2b versus observation in patients with stage IIb/III melanoma (EORTC 18952): randomised controlled trial. *Lancet* **2005,** 366, (9492), 1189-96.

275. Kirkwood, J. M.; Strawderman, M. H.; Ernstoff, M. S.; Smith, T. J.; Borden, E. C.; Blum, R. H., Interferon alfa-2b adjuvant therapy of high-risk resected cutaneous melanoma: the Eastern Cooperative Oncology Group Trial EST 1684. *J Clin Oncol* **1996,** 14, (1), 7-17.

276. Garbe, C.; Amaral, T.; Peris, K.; Hauschild, A.; Arenberger, P.; Bastholt, L.; Bataille, V.; Del Marmol, V.; Dreno, B.; Fargnoli, M. C.; Grob, J. J.; Holler, C.; Kaufmann, R.; Lallas, A.; Lebbe, C.; Malvehy, J.; Middleton, M.; Moreno-Ramirez, D.; Pellacani, G.; Saiag, P.; Stratigos, A. J.; Vieira, R.; Zalaudek, I.; Eggermont, A. M. M.; European Dermatology Forum, t. E. A. o. D.-O.; the European Organization for, R.; Treatment of, C., European consensus-based

interdisciplinary guideline for melanoma. Part 2: Treatment - Update 2019. *Eur J Cancer* **2020,** 126, 159-177.

277. Hargadon, K. M.; Johnson, C. E.; Williams, C. J., Immune checkpoint blockade therapy for cancer: An overview of FDA-approved immune checkpoint inhibitors. *Int Immunopharmacol* **2018,** 62, 29-39.
278. Robert, C.; Long, G. V.; Brady, B.; Dutriaux, C.; Maio, M.; Mortier, L.; Hassel, J. C.; Rutkowski, P.; McNeil, C.; Kalinka-Warzocha, E.; Savage, K. J.; Hernberg, M. M.; Lebbe, C.; Charles, J.; Mihalcioiu, C.; Chiarion-Sileni, V.; Mauch, C.; Cognetti, F.; Arance, A.; Schmidt, H.; Schadendorf, D.; Gogas, H.; Lundgren-Eriksson, L.; Horak, C.; Sharkey, B.; Waxman, I. M.; Atkinson, V.; Ascierto, P. A., Nivolumab in previously untreated melanoma without BRAF mutation. *N Engl J Med* **2015,** 372, (4), 320-30.
279. Hodi, F. S.; O'Day, S. J.; McDermott, D. F.; Weber, R. W.; Sosman, J. A.; Haanen, J. B.; Gonzalez, R.; Robert, C.; Schadendorf, D.; Hassel, J. C.; Akerley, W.; van den Eertwegh, A. J.; Lutzky, J.; Lorigan, P.; Vaubel, J. M.; Linette, G. P.; Hogg, D.; Ottensmeier, C. H.; Lebbe, C.; Peschel, C.; Quirt, I.; Clark, J. I.; Wolchok, J. D.; Weber, J. S.; Tian, J.; Yellin, M. J.; Nichol, G. M.; Hoos, A.; Urba, W. J., Improved survival with ipilimumab in patients with metastatic melanoma. *N Engl J Med* **2010,** 363, (8), 711-23.
280. Hodi, F. S.; Chiarion-Sileni, V.; Gonzalez, R.; Grob, J. J.; Rutkowski, P.; Cowey, C. L.; Lao, C. D.; Schadendorf, D.; Wagstaff, J.; Dummer, R.; Ferrucci, P. F.; Smylie, M.; Hill, A.; Hogg, D.; Marquez-Rodas, I.; Jiang, J.; Rizzo, J.; Larkin, J.; Wolchok, J. D., Nivolumab plus ipilimumab or nivolumab alone versus ipilimumab alone in advanced melanoma (CheckMate 067): 4-year outcomes of a multicentre, randomised, phase 3 trial. *Lancet Oncol* **2018,** 19, (11), 1480-1492.
281. McDermott, D. F.; Shah, R.; Gupte-Singh, K.; Sabater, J.; Luo, L.; Botteman, M.; Rao, S.; Regan, M. M.; Atkins, M., Quality-adjusted survival of nivolumab plus ipilimumab or nivolumab alone versus ipilimumab alone among treatment-naive patients with advanced melanoma: a quality-adjusted time without symptoms or toxicity (Q-TWiST) analysis. *Qual Life Res* **2019,** 28, (1), 109-119.
282. Bajwa, R.; Cheema, A.; Khan, T.; Amirpour, A.; Paul, A.; Chaughtai, S.; Patel, S.; Patel, T.; Bramson, J.; Gupta, V.; Levitt, M.; Asif, A.; Hossain, M. A., Adverse Effects of Immune Checkpoint Inhibitors (Programmed Death-1 Inhibitors and

Cytotoxic T-Lymphocyte-Associated Protein-4 Inhibitors): Results of a Retrospective Study. *J Clin Med Res* **2019,** 11, (4), 225-236.

283. Guleria, I.; Gubbels Bupp, M.; Dada, S.; Fife, B.; Tang, Q.; Ansari, M. J.; Trikudanathan, S.; Vadivel, N.; Fiorina, P.; Yagita, H.; Azuma, M.; Atkinson, M.; Bluestone, J. A.; Sayegh, M. H., Mechanisms of PDL1-mediated regulation of autoimmune diabetes. *Clin Immunol* **2007,** 125, (1), 16-25.
284. Sansom, D. M.; Walker, L. S., The role of CD28 and cytotoxic T-lymphocyte antigen-4 (CTLA-4) in regulatory T-cell biology. *Immunol Rev* **2006,** 212, 131-48.
285. Liu, B. L.; Robinson, M.; Han, Z. Q.; Branston, R. H.; English, C.; Reay, P.; McGrath, Y.; Thomas, S. K.; Thornton, M.; Bullock, P.; Love, C. A.; Coffin, R. S., ICP34.5 deleted herpes simplex virus with enhanced oncolytic, immune stimulating, and anti-tumour properties. *Gene Ther* **2003,** 10, (4), 292-303.
286. Andtbacka, R. H.; Kaufman, H. L.; Collichio, F.; Amatruda, T.; Senzer, N.; Chesney, J.; Delman, K. A.; Spitler, L. E.; Puzanov, I.; Agarwala, S. S.; Milhem, M.; Cranmer, L.; Curti, B.; Lewis, K.; Ross, M.; Guthrie, T.; Linette, G. P.; Daniels, G. A.; Harrington, K.; Middleton, M. R.; Miller, W. H., Jr.; Zager, J. S.; Ye, Y.; Yao, B.; Li, A.; Doleman, S.; VanderWalde, A.; Gansert, J.; Coffin, R. S., Talimogene Laherparepvec Improves Durable Response Rate in Patients With Advanced Melanoma. *J Clin Oncol* **2015,** 33, (25), 2780-8.
287. Chou, J.; Chen, J. J.; Gross, M.; Roizman, B., Association of a M(r) 90,000 phosphoprotein with protein kinase PKR in cells exhibiting enhanced phosphorylation of translation initiation factor eIF-2 alpha and premature shutoff of protein synthesis after infection with gamma 134.5- mutants of herpes simplex virus 1. *Proc Natl Acad Sci U S A* **1995,** 92, (23), 10516-20.
288. Watanabe, T.; Imamura, T.; Hiasa, Y., Roles of protein kinase R in cancer: Potential as a therapeutic target. *Cancer Sci* **2018,** 109, (4), 919-925.
289. Goldsmith, K.; Chen, W.; Johnson, D. C.; Hendricks, R. L., Infected cell protein (ICP)47 enhances herpes simplex virus neurovirulence by blocking the CD8+ T cell response. *J Exp Med* **1998,** 187, (3), 341-8.
290. Kohno, S.; Luo, C.; Goshima, F.; Nishiyama, Y.; Sata, T.; Ono, Y., Herpes simplex virus type 1 mutant HF10 oncolytic viral therapy for bladder cancer. *Urology* **2005,** 66, (5), 1116-21.

291. Watanabe, D.; Goshima, F.; Mori, I.; Tamada, Y.; Matsumoto, Y.; Nishiyama, Y., Oncolytic virotherapy for malignant melanoma with herpes simplex virus type 1 mutant HF10. *J Dermatol Sci* **2008,** 50, (3), 185-96.

292. Sahin, T. T.; Kasuya, H.; Nomura, N.; Shikano, T.; Yamamura, K.; Gewen, T.; Kanzaki, A.; Fujii, T.; Sugae, T.; Imai, T.; Nomoto, S.; Takeda, S.; Sugimoto, H.; Kikumori, T.; Kodera, Y.; Nishiyama, Y.; Nakao, A., Impact of novel oncolytic virus HF10 on cellular components of the tumor microenviroment in patients with recurrent breast cancer. *Cancer Gene Ther* **2012,** 19, (4), 229-37.

293. Zamarin, D.; Martinez-Sobrido, L.; Kelly, K.; Mansour, M.; Sheng, G.; Vigil, A.; Garcia-Sastre, A.; Palese, P.; Fong, Y., Enhancement of oncolytic properties of recombinant newcastle disease virus through antagonism of cellular innate immune responses. *Mol Ther* **2009,** 17, (4), 697-706.

294. Zamarin, D.; Vigil, A.; Kelly, K.; Garcia-Sastre, A.; Fong, Y., Genetically engineered Newcastle disease virus for malignant melanoma therapy. *Gene Ther* **2009,** 16, (6), 796-804.

295. Atkins, M. B.; Lotze, M. T.; Dutcher, J. P.; Fisher, R. I.; Weiss, G.; Margolin, K.; Abrams, J.; Sznol, M.; Parkinson, D.; Hawkins, M.; Paradise, C.; Kunkel, L.; Rosenberg, S. A., High-dose recombinant interleukin 2 therapy for patients with metastatic melanoma: analysis of 270 patients treated between 1985 and 1993. *J Clin Oncol* **1999,** 17, (7), 2105-16.

296. Vigil, A.; Park, M. S.; Martinez, O.; Chua, M. A.; Xiao, S.; Cros, J. F.; Martinez-Sobrido, L.; Woo, S. L.; Garcia-Sastre, A., Use of reverse genetics to enhance the oncolytic properties of Newcastle disease virus. *Cancer Res* **2007,** 67, (17), 8285-92.

297. Cassel, W. A.; Murray, D. R., A ten-year follow-up on stage II malignant melanoma patients treated postsurgically with Newcastle disease virus oncolysate. *Med Oncol Tumor Pharmacother* **1992,** 9, (4), 169-71.

298. Batliwalla, F. M.; Bateman, B. A.; Serrano, D.; Murray, D.; Macphail, S.; Maino, V. C.; Ansel, J. C.; Gregersen, P. K.; Armstrong, C. A., A 15-year follow-up of AJCC stage III malignant melanoma patients treated postsurgically with Newcastle disease virus (NDV) oncolysate and determination of alterations in the CD8 T cell repertoire. *Mol Med* **1998,** 4, (12), 783-94.

299. Murray, D. R.; Cassel, W. A.; Torbin, A. H.; Olkowski, Z. L.; Moore, M. E., Viral oncolysate in the management of malignant melanoma. II. Clinical studies. *Cancer* **1977,** 40, (2), 680-6.

300. Pecora, A. L.; Rizvi, N.; Cohen, G. I.; Meropol, N. J.; Sterman, D.; Marshall, J. L.; Goldberg, S.; Gross, P.; O'Neil, J. D.; Groene, W. S.; Roberts, M. S.; Rabin, H.; Bamat, M. K.; Lorence, R. M., Phase I trial of intravenous administration of PV701, an oncolytic virus, in patients with advanced solid cancers. *J Clin Oncol* **2002,** 20, (9), 2251-66.

301. Subbarao, K.; Joseph, T., Scientific barriers to developing vaccines against avian influenza viruses. *Nature Reviews Immunology* **2007,** 7, (4), 267.

302. Arias, C. F.; Escalera-Zamudio, M.; Soto-Del Rio Mde, L.; Cobian-Guemes, A. G.; Isa, P.; Lopez, S., Molecular anatomy of 2009 influenza virus A (H1N1). *Arch Med Res* **2009,** 40, (8), 643-54.

303. El Najjar, F.; Schmitt, A. P.; Dutch, R. E., Paramyxovirus glycoprotein incorporation, assembly and budding: a three way dance for infectious particle production. *Viruses* **2014,** 6, (8), 3019-54.

304. International Atomic Energy Agency, Sterility assurance level. *Guidelines for Industrial Radiation Sterilisation of Disposable Medical Products (Cobalt-60 Gamma-Irradiation)* **1990,** Vol IAEA-TECDOC-539, 39.

305. Shahrudin, S.; Chen, C.; David, S. C.; Singleton, E. V.; Davies, J.; Kirkwood, C. D.; Hirst, T. R.; Beard, M.; Alsharifi, M., Gamma-irradiated rotavirus: A possible whole virus inactivated vaccine. *PLoS One* **2018,** 13, (6), e0198182.

306. Reed, L. J.; Muench, H., A simple method of estimating fifty per cent endpoints. *American Journal of Epidemiology* **1938,** 27, (3), 493-497.

307. Sommers, C. H.; Rajkowski, K. T., Radiation inactivation of foodborne pathogens on frozen seafood products. *J Food Prot* **2011,** 74, (4), 641-4.

308. McClain, M. E.; Spendlove, R. S., Multiplicity reactivation of reovirus particles after exposure to ultraviolet light. *J Bacteriol* **1966,** 92, (5), 1422-9.

309. Brena-Valle, M.; Serment-Guerrero, J., SOS induction by gamma-radiation in *Escherichia coli* strains defective in repair and/or recombination mechanisms. *Mutagenesis* **1998,** 13, (6), 637-41.

310. Gasc, A. M.; Sicard, N.; Claverys, J. P.; Sicard, A. M., Lack of SOS repair in *Streptococcus pneumoniae*. *Mutat Res* **1980,** 70, (2), 157-65.

311. Sicard, N.; Estevenon, A. M., Excision-repair capacity in *Streptococcus pneumoniae*: cloning and expression of a uvr-like gene. *Mutat Res* **1990,** 235, (3), 195-201.

312. Dolling, J. A.; Boreham, D. R.; Brown, D. L.; Mitchel, R. E.; Raaphorst, G. P., Modulation of radiation-induced strand break repair by cisplatin in mammalian cells. *International journal of radiation biology* **1998,** 74, (1), 61-9.

313. Hafer, K.; Iwamoto, K. S.; Scuric, Z.; Schiestl, R. H., Adaptive response to gamma radiation in mammalian cells proficient and deficient in components of nucleotide excision repair. *Radiation research* **2007,** 168, (2), 168-74.

314. Le, D. T.; Picozzi, V. J.; Ko, A. H.; Wainberg, Z. A.; Kindler, H.; Wang-Gillam, A.; Oberstein, P.; Morse, M. A.; Zeh, H. J., 3rd; Weekes, C.; Reid, T.; Borazanci, E.; Crocenzi, T.; LoConte, N. K.; Musher, B.; Laheru, D.; Murphy, A.; Whiting, C.; Nair, N.; Enstrom, A.; Ferber, S.; Brockstedt, D. G.; Jaffee, E. M., Results from a Phase IIb, Randomized, Multicenter Study of GVAX Pancreas and CRS-207 Compared with Chemotherapy in Adults with Previously Treated Metastatic Pancreatic Adenocarcinoma (ECLIPSE Study). *Clin Cancer Res* **2019,** 25, (18), 5493-5502.

315. Dranoff, G.; Jaffee, E.; Lazenby, A.; Golumbek, P.; Levitsky, H.; Brose, K.; Jackson, V.; Hamada, H.; Pardoll, D.; Mulligan, R. C., Vaccination with irradiated tumor cells engineered to secrete murine granulocyte-macrophage colony-stimulating factor stimulates potent, specific, and long-lasting anti-tumor immunity. *Proc Natl Acad Sci U S A* **1993,** 90, (8), 3539-43.

316. Baureus-Koch, C.; Nyberg, G.; Widegren, B.; Salford, L. G.; Persson, B. R., Radiation sterilisation of cultured human brain tumour cells for clinical immune tumour therapy. *Br J Cancer* **2004,** 90, (1), 48-54.

317. Ormerod, M. G., Free-Radical Formation in Irradiated Deoxyribonucleic Acid. *Int J Radiat Biol Relat Stud Phys Chem Med* **1965,** 9, 291-300.

318. Grieb, T.; Forng, R. Y.; Brown, R.; Owolabi, T.; Maddox, E.; McBain, A.; Drohan, W. N.; Mann, D. M.; Burgess, W. H., Effective use of gamma irradiation for pathogen inactivation of monoclonal antibody preparations. *Biologicals* **2002,** 30, (3), 207-216.

319. Gibbs, C. J., Jr.; Gajdusek, D. C.; Latarjet, R., Unusual resistance to ionizing radiation of the viruses of kuru, Creutzfeldt-Jakob disease, and scrapie. *Proc Natl Acad Sci U S A* **1978,** 75, (12), 6268-70.

320. Putri, W.; Muscatello, D. J.; Stockwell, M. S.; Newall, A. T., Economic burden of seasonal influenza in the United States. *Vaccine* **2018,** 36, (27), 3960-3966.

321. Furuya, Y., Return of inactivated whole-virus vaccine for superior efficacy. *Immunology and Cell Biology* **2011,** 90, (6), 571.

322. National, H.; Medical Research, C., *Australian code of practice for the care and use of animals for scientific purposes*. 8th ed.; National Health and Medical Research Council: Canberra, 2013.

323. Martin, S. S.; Bakken, R. R.; Lind, C. M.; Garcia, P.; Jenkins, E.; Glass, P. J.; Parker, M. D.; Hart, M. K.; Fine, D. L., Comparison of the immunological responses and efficacy of gamma-irradiated V3526 vaccine formulations against subcutaneous and aerosol challenge with Venezuelan equine encephalitis virus subtype IAB. *Vaccine* **2010,** 28, (4), 1031-40.

324. Miller, J. L.; Anders, E. M., Virus-cell interactions in the induction of type 1 interferon by influenza virus in mouse spleen cells. *J Gen Virol* **2003,** 84, (Pt 1), 193-202.

325. Margine, I.; Hai, R.; Albrecht, R. A.; Obermoser, G.; Harrod, A. C.; Banchereau, J.; Palucka, K.; Garcia-Sastre, A.; Palese, P.; Treanor, J. J.; Krammer, F., H3N2 influenza virus infection induces broadly reactive hemagglutinin stalk antibodies in humans and mice. *J Virol* **2013,** 87, (8), 4728-37.

326. Krystal, M.; Elliott, R. M.; Benz, E. W., Jr.; Young, J. F.; Palese, P., Evolution of influenza A and B viruses: conservation of structural features in the hemagglutinin genes. *Proc Natl Acad Sci U S A* **1982,** 79, (15), 4800-4.

327. Wu, N. C.; Thompson, A. J.; Lee, J. M.; Su, W.; Arlian, B. M.; Xie, J.; Lerner, R. A.; Yen, H. L.; Bloom, J. D.; Wilson, I. A., Different genetic barriers for resistance to HA stem antibodies in influenza H3 and H1 viruses. *Science* **2020,** 368, (6497), 1335-1340.

328. Cote, C. K.; Buhr, T.; Bernhards, C. B.; Bohmke, M. D.; Calm, A. M.; Esteban-Trexler, J. S.; Hunter, M.; Katoski, S. E.; Kennihan, N.; Klimko, C. P.; Miller, J. A.; Minter, Z. A.; Pfarr, J. W.; Prugh, A. M.; Quirk, A. V.; Rivers, B. A.; Shea, A. A.; Shoe, J. L.; Sickler, T. M.; Young, A. A.; Fetterer, D. P.; Welkos, S. L.; Bozue, J. A.; McPherson, D.; Fountain, A. W., 3rd; Gibbons, H. S., A Standard Method To Inactivate Bacillus anthracis Spores to Sterility via Gamma Irradiation. *Appl Environ Microbiol* **2018,** 84, (12).

329. Epstein, J. E.; Tewari, K.; Lyke, K. E.; Sim, B. K.; Billingsley, P. F.; Laurens, M. B.; Gunasekera, A.; Chakravarty, S.; James, E. R.; Sedegah, M.; Richman, A.; Velmurugan, S.; Reyes, S.; Li, M.; Tucker, K.; Ahumada, A.; Ruben, A. J.; Li, T.; Stafford, R.; Eappen, A. G.; Tamminga, C.; Bennett, J. W.; Ockenhouse, C. F.; Murphy, J. R.; Komisar, J.; Thomas, N.; Loyevsky, M.; Birkett, A.; Plowe, C. V.; Loucq, C.; Edelman, R.; Richie, T. L.; Seder, R. A.; Hoffman, S. L., Live attenuated malaria vaccine designed to protect through hepatic CD8(+) T cell immunity. *Science* **2011,** 334, (6055), 475-80.

330. Cattoli, G.; Susta, L.; Terregino, C.; Brown, C., Newcastle disease: a review of field recognition and current methods of laboratory detection. *J Vet Diagn Invest* **2011,** 23, (4), 637-56.

331. Nanthakumar, T.; Kataria, R. S.; Tiwari, A. K.; Butchaiah, G.; Kataria, J. M., Pathotyping of Newcastle disease viruses by RT-PCR and restriction enzyme analysis. *Vet Res Commun* **2000,** 24, (4), 275-86.

332. Absalon, A. E.; Cortes-Espinosa, D. V.; Lucio, E.; Miller, P. J.; Afonso, C. L., Epidemiology, control, and prevention of Newcastle disease in endemic regions: Latin America. *Trop Anim Health Prod* **2019,** 51, (5), 1033-1048.

333. Putri, D. D.; Handharyani, E.; Soejoedono, R. D.; Setiyono, A.; Mayasari, N.; Poetri, O. N., Pathotypic characterization of Newcastle disease virus isolated from vaccinated chicken in West Java, Indonesia. *Vet World* **2017,** 10, (4), 438-444.

334. Ibrahim, A. L.; Chulan, U.; Babjee, A. M., An assessment of the Australian V4 strain of Newcastle disease virus as a vaccine by spray, aerosol and drinking water administration. *Aust Vet J* **1981,** 57, (6), 277-80.

335. Westbury, H. A., Comparison of the immunogenicity of Newcastle disease virus strains V4, B1 and La Sota in chickens. 1. Tests in susceptible chickens. *Aust Vet J* **1984,** 61, (1), 5-9.

336. Miller, P. J.; Afonso, C. L.; El Attrache, J.; Dorsey, K. M.; Courtney, S. C.; Guo, Z.; Kapczynski, D. R., Effects of Newcastle disease virus vaccine antibodies on the shedding and transmission of challenge viruses. *Dev Comp Immunol* **2013,** 41, (4), 505-13.

337. Centers for Disease, C.; Prevention, D. o. H.; Human, S., Possession, use, and transfer of select agents and toxins. Final rule. *Fed Regist* **2008,** 73, (201), 61363-6.

338. Hofmeister, Y.; Planitzer, C. B.; Farcet, M. R.; Teschner, W.; Butterweck, H. A.; Weber, A.; Holzer, G. W.; Kreil, T. R., Human IgG subclasses: in vitro neutralization of and in vivo protection against West Nile virus. *J Virol* **2011,** 85, (4), 1896-9.

339. Mathiesen, T.; Persson, M. A.; Sundqvist, V. A.; Wahren, B., Neutralization capacity and antibody dependent cell-mediated cytotoxicity of separated IgG subclasses 1, 3 and 4 against herpes simplex virus. *Clin Exp Immunol* **1988,** 72, (2), 211-5.

340. Cavacini, L. A.; Kuhrt, D.; Duval, M.; Mayer, K.; Posner, M. R., Binding and neutralization activity of human IgG1 and IgG3 from serum of HIV-infected individuals. *AIDS Res Hum Retroviruses* **2003,** 19, (9), 785-92.

341. Scharf, O.; Golding, H.; King, L. R.; Eller, N.; Frazier, D.; Golding, B.; Scott, D. E., Immunoglobulin G3 from polyclonal human immunodeficiency virus (HIV) immune globulin is more potent than other subclasses in neutralizing HIV type 1. *J Virol* **2001,** 75, (14), 6558-65.

342. Salem, M. L.; El-Naggar, S. A.; Kadima, A.; Gillanders, W. E.; Cole, D. J., The adjuvant effects of the toll-like receptor 3 ligand polyinosinic-cytidylic acid poly (I:C) on antigen-specific CD8+ T cell responses are partially dependent on NK cells with the induction of a beneficial cytokine milieu. *Vaccine* **2006,** 24, (24), 5119-32.

343. Billiau, A.; Matthys, P., Modes of action of Freund's adjuvants in experimental models of autoimmune diseases. *Journal of Leukocyte Biology* **2001,** 70, (6), 849-860.

344. Mawas, F.; Feavers, I. M.; Corbel, M. J., Serotype of Streptococcus pneumoniae capsular polysaccharide can modify the Th1/Th2 cytokine profile and IgG subclass response to pneumococal-CRM(197) conjugate vaccines in a murine model. *Vaccine* **2000,** 19, (9-10), 1159-66.

345. Brewer, J. M.; Conacher, M.; Hunter, C. A.; Mohrs, M.; Brombacher, F.; Alexander, J., Aluminium hydroxide adjuvant initiates strong antigen-specific Th2 responses in the absence of IL-4- or IL-13-mediated signaling. *J Immunol* **1999,** 163, (12), 6448-54.

346. Lazar, I.; Yaacov, B.; Shiloach, T.; Eliahoo, E.; Kadouri, L.; Lotem, M.; Perlman, R.; Zakay-Rones, Z.; Panet, A.; Ben-Yehuda, D., The oncolytic activity of Newcastle disease virus NDV-HUJ on chemoresistant primary melanoma cells is

dependent on the proapoptotic activity of the inhibitor of apoptosis protein Livin. *J Virol* **2010,** 84, (1), 639-46.

347. Ahlert, T.; Schirrmacher, V., Isolation of a human melanoma adapted Newcastle disease virus mutant with highly selective replication patterns. *Cancer Res* **1990,** 50, (18), 5962-8.
348. Li, Q.; Wei, D.; Feng, F.; Wang, X. L.; Li, C.; Chen, Z. N.; Bian, H., alpha2,6-linked sialic acid serves as a high-affinity receptor for cancer oncolytic virotherapy with Newcastle disease virus. *J Cancer Res Clin Oncol* **2017,** 143, (11), 2171-2181.
349. Jarahian, M.; Watzl, C.; Fournier, P.; Arnold, A.; Djandji, D.; Zahedi, S.; Cerwenka, A.; Paschen, A.; Schirrmacher, V.; Momburg, F., Activation of natural killer cells by newcastle disease virus hemagglutinin-neuraminidase. *J Virol* **2009,** 83, (16), 8108-21.
350. Zeng, J.; Fournier, P.; Schirrmacher, V., Induction of interferon-alpha and tumor necrosis factor-related apoptosis-inducing ligand in human blood mononuclear cells by hemagglutinin-neuraminidase but not F protein of Newcastle disease virus. *Virology* **2002,** 297, (1), 19-30.
351. Ren, S.; Rehman, Z. U.; Shi, M.; Yang, B.; Qu, Y.; Yang, X. F.; Shao, Q.; Meng, C.; Yang, Z.; Gao, X.; Sun, Y.; Ding, C., Syncytia generated by hemagglutinin-neuraminidase and fusion proteins of virulent Newcastle disease virus induce complete autophagy by activating AMPK-mTORC1-ULK1 signaling>. *Vet Microbiol* **2019,** 230, 283-290.
352. Altomonte, J.; Marozin, S.; Schmid, R. M.; Ebert, O., Engineered newcastle disease virus as an improved oncolytic agent against hepatocellular carcinoma. *Mol Ther* **2010,** 18, (2), 275-84.
353. Li, P.; Chen, C. H.; Li, S.; Givi, B.; Yu, Z.; Zamarin, D.; Palese, P.; Fong, Y.; Wong, R. J., Therapeutic effects of a fusogenic newcastle disease virus in treating head and neck cancer. *Head Neck* **2011,** 33, (10), 1394-9.
354. Song, K. Y.; Wong, J.; Gonzalez, L.; Sheng, G.; Zamarin, D.; Fong, Y., Antitumor efficacy of viral therapy using genetically engineered Newcastle disease virus [NDV(F3aa)-GFP] for peritoneally disseminated gastric cancer. *J Mol Med (Berl)* **2010,** 88, (6), 589-96.
355. Molouki, A.; Yusoff, K., NDV-induced apoptosis in absence of Bax; evidence of involvement of apoptotic proteins upstream of mitochondria. *Virol J* **2012,** 9, 179.

356. Schultz, M. J.; Swindall, A. F.; Wright, J. W.; Sztul, E. S.; Landen, C. N.; Bellis, S. L., ST6Gal-I sialyltransferase confers cisplatin resistance in ovarian tumor cells. *J Ovarian Res* **2013,** 6, (1), 25.

357. Meng, S.; Zhou, Z.; Chen, F.; Kong, X.; Liu, H.; Jiang, K.; Liu, W.; Hu, M.; Zhang, X.; Ding, C.; Wu, Y., Newcastle disease virus induces apoptosis in cisplatin-resistant human lung adenocarcinoma A549 cells in vitro and in vivo. *Cancer Lett* **2012,** 317, (1), 56-64.

358. Spranger, S.; Spaapen, R. M.; Zha, Y.; Williams, J.; Meng, Y.; Ha, T. T.; Gajewski, T. F., Up-regulation of PD-L1, IDO, and T(regs) in the melanoma tumor microenvironment is driven by CD8(+) T cells. *Sci Transl Med* **2013,** 5, (200), 200ra116.

359. Ji, R. R.; Chasalow, S. D.; Wang, L.; Hamid, O.; Schmidt, H.; Cogswell, J.; Alaparthy, S.; Berman, D.; Jure-Kunkel, M.; Siemers, N. O.; Jackson, J. R.; Shahabi, V., An immune-active tumor microenvironment favors clinical response to ipilimumab. *Cancer Immunol Immunother* **2012,** 61, (7), 1019-31.

360. Haas, C.; Ertel, C.; Gerhards, R.; Schirrmacher, V., Introduction of adhesive and costimulatory immune functions into tumor cells by infection with Newcastle Disease Virus. *Int J Oncol* **1998,** 13, (6), 1105-15.

361. Termeer, C. C.; Schirrmacher, V.; Brocker, E. B.; Becker, J. C., Newcastle disease virus infection induces B7-1/B7-2-independent T-cell costimulatory activity in human melanoma cells. *Cancer Gene Ther* **2000,** 7, (2), 316-23.

362. Zorn, U.; Dallmann, I.; Grosse, J.; Kirchner, H.; Poliwoda, H.; Atzpodien, J., Induction of cytokines and cytotoxicity against tumor cells by Newcastle disease virus. *Cancer Biother* **1994,** 9, (3), 225-35.

363. Miller, C. G.; Fraser, N. W., Requirement of an integrated immune response for successful neuroattenuated HSV-1 therapy in an intracranial metastatic melanoma model. *Mol Ther* **2003,** 7, (6), 741-7.

364. Gao, Y.; Bergman, I., Potent Antitumor T-Cell Memory Is Generated by Curative Viral Oncolytic Immunotherapy But Not Curative Chemotherapy. *Anticancer Res* **2018,** 38, (12), 6621-6629.

365. Overwijk, W. W.; Restifo, N. P., B16 as a mouse model for human melanoma. *Curr Protoc Immunol* **2001,** Chapter 20, Unit 20 1.

366. Vlkova, M.; Rohousova, I.; Hostomska, J.; Pohankova, L.; Zidkova, L.; Drahota, J.; Valenzuela, J. G.; Volf, P., Kinetics of antibody response in BALB/c and

C57BL/6 mice bitten by Phlebotomus papatasi. *PLoS Negl Trop Dis* **2012,** 6, (7), e1719.

367. Fornefett, J.; Krause, J.; Klose, K.; Fingas, F.; Hassert, R.; Benga, L.; Grunwald, T.; Muller, U.; Schrodl, W.; Baums, C. G., Comparative analysis of humoral immune responses and pathologies of BALB/c and C57BL/6 wildtype mice experimentally infected with a highly virulent Rodentibacter pneumotropicus (Pasteurella pneumotropica) strain. *BMC Microbiol* **2018,** 18, (1), 45.
368. Guyach, S. E.; Bryan, M. A.; Norris, K. A., Differences in antibody and immune responses between Balb/c and C57Bl/6 mice infected with Trypanosoma cruzi (129.5). *The Journal of Immunology* **2009,** 182, (1 Supplement), 129.5.
369. Cote, C. K.; Buhr, T.; Bernhards, C. B.; Bohmke, M. D.; Calm, A. M.; Esteban-Trexler, J. S.; Hunter, M. C.; Katoski, S. E.; Kennihan, N.; Klimko, C. P.; Miller, J. A.; Minter, Z. A.; Pfarr, J. W.; Prugh, A. M.; Quirk, A. V.; Rivers, B. A.; Shea, A. A.; Shoe, J. L.; Sickler, T. M.; Young, A. A.; Fetterer, D. P.; Welkos, S. L.; Bozue, J. A.; McPherson, D.; Fountain, A. W.; Gibbons, H. S., A Standard Method to Inactivate Bacillus anthracis Spores to Sterility Using γ-Irradiation. *Applied and Environmental Microbiology* **2018**.
370. Stewart, D.; Fulton, W. B.; Wilson, C.; Monitto, C. L.; Paidas, C. N.; Reeves, R. H.; De Maio, A., Genetic contribution to the septic response in a mouse model. *Shock* **2002,** 18, (4), 342-7.
371. Mills, C. D.; Kincaid, K.; Alt, J. M.; Heilman, M. J.; Hill, A. M., M-1/M-2 macrophages and the Th1/Th2 paradigm. *J Immunol* **2000,** 164, (12), 6166-73.
372. Thomas, C. E.; Ehrhardt, A.; Kay, M. A., Progress and problems with the use of viral vectors for gene therapy. *Nat Rev Genet* **2003,** 4, (5), 346-58.
373. Marshall, E., Gene therapy death prompts review of adenovirus vector. *Science* **1999,** 286, (5448), 2244-5.
374. Assessment of adenoviral vector safety and toxicity: report of the National Institutes of Health Recombinant DNA Advisory Committee. *Hum Gene Ther* **2002,** 13, (1), 3-13.
375. Cavazzana-Calvo, M.; Hacein-Bey, S.; de Saint Basile, G.; Gross, F.; Yvon, E.; Nusbaum, P.; Selz, F.; Hue, C.; Certain, S.; Casanova, J. L.; Bousso, P.; Deist, F. L.; Fischer, A., Gene therapy of human severe combined immunodeficiency (SCID)-X1 disease. *Science* **2000,** 288, (5466), 669-72.

376. Hacein-Bey-Abina, S.; von Kalle, C.; Schmidt, M.; Le Deist, F.; Wulffraat, N.; McIntyre, E.; Radford, I.; Villeval, J. L.; Fraser, C. C.; Cavazzana-Calvo, M.; Fischer, A., A serious adverse event after successful gene therapy for X-linked severe combined immunodeficiency. *N Engl J Med* **2003,** 348, (3), 255-6.

377. Coley, W. B., Late results of the treatment of inoperable sarcoma by the mixed toxins of erysipelas and bacillus prodigiosus. *Trans Southern Surg Gynecol Ass* **1906,** 18, 197.

378. Pawelek, J. M.; Low, K. B.; Bermudes, D., Tumor-targeted Salmonella as a novel anticancer vector. *Cancer Res* **1997,** 57, (20), 4537-44.

379. Baban, C. K.; Cronin, M.; O'Hanlon, D.; O'Sullivan, G. C.; Tangney, M., Bacteria as vectors for gene therapy of cancer. *Bioeng Bugs* **2010,** 1, (6), 385-94.

380. Ishii, N.; Sakashita, T.; Takeda, H.; Kubota, Y.; Fuma, S.; Doi, M.; Takahashi, S., Impact of gamma irradiation on the transformation efficiency for extracellular plasmid DNA. *J Environ Radioact* **2007,** 97, (2-3), 159-67.

381. Lyons, C. R.; Lovchik, J.; Hutt, J.; Lipscomb, M. F.; Wang, E.; Heninger, S.; Berliba, L.; Garrison, K., Murine model of pulmonary anthrax: kinetics of dissemination, histopathology, and mouse strain susceptibility. *Infect Immun* **2004,** 72, (8), 4801-9.

382. Zhang, P.; Ding, Z.; Liu, X.; Chen, Y.; Li, J.; Tao, Z.; Fei, Y.; Xue, C.; Qian, J.; Wang, X.; Li, Q.; Stoeger, T.; Chen, J.; Bi, Y.; Yin, R., Enhanced Replication of Virulent Newcastle Disease Virus in Chicken Macrophages Is due to Polarized Activation of Cells by Inhibition of TLR7. *Front Immunol* **2018,** 9, 366.

383. Huang, Z.; Panda, A.; Elankumaran, S.; Govindarajan, D.; Rockemann, D. D.; Samal, S. K., The hemagglutinin-neuraminidase protein of Newcastle disease virus determines tropism and virulence. *J Virol* **2004,** 78, (8), 4176-84.

384. Shultz, L. D.; Ishikawa, F.; Greiner, D. L., Humanized mice in translational biomedical research. *Nat Rev Immunol* **2007,** 7, (2), 118-30.

385. Simpson-Abelson, M. R.; Sonnenberg, G. F.; Takita, H.; Yokota, S. J.; Conway, T. F., Jr.; Kelleher, R. J., Jr.; Shultz, L. D.; Barcos, M.; Bankert, R. B., Long-term engraftment and expansion of tumor-derived memory T cells following the implantation of non-disrupted pieces of human lung tumor into NOD-scid IL2Rgamma(null) mice. *J Immunol* **2008,** 180, (10), 7009-18.

386. Hodi, F. S.; Mihm, M. C.; Soiffer, R. J.; Haluska, F. G.; Butler, M.; Seiden, M. V.; Davis, T.; Henry-Spires, R.; MacRae, S.; Willman, A.; Padera, R.; Jaklitsch, M. T.;

Shankar, S.; Chen, T. C.; Korman, A.; Allison, J. P.; Dranoff, G., Biologic activity of cytotoxic T lymphocyte-associated antigen 4 antibody blockade in previously vaccinated metastatic melanoma and ovarian carcinoma patients. *Proc Natl Acad Sci U S A* **2003,** 100, (8), 4712-7.

387. Curran, M. A.; Montalvo, W.; Yagita, H.; Allison, J. P., PD-1 and CTLA-4 combination blockade expands infiltrating T cells and reduces regulatory T and myeloid cells within B16 melanoma tumors. *Proc Natl Acad Sci U S A* **2010,** 107, (9), 4275-80.
388. Sznol, M.; Chen, L., Antagonist antibodies to PD-1 and B7-H1 (PD-L1) in the treatment of advanced human cancer. *Clin Cancer Res* **2013,** 19, (5), 1021-34.
389. Roberts, E. W.; Broz, M. L.; Binnewies, M.; Headley, M. B.; Nelson, A. E.; Wolf, D. M.; Kaisho, T.; Bogunovic, D.; Bhardwaj, N.; Krummel, M. F., Critical Role for CD103(+)/CD141(+) Dendritic Cells Bearing CCR7 for Tumor Antigen Trafficking and Priming of T Cell Immunity in Melanoma. *Cancer Cell* **2016,** 30, (2), 324-336.
390. Broz, M. L.; Binnewies, M.; Boldajipour, B.; Nelson, A. E.; Pollack, J. L.; Erle, D. J.; Barczak, A.; Rosenblum, M. D.; Daud, A.; Barber, D. L.; Amigorena, S.; Van't Veer, L. J.; Sperling, A. I.; Wolf, D. M.; Krummel, M. F., Dissecting the tumor myeloid compartment reveals rare activating antigen-presenting cells critical for T cell immunity. *Cancer Cell* **2014,** 26, (5), 638-52.
391. Whyte, C. E.; Osman, M.; Kara, E. E.; Abbott, C.; Foeng, J.; McKenzie, D. R.; Fenix, K. A.; Harata-Lee, Y.; Foyle, K. L.; Boyle, S. T.; Kochetkova, M.; Aguilera, A. R.; Hou, J.; Li, X. Y.; Armstrong, M. A.; Pederson, S. M.; Comerford, I.; Smyth, M. J.; McColl, S. R., ACKR4 restrains antitumor immunity by regulating CCL21. *J Exp Med* **2020,** 217, (6).

APPENDICES

- Gating strategies for flow cytometry (Supplementary Figure 1)
- Statement of Authorship Form (Chapter 2)
- Manuscript published in *Journal of Radiation Research*

Flow cytometry gating strategy

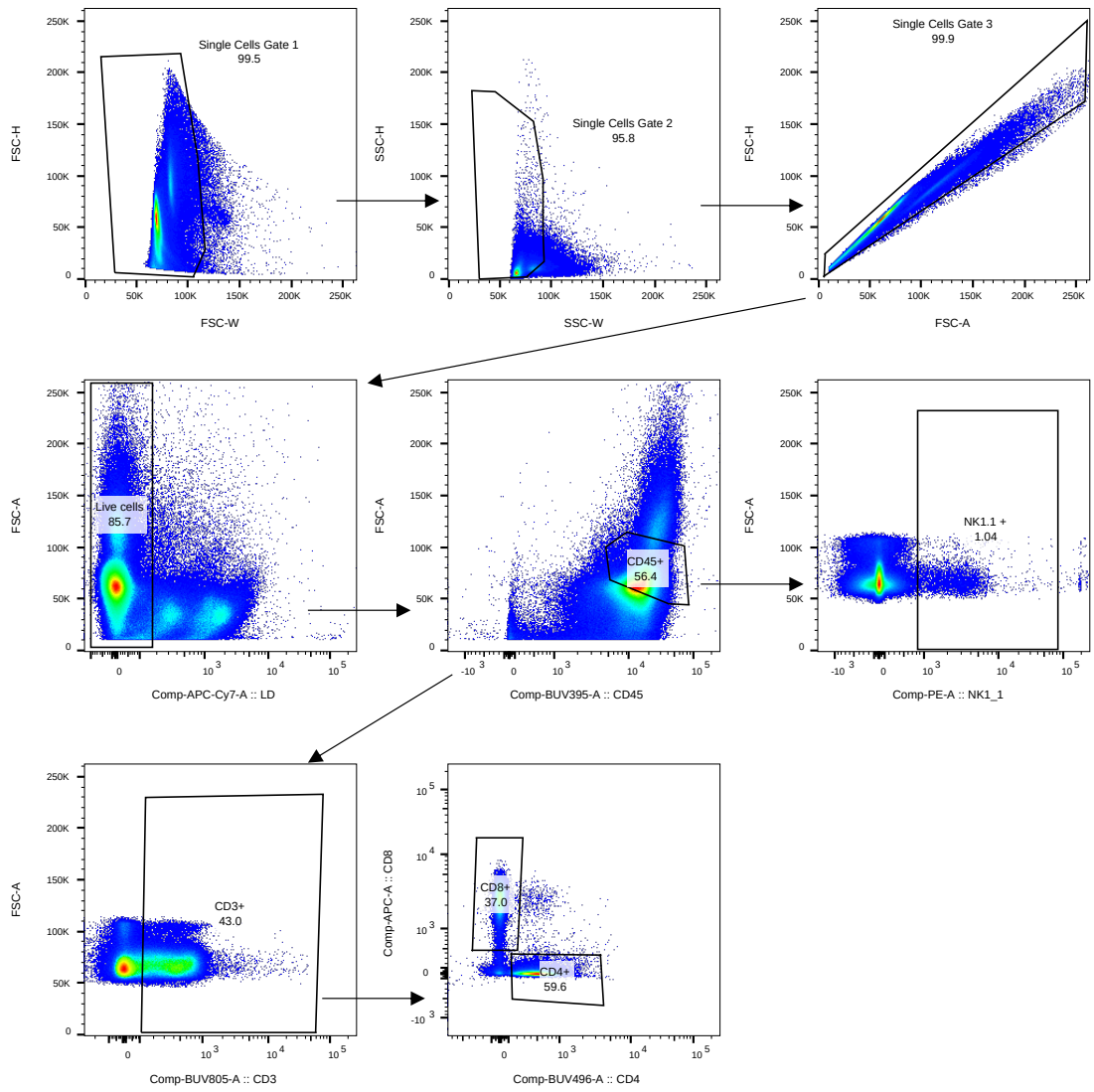

Supplementary Figure 1. Gating strategy for flow cytometry. Cells were first gated based on size and singularity, followed by exclusion of dead cells. Lymphocytes were identified based on expression of CD45 (BUV395) and expected lymphocyte size. Lymphocytes were then gated on NK1.1 (PE) to identify NK cells on CD3 (BV805) to identify T cells. T cells were then gated further on CD8 (APC) and CD4 (BUV496). The same gating strategy was applied to tumours, spleens and draining lymph nodes.

Statement of Authorship

Title of Paper	Sterility of gamma-irradiated pathogens: a new formula to calculate sterilising doses.
Publication Status	☐ Published ☐ Accepted for Publication ☑ Submitted for Publication ☐ Unpublished and Unsubmitted work written in manuscript style
Publication Details	**Singleton, EV.**, David, SC., Davies, JB., Hirst, TR., Paton, JC., Beard, MR., Hemmatzadeh, F., Alsharifi, M. 'Sterility of gamma-irradiated pathogens: a new formula to calculate sterilising doses' (2020), *Journal of Radiation Research*. **Accepted with minor revisions**

Principal Author

Name of Principal Author (Candidate)	Eve Singleton		
Contribution to the Paper	Designed and performed experiments, performed analysis on all data, and wrote the manuscript.		
Overall percentage (%)	85%		
Certification:	This paper reports on original research I conducted during the period of my Higher Degree by Research candidature and is not subject to any obligations or contractual agreements with a third party that would constrain its inclusion in this thesis. I am the primary author of this paper.		
Signature		Date	28/07/2020

Co-Author Contributions

By signing the Statement of Authorship, each author certifies that:

i. the candidate's stated contribution to the publication is accurate (as detailed above);

ii. permission is granted for the candidate in include the publication in the thesis; and

iii. the sum of all co-author contributions is equal to 100% less the candidate's stated contribution.

Name of Co-Author	Shannon David		
Contribution to the Paper	Performed experiments and prepared reagents. Edited the manuscript.		
Signature		Date	28/07/2020

Name of Co-Author	Justin Davies		
Contribution to the Paper	Prepared reagents, aided in statistical analysis and edited the manuscript. Supervised the study.		
Signature		Date	29/07/2020

Name of Co-Author	Tim Hirst		
Contribution to the Paper	Aided in data interpretation and edited the manuscript		
Signature		Date	29-Jul-2020

Name of Co-Author	James Paton		
Contribution to the Paper	Provided reagents and edited the manuscript		
Signature		Date	30/7/20

Name of Co-Author	Michael Beard		
Contribution to the Paper	Provided reagents and supervised the study		
Signature		Date	29/07/20

Name of Co-Author	Farhid Hemmatzadeh		
Contribution to the Paper	Provided reagents and supervised the study. Edited the manuscript		
Signature		Date	29.07.20

Name of Co-Author	Mohammed Alsharifi		
Contribution to the Paper	Conceived, designed and supervised the study. Aided in data interpretation, statistical analysis and manuscript editing. Was the corresponding author.		
Signature		Date	28/07/2020

Journal of Radiation Research, 2020, pp. 1–9
doi: 10.1093/jrr/rraa076

Sterility of gamma-irradiated pathogens: a new mathematical formula to calculate sterilizing doses

Eve V. Singleton[1], Shannon C. David[1], Justin B. Davies[2], Timothy R. Hirst[1,3,4], James C. Paton[1,4], Michael R. Beard[1], Farhid Hemmatzadeh[5] and Mohammed Alsharifi[1,3,4,*]

[1]Research Centre for Infectious Diseases, and Department of Molecular and Biomedical Sciences, University of Adelaide, Adelaide, SA, 5005, Australia
[2]Australian Nuclear Science and Technology Organisation, Lucas Heights, NSW, 2234, Australia
[3]Gamma Vaccines Pty Ltd, Mountbatten Park, Yarralumla, ACT, 2600, Australia
[4]GPN Vaccines Pty Ltd, Mountbatten Park, Yarralumla, ACT, 2600, Australia
[5]School of Animal and Veterinary Sciences, University of Adelaide, Roseworthy, SA, 5371, Australia
*Corresponding author. Research Centre for Infectious Diseases, University of Adelaide, Adelaide, SA, 5005, Australia.
Email: mohammed.alsharifi@adelaide.edu.au
(Received 19 February 2020; revised 19 June 2020; editorial decision 6 August 2020)

ABSTRACT

In recent years there has been increasing advocacy for highly immunogenic gamma-irradiated vaccines, several of which are currently in clinical or pre-clinical trials. Importantly, various methods of mathematical modelling and sterility testing are employed to ensure sterility. However, these methods are designed for materials with a low bioburden, such as food and pharmaceuticals. Consequently, current methods may not be reliable or applicable to estimate the irradiation dose required to sterilize microbiological preparations for vaccine purposes, where bioburden is deliberately high. In this study we investigated the applicability of current methods to calculate the sterilizing doses for different microbes. We generated inactivation curves that demonstrate single-hit and multiple-hit kinetics under different irradiation temperatures for high-titre preparations of pathogens with different genomic structures. Our data demonstrate that inactivation of viruses such as Influenza A virus, Zika virus, Semliki Forest virus and Newcastle Disease virus show single-hit kinetics following exposure to gamma-irradiation. In contrast, rotavirus inactivation shows multiple-hit kinetics and the sterilizing dose could not be calculated using current mathematical methods. Similarly, *Streptococcus pneumoniae* demonstrates multiple-hit kinetics. These variations in killing curves reveal an important gap in current mathematical formulae to determine sterility assurance levels. Here we propose a simple method to calculate the irradiation dose required for a single $\log_{10}$ reduction in bioburden (D_{10}) value and sterilizing doses, incorporating both single- and multiple-hit kinetics, and taking into account the possible existence of a resistance shoulder for some pathogens following exposure to gamma-irradiation.

Keywords: gamma-irradiation; inactivation curve; sterilizing dose; sterility assurance level

INTRODUCTION

Gamma (γ) radiation is widely used to sterilize materials in a variety of settings. It is used in the food [1], pharmaceutical [2] and medical industries [3, 4] due to the ability of γ-radiation to inactivate pathogens through nucleic acid damage, whilst leaving proteins and other structures largely intact. Consequently, γ-radiation has also been proposed as an inactivation method to generate highly immunogenic vaccines [5]. Several groups have demonstrated the superiority of γ-radiation to traditional methods of vaccine inactivation, including formalin and β-propiolactone [6, 7]. In addition, previous publications illustrated the development of highly immunogenic γ-irradiated vaccines against influenza A virus (IAV) [5, 7–9] and *Streptococcus*

pneumoniae [10, 11]. Furthermore, γ-irradiated vaccines against human immunodeficiency virus (HIV) [12], and malaria [13, 14] are currently in clinical trials.

In order to ensure vaccine safety and immunogenicity, estimating the sterilizing dose (DS) under different irradiation conditions must be carefully considered. The radiosensitivity of a pathogen can be influenced by multiple factors including genome structure [15, 16], irradiation temperature [17–19], water [20] and oxygen levels [21, 22], and the presence of free-radical scavengers [23]. Importantly, resistance to γ-radiation is inversely related to genome size [15], as the chances of a single γ-ray interacting with the genome of a given pathogen is increased if the genome is larger. Accordingly, the DSs required for bacterial species are usually lower than those required for viruses [24]. In addition, it is hypothesized that viruses with more complex genomes are more radioresistant compared to viruses with simple genome structures, as a virus with a double stranded or segmented genome may require inactivation of multiple strands or segments to prevent non-damaged segments from re-assorting in a host cell. Importantly, current standard-operating procedures related to sterilization of pathogens were developed to deal with low levels of bioburden or contamination [25–27], and a dose of 50 kGy is routinely used for sterilizing pathogens that pose a biosecurity risk [28]. In this study, we investigated the effect of irradiation conditions on the irradiation dose required to sterilize highly concentrated or radioresistant pathogens, and assessed the validity of considering 50 kGy to be a widely applicable DS.

In general, DS is calculated based on the concept of a sterility assurance level (SAL). For irradiated materials, the SAL is a given probability that any single pathogen within a sample may escape inactivation following an exposure to γ-irradiation. The International Atomic Energy Agency (IAEA) recommends a SAL of 10^{-6} for products intended to come into contact with compromised tissues [25], and so this should be applied to γ-irradiated vaccines. A SAL of 10^{-6} means that there is a one in a million chance of a single infectious particle remaining following irradiation [28]. Currently, the irradiation dose required to achieve sterility at the recommended SAL of 10^{-6} (DS_{SAL}) is calculated using the formula

$$DS_{SAL} = n \times D_{10} \quad (1)$$

where n is the number of $\log_{10}$ reductions in bioburden required to reach a theoretical SAL of 10^{-6} and D_{10} is the irradiation dose required for a single $\log_{10}$ reduction in bioburden. Equation 1 assumes a log–linear inactivation curve, which is likely observed for viruses with simple genome structure that follow one-hit kinetics (Fig. 1A). Our recent publications, however, have shown non-linear inactivation curves (Fig. 1B) for rotavirus (RV) [29] and *S. pneumoniae* [30], demonstrating multiple-hit kinetics for complicated pathogens. While a D_{10} value is usually calculated based on the linear portion of the curve [22], ignoring the shoulder of resistance could lead to miscalculation of the irradiation dose required to achieve a SAL of 10^{-6} (or DS_{SAL}).

In this study we analyse the differences in D_{10} and DS_{SAL} for pathogens with different genomic structures irradiated at different temperatures. Our data show both single-hit and multiple-hit inactivation kinetics and we have formulated a simple method to calculate the DS_{SAL}. This method will ensure the shoulder of resistance is accounted for in multiple-hit inactivation models and thus allows for more accurate calculation of the SAL.

MATERIALS AND METHODS

Cells

Madin–Darby canine kidney (MDCK) and African green monkey kidney (Vero and MA104) cells were maintained in Dulbecco's Modified Eagle's Medium (DMEM) with 10% foetal bovine serum (FBS), 1% penicillin/streptomycin (P/S) and 1% 2 mM L-glutamine. For MA104 cells, 0.5% 200 mM sodium pyruvate was also added. Cells were maintained at 37°C with 5% CO_2 in a humidified environment. Primary chicken embryo fibroblasts (CEF) were prepared from 10-day-old chicken embryos by removing the head, limbs and viscera. Bodies were fragmented then pushed through a 70 μm single cell strainer (BD). Cells were washed three times with phosphate buffer saline (PBS) by centrifugation at 1831 × *g*, then seeded into a 75cm² tissue culture flask in DMEM +10% FBS and 1% P/S and kept at 37°C with 5% CO_2 in a humidified environment. After 24 h, non-adherent cells were removed by three washes with PBS and fresh medium was added.

Viruses

Handling of all pathogens was carried out in accordance with guidelines of the biosafety committee at the University of Adelaide and all viruses were handled inside a Class II Biosafety Cabinet. Influenza A virus (IAV) A/Puerto Rico/8/1934 (A/PR8) H1N1 and Newcastle disease virus (NDV) V4 strain were grown in the allantoic cavity of 10 day old embryonated chicken eggs (ECE). Viruses were injected at 1×10^3 50% tissue culture infectious dose ($TCID_{50}$)/egg in PBS containing 1% P/S. Eggs were incubated at 37°C for 48 h then chilled at 4°C overnight. Infected allantoic fluid was harvested and clarified by centrifugation at 3256 × *g* at 4°C for 10 min, then stored at −80°C until required.

Semliki Forest virus (SFV) A7 strain and Zika virus (ZIKV) MRC766 (Uganda 1947) strain were grown in Vero cells and rotavirus (RV) Rh452 was grown in MA104 cells. Viruses were propagated in DMEM + 1% P/S + 1% L-Glutamine RV was additionally activated by incubation at 37°C for 1 h with 10 μg/mL TPCK-trypsin (Sigma) prior to adding to cells. Viruses were all added at an multiplicity of infection (MOI) of 0.01, and infected flasks were stored at 37°C for 24–48 h until a cytopathic effect (CPE) of ∼50% of the cell monolayer was observed. Virus-containing cell culture supernatants were collected and clarified by centrifugation at 3256 × *g* at 4°C for 10 min and stored at −80°C until required.

IAV and NDV were titrated by $TCID_{50}$ in MDCK or CEF cells, respectively, in a 96-well round-bottomed microtitre plate. Virus was activated with 0.004% trypsin then 10-fold dilutions were added to confluent cell monolayers. Plates were incubated for 3 days at 37°C with 5% CO_2. The presence of infectious virus was determined by agglutination of 50 μL of 0.6% chicken red blood cells (cRBC) in each well. The 50% infectious dose was determined using the method described by Reed and Muench [31] and titres were given as $TCID_{50}$/mL.

SFV and ZIKV were titrated by plaque forming assay (PFA). Confluent monolayers of Vero cells were infected with serial dilutions of virus. Adsorption of virus was allowed for 1 h then a 0.9% agar overlay

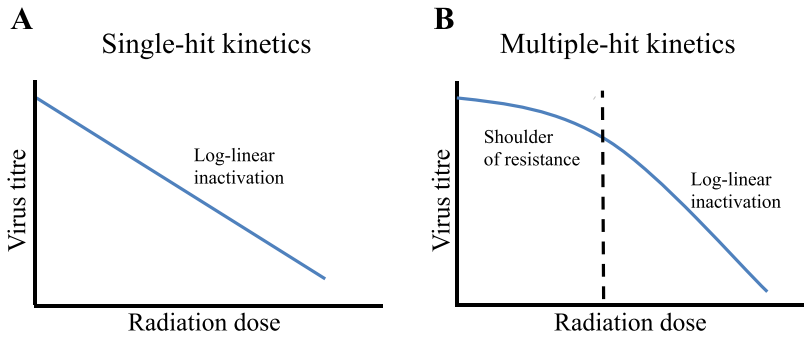

Fig. 1. Inactivation kinetics of viruses demonstrating a model of (A) single-hit kinetics or (B) multiple-hit kinetics. Single-hit kinetics follows log–linear inactivation, whereas multiple-hit kinetics has a shoulder of resistance before damage is accumulated and log–linear inactivation occurs.

was added and plates were incubated for 3 days (SFV) or 5 days (ZIKV). Cells were fixed with 5% formalin for 1 h at room temperature (RT). Overlays were removed and cells were stained with 0.2% crystal violet. Plaques were enumerated and titre was calculated as plaque-forming units (PFU)/mL.

RV was titrated by focus-forming assay (FFA) as described previously [29]. Briefly, MA104 cells were seeded in 96-well flat-bottomed microtitre plates at 6.4×10^3 cells/well and plates were incubated at 37°C for 3 days until a confluent monolayer had formed. RV was activated by 10 μg/mL TPCK-trypsin for 30 min at 37°C. RV, 10-fold serially diluted, was added to wells and incubated at 37°C for 1 h to allow virus to adhere to cells. Inoculum was removed and replaced with DMEM + 1% P/S + 1% L-glutamine + 0.5% sodium pyruvate and plates were incubated for a further 18 h at 37°C. Cells were then washed, and fixed and permeabilized using acetone:methanol (1:1 ratio). RV was visualized by primary staining with a polyclonal mouse anti-RV serum for 1 h at 4°C followed by Alexa Fluor® 555 goat anti-mouse IgG (Life Technologies, USA) secondary antibody for 1 h at 4°C in the dark. Cells were also stained with 1 μg/mL DAPI (Sigma) for 10 min at RT. RV-positive cells were visualized using a Nikon Eclipse Ti fluorescent microscope and NIS-Elements AR software. Titre was calculated as focus-forming units (FFU)/mL.

Streptococcus pneumoniae

Streptococcus pneumoniae strain Rx1, a capsule-deficient derivative of D39 containing two additional mutations (ΔLytA, PdT) that has been described previously [10], was used. *Streptococcus pneumoniae* was inoculated into Todd Hewitt Broth supplemented with 0.5% yeast extract (THY) medium at a starting OD_{600} of 0.02 and then grown at 37°C + 5% CO_2 until OD reached 0.65. Bacteria were centrifuged at 4000 × *g* for 10 min at 4°C then resuspended and washed thrice in PBS. Bacteria were then resuspended in PBS + 13% glycerol at ~10^{10} colony forming unit (CFU)/mL then frozen at −80°C until required. Viable titres were measured by CFU counts on blood agar plates.

Gamma-irradiation

Virus and bacteria stocks were shipped to the Australian Nuclear Science and Technology Organisation (ANSTO) whilst frozen on dry ice. Samples were thawed on ice or at RT, or kept frozen on dry ice as specified and were exposed to increasing doses (0–50 kGy) of γ-radiation at different conditions [RT (24–27°C), cold on ice water (4–8°C) or frozen on dry-ice]. Gamma-irradiation was performed using a ^{60}Co source at the ANSTO (NSW). Radiation doses were measured using calibrated Fricke or ceric cerous dosimeters. Pathogens were then titrated to measure loss of infectivity at different radiation doses. Non-irradiated controls were treated with the same conditions (room-temperature, ice or dry ice) without exposure to γ-radiation. After irradiation all samples were stored at −80°C until required.

RESULTS

Inactivation curves

Different pathogens were exposed to incremental doses of γ-radiation and titres at each radiation dose were determined. IAV and NDV were both grown in 10-day-old ECEs and they are expected to have the same medium composition. This enabled a comparison between radiation-sensitivity of a non-segmented single-stranded RNA genome (ssRNA) genome (NDV) and a segmented ssRNA genome (IAV). Our data demonstrate log–linear inactivation for both viruses (Fig. 2), indicating single-hit inactivation kinetics.

Next, we compared the inactivation curves of SFV and ZIKV under different irradiation temperatures. Both viruses have ssRNA genomes of a comparable size, and were both grown in Vero cells using DMEM with similar medium composition. Both viruses demonstrated single-hit inactivation kinetics, with increased radiosensitivity at higher temperatures, as expected (Fig. 3).

We then analysed the inactivation curve of RV, a more complex virus with a segmented and double-stranded RNA genome (dsRNA) genome structure. We have previously reported that the inactivation curve for dry ice-irradiated RV is non-linear and confirmed that here using a different strain of RV (Fig. 4). The curve shows two distinct regions. A large shoulder of resistance is observed initially, with an ~2 log loss of titre occurring between 0 to 40 kGy. After this point, a rapid decline in viable titre was observed with increased radiation dose. Importantly, calculating the DS using this inactivation curve would not be possible using current mathematical models (equation

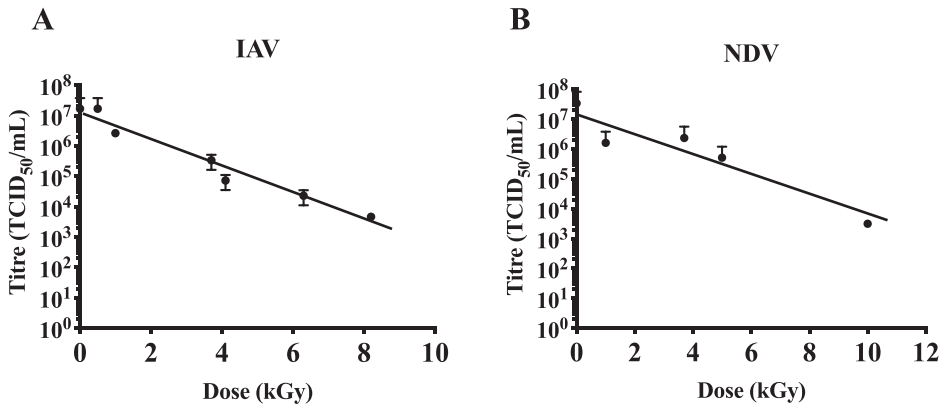

Fig. 2. Log–linear inactivation curves of ssRNA viruses in allantoic fluid. (A) Influenza A virus and (B) Newcastle disease virus were exposed to increasing doses of γ-irradiation on dry ice. Reduced virus titre (as measured by $TCID_{50}$/ml) for increasing irradiation doses helped to generate inactivation curves and log–linear inactivation was observed for both viruses. Data are expressed as mean ± SEM ($n = 2$). Horizontal dashed line represents background binding of virus to RBCs in the absence of a cell monolayer.

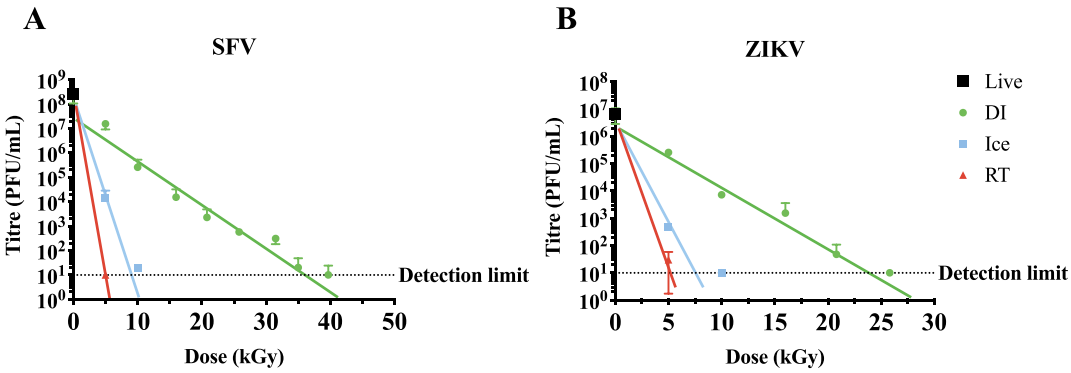

Fig. 3. Log–linear inactivation of ssRNA viruses at different irradiation temperatures. (A) Semliki Forest virus and (B) Zika virus were exposed to increased doses of γ-irradiation on dry ice (DI) (green circles), ice (blue squares) or at room temperature (RT) (red triangles). The reduction in virus titre was estimated using plaque assay and inactivation curves were generated. Log–linear inactivation was observed for all three temperature conditions. Non-irradiated live virus was used as the starting point. Data are presented as mean ± SEM ($n = 3$). Horizontal dashed line represents detection limit.

1). Interestingly, we did not detect the multiple-hit inactivation curve for RV materials irradiated on ice or at RT (Fig. 4). This could indicate that indirect damage caused by free radicals following irradiation at higher temperatures may counteract the radioresistance of pathogens with more complex genomes.

Calculating sterilizing doses

For viruses demonstrating single-hit kinetics, exponential lines of best fit could be determined using the equation:

$$y = ae^{-bx} \tag{2}$$

where y is the titre at a given radiation dose x, a is the starting titre, and b is a constant that is determined experimentally for each individual virus under a given set of irradiation conditions. Equation (2) can then be rearranged to determine the D_{10} value (x), when $y = 0.1a$ (i.e. a 90% loss of starting titre):

$$D_{10} = \frac{\ln(0.1)}{-b} \tag{3}$$

Therefore, the D_{10} is higher where b is lower, as would be expected for more radioresistant pathogens. The line of best fit, D_{10} values and

Table 1. Inactivation formulae and sterility assurance levels of NDV and IAV

Virus	Formula[a]	Starting titre ($TCID_{50}$/mL)	D_{10} (kGy)	DS (kGy)
IAV	$y = 2 \times 10^7 \times e^{-1.097x}$	1.69×10^7	2.1 ± 0.16	27.77
NDV	$y = 2 \times 10^7 \times e^{-0.823x}$	3.41×10^7	2.8 ± 0.53	37.86

[a]Units for x are kGy.

Table 2. Inactivation formulae and sterility assurance levels of ZIKV, SFV and RV

Virus	Irradiation condition[a]	Formula[b]	Starting titre[c]	D_{10} (kGy)	DS (kGy)
SFV	DI	$y = 5 \times 10^7 \times e^{-0.418x}$	2.55×10^8	5.5 ± 0.43	79.36
	Ice	$y = 3 \times 10^8 \times e^{-1.968x}$		1.2 ± 0.23	16.86
	RT	$y = 3 \times 10^8 \times e^{-3.871x}$		<1	14.41
ZIKV	DI	$y = 7 \times 10^6 \times e^{-0.625x}$	6.75×10^6	4.2 ± 0.35	54.10
	Ice	$y = 9 \times 10^6 \times e^{-1.986x}$		1.2 ± 0.06	14.87
	RT	$y = 9 \times 10^6 \times e^{-2.533x}$		0.9 ± 0.31	11.66
RV	Ice	$y = 1 \times 10^5 \times e^{-0.506x}$	1.05×10^6	4.6 ± 1.1	54.71
	RT	$y = 1 \times 10^5 \times e^{-0.521x}$		4.4 ± 0.02	53.13

[a]DI = Dry ice, RT = room temperature.
[b]Units for x are kGy.
[c]Virus titre was measured as PFU/mL for SFV and ZIKV, and FFU/mL for RV.

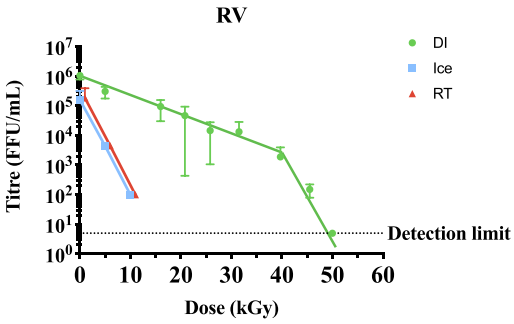

Fig. 4. Inactivation curve of RV at different irradiation temperatures. RV was exposed to increasing doses of γ-radiation on dry ice (DI) (green circles), ice (blue squares) or at room temperature (RT) (red circles). Titre was measured by focus forming units. In contrast to both ice and RT, irradiation on DI shows an inactivation curve with multiple-hit kinetics. A shoulder of resistance appears to require an irradiation dose of 40 kGy. Data are presented as mean ± SEM ($n = 2$).

DS_{SAL} were determined for IAV and NDV (Table 1), and ZIKV and SFV (Table 2). The D_{10} values of IAV and NDV were comparable (2.1 and 2.8 kGy, respectively), whereas SFV had a higher D_{10} than ZIKV for dry-ice irradiation (5.5 compared to 4.2 kGy). The D_{10} values were also calculated for ice and RT and were comparable, however an exact D_{10} value for RT-irradiated SFV could not be determined since virus was undetectable at the lowest irradiation dose used (5 kGy) in our experimental settings. Importantly, calculating a D_{10} value for pathogens with single-hit kinetics allowed us to calculate the DS_{SAL} using equation (1), as shown in Tables 1 and 2. However, calculating the DS using equation (1) would not be possible for pathogens with multiple-hit kinetics as ignoring the shoulder of resistance would result in a miscalculation of the DS. Therefore, we propose a new formula to calculate the DS_{SAL} that could accommodate both single-hit and multiple-hit inactivation kinetics:

$$DS_{SAL} = R + (n \times D_{10}) \quad (4)$$

where R refers to the irradiation dose required to overcome the shoulder of resistance with a value of 'R = 0' for pathogens that show linear inactivation curves (single-hit kinetics). This formula takes into account the distinct regions of multiple-hit curves and should allow for more accurate calculation of DSs.

When considering the inactivation curve of dry-ice irradiated RV (Fig. 4), we could consider 40 kGy to be required to overcome the radioresistance (R value). We could also calculate the D_{10} for the radiation sensitive portion of the curve (above 40 kGy) using equation (3). The D_{10} for the linear portion of the curve was calculated to be 3.2 kGy (based on the formula $y = 7 \times 10^{15} \times e^{-0.718x}$). To calculate DS_{SAL} using equation (4), we need to estimate the number of $\log_{10}$ reduction in virus titre (n) required to achieve the internationally acceptable SAL of 10^{-6}. For this calculation, the viable titre at $x = 40$ kGy was determined to be 2.4×10^3 FFU/mL. Thus, a further reduction of 9.4 $\log_{10}$ will be required to meet a SAL of 10^{-6}. Hence the DS_{SAL} for dry-ice irradiated RV could be calculated based on equation (4) as follows:

$$DS_{SAL} = 40 + (9.4 \times 3.2) = 70.08 \text{ kGy}.$$

To confirm the applicability of this method, we considered the inactivation curve of the bacterial pathogen *S. pneumoniae*. This pathogen

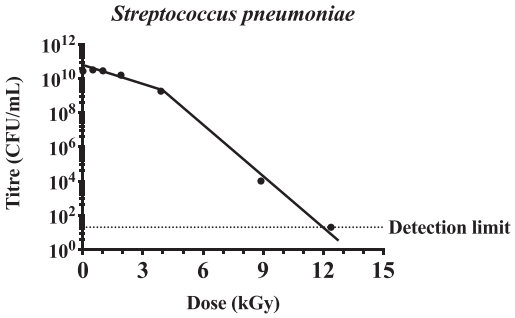

Fig. 5. Inactivation curve of *S. pneumoniae* demonstrates multiple-hit kinetics. *Streptococcus pneumoniae* was irradiated on dry-ice (DI) at the indicated doses. Titre was measured by colony forming units and data are presented as mean ± SEM ($n = 4$). Inactivation curve demonstrates a multiple hit kinetics and a shoulder of resistance that require an irradiation dose of 4 kGy.

has a double-stranded genome, and the inactivation curve is non-linear (Fig. 5). The shoulder of resistance, or R value, was determined to be 4 kGy. At $x = 4$ kGy the titre was 1.7×10^9 CFU/mL, thus 15.2 $\log_{10}$ reductions ($n = 15.2$) were required to reach the accepted SAL level of 10^{-6}. We calculated the D_{10} value for the log–linear curve (after 4 kGy) using the formula $y = 6 \times 10^{13} \times e^{-2.611x}$, which shows a value of 0.88 kGy. Therefore, the DS_{SAL} for *S. pneumoniae* irradiated on dry-ice could be calculated using equation (4) as follows:

$$DS_{SAL} = 4 + (15.2 \times 0.88) = 17.38 \text{ kGy}.$$

DISCUSSION

Current recommendations for calculating DSs are based on concepts and formulae generated to meet requirements to sterilize food, medical equipment and other health care products [25, 27, 32]. A dose of 25 kGy is considered the 'gold standard' [25] and is often substantiated for a low bioburden. In general, the contaminating species are typically bacteria, which are more sensitive to γ-radiation than viruses [24] and spores [33]. In addition, the The International Organization for Standardization (ISO) suggests that a bioburden of 10^6 infectious units is unusually high [27]. However, materials prepared for biomedical analysis as well as for vaccine purposes are expected to have bioburden levels much higher than 10^6 infectious units. Consequently, a DS_{SAL} <25 kGy was not observed for any of the viruses irradiated on dry ice (Tables 1 and 2). Accordingly, 25 kGy should not be considered a DS for virally contaminated materials, nor for vaccine inactivation purposes, without properly addressing the inactivation curve and D_{10} value, particularly when frozen materials are irradiated using dry ice. For pathogens that pose a biosecurity concern a dose of 50 kGy is usually considered sufficient [28]. However, a SAL of 10^{-6} could not be reached following irradiation with 50 kGy on dry ice for ZIKV or SFV, or at 50 kGy using all irradiation conditions (dry ice, ice and RT) for RV (Table 2). Therefore, existing concepts that govern the use of γ-irradiation to sterilize highly infectious pathogens should be carefully considered to ensure sterility at internationally accepted levels. This will be essential for the development of highly safe and immunogenic γ-irradiated vaccines.

Inactivation curves typically follow single-hit or multiple-hit kinetics. It was expected that inactivation of single-stranded, non-segmented RNA viruses would follow single-hit kinetics. This was confirmed with NDV (Fig. 2B), SFV and ZIKV (Fig. 3), as well as previous publications [16, 34]. Interestingly, IAV also appeared to follow single-hit inactivation kinetics despite having segmented single-stranded RNA genomes (Fig. 2A). We have previously demonstrated log–linear inactivation of IAV [35]. Previous reports of inactivation curves of viruses with single-stranded segmented genomes have also demonstrated first-order kinetics [17, 36]. Conversely, the inactivation curves of RV (Fig. 4) and *S. pneumoniae* (Fig. 5) demonstrate multiple-hit inactivation kinetics where an accumulation of damage is required to sterilize each pathogen. Unlike other viruses used in this study, the genome of RV is comprised of 11 dsRNA segments and sufficient damage to both strands will be required to completely inactivate any genome segment. In addition, reassortment of RV is relatively frequent, and has been shown to enhance resistance in response to UV treatment [37]. Thus, incomplete inactivation of dsRNA segments accompanied by reassortment can rescue the infectivity of RV. This could explain the large shoulder of 40 kGy observed for RV. In contrast, *S. pneumoniae* cannot reassort, and SOS repair used by other bacterial species such as *Escherichia coli* [38] in response to γ-radiation do not appear to occur in *S. pneumoniae* [39]. However *S. pneumoniae* does utilize some repair mechanisms, such as excision repair [40]. It is also important to consider that *S. pneumoniae* has double-stranded genomes which could enhance resistance as both strands may need to be damaged to ensure inactivation. Conversely, mammalian cells are highly susceptible to γ-radiation despite having double-stranded genomes and repair mechanisms [41, 42]. This is particularly relevant to the development of γ-irradiated cancer vaccines such as GVAX, which is currently in clinical trials [43]. DSs reported are typically between 35 [44] and 100 Gy [45]. The radiosensitivity of mammalian cells is explained by a considerably larger genome than viruses and bacteria.

The ISO recommendations for calculating the DS involves setting a dose based on the calculated bioburden and a standard distribution of resistances (SDR) based on a D_{10} of between 2 and 3 kGy [27]. Where radioresistance is higher than the SDR (as would be the case for most viruses), the preparation is subjected to incremental increases in radiation dose and the proportion of positive samples is used to calculate the DS (i.e. at a SAL of 10^{-2}, there should be 0, 1 or 2 positive samples out of 100 for statistically significant substantiation of the dose used). However, extrapolating this data for a SAL of 10^{-6} does not take into account the potential for non-linear inactivation. We have proposed an alternative method where the shoulder of resistance is calculated and accounted for as well as log–linear inactivation. To ensure the sterility and safety of irradiated materials, it is important to take into account the shape of the inactivation curve when considering the SAL, and equation (4) allows the shoulder of resistance to be incorporated when calculating the DS for pathogens that display multiple-hit inactivation kinetics. Importantly, mathematical modelling must also be coupled with rigid sterility testing.

It is important to note that γ-rays cause damage to pathogens by directly interacting with genomes to cause cross-linking, and single- and double-stranded breaks [46–49], and can interact with water or oxygen molecules to form free radicals. Oxidative damage causes most of the protein damage [20], but the formation and movement of free radicals can be reduced in frozen samples [50, 51]. In fact, irradiating frozen prions at incredibly high doses of up to 200 kGy showed minimal loss of transmission [52], demonstrating the resistance of proteins to γ-radiation at low temperatures. Thus, while irradiating at higher temperatures is more effective for sterilization (Figs 3 and 4, [16, 17, 19]), irradiating frozen samples is expected to better maintain structural integrity [35, 53]. Therefore, γ-irradiation has routinely been performed at low temperatures to obtain more effective results for both biomedical analysis and vaccine immunogenicity. However, our data clearly illustrate that sterility at an internationally accepted level based on SAL of 10^{-6} could not be achieved when irradiating high titres of some pathogens with 50 kGy using dry-ice conditions, and even when using room-temperature irradiation for radioresistant pathogens such as RV. Therefore, to ensure the safety of irradiated materials, the irradiation temperature, the appropriate method to calculate DS_{SAL} and rigid sterility testing must be considered. Overall, this study highlighted a serious gap in current practices, and we propose a new mathematical formula to calculate both the D_{10} value and DS_{SAL} to ensure the safety of irradiated materials for vaccine and research purposes.

ACKNOWLEDGEMENT

This work was presented at the Australian Nuclear Science and Technology Organisation (ANSTO) User Meeting, Sydney Australia, December 2019.

CONFLICT OF INTEREST

M.A. is head of the Vaccine Research Group at the University of Adelaide and the Chief Scientific Officer of Gamma Vaccines Pty Ltd and Director of GPN Vaccines Pty Ltd, J.C.P. is a Director of GPN Vaccines Pty Ltd, and T.R.H. is the Executive Chairman of Gamma Vaccines Pty Ltd and GPN Vaccines Pty Ltd. This does not alter adherence to policies on sharing data and materials. Both Gamma Vaccines Pty Ltd and GPN Vaccines Pty Ltd have no role in the study design, data collection and analysis, decision to publish, and preparation of the manuscript.

FUNDING

This work was supported by the following funding sources: an Australian Institute of Nuclear Science and Engineering (AINSE) Research Award (ALNGRA15517; to M.A.); an Australian Government Research Training Program (RTP) Scholarship (to E.V.S.); and a National Health and Medical Research Council Senior Principal Research Fellowship (awarded to J.C.P.).

AUTHORS' CONTRIBUTIONS

M.A. and E.V.S. conceived and designed the study. E.V.S., S.C.D. and J.B.D. performed the experiments. E.V.S. and M.A. wrote the manuscript. F.H., T.R.H., J.C.P. and M.R.B. assisted in experimental design and preparation of the manuscript and provided reagents. M.A. supervised the study.

REFERENCES

1. Food and Drug Administration (FDA). Irradiation in the production, processing and handling of food. 2017.
2. International Atomic Energy Agency. Manual on radiation sterilization of medical and biological materials. 1973.
3. Singh, R, Singh, D, Singh, A. Radiation sterilization of tissue allografts: A review. *World J Radiol* 2016; 8(4): 355–69.
4. Doue B. Radiation doses and dose distribution during industrial sterilization by gamma rays and acclerated electron beams (part I). *Medical Device Technol* 2001;32–5.
5. Alsharifi, M, Mullbacher, A. The γ-irradiated influenza vaccine and the prospect of producing safe vaccines in general. *Immunology and Cell Biology* 2009; 88(2): 103.
6. Wiktor, TJ, Aaslestad, HG, Kaplan, MM. Immunogenicity of rabies virus inactivated by β-propiolactone, acetylethyleneimine, and ionizing irradiation. *Appl Microbiol* 1972; 23(5): 914–8.
7. Furuya, Y, Regner, M, Lobigs, M et al. Effect of inactivation method on the cross-protective immunity induced by whole 'killed' influenza a viruses and commercial vaccine preparations. *The Journal of general virology* 2010; 91(Pt 6): 1450.
8. Alsharifi, M, Furuya, Y, Bowden, TR et al. Intranasal flu vaccine protective against seasonal and H5N1 avian influenza infections. *PLoS One* 2009; 4(4): e5336.
9. Furuya, Y, Chan, J, Wan, E-C et al. Gamma-irradiated influenza virus uniquely induces IFN-I mediated lymphocyte activation independent of the TLR7/MyD88 pathway (immune responses to inactivated influenza viruses). *PLoS ONE* 2011; 6(10): e25765.
10. Babb, R, Chen, A, Hirst, TR et al. Intranasal vaccination with gamma-irradiated Streptococcus pneumoniae whole-cell vaccine provides serotype-independent protection mediated by B-cells and innate IL-17 responses. *Clin Sci (Lond)* 2016; 130(9): 697–710.
11. Babb, R, Chen, A, Ogunniyi, AD et al. Enhanced protective responses to a serotype-independent pneumococcal vaccine when combined with an inactivated influenza vaccine. *Clin Sci (Lond)* 2017; 131(2): 169–80.
12. Choi, E, Michalski, CJ, Choo, SH et al. First phase I human clinical trial of a killed whole-HIV-1 vaccine: Demonstration of its safety and enhancement of anti-HIV antibody responses. *Retrovirology* 2016; 13(1): 82.
13. Seder, RA, Chang, LJ, Enama, ME et al. Protection against malaria by intravenous immunization with a nonreplicating sporozoite vaccine. *Science* 2013; 341(6152): 1359–65.
14. Ishizuka, AS, Lyke, KE, DeZure, A et al. Protection against malaria at 1 year and immune correlates following PfSPZ vaccination. *Nat Med* 2016; 22(6): 614–23.
15. Jordan, RT, Kempe, LL. Inactivation of some animal viruses with gamma radiation from cobalt-60. *Proc Soc Exp Biol Med* 1956; 91(2): 212–5.
16. Sullivan, R, Fassolitis, AC, Larkin, EP et al. Inactivation of thirty viruses by gamma radiation. *Appl Microbiol* 1971; 22(1): 61–5.

17. Elliott, LH, Mccormick, JB, Johnson, KM. Inactivation of Lassa, Marburg, and Ebola viruses by gamma-irradiation. *Journal of Clinical Microbiology* 1982; 16(4): 704–8.
18. Kempner, ES, Haigler, HT. The influence of low temperature on the radiation sensitivity of enzymes. *J Biol Chem* 1982; 257(22): 13297–9.
19. Thayer, DW, Boyd, G. Effect of irradiation temperature on inactivation of Escherichia coli O157:H7 and Staphylococcus aureus. *J Food Prot* 2001; 64(10): 1624–6.
20. Feldberg, RS, Carew, JA. Water radiolysis products and nucleotide damage in gamma-irradiated DNA. *Int J Radiat Biol Relat Stud Phys Chem Med* 1981; 40(1): 11–7.
21. Teoule, R, Bonicel, A, Bert, C et al. Identification of radioproducts resulting from the breakage of thymine moiety by gamma irradiation of E. coli DNA in an aerated aqueous solution. *Radiation research* 1974; 57(1): 46–58.
22. Gazso L. Physical, chemical and biological dose modifying factors. In: Gazso LP (ed). CC*Nato Sci Ser I Life*. Amsterdam: IOS Press, 2005, 59–68.
23. Sullivan, R, Scarpino, PV, Fassolitis, AC et al. Gamma radiation inactivation of coxsackievirus B-2. *Appl Microbiol* 1973; 26(1): 14–7.
24. Farkas J. In: Doyle MP (ed). BL*Physical Methods of Food Preservation*. 2007.
25. International Atomic Energy Agency. Good radiation practice (GRP). IAEA Guidelines for industrial radiation and sterilization of disposable medical products (cobalt-60 gamma irradiation). 1990.
26. International Atomic Energy Agency. Sterility assurance level. Guidelines for Industrial Radiation Sterilisation of Disposable Medical Products (Cobalt-60 Gamma-Irradiation). 1990Vol IAEA-TECDOC-539;39.
27. International Organisation for Standardization. Sterilization of health care products - radiation - part 2: Establishing the sterilization dose. 2013 ISO 11137-2:2013, 2013.
28. Department of Agriculture Fisheries and Forestry Biosecurity. Gamma irradiation as a treatment to address pathogens of animal biosecurity concern - final policy Review'. Canberra, CC BY 3.0 2014.
29. Shahrudin, S, Chen, C, David, SC et al. Gamma-irradiated rotavirus: A possible whole virus inactivated vaccine. *PLoS One* 2018; 13(6): e0198182.
30. David SC, Laan Z, Minhas V et al. Enhanced safety and immunogenicity of a psaA mutant whole-cell inactivated pneumococcal vaccine. *Immunology and Cell Biology* 2019.
31. Reed, LJ, Muench, H. A simple method of estimating fifty per cent endpoints. *American Journal of Epidemiology* 1938; 27(3): 493–7.
32. Hendry JH. *Radiation Sterilization of Tissue Allografts: Requirements for Validation and Routine Control : a Code of Practice*. International Atomic Energy Agency, 2007.
33. Sommers, CH, Rajkowski, KT. Radiation inactivation of foodborne pathogens on frozen seafood products. *J Food Prot* 2011; 74(4): 641–4.
34. Hume, AJ, Ames, J, Rennick, LJ et al. Inactivation of RNA viruses by gamma irradiation: A study on mitigating factors. *Viruses* 2016; 8(7).
35. David, SC, Lau, J, Singleton, EV et al. The effect of gamma-irradiation conditions on the immunogenicity of whole-inactivated influenza a virus vaccine. *Vaccine* 2017; 35(7): 1071–9.
36. Thomas, FC, Davies, AG, Dulac, GC et al. Gamma ray inactivation of some animal viruses. *Can J Comp Med* 1981; 45(4): 397–9.
37. McClain, ME, Spendlove, RS. Multiplicity reactivation of reovirus particles after exposure to ultraviolet light. *J Bacteriol* 1966; 92(5): 1422–9.
38. Brena-Valle, M, Serment-Guerrero, J. SOS induction by gamma-radiation in Escherichia coli strains defective in repair and/or recombination mechanisms. *Mutagenesis* 1998; 13(6): 637–41.
39. Gasc, AM, Sicard, N, Claverys, JP et al. Lack of SOS repair in Streptococcus pneumoniae. *Mutation research* 1980; 70(2): 157–65.
40. Sicard, N, Estevenon, AM. Excision-repair capacity in Streptococcus pneumoniae: Cloning and expression of a uvr-like gene. *Mutation research* 1990; 235(3): 195–201.
41. Dolling, JA, Boreham, DR, Brown, DL et al. Modulation of radiation-induced strand break repair by cisplatin in mammalian cells. *International journal of radiation biology* 1998; 74(1): 61–9.
42. Hafer, K, Iwamoto, KS, Scuric, Z et al. Adaptive response to gamma radiation in mammalian cells proficient and deficient in components of nucleotide excision repair. *Radiation research* 2007; 168(2): 168–74.
43. Le, DT, Picozzi, VJ, Ko, AH et al. Results from a phase IIb, randomized, Multicenter study of GVAX pancreas and CRS-207 compared with chemotherapy in adults with previously treated metastatic pancreatic adenocarcinoma (ECLIPSE study). *Clin Cancer Res* 2019; 25(18): 5493–502.
44. Dranoff, G, Jaffee, E, Lazenby, A et al. Vaccination with irradiated tumor cells engineered to secrete murine granulocyte-macrophage colony-stimulating factor stimulates potent, specific, and long-lasting anti-tumor immunity. *Proc Natl Acad Sci U S A* 1993; 90(8): 3539–43.
45. Baureus-Koch, C, Nyberg, G, Widegren, B et al. Radiation sterilisation of cultured human brain tumour cells for clinical immune tumour therapy. *Br J Cancer* 2004; 90(1): 48–54.
46. Schulte-Frohlinde, D, Opitz, J, Gorner, H et al. Model studies for the direct effect of high-energy irradiation on DNA. Mechanism of strand break formation induced by laser photoionization of poly U in aqueous solution. *Int J Radiat Biol Relat Stud Phys Chem Med* 1985; 48(3): 397–408.
47. Henner, WD, Grunberg, SM, Haseltine, WA. Sites and structure of gamma radiation-induced DNA strand breaks. *J Biol Chem* 1982; 257(19): 11750–4.
48. Lomax, ME, Folkes, LK, O'Neill, P. Biological consequences of radiation-induced DNA damage: Relevance to radiotherapy. *Clin Oncol (R Coll Radiol)* 2013; 25(10): 578–85.
49. Van Der Schans, GP. Gamma-ray induced double-strand breaks in DNA resulting from randomly-inflicted single-strand breaks: Temporal local denaturation, a new radiation phenomenon? *Int J Radiat Biol Relat Stud Phys Chem Med* 1978; 33(2): 105–20.
50. Ormerod MG. Free-radical formation in irradiated deoxyribonucleic acid. *Int J Radiat Biol Relat Stud Phys Chem Med* 1965;9:291–300.

51. Grieb, T, Forng, RY, Brown, R et al. Effective use of gamma irradiation for pathogen inactivation of monoclonal antibody preparations. *Biologicals* 2002; 30(3): 207–16.
52. Gibbs, CJ, Jr., Gajdusek, DC, Latarjet, R. Unusual resistance to ionizing radiation of the viruses of kuru, Creutzfeldt-Jakob disease, and scrapie. *Proc Natl Acad Sci U S A* 1978; 75(12): 6268–70.
53. Kitchen, AD, Mann, GF, Harrison, JF et al. Effect of gamma irradiation on the human immunodeficiency virus and human coagulation proteins. *Vox sanguinis* 1989; 56(4): 223–9.